Biomass accumulation in secondary forests of the Brazilian Amazon

Mr Joshua Aidan Howard Jones

A thesis submitted in fulfilment of the requirements for the degree of Doctor of Philosophy

9^{th} May, 2017

Aberystwyth University

Supervisors: Dr Peter Bunting, Dr George Petropoulos,

Prof Richard Lucas & Dr João Carreiras

Declaration and Statements

Declaration

This work has not previously been accepted in substance for any degree and is not being concurrently submitted in candidature for any degree.

Signed ..... Date .....

Statement 1

This thesis is the result of my own investigations expect where otherwise stated. Where correction services have been used, the extent and nature of the correction is clearly marked in footnote(s). Other sources area acknowledged by footnotes and giving explicit references. A bibliography is appended.

Signed ..... Date .....

Statement 2

I hereby give consent for my thesis, if accepted, to be available for photocopying and for inter-library loan, and for the title and summery to be made available to outside organisations.

Signed ..... Date .....

Acknowledgements

I would like to thank my main supervisor Dr Peter Bunting for his support throughout my PhD and work in leading a successful research group that was a pleasure to be a part of. My thanks to Prof. Richard Lucas for giving me the opportunity to take up a PhD at Aberystwyth University; his supervision throughout the first two years of my thesis and for sharing his knowledge whilst on field work. Dr George Petropoulos's guidance proved invaluable in conducting my analysis and thesis writing. João Carreiras for co-authorship; critical comments on my thesis and his work as PI of Regrowth-BR (PTDC/AGR-CFL/114908/2009) which provided field data and funding. Additional field data was provided by NERC TIGER project (GST/02/604).

Besides my supervisor team, I would like to thank the rest of the Earth Observation and Ecosystem Dynamics research group, past and present: Dr Nathan Thomas, Dr Sizwe Mabaso, Dr Andrew Hardy, Dr Alisdair Cunningham, Dr Rebecca Charnock, Gwawr Jones, Sarah Perry and Dr Heather Crump,.

Last but not least, I would like to thank my mother and dyslexia tutor Victoria Wade and my fiancée Morgan Gibson for reading endless iterations of my thesis and accommodating me when the pressure was on.

Abstract

Across the world, particularly in the tropics, the extent of forest clearance has been widespread. At present, few studies have been undertaken and little is known on the long-term effect of land use history following clearance, on forest recovery, a significant sink for atmospheric CO_2. This study aimed at quantifying the capacity of regenerating forests in the Brazilian Legal Amazon (BLA) to recover carbon using a combination of Earth Observation (EO) data and the 3-PG forest growth model. Three sites were selected within the BLA, representative of different clearance histories on which extensive deforestation has occurred. Land use history and forest age for these areas was obtained from time-series analysis of Landsat images (1974 - 2011). Long term trends of aboveground biomass (AGB) accumulation in secondary forests were studied using field inventory data from 52 secondary forest plots north of Manaus from 1993, 1995 and 2014. Plots were representative of different clearance histories; a combination of clearance frequency and period of active land use prior to abandonment. A variance based global sensitivity analysis (SA) was carried out on the 3-PG forest growth model to identify its most sensitive model inputs when applying it to a mixed tropical rainforest. A parameter set for mixed tropical forests was identified using a Monte-Carlo simulation and by comparing simulated outputs to field data. These parameters were used within 3-PG to provide estimates of total carbon sequestration and model sensitivity to future climate change.

Results of this thesis showed that forest age derived from remote sensing time series was comparable to that derived from field observations and interviews. Sites with a higher land use intensity did not accumulate biomass at a significantly slower rate than those used less intensively. Accumulation rates predicted from the model closely matched those calculated from the forest inventory data gathered at each plot. SA results demonstrated scientifically credible behaviour of the model and allowed identification of the most responsive model inputs and interactions. Findings illustrated the suitability and potential of combining a process based model with EO data as a way to forecast the productivity of mixed secondary forest in Brazil. Comparisons with existing estimates highlight uncertainties in deriving secondary forest AGB from remote sensing using relationships fitted to primary forests. Development of these methodologies has applications to other tropical ecosystems that have experienced a similar history of disturbance and can provide invaluable information for future land-use planning and REDD+ monitoring.

List of Publications

The following is a list of Papers which have been published in a journal during the course of this study:

Journal

Carreiras, J.M.B., Jones, J., Lucas, R.M., Gabriel, C. (2014) Land Use and Land Cover Change Dynamics across the Brazilian Amazon: Insights from Extensive Time-Series Analysis of Remote Sensing Data. *PLoS ONE*. 9(8)

Carreiras, J.M.B., Jones, J., Lucas, R.M., Shimabukuro, Y.E. (2017) Mapping major land cover types and retrieving the age of secondary forests in the Brazilian Amazon by combining single-date optical and radar remote sensing data. *Remote Sensing of the Environment*

Abbreviations and Units

Table 1: List of abbreviations and definitions used in the thesis.

Abbreviation	**Definition**
ρ	Specific wood density
fPAR	photosynthetically active radiation
3-PG	Physiological Principles Predicting Growth. Forest growth model.
3-PG$_2$	Most recent version of Physiological Principles Predicting Growth as of 2007. Forest growth model.
AGB	Above ground biomass
AGC	Above ground carbon
AIRSAR	Airborne Synthetic Aperture Radar
ALOS PALSAR	Advanced Land Observation Satellite Phased Array type L-band Synthetic Aperture Radar
ASF	Age of secondary forest. Sum of time (in years) that each pixel was occupied by secondart forest since the last clearance event
ASW	Available soil water
avDBH	Average diameter at breast height. Measured in cm
AVHRR	Advanced Very High Resolution Radiometer
BA	Basal area m^2 ha^{-1}
BACCO	Bayesian Analysis of Computer Code Outputs
BDFFP	Biological Dynamics of Forest Fragments Project
BDMEP	Banco de Dados Meteorológicos para Ensino e Pesquisa
BGB	Below ground biomass
BIOMASS	P-band synethic aperture radar
BLA	Brazilian Legal Amazon

Continued on next page

Table 1 – *Continued from previous page*

Abbreviation	**Definition**
CARLUC	CARbon and Land-Use Change. Process based forest growth model.
CBD	Convention on Biological Diversity
CDM	Clean Development Mechanism
CUs	Conservation units
CV	Coefficient of variation
DBH	Diameter at breast height is measured at 1.3 m above the ground in cm.
DGSM	Derivative-based Global Sensitivity Measure
DGVM	Dynamic Global Vegetation Models
DMF	Dry mass fraction (dry mass/fresh mass)
EC	European Commission
ENSO	El Niño Southern Oscillation
ENVI	Environment for Visualizing Images
Envisat ASAR	Advanced Synthetic Aperture Radar
EO	Earth Observation
ESA	European Space Agency
FAO	Food and Agriculture Organisation
FAST	Fourier amplitude sensitivity analysis
fASW	Fraction of available soil water
FC	Frequency of clearance. Sum of frequency of transitions from forest to non-forest
FCPF	Forest Carbon Partnership Facility
FLEGT	Forest Law Enforcement, Governance and Trade
FORMIND	Individual based forest gap model.
FORMIX	Individual-based mixed rainforest growth simulator
GCC	Global carbon cycle
GHG	Green house gases
GLAS	Geoscience Laser Altimeter System
GloPEM	Global Production Efficiency Model

Continued on next page

Table 1 – *Continued from previous page*

Abbreviation	**Definition**
GPP	Gross primary productivity
H	Tree height. Measured in m
HPC	High-performance computing
HRV	High resolution visible
ICESat	Ice, Cloud and Land Elevation Satellite
IDL	Interactive Data Language
INPA	Instituto Nacional de Pesquisas da Amaznia. National Institute of Amazonian Research
INPE	Instituto Nacional De Pesquisas Espaciais. National Institute for Space Research
IPCC	Intergovernmental Panel on Climate Change
iStocking	initial stocking of trees
iWF	initial foliage weight
iWR	initial root weight
iWS	initial stem weight
JABOWA	Forest growth model named after the initials of its authors.
JERS-1	Japanese Earth Resources Satellite -1
LAI	Leaf area index
Landsat ETM+	Landsat Enhanced Thematic Mapper Plus
Landsat MSS	Landsat Multispectral Scanner System
Landsat TM	Landsat Thematic Mapper
LiDAR	Light detection and ranging
LOOCV	Leave one out cross validation
LUE	Light use efficiency g_{DM} MJ^{-1}
LULCC	Land use and land cover change
MCT	Brazilian Ministry of Science and Technology
MF	Mature forest
MMA	Brazilian Ministry of the Environment
MODIS	Moderate-resolution imaging spectroradiometer

Continued on next page

Table 1 – *Continued from previous page*

Abbreviation	**Definition**
MRV	Measuring, reporting and verifying
NAPAs	National adaptation programme of actions
NASA	National Aeronautics and Space Administration
NDVI	Normalized Difference Vegetation Index
NDWI	Normalized Difference Water Index
NERC	Natural Environment Research Council
NF	Non-forest
NIR	Near infrared
NOAA	National Oceanic and Atmospheric Administration
NPP	Net primary productivity
OAT	One factor-at-a-time
PALU	Period of active land use. Difference (in years) between the time of initial forest clearance and the onset of regeneration
PBM	Process-based model
PC	Perenial crops
POLONORDESTE	Northwest Region Integrated Development Program
Q_{int}	Intercepted radiation
REDD+	Reduced Emissions from Deforestation and Degradation
RI	Relative incidence
RMSE	Root mean squared error
RS	Remote sensing
SA	Sensitivity analysis
SAR	Synthetic Aperture Radar
Sentinel 1	European Space Agency C-band synthetic aperture radar
SF	Secondary forest. Forests regenerating largely through natural processes after total abandonment of alternative land use (plantations, agriculture, pasture, etc.) on formerly forested lands.
SI	Smithsonian Institution
SIR-C	Spaceborne Imaging Radar C-band

Continued on next page

Table 1 – *Continued from previous page*

Abbreviation	**Definition**
SI's	Sensitivity indices
SOM	Soil organic matter
SOTER	Soil and Terrain Databas
SPOT–4	Satellite Pour l'Observation de la Terre
StandVol	Stand volume m^3
StemNo	Stem density stem ha $^{-1}$
SWIR	Shortwave infrared
TC	Tree crops
TerraSAR-X	Phased array X-band synthetic aperture radar
TIGER	Terrestrial Initiative in Global Environmental Research
TOA	Top of atmosphere reflectance
UN	United Nations
UNFCCC	United Nations Framework Convention on Climate Change
USGS	United States Geological Survey
VHR	Very high resolution
VPD	Vapour pressure deficit. Difference between the amount of moisture in the air and how much moisture the air can hold when it is saturated.
WF	Foilage weight in 3-PG
WIMOVAC	Windows Intuitive Model of Vegetation response to Atmospheric and Climate Change
WR	Root weight in 3-PG
WS	Stem weight in 3-PG

Table 2: List of International System of Units used in the thesis.

Units	**Definition**
℃	Degrees Celcius
$molCmolPAR^{-1}$	Moles of carbon per moles of photosynthetically active radiation
cm	Centimetres
gcm^{-3}	Grams per centimetre cubed
GtC yr^{-1}	Giga tons of carbon per year
ha	Hectare
kg	Kilograms
kg $tree^{-1}$	Kilograms per tree
km	Kilometres
m	Metres
m s^{-1}	Meters per second
m^2 kg^{-1}	Metres squared per kilogram
$mBar^{-1}$	per millibar
Mg C ha^{-1}	Mega grams of carbon per hectare
Mg ha^{-1}	Mega grams per hectare
Mg ha^{-1} mm^{-1}	Mega grams per hectare per millimetre
Mg ha^{-1} yr^{-1}	Mega grams per hectare per year
Mha	Mega hectares
MJ m^{-2} d^{-1}	Mega joules per square meter per day
mm	millimetre
mm d^{-1}	Millimetres per day
mm hr^{-1}	Millimetres per hour
$month^{-1}$	Per month
Pg C	Peta grams of carbon
ppm	Parts per million
$year^{-1}$	Per year

Table of Contents

List of Figures

List of Tables

Chapter 1

Introduction

1.1 The importance of tropical rainforests

Approximately 85 countries contain tropical forest ecosystems covering an area of 18 million km^2 (Hartshorn, 2013). They provide an invaluable range of environmental and socio-economic services. These include high biodiversity; provision of medicines; food; fuel wood; climate regulation; CO_2 sequestration and services related to flood prevention and soil stabilisation. They also exchange more water, through evapotranspiration, and CO_2 with the atmosphere than any other biome (Foley et al., 2005).

It is extremely likely that human influence has been the dominant cause of observed warming of the atmosphere and oceans since the mid-20^{th} century (Alexander et al., 2013). The largest contribution to total radiative forcing, the difference of insolation (sunlight) absorbed by the Earth and energy radiated back to space, is caused by the increase in atmospheric concentration of CO_2 since 1750 (Alexander et al., 2013). Hence, the carbon sequestration performed by these forests, influenced by their ecosystem structure and function, constitutes a globally important environmental service. Terrestrial ecosystems have been widely recognised as playing a vital role in the global carbon cycle and biodiversity hotspots (Heimann and Reichstein, 2008). The abundance of tropical rainforests at the Earth's equator is ackwoledged as being particularly crucial in this role (Gibson et al., 2011; Pan et al., 2011). As a consequence there have been various international efforts in recent decades to reduce greenhouse gas (GHG) emissions (United Nations Framework Convention on Climate Change, UNFCCC 1992) and to preserve

biological diversity (Convention on Biological Diversity, CBD 1992). The UNFCCC has put in place investment mechanisms and market based carbon transactions in reaction to high rates of tropical land use and land cover change (LULCC) and the subsequent reduction in biodiversity and loss of the ecosystem services it supports. These measures are aimed at enhancing forest carbon stocks and the reduction of deforestation and forest degradation whilst promoting sustainable development in developing countries (UNFCCC Non-Annex 1 countries). The UNFCCC Clean Development Mechanism (CDM) initiative and post-Kyoto Protocol Reduced Emissions from Deforestation and Degradation (REDD+) program (Lederer, 2011) are two of the implemented mechanisms. The Aichi CBD set a strategic plan consisting of 20 targets to be met by 2020. Target 5 aims at reducing the rate of loss of all natural habitats, including forests, to half, and, where feasible, close to zero whilst significantly reducing degradation and fragmentation (Aichi, 2011). These targets and agreements are also a priority for the European Commission (EC) who support the REDD+ Partnership, the Forest Carbon Partnership Facility (FCPF), and the UN-REDD programme. The EC has provided financial support for REDD+ projects in Asia, Africa and Latin America through the Forest Law Enforcement, Governance and Trade (FLEGT) Action Plan (Ochieng et al., 2013).

1.2 Tropical rainforest in Amazonia

The Amazon Basin supports the largest continuous extent of tropical rainforest and associated ecosystems (mangroves, swamp forest) in the world (Table 1.1). These are currently believed to be sequestering carbon through enhanced vegetative growth associated with increased CO_2 levels in the atmosphere otherwise known as carbon fertilisation (Baker et al., 2004; Malhi et al., 2008; Affum-baffoe et al., 2009). This has, however, been recently challenged by Brienen et al. (2015) who showed increased tree mortality across forest plots in Amazonia, resulting in an overall decline in the Amazon biomass carbon sink. Historically much of the region has remained relatively unchanged except for disturbance by natural events (e.g., windblown) and subsistence agriculture. However, since the early 1970s approximately 20 % (mainly within the Brazilian Legal Amazon, BLA) has been deforested for both small scale and large scale agriculture (Ferreira et al., 2007). Deforestation is defined as the removal of tree cover

to less than 10 % (Chazdon, 2012). Most of this deforestation has occurred in the south eastern Brazilian states of Rondônia, Mato Grosso, Pará, Tocantins and Maranhão in what is often referred to as the arc of deforestation (INPE, 2013). Several states to the north and west, such as Amapa, Acre, Roraima and Amazonas, have remained relatively intact (Figure 1.1).

Table 1.1: Tropical forest cover and annual rates of change for the ten countries with the largest coverage (Hansen et al., 2010)

Rank	**Country**	**Forests (km^2)**	**Cover (%)**	**Annual change (%)**
1	Brazil	5,195,220	62	-0.42
2	Dem. Rep. Congo	1,541,350	68	-0.20
3	Indonesia	944,320	52	-0.71
4	Sudan	699,490	29	-0.08
5	India	684,340	23	0.22
6	Peru	679,920	53	-0.22
7	Colombia	604,990	55	-0.17
8	Angola	584,480	47	-0.21
9	Bolivia	571,960	53	-0.53
10	Venezuela	462,750	52	-0.61
	Subtotal top 10	11,968,820	49	-0.34

1.3 Regeneration of cleared land

Although extensive deforestation has occurred, over 21 - 30 % of the cleared land is now supporting forests at various stages of regeneration (Lucas et al., 2000; Carreiras et al., 2006b; INPE, 2011; de Almeida et al., 2016; Chazdon et al., 2016). Forest regeneration is the process of forest regrowth on land that was formerly forested (Chazdon, 2012). These areas make a considerable contribution to the carbon sink capacity of the Amazon region. Despite this, the capacity of these forests to accumulate biomass is highly dependent on climate, soil fertility; type, duration and intensity of prior land use and distance to remnant forests (Chambers et al., 2007). By understanding the contribution of different land use practices over time in conjunction with abiotic factors such as climate, the carbon sink potential for the deforested land area can be established. This is in relation to the ability of forests to accumulate biomass regardless of whether they currently support regrowth forest. Such information can provide a vital and highly valuable planning tool for restoring forests through a range of initiatives relating to sustainable land use; CBD and REDD+ (Campbell et al., 2009). In particular, target 15 of the

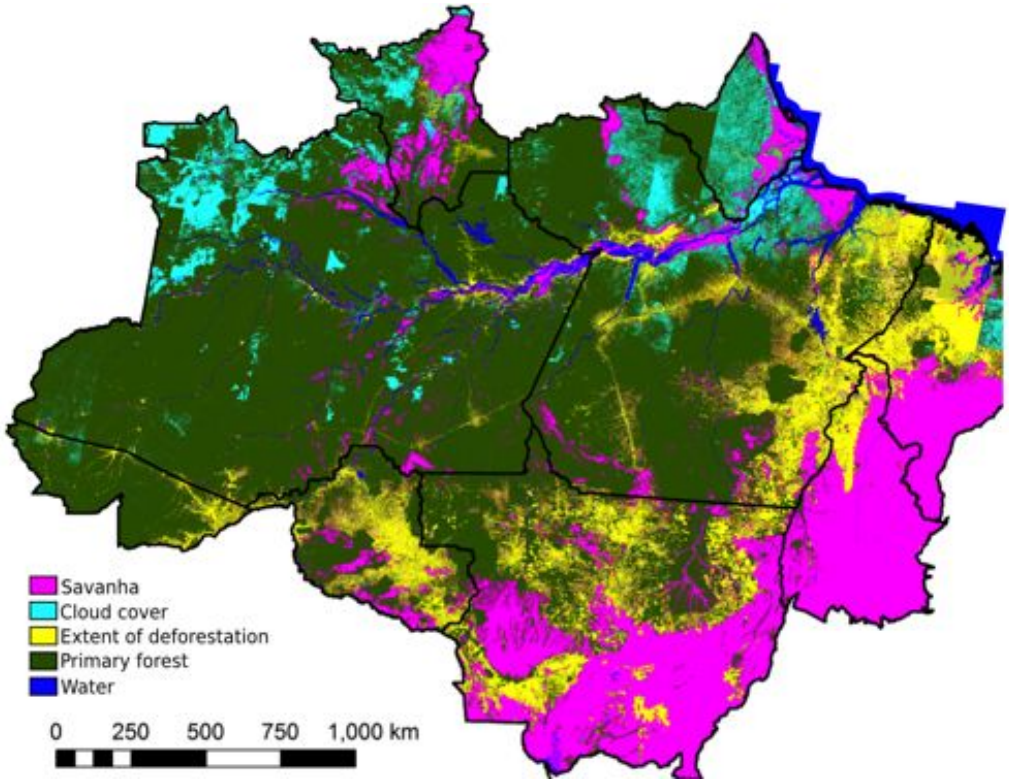

Figure 1.1: Extent of deforestation in the BLA, 2013 (INPE, 2013)

Aichi CBD aims, through conservation and restoration, to enhance ecosystem resilience and the contribution of biodiversity to carbon stocks. This includes restoration of at least 15 % of degraded ecosystems, thereby contributing to climate change mitigation and adaptation (Aichi, 2011).

1.4 Remote sensing of the Brazilian Amazon

Remote sensing (RS) provides many advantages for assessing trends in LULCC. The variety of sensors allow for multiple observations at different spatial and temporal scales, resolutions and spectral regions, offering a wealth of information on the properties of land surface targets. It is often the only practical way to repeatedly obtain data for large inaccessible regions such as the Amazonian rainforest. It provides a cost effective, repetitive method for collecting data on the Earth's surface allowing time series studies to be carried out at frequent regular intervals, on temporal scales far exceeding the duration of most research projects. This is particularly useful for studying ecosystem dynamics.

Since 1988, the history of deforestation in the BLA has been mapped annually by

Brazil's National Institute for Space Research (INPE) using wall-to-wall coverage of 30 m spatial resolution Landsat sensor data (INPE, 2013). More recently, Synthetic Aperture Radar (SAR) such as the Advanced Land Observation Satellite Phased Array type L-band Synthetic Aperture Radar (ALOS PALSAR), has allowed systematic annual and cloud free observations at L-band wavelength microwaves for the globe. Walker and Stickler (2010); Shimada et al. (2011, 2014) and Grover et al. (1999) have demonstrated the capability of SAR for monitoring deforestation. These efforts have focused on mapping the deforested area but not the areas of regrowth. A recent attempt to quantify the global extent of intact forest and forest gain is that by Hansen et al. (2013); however this work did not distinguish forest gain from plantations or that which began growing before 2000 from intact forest. This lack of distinction between forest gain present in 2000 and intact forest cannot therefore be used to monitor secondary forest regeneration before 2000.

Regrowth forests have been mapped using the same optical data that is available through the United States Geological Survey (USGS) archive free of charge. Most estimates of the extent of regenerating tropical forest are based on single-date studies (Lucas et al., 2000; Carreiras et al., 2006a; Neeff et al., 2006; INPE, 2011; de Almeida et al., 2016; Chazdon et al., 2016).Annual maps of primary rainforest; secondary or regrowth forest; non-forest (including agriculture and tree crops) can then be combined to establish the age of regenerating forests (Sant'Anna et al., 1995) and information relating to land use history such as the number of cultivation cycles (**?**). Estimating these metrics at this scale provides the opportunity to quantify the effects land use has on future recovery of the Brazilian Amazon. Hence, there is clearly a need to promote the acquisition of sufficient and appropriate RS data that is comparable over time and appropriate for use in monitoring changes in the Earth's environments. In other words, there is a continuing requirement for consistent data and classification schemes to allow comparison at a country wide scale which is only possible using Earth Observation (EO) technology (Reiche et al., 2016).

Depending on the wavelength, SAR sensors interact with different components in the forest structure. The backscatter of P-band sensors (e.g. AIRSAR) and L-band (e.g. JERS-1 and ALOS PALSAR 1 and 2) is attenuated by the tree trunks and large branches, whilst C-band sensors (e.g. Envisat ASAR, Sentinel 1 and SIR-C) and X-band sensors

(e.g. TerraSAR-X) are sensitive to the smaller components of the canopy (Le Toan et al., 1992; Fleischman et al., 1996; Imhoff, 1995). These attributes make active RS an ideal candidate for studying the spatial distribution of above ground biomass (AGB) in forests (e.g., Sarker and Nichol, 2013; Solberg et al., 2015). The ability of these sensors to measure biomass is primarily dependent on their wavelength, which in turn governs how far into the canopy they penetrate. Longer wavelengths, e.g. P-band and L-band, penetrate further (Le Toan et al., 1992; Santos et al., 2009). It has been shown that these longer wavelengths are more sensitive to changes in biomass as evidenced by an increasing backscatter range (Wang et al., 1995; Luckman et al., 1997; Lu et al., 2007). However these biomass estimations are only valid up to a threshold where saturation occurs, that is, where the slope of the biomass-backscatter coefficient curve approaches zero (Lucas et al., 2007; Mitchard et al., 2009). In tropical forests this is ≈300 Mg ha^{-1} for P-band and ≈150 Mg ha^{-1} for airbourne L-band (Saatchi et al., 2011b). This data has a resolution of 10 m making them ideal for studying small patches of SF. However, the BIOMASS spacebourne P-band sensor will have a resolution of 200 m (Le Toan et al., 2011), therefore limiting their applicability to studying small scale SF biomass. The 25 m resolution of spacebourne dual polarisation L-band sensors, e.g. ALOS PALSAR, is suitable for characterising small SF patches. However, AGB can exceed 250–300 Mg ha^{-1} in central and eastern Amazonia, depending on the allometric model in estimating the AGB from field measurements (Baker et al., 2004). Beyond the point of saturation for L-band sensors in this environment (Cutler et al., 2012).

Although young secondary tropical forests have biomass densities lower than 100 Mg ha^{-1} their fast growth means that they can accumulate >150 Mg ha^{-1} within 20 years (Brown and Lugo, 1990) exceeding that which can be detected by SAR. However the use of radar backscatter as a 'direct measure' of forest biomass is contentious (Woodhouse et al., 2012). Whilst it is agreed that radar backscatter is influenced by a variety of vegetation structural properties which vary between forest types this may, or may not, directly correlate with AGB. The only direct measure of AGB can come from destructive harvesting (Clark and Kellner, 2012). As this is impractical at the global scale, Saatchi et al. (2012) states that proper experimental design, consisting of remote sensing specific field inventory data and long wavelength (>0.7 m) SAR, such as BIOMASS (Le Toan et al., 2011), provides the only method for circumnavigating

these limitations encountered by field only studies.

One of the largest sources of uncertainty in GHG accounting rests in the spatial variation of above ground carbon stocks and stock changes in primary and secondary forests and on fallow land (Asner, 2011). This uncertainty can be reduced using information on land use intensity and age distribution of secondary forest are adequate measures from which to estimate the carbon accumulation potential (Orihuela-Belmonte et al., 2013). Whilst it is unable to directly quantify aboveground biomass, using time-series optical or SAR data, RS is well-placed to address these uncertainties at a landscape scale. Using a detailed timeseries analysis it is possible to provide estimates of the current extent along with information on land use intensity and age distribution of secondary forest (Prates-Clark et al., 2009).

1.5 Forest growth modelling in the Brazilian Amazon

Where RS alone is unable to estimate current standing AGB across a variety of forest types, forest growth modelling has been shown to be capable of estimating current standing AGB (e.g. Nightingale et al., 2008b). Modelling forest growth allows the prediction of future biomass accumulation in areas of deforestation. This attribute can also be used as a tool for assessing the impacts of future climate change and other types of disturbance (e.g. Groeneveld et al., 2009; Dislich and Huth, 2012).

Through anthropogenic climate change increased temporal and spatial climate variability has been predicted (Malhi and Wright, 2004). As temperature and precipitation are key drivers of plant growth these rapid changes in environmental conditions will have an effect on carbon cycling throughout the globes tropical rainforests and associated ecosystems (Cleveland et al., 2011; Toledo et al., 2011a). Forest growth models that incorporate these parameters allow for these effects to be quantified.

The majority of modelling attempts in Brazil have been empirically based and are only applicable to the location or vegetation type of the data from which they were developed. Empirical modelling estimates (e.g. Silva, 1989; Alder and Silva, 2012; Espírito-Santo et al., 2014) require a wealth of time series and often chronosequences of forest inventory

datasets (Chazdon et al., 2016). Where datasets are not readily available, such as for the entire BLA, process-based models have been implemented such as CARLUC (Hirsch et al., 2004; Oliveira et al., 2013) and 3-PG (White et al., 2006). Whereas empirical models are location and/or vegetation type specific process-based models such as FORMIND (Köhler and Huth, 1998), JABOWA (Botkin et al., 1972) and 3-PG (Landsberg and Waring, 1997) have been used widely for modelling the growth of mixed species forests and plantations.

The majority of applications of process based forest growth models to tropical forest have been in Asia (e.g. using the FORMIND model) with fewer studies focusing on the tropical rainforests of South America. Parameterising a process based model for mixed secondary forest allows for estimates of forest regeneration on pastoral and agricultural land which has yet to be abandoned. Estimating the potential carbon sequestration capacity of these deforested areas at a large spatial scale will prove to be a valuable output for various REDD+ activities in Brazil and the other countries mentioned in Table 1.1 experiencing deforestation and degradation of their tropical forests.

1.6 Aim and objectives

The aim of this research is to quantify the impact of land use on tropical rainforests in Brazil to recover biomass, and therefore carbon, on sites of abandoned agriculture. To achieve this aim the following objectives are addressed:

1. Estimate frequency of forest clearance and the period of active land use for areas of abandoned agriculture in the Brazilian Amazon at a local scale and their effects on above ground biomass accumulation.

2. Parameterise and validate the process based forest growth model 3-PG_2 for use in mixed secondary forest to estimate above ground biomass accumulation.

3. Determine the extent to which secondary forests contribute to the carbon budget within the BLA and reassess regional above ground biomass estimates

4. Assess the sensitivity of the process based forest growth model 3-PG_2 to changes in temperature and precipitation

1.7 Thesis Outline

This thesis is presented in eight chapters as follows.

Chapter One has provided an introduction and outlined the thesis aim and objectives.

Chapter Two provides an critical overview of tropical forest growth and successional dynamics following anthropogenic disturbances.

Chapter Three provides a description of the three study sites examined in this work; the Manaus Biological Dynamics of Forest Fragments Project (BDFFP); the area of agriculture adjacent to the Tapajós national forest and the region of intense deforestation south of Machadinho d'Oeste, Rondonia, Brazil. Information on climate, geology and soil, vegetation types and land use history of those sites is presented.

Chapter Four details the estimation of land use history through the use of remote sensing. This includes outlines of, data collection, pre-processing of remotely sensed datasets, classification methods and the time series analysis used to estimate land use history. The results are discussed in relation to land use history and land cover differences between the three study sites and the Brazilian Legal Amazon. This work was published in Carreiras et al. (2014). The PhD candidate is the second author.

Chapter Five summarises the analysis of field inventory data to obtain aboveground biomass. The results demonstrate regrowth dynamics of secondary forests more than 30 years old and the effect of varying land use history. These results are then used on model parameterisation in Chapter 6.

Chapter Six assesses the structure of the forest growth model, 3-PG_2, and the input parameters via an extensive sensitivity analysis. The chapter provides a validated parameter set with confidence intervals for predicting secondary forest biomass accumulation. The findings of Chapter Six are then used to parameterise and validate 3-PG_2 for use in secondary forests in the Brazilian Amazon.

Chapter Seven uses the parameter set defined in Chapter Six to estimate potential above ground biomass accumulation under current and future IPCC climate predictions. There is also a comparison with other published above ground biomass estimates.

Chapter Eight provides a reflective discussion on the methods and results from each chapter in relation to each other and, similar studies of the tropical secondary forest of Amazonia. Following this, conclusions are drawn from the outcomes of this study whilst highlighting potential directions for future research.

Chapter 2

Background

2.1 Tropical rainforest: an overview

The Food and Agriculture Organisation (FAO) defines a forest as "land spanning more than 0.5 ha with trees higher than 5m and a canopy cover of more than 10 percent". The tropical rainforest biome occurs between 28°north and south of the equator in of South America, Africa and South-East Asia. This biome is characterised by mean monthly temperatures >18℃ (Woodward, 2008) and mean annual rainfall >1660 mm (Newman, 2002). The dominant land cover type in this environment is a dense broadleaf evergreen forest ecosystem that is species rich and exhibits high levels of above and below ground biomass (AGB and BGB, respectively). These forests consist of a mixture of forest types including lowland, montane, flooded, peat, heath and mangrove forests. Primary forest represents the climax forest type, an environment that is considered stable but not necessarily static (Chokkalingam and De Jong, 2001), for the given region. Alongside these primary forests are secondary forests. These are forests that regenerate largely through natural process following removal or partial disturbance of the original forest vegetation (Blay, 2002). These disturbances can include tree falls, fires, lightning strikes, landslides, floods, blowdowns and anthropogenic clearing.

The Amazon rainforest of South America is located in the Amazon basin, otherwise known as Amazonia. This is defined as the area of South America drained by the Amazon River and its tributaries. It is located in of Bolivia, Brazil, Colombia, Ecuador, Guyana, Peru, Suriname and Venezuela (Goulding et al., 2003). The forest type in

this region is predominantly lowland equatorial evergreen rainforest (Corlett, 2014). The legal definition of the extent of Amazon rainforest in Brazil is the Brazilian Legal Amazon (BLA), the socio-geographic division that contains the 9 states in the Amazon basin (Laurance et al., 2001). The BLA covers an area of ≈5 million km^2 of which 65.8 % is primary rainforest, 10.6 % savannah, 19.3 % agriculture, 1.5 % water bodies and 2.8 % secondary forest (SF), as of 2000 (Carreiras et al., 2006b). Updated estimates of secondary vegetation indicate that the area of SF in the BLA is increasing with up to 4 % of the BLA occupied by SF (Hansen et al., 2013; de Almeida et al., 2016).

2.1.1 Tropical rainforest ecosystem

Tropical rainforests in Brazil are characterised by high average annual temperatures (25 ℃) and high average annual rainfall (>2000 mm). In addition to this its position at the equator affords little seasonal variation in day length and solar radiation (De Oliveira and Mori, 1999). These conditions support both high fauna, fungi and flora species diversity (Fine, 2015). These primary, or mature, forests are defined as "naturally regenerated forests of native species, where there are no clearly visible indications of human activities and the ecological processes are not significantly disturbed" (MacDicken, 2012). These forests show natural characteristics such as forest dynamics, species composition, age structure and regeneration processes.

The rainforest canopy can generally be divided into strata that develop over time, although this is not always the case (Dial et al., 2004). These layers can be grouped in three classes; emergents which reach heights of up to 55 m (Laurance et al., 2004); the canopy which is occupied by a majority of large trees; below which is the understory of palms, early stage mature forest trees, lianas and epiphytes supported by other plants; at ground level is the forest floor (Figure 2.1).

Due to their position above the canopy emergents experience an extreme range of microhabitats, from ground level to above the canopy. They are often the largest organisms in tropical rainforests and therefore play a significant role in the carbon storage of Amazonia (Nascimento and Laurance, 2002). Canopy species have high juvenile survival rates and show a large increase in growth rates when exposed to high light environments (Rüger et al., 2012). Levels of incident solar radiation above the

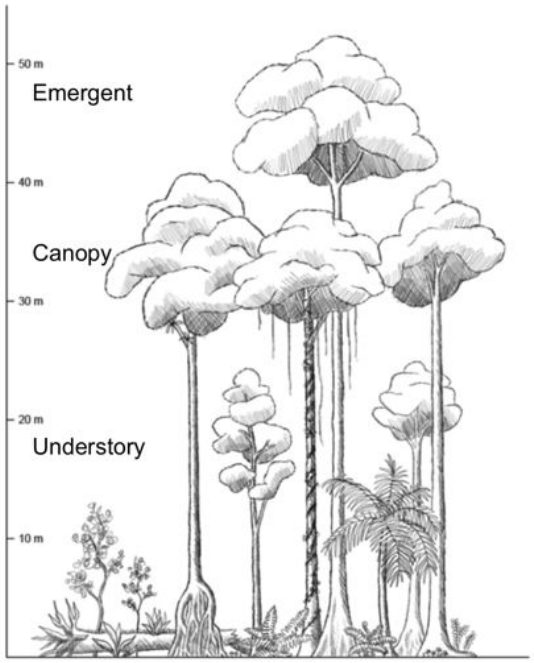

Figure 2.1: Typical rainforest canopy layer structure (`https://en.wikibooks.org/wiki/HKDSE_Geography/M6/Vegetation`)

canopy can vary by 50 % between cloud-free and over-cast months (van Schaik et al., 1993). Whilst below the canopy, there is a strong vertical control on levels of incident solar radiation where it is sometimes <1 % of that above the canopy (Niinemets, 2010). These low light levels lead to relatively slower growth rates in understory species, making them smaller in stature when at maturity with high mortality rates (Turner, 2001). Trees which develop below the canopy are shade tolerant and are able to achieve a lower rate of respiration in low light levels than leaves in direct sunlight (Valladares and Niinemets, 2008). At the forest floor fungi and other organisms play vital biological and mechanical roles in decomposing and recycling nutrients as tropical rainforest soils are typically nutrient poor (Lodge et al., 2014).

2.1.2 Secondary forest succession

Secondary succession is the process of regeneration and species turnover of, predominantly, woody vegetation on land that was formerly forested. It is a continuous process but is often initiated by disturbance of the canopy cover causing an influx of solar radiation (Chazdon, 2014). As succession progresses with increasing forest age it can be conceptualised as different successional stages (Table 2.1). Forbs, grasses and sedge species are the first to colonise pastoral and agricultural land after abandonment (Uhl et al., 1988). Following shortly behind, light demanding pioneers, e.g. *Cecropia* species, begin to establish and complete canopy closure can occur within 4 years (Lucas et al., 2002). An understory comprised of, shade tolerant, later successional, e.g. *Chrysophyllum* species, and climax species develops beneath the canopy formed by the pioneer species. The more intermediate and later successional species emerge through the pioneer canopy after 15 – 20 years (Uhl, 1987). This succesional stage eventually gives way to the climax species that will make up the mature forest. This final stage is not static as previously assumed (Richards, 1955) but rather in a dynamic state of equilibrium (Chanthorn et al., 2015). Its complex and diverse structure is maintained by frequent disturbances causing irregular mortality and recruitment of trees at small spatial and temporal scales (Brokaw, 1982; Chambers et al., 2013). Patterns of dominant processes in vegetation establishment vary at each stage of succession (Table 2.2). These patterns of succession are often visible in secondary forests in the Brazilian Amazon (Figure 2.2).

Table 2.1: Comparison of successional stages of tropical forests under several proposed classification schemes (Franklin, 2003).

Time since disturbance (years)	Budowski (1965)	Gómez-Pompa and Vázquez-Yanes (1985)	Finegan (1996)	Oliver and Larson (1990); Chazdon (2008)
0–1	Pioneer	Herbaceous phase	Herbaceous/ shrub/climber stage	Stand initiation stage
1–3		Shrub stage		
3–15	Early secondary	Pioneer tree stage	Short-lived pioneer stage	
20–50	Late secondary	Secondary tree stage	Long-lived pioneer stage	Stem exclusion stage
30–80		Mature tree stage	Recruitment of shade tolerant tree species	Understory re-initiation stage
100–200	Climax			
>200			Old-growth stage	Old-growth stage

2.2 Importance of tropical rainforests

Quantifying the global carbon cycle (GCC) is a critical element in controlling and reducing the widely acknowledged changes occurring in the Earth's climate through the increasing concentration of atmospheric CO_2, which recently exceeded 400 ppm (Jones,

Table 2.2: Processes of vegetation dynamics associated with stages of secondary succession in tropical forests (Chazdon, 2008). Successional stages based on the framework of Oliver and Larson (1990).

Stand initiation	**Stem exclusion stage**	**Understory re-initiation stage**	**Old-growth stage**
Germination of seeds in seed bank	Canopy closure	Mortality of canopy trees	Mortality of pioneer cohort in canopy
Resprouting of remnant trees	High mortality of lianas and shrubs	Formation of small canopy gaps	Range of gap sizes
Colonisation of short- and long-lived pioneer trees	Recruitment of shade-tolerant seedlings, saplings, and trees	Canopy recruitment and reproductive maturity of early-colonising species	Recruitment of shade tolerant and gap requiring canopy species and emergents
Rapid height and diameter growth of woody species	Growth suppression of shade intolerant trees in understory and subcanopy	Increased heterogeneity in understory light availability	Spatial heterogeneity in biomass and microtopography
High mortality of herbaceous species	High mortality of short-lived, pioneer trees	Seedlings and sapling establishmentof shade tolerant tree species	Large woody debris
High rates of seed predation	Dominance of long-lived pioneer trees	Tree recruitment of early-establishing shade tolerant species	Maximum diversification of trees and epiphytes
Seedling establishment of shade tolerant tree species	Development of canopy and understory tree strata Seedling establishment of shade tolerant tree species		

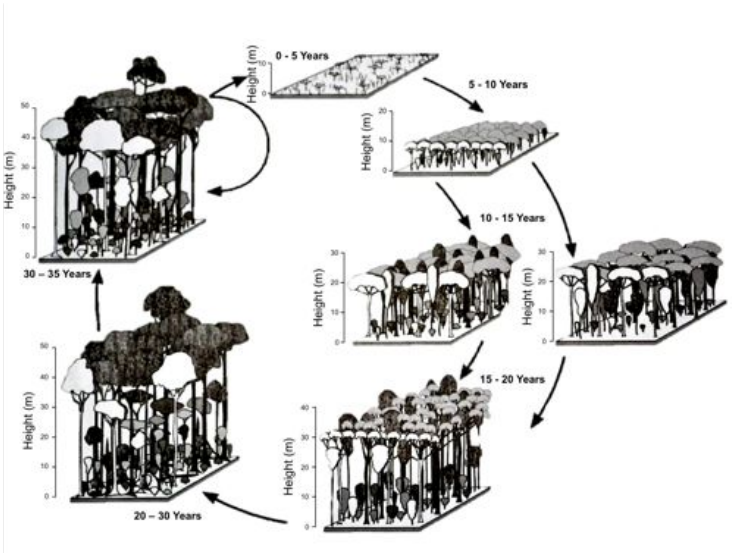

Figure 2.2: Sequence of tropical forest succession regenerating on abandoned land pasture in Amazonia (Lucas et al., 2004).

2013). Plants, primarily forests, have the largest fluxes of carbon to and from the atmosphere (Table 2.3). Alongside land use change (e.g. deforestation), these elements of the GCC are arguably one of the easiest for us to influence. Therefore, projects such as the United Nations (UN) initiative for Reducing Emissions from Deforestation and Forest Degradation (REDD+) are aiming to create conditions to minimise emissions due to land use change and disturbance. In the BLA tropical forests represent 25 % of intact forest landscapes globally (Hansen et al., 2013) and therefore play an important role in the GCC.

Table 2.3: Summarised sources and sinks of carbon globally (Quéré et al., 2015)

	Stored (GtC)	**Flux into (GtC yr^{-1})**	**Flux out from (GtC yr^{-1})**	**Diff (GtC yr^{-1})**
Crust	10×10^7	-	-	-
Ocean	10×10^7	92	90	+2
Plants	560	122	60 (atmo) 61 (soil)	+1
Soil	1500	61	60	+1
Land use	-	-	3	-1
Fossil Fuel	-	-	7	-7
Atmosphere	750	220	214	+6

These ecosystems support high levels of biodiversity, including 93,500 plant species in the tropical forests of South America alone (Primack and Corlett, 2005) and 40,000–53,000 tree species across the tropics (Slik et al., 2015). In addition to these valuable assets, tropical rainforests provide a range of ecosystem goods and services. They refer to the supply of valuable products and materials (including agricultural, forest, mineral,and pharmaceutical commodities); the support and regulation of environmental conditions (through processes like pollination, flood control, and water purification) and the provision of cultural and aesthetic benefits (including ecotourism, heritage, and sense of place) by ecosystems (Powledge, 2006).

2.2.1 Importance of regrowth forests

Globally there has been a loss of 2.3 million square kilometres of forest cover from 2000 to 2012 (Hansen et al., 2013). Whilst there has been a gain of 0.8 million square kilometres of forest cover in the form of secondary forest and plantations for the same period. In Brazil, de Almeida et al. (2016) showed that in 2012 the BLA was comprised of 4 % secondary forest primarily due to practices such as shifting agriculture. This approximates to 200,000 ha of regrowth. Assuming an average SF age of 10 years

and an average AGB accumulation rate of 6.1 Mg ha^{-1} yr^{-1} (Poorter et al., 2016) this equates to 12.2 million Mg ha^{-1} or approximately 1.9 % of the total AGB of the Amazon (≈640 million Mg ha^{-1}, Avitabile et al., 2015). If these regrowth forests attain an AGB equivalent to mature forest median of the BLA (252 Mg ha^{-1}, Avitabile et al., 2015) these forests would account for 6.3 % of the Amazon's AGB. This demonstrates secondary forests current and potential contribution to the carbon sink capacity of the BLA. In fact, forests regenerating in tree fall gaps, have already been shown to be a net carbon sink in the BLA (Espírito-Santo et al., 2014).

In some studies (e.g. Uhl et al., 1988; Mesquita et al., 2001; Wandelli and Fearnside, 2015), the capacity of these forests to accumulate biomass was found to be highly dependent on the intensity of land use prior to abandonment and they had yet to attain the same AGB as primary forests. The land use intensity is therefore crucial to understanding the successional ecology of these forests for determining their AGB accumulation potential. By determining the area and age of secondary forests, the carbon sink potential for the deforested land area can be established. This is in relation to the ability of forests to accumulate biomass regardless of whether they currently support regrowth forest. Such information can provide a vital and highly valuable planning tool for restoring forests through a range of initiatives relating to sustainable land use; Convention on Biodiversity (CBD) and REDD+ (Campbell et al., 2009). In particular, Target 15 of the Aichi CBD aims through conservation and restoration to enhance ecosystem resilience and the contribution of biodiversity to carbon stocks. This includes restoration of at least 15% of degraded ecosystems, thereby contributing to climate change mitigation and adaptation (Aichi, 2011).

The presence of early secondary forest restores soil organic matter (SOM) pools (Aweto, 1981; Lugo et al., 1986) through above and below ground (root turnover) litter inputs. This makes conditions more favourable for the species which succeed the pioneer species. In addition, forest regrowth benefits many other ecosystem processes enabling recovery of other forest parameters besides tree growth and diversity (Table 2.4).

Table 2.4: Benefits of forest regrowth to the forest ecosystem following deforestation and abandonment.

Characteristics	Source
Allow recolonisation of mycorrhizae after agriculture	Bini et al. (2013); Ewel (1986)
Restore soil organic matter (SOM)	Bini et al. (2013); Don et al. (2011); Martin et al. (2014)
Restore soil nutrient levels	Bini et al. (2013); Gehring et al. (2005b)
Biomass accumulation by tree growth can counter losses from disturbances	Espírito-Santo et al. (2014)
Facilitate persistence of forest species in human-modified landscapes	Chazdon et al. (2009)

2.3 Factors influencing forest growth and regeneration

Abandoned croplands and pastures in tropical regions give rise to rapid establishment of secondary forests, with consequent carbon accumulation and potential restoration of biodiversity. However, the age, type and composition of these forests established on abandoned lands are a consequence of several factors, such as land use history, soil fertility, and distance to mature (primary) forests (Guariguata and Ostertag, 2001). In addition, environmental factors such as topography, soil structure, seed dispersal traits and the local microclimate play an important role in determining a secondary forest's recovery towards a mature forest state.

2.3.1 Climatic controls on growth

Plant growth, through photosynthesis, requires solar radiation, water, carbon dioxide (CO_2) and nutrients. Persistently high levels of incident solar radiation at the tropics, which drive high annual air temperatures, result in highly productive ecosystems (Monteith, 1972). Water availability is an important control on plant growth in the tropics (e.g. Kapos, 1989; Metcalfe et al., 2008; Rowland et al., 2014b) and is intrinsically linked to the air temperature. Reduced water availability is often a symptom of severe droughts, climactic conditions characterised by prolonged periods of abnormally low rainfall. These conditions are becoming more frequent in the region. In 2005 air temperatures were 3–5 ℃ higher than average in south western Amazonia (Marengo et al., 2008). Whilst in 2010, 57% of Amazonia experienced lower than average rainfall in comparison to 37 % in the 2005 drought (Lewis et al., 2011). These conditions, which induced water stress in trees (Phillips et al., 2009), are predicted to increase over the 21st century in Amazonia (Williams et al., 2007; Malhi et al., 2009a). Drought conditions are exacerbated by land cover change (deforestation) through an increased latent heat flux.

This reduces precipitation and increases the amplitude of droughts in the region (Bagley et al., 2013). The effects of these droughts are furthered through positive feedbacks when coupled with forest loss, fragmentation and fire. Greater drought stress leads to increased vulnerability of forests to fires, especially at forest edges adjacent to pastures where fire is used as a management tool (Laurance and Williamson, 2001). In addition to increased fire risks, these drought conditions are responsible for heightened mortality rates in large trees and lianas post drought (Nepstad et al., 2007; Doughty et al., 2015). However, these forests are adapted to the more typical, less severe, dry seasons. Huete et al. (2006) observed a 'greening-up' of the Amazon rainforests in the dry seasons preceding recent drought as incident solar radiation levels increased.

In deforested areas forest hydrology is disrupted due to a higher albedo and decreased evapotranspiration (lower leaf area and deep root systems), water demand and canopy interception, particularly at the forest edge (Laurance et al., 2010). These microclimate alterations can lead to localised flooding in the wet season and stream failure in the dry season because of increased temporal variability (Trancoso et al., 2007). This variability can reduce successful germination and establishment of shade tolerant mature forest species such as *Tapirira mexicana* (Sugiyama and Peterson, 2013). Additional symptoms of water stress are observable in the canopy (Lee et al., 2013; Saatchi et al., 2013a,b) and result in lower ecosystem net primary productivity (NPP) (Tian et al., 1998; Nepstad et al., 2004).

It is uncertain whether forest regeneration will lessen the effects of forests edges in comparison to open pasture (Wolf et al., 2011). However afforestation is being pursued through the UNFCCC REDD+ scheme in an attempt to mitigate some of the effects of climate change and the positive feedbacks inherent in the degraded system (Ravindranath, 2007).

2.3.2 Soil Nutrient Status

Nutrients such as nitrogen (N) and phosphorus (P) are important elements for plant growth. N is important in leaf growth and photosynthesis (dos Santos et al., 2006) whilst P is used in production of biomass tissues (Mustonen et al., 2014).

Nutrient turnover, the cycling of nutrients between pools, in tropical forests is typically

high and relies upon the mycorrhiza and decomposers present in the litter layer (Kaspari et al., 2008). This counters the low nutrient content of soils typical to Amazonia e.g. Oxisols (Negreiros et al., 2009).

Nutrient limitation of tree growth has been demonstrated in the lowland tropical forests of Panama. This is evidenced in nutrient addition experiments by increased fine-litter production; significant decreases in fine-root biomass; increased basal area (BA); decreased allocation to roots and increases in stem growth rates of seedlings, saplings and pole (Wright et al., 2011; Santiago et al., 2012; Alvarez-Clare et al., 2013; Mayor et al., 2014). In addition, the highly weathered, relatively nutrient poor, soils of Amazonia have exhibited N and P limitations on NPP (Davidson et al., 2004). However in Eastern Amazonia, enhanced P and N conditions only increased the growth of grasses and forbs (Uhl, 1987), suggesting that there was no nutrient limitation of forest growth in the SF being studied.

Nutrients accumulate as leaf litter and other dead plant material are decomposed at the forest floor. In SF this occurs rapidly, as evidenced by concentrations of N and P in the soil being in excess of those found in the vegetation and leaf litter (Feldpausch et al., 2004). Concentrations similar to those found in mature forest often occurring within five years (Uhl and Jordan, 1984).

2.3.3 Seed dispersal

Seed dispersal has important implications for the demographic and genetic structure of plant populations (Hamrick et al., 1993; Dick et al., 2008). Seed dispersal mechanisms include anemochory, primarily carried out by taller trees as the shorter trees of the understory are rarely exposed to high winds (Turner, 2001); autochory is often found in pioneer species (van der Pijl, 1982); hydrochory is common in riverine species (Parolin et al., 2013) and zoochory, both endo and epizoochory. Secondary dispersal is often carried out by ants which remove seeds from faeces of frugivores (Henao-Gallego et al., 2012).

Seed source availability regulates the recovery of a diverse range of species in forests that regenerate by seed (Uhl and Clark, 1983). Impoverishment of the seed bank in the pasture soil affects species composition of the regenerating forest (Vieira et al.,

1994). This is particularly important for secondary forests growing in large disturbed areas. When seed sources are far from the damaged site, seed vectors determine the rehabilitation of species richness (Uhl et al., 1988).

Spatial constraints to seed dispersal are a critical barrier to succession (Guariguata and Ostertag, 2001). Forest fragmentation influences the movement of frugivorous bats as they prefer to forage near intact forests and not open pasture (Vulinec, 2013). Where as Silva et al. (1996) observed small (<50 g) frugivorous birds distributing small seeds in abandoned pasture. These birds often use remnant trees, within the abandoned pasture, as perches which has been shown to lead to a high number of seeds present in the micro-climate underneath the canopy of these shrubs and young trees (Nepstad et al., 1996).

2.3.4 Geometries of regenerating areas

The rate of forest recovery towards a mature forest state is often determined by the size and dimension of cleared areas. These factors determine their proximity to seed sources within mature forest. Fragmentation of forest habitat occurs when forests are cut down in a manner that leaves small, isolated patches of intact forest (Sahney et al., 2010). It is considered a major driver of biodiversity loss (e.g. ArroyoRodríguez et al., 2012; Tabarelli et al., 2012; Bregman et al., 2014) and disrupts seed dispersal and colonisation (Collingham and Huntley, 2000; De Melo et al., 2006). The size of the disturbances is important for seed dispersal however, Aide and Cavelier (1994) reported almost no dispersed seeds in pastures only 20 m away from the nearest forested patches which were 0.1 ha to 3.3 ha in size. Whilst in smaller cleared fragments, <1 ha, external seed rain compensates for 65% of fragmentation (Laurance et al., 2011).

Increased fragmentation leads to a greater area of forest edge. At this interface between the dense forest and pasture or road, edge effects can be detrimental to forest structure and growth. Edge effects include higher dessication through alteration of the forests microclimate (Kunert et al., 2015) and an increased mortality rate (Laurance et al., 1997), particularly of species intolerant of abundant light conditions whilst light demanding species and r-selected species (an emphasis on high growth rate and many offspring) are favoured (Tabarelli et al., 2012).

2.4 Anthropogenic influences on tropical rainforests

Understanding anthropogenic influences is fundamental to determining the pathway followed forest regeneration i.e. secondary forest growth and succession (Orihuela-Belmonte et al., 2013). These influences may be defined by the type of clearance and subsequent land use practices. The method by which the primary, or secondary, forest is cleared, is in part responsible for the recovery rate of the forest (Watt et al., 1997; Nortcliff, 1998). A number of methods are employed to clear forests in the BLA. Traditional 'slash and burn', in which vegetation is cleared manually before burning the cut material in situ., is practised on a small scale. Tractor and chain, involves a chain being dragged across an area to uproot the vegetation and is used to clear larger areas (>5 ha) (Alves et al., 2009). Logging is either complete removal of trees or selective removal of high value individual trees. The latter clearance method may involve heavy machinery in implementation.

These methods may be used in combination over a period of time. The intensity and frequency of anthropogenic clearing determines subsequent regrowth of the forest (Laurance et al., 2006; Barlow et al., 2012; Aragão et al., 2014). Selective logging may only occur once where as 'slash and burn' may be used repeatedly. Following clearance of the primary or secondary forest the type of land use and the intensity with which it is practised can alter the pathway of succession and AGB accumulation (Mesquita et al., 2001; Lucas et al., 2002). There are several land use practices on cleared land in the BLA.

Small-scale agricultural practices such as shifting, or swidden agriculture, account for 10 million ha of land cover in the BLA (INPE, 2011). This sustains half a million people and provides approximately 80% of the region's food production (Serráo, 1995). It is predominantly a cyclic subsistence farming method, widely used throughout the tropics. It involves cutting and burning of small patches of forest, followed by several years of crop cultivation. This is succeeded by a period of fallow during which the forest regenerates. Fallow phases between crop cycles are important for the regeneration of forest vegetation and accumulation of soil nutrient stocks (De Rouw, 1995).

Cattle grazing is a relatively modern practice in South America and the BLA (Kent, 2006). More than 80% of the rainforest that is cleared in the BLA provides pasture for cattle ranching (Nepstad et al., 2009). The Brazilian heard is still increasing from 147 million head of cattle in 1990 to ≈ 200 million in 2007 (Bowman et al., 2012). Clearing of rainforest for crops in the BLA accounted for 7% of land cover change between 1980 and 1995 (Cardille and Foley, 2003). These may include sugarcane, soybeans, maize or tree crops such as oil palm.

In addition to land use type, the duration for which a parcel of rainforest is kept clear for crops or grazing is fundamental in determining is ability to recover (Uhl, 1987). Swidden agriculture may use the same piece of land for three to seven years before being abandoned (Jakovac et al., 2015).

2.5 Forest regeneration following anthropogenic disturbances

A variety of human activities are responsible for the clearing of primary forest. Included in these are mining; plantation development; cattle ranching; commercial agriculture; subsistence farming; selective and clear-cut logging; large scale hydroelectic projects; planned and unplanned settlements and the development of supporting infrastructure (Kirby et al., 2006; Rudel et al., 2009; Barona et al., 2010; Lenzen et al., 2013; Barber et al., 2014). These disturbances encompass a variety of clearance methods and subsequent land use varying in intensity and extent. Secondary forest forms as a consequence of abandonment of these lands impacted by humans. Typically, the first 15 years of growth development in SF are characterized by rapid biomass accumulation up to 100 Mg ha^{-1} (Brown and Lugo, 1990); after 15 years forest stands may diverge in the amount of biomass accumulation. This has been related to the history of disturbance. For example, Kellman (1970) found that slightly disturbed sites had higher biomass than severely disturbed sites. Large areas of forest considered to be primary or mature may be late secondary forests generated after historic land use practices such as shifting cultivation (Richards, 1955; Budowski, 1970; Gómez-Pompa and Vazquez-Yanes, 1974).

2.5.1 Selective logging

Between 1999 and 2002 the area of land subjected to selective logging rose from 12,075 to 19,823 km^2 in the top 5 timber producing states of Brazil (Asner et al., 2005). The main disturbance associated with selective logging comes from peripheral activities e.g. access roads and the removal of timber. The practice increases fire risk and reduces leaf litter nutrient content and mean canopy height (Villela et al., 2006). Regeneration in affected areas is analogous to that which occurs in natural gaps in the canopy (Toledo et al., 2011b). However, West et al. (2014) showed that after 16 years of regrowth, areas logged using these methods had only recovered 77% of their original AGB compared to reduced impact methods which recovered 100%, similar to natural gaps.

2.5.2 Regeneration associated with shifting agriculture

Cleared land parcels rapidly lose productivity as the land is depleted of nutrients (Neill et al., 2013). In shifting agriculture the cycle is repeated, i.e. the plot is recultivated, after 1 to 12 years (Scatena et al., 1996). The fallow period allows rapid build-up of SOM (Don et al., 2011) and valuable nutrients (Szott et al., 1999). However, Sirois et al. (1998) concluded that the nutrient content of the soil decreased over an 8-year fallow period.

Growing populations have increased demand on these areas to sustain productivity. This has resulted in a less time between rotations and a reduction in productive capacity (Laurance et al., 2014; Palm et al., 2013). This causes further implications as the utilisation of marginal lands, which may not have been previously considered, increases (Laurance and Balmford, 2013). Such land often has steep slopes; poor drainage or nutrient poor soil. Regeneration on these lands will be slower than in other secondary forests (Feldpausch et al., 2004).

Nutrient limitation is a feature of Amazonian secondary forests where fire has been used to clear and manage vegetation, e.g. 'slash and burn' agriculture. Fertility is greatly reduced as soil minerals (nitrogen, sulphur, phosphorus, potassium, calcium and magnesium) are volatilised during burning (Mackensen et al., 1996; Sommer et al., 2000; Davidson et al., 2004). Much of the soil organic matter, sometimes up to 25% (Whitmore, 1990) is lost when fire is used as a clearance and management method.

In addition to nutrient loss during burning, productivity diminishes as soil acidity increases. This occurs as aluminium (Al) becomes more soluble as cations are depleted. Phosphorus (P) quickly combines with Al making the P unavailable for plant growth. Native woody species can often cope with these conditions owing to mycorrhizal associations with their root systems (De Grandcourt et al., 2004).

Studies of areas previously cleared by 'slash and burn' and cultivated under shifting agriculture have shown the effect of varying land use intensities on the AGB accumulation in SF. Zarin et al. (2005) found carbon accumulation in the BLA to be reduced by half after five burns (an intensive fire regime) compared to sites where fire hadn't been used as a clearance tool. At sites in central Amazonia which were subject to first-cycle 'slash and burn' and long-term land use, biomass accumulation was in the form of a saturation curve. This indicated rapid initial biomass accumulation followed by a slow down later in succession (Gehring et al., 2005a). Biomass accumulation was reduced by 5 - 35% at long-term use sites which had gone through a second cycle of 'slash and burn' or extended cultivation (Uhl, 1987).

Hughes et al. (1999) found that carbon pool sizes were negatively correlated with the duration of the land use prior to abandonment. Kauffman et al. (2009) found similar relationships between biomass stocks and accumulation rates with the length of cultivation period. Eaton and Lawrence (2009) noted a similar relationships with the number of cultivation cycles. Along with the age and region it significantly affected the carbon stocks in live AGB and coarse woody debris, the most dynamic and the second largest pool of carbon. Both of these carbon pools declined with the number of cultivation-fallow cycles (Eaton and Lawrence, 2009). However, Hughes et al. (2000) and Steininger (2000) found that two to four cycles of shifting cultivation in Brazil and Bolivia had no significant effect on the live biomass carbon pool.

In dry years there is often more burning (Mesquita et al., 2001) and less growth. Whilst in wet years there is less and CO_2 output to the atmosphere is lower and growth is higher. This was noted north of Manaus where SF were subject to different clearance histories as a result of wet or dry years. This led to the formation of differing species compositions or successional pathways (Lucas et al., 2002; Mesquita et al., 2001).

Effects of the previous land use were manifested in structural differences when compared

to undisturbed mature forest. At first-cycle regrowth sites 60% of the biomass was found in single stem plants whilst only 31% of the biomass present in recovering long-term use sites was constituted of single stems (Gehring et al., 2005a). Long-term land use can result in a higher biomass share of lianas; lower biomass share of palms and very high biomass share of multiple-stem plants. The latter of which can be linked to an increase in vegetative resprouting (Mesquita et al., 2001, 2015).

2.5.3 Regeneration on clear felled logging areas

Clear fell logging is predominantly carried out for timber extraction. This land use has a low frequency of clearance as the large trees can only be felled once. Following clearing the subsequent land uses can vary. The cleared land is sometimes turned into cattle pasture which can result in further clearing and weed control through burning (Uhl et al., 1988). Crops are often planted and this can involve tilling of the land by heavy machinery. Generally the regeneration following abandonment of these lands is then commensurate with the successions described below. However additional compaction through the use of heavy logging machinery may further inhibit successful regrowth (Asner et al., 2004).

2.5.4 Regeneration on cattle pasture

Cattle ranching is sometimes unprofitable owing to external market forces (Mesquita, 2000; Sirén, 2007) resulting in grazing land being abandoned after a few years. Natural vegetation re-colonises the area from any remaining seed trees (Whitmore, 1990). This regeneration is limited by soil water availability; nutrient deficiencies and denuded seed and seedling banks (Comita and Engelbrecht, 2009; Mesquita et al., 2015). 'Slash and burn' methods are often used in initial clearing the forest for cattle pasture and periodic weed control. Grazing can lead to an increase in SOM; soil carbon and pH (de Moraes et al., 1996; Neill et al., 1996). SOM is important for: soil structure and porosity which determine water infiltration rate; moisture holding capacity; diversity and biological activity of soil organisms; and plant nutrient availability (Bot and Benites, 2005). SOM is positively correlated with AGB accumulation following conversion (Laurance et al., 1999). The pH was found to be 1–2 units higher in pastures that were three to twenty years old compared to levels in primary forest (de Moraes et al., 1996). Typical pioneer

genera such as *Vismia* and *Ceiba* are adapted to a pH that is up to 2.5 units less than that found in these pastures (Menyailo et al., 2003).

Soil condition and surface drainage decreases with pasture age. This is often the result of compaction which reduces air spaces within the soil and makes it more impermeable. This reduction of aeration and oxygen diffusion decreases microbial activity and the turnover of carbon and nitrogen. Compaction can lead to increases in bulk density which in turn raises the soils resistance to root penetration (Martinez and Zinck, 2004). Soil erosion, linked to a reduction of the vegetation cover, is evident in cattle pasture leading to nutrient leaching during high rainfall (Nepstad et al., 1990, 1996). Despite these limitations BGB is recovered faster on abandoned cattle pasture than on sites subjected to shifting agriculture (Martin et al., 2014).

Some pioneer tree species, such as *Cecropia* are unable to regenerate vegetatively after cutting, e.g. grazing by cattle. Therefore it is dependant on the seed bank and dispersal from primary forest to re-establish. In contrast to *Vismia* and other resprouter species (Mesquita et al., 2001; Norden et al., 2011; Williamson et al., 2014). It could be argued therefore that this denudation of the seedling bank is be responsible for limiting species diversity in early successional stands. Secondary forests regenerating after repeated burning an mechanical clearance of tree roots before being turned into cattle pasture only accumulated 5% of that in sites that were abandoned almost immediately (Uhl et al., 1988).

Studies, such as those by Mesquita et al. (2001); Feldpausch et al. (2004, 2007); Norden et al. (2011); Williamson et al. (2014); Mesquita et al. (2015), have demonstrated that SF regenerating on cattle pasture accumulated AGB at a slower rate than forest regenerating on areas which had been clear cut or subject to ‘slash and burn’. The same was true for the recovery of other stand properties such as basal area and species diversity

2.5.5 Regeneration on croplands

It has long been a misconception that tropical rainforest soil fertility in the BLA would be sustainable for the cultivation of crops after removal of the forest. In some parts this has led to a shift towards large scale agriculture (Carvalho et al., 2002; Simon and

Garagorry, 2005; Morton et al., 2006; Buys, 2007; Barona et al., 2010). A continuous cycling of nutrients into biomass above the ground gives the impression of a productive system. Removal of the original forest cover curtails the nutrient cycle between the soil and forest canopy. These are highly weathered soils which require continuous addition of nutrients to sustain their fertility for the production of crops as soil carbon is depleted (Steiner et al., 2007). This fall in productivity leads to abandonment (Silver et al., 2000a), allowing the regeneration of natural vegetation. However, the tree species diversity and AGB in the secondary vegetation is limited by cultivation practices, e.g. SF derived from abandoned coffee plantations, were less species rich than those derived from agriculture as only those species used as shade trees prevailed (Brown and Lugo, 1990). Few other studies have focused on the regeneration of forest cover after this land use.

2.6 Remote sensing of tropical rainforests

Remote sensing of tropical rainforests is capable of providing systematic, repetitive and consistent observations on a range of forest resource information. This includes information on forest extent and change dynamics; forest type and forest biophysical and biochemical properties. The greatest spatial and temporal coverage is afforded to spacebourne optical and synthetic aperture radar (SAR) sensors such as the Landsat programme and JAXAs JERS-1, ALOS and ALOS-2 satellites. More recently, spacebourne LiDAR has made estimations of height and biomass possible at similar spatial scales (e.g. Saatchi et al., 2007). Details of studies which utilise remote sensing in tropical rainforests are shown in Table 2.5.

With the availability of long term observations, such as Landsat Multispectral Scanner System (1972) to Landsat Operational Land Imager (present) it is possible to study change over >40 years (Fickas et al., 2015; Vogelmann et al., 2016). Various change detection methods have been used in conjunction which such datasets. Bi-temporal and multi-temporal change analysis is the direct comparison of pairs of images, or multiple images, or characterizations (Coppin et al., 2004). In these methods, change is quantified through image or characterization contrast (Hansen and Loveland, 2012). These methods are prone to the multiplication of errors in each individual characterization. However

Table 2.5: Examples of studies which utilise remote sensing data to characterise tropical rainforests.

Examples	**Sensor type**	**Tropical rainforest property**
Dubayah et al. (2010); Saatchi et al. (2011a); Baccini et al. (2012)	LiDAR	Canopy height and biomass
Girardin et al. (2010); Jordan et al. (2013); Hilker et al. (2013); Cleveland et al. (2015)	Optical	Productivity
Espírito-Santo et al. (2014); DeVries et al. (2015); Moore et al. (2016)	Optical and SAR	Disturbance
Shimada et al. (2011, 2014); Hansen et al. (2013); INPE (2013); Margono et al. (2014); Stibig et al. (2014)	Optical and/or SAR	Landcover and landcover change
Englhart et al. (2011); Dinh et al. (2012); Minh et al. (2014)	SAR	Biomass
Cutler et al. (2012); Fedrigo et al. (2013); Hame et al. (2013)	SAR and Optical	Biomass
Huete et al. (2014); Saleska et al. (2016); Zhu et al. (2016)	Optical	Canopy health

these issues is can be reduced through the consideration of joint probabilities of land cover change (Caccetta et al., 2007) and the use of a continuous index as a basis for comparison (Masek et al., 2008).

It is possible to characterise forest loss through the use of all spectral inputs in the times series. The combination of optimal single date imagery, or composite imagery, from both time periods, in the same feature space was used to characterise forest cover change in European Russia, Congo and Indonesia (Broich et al., 2011; Potapov et al., 2011, 2012). Such methods often provide difficulties in labelling change classes (Hussain et al., 2013) and do not provide a complete change matrix (Jensen, 2005).

The use of spectral vectors or change indices from a reference state does not rely on the characterization of all areas in the latest image. Only those areas of change are identified by interactive thresholding (Xian et al., 2009). Each pixel value is treated as a vector and change vectors are calculated by subtracting vectors for all pixels at each date (Lambin and Strahlers, 1994). The type of change is shown by the direction of the vector and its magnitude by the vector length. This method is limited by the

requirement for all remotely sensed data to be from the same phonological period (Chen et al., 2003).

2.7 Forest growth modelling

There are several methods of modelling the growth of a forest. Yield tables and empirical models are frequently used in plantation management (Yaussy, 2000). A yield table is a tabular statement which summarizes, on a per unit area basis, all essential data relating to the development of a fully-stocked; regularly thinned; even-aged crop at periodic intervals covering the greater part of its useful life (Vanclay, 1994). Plantation managers have access to repeated measurements of variables, such as diameter at breast height (DBH) and height, from trees on permanent plots. These parameters are a result of tree growth processes that can be empirically modelled to determined future timber values. As these empirically based models can only be developed using an extensive time-series and, occasionally, chronosequence forest inventory datasets (Silva, 1989; Neeff, 2005; Neeff and dos Santos, 2005; Alder and Silva, 2012), they are only applicable to the location or vegetation type of the data from which they were developed. There are extensive networks of field plots in primary forest in the BLA e.g. RADAMBRASIL, LBA and RAINFOR (Saatchi et al., 2007; Lefsky et al., 2005; Malhi et al., 2002). Such comprehensive datasets are not available for secondary forests in the Brazilian Amazon, although a few, spatially clustered datasets, exist (e.g. Laurance et al., 2011). To overcome these knowledge gaps, process-based models (PBM) have been implemented at the regional scale e.g. CARLUC (Hirsch et al., 2004) and 3-PG (White et al., 2006). Although these models often have extensive parameter sets (>50 parameters) their base in physiological processes allows them to be applied across different forest types and climates.

A variety of models have been developed to describe forest growth in terms of the physiological and physical processes that govern CO_2 uptake by photosynthesis and losses by respiration. These models operate from the level of leaf-scale processes, e.g. the Windows Intuitive Model of Vegetation response to Atmospheric and Climate Change (WIMOVAC) (Humphries and Long, 1995), to those at the ecosystem scale, e.g. the Global Production Efficiency Model (GloPEM) (Cramer et al., 1999). These

models are adaptable and therefore applicable across different sites, often with little or no alternation (Almeida et al., 2003). However they have a tendency to oversimplify biological processes such as respiration (Gillooly et al., 2001).

These models are capable of simulating canopy processes, water usage, nutrient budgets, mortality, recruitment and dynamic biomass partitioning (Running and Coughlan, 1988; Running and Gower, 1991; Landsberg and Waring, 1997; Yaussy, 2000; Ménard et al., 2002; Almeida et al., 2007a). These attributes allow such models to be used in the estimation of the impact of future changes in climate (Prentice et al., 1993; Keane et al., 2001; Lasch et al., 2002; Fischer et al., 2014); management practices (Peng et al., 2002; Monserud, 2003; Battaglia et al., 2004); logging (Köhler, 2000); fire regimes (Scheller and Mladenoff, 2004; Hogg and Wein, 2005); and succession (Doyle, 1981; Huth et al., 1998; Köhler and Huth, 1998; Dislich and Huth, 2012).

2.8 Summary

Tropical rainforests, particularly those in the BLA, are highly productive environments. Deforestation during the second half of the twentieth century has led to the formation of a mosaic of different land uses. Abandonment of these cleared lands has allowed natural secondary vegetation to regenerate. The intensity and duration of anthropogenic influences, i.e. clearance method and subsequent land use practices, determine the rate of recovery of the forest.

Chapter 3

Study sites

3.1 The Brazilian Legal Amazon: an overview

The legal definition of the extent of Amazon rainforest in Brazil is the Brazilian Legal Amazon (BLA, upper left: 73°59'37.01"W, 5°16'18.00"N, lower right: 43°41'49.24"W, 18°7'42.75"S, Figure 3.1), the socio-geographic division that contains nine states in the Amazon basin (Laurance et al., 2001): Roraima, Amapá, Amazonas, Pará, Maranhão, Acre, Rondônia, Mato Grosso and Tocantins.

The climate of the region is characterised by consistently high air temperatures and seasonal precipitation. Air temperatures range from 20 to 31 ℃ annually across the Amazon basin, with fires often occurring during the drier months of September and October (Mesquita et al., 2001). Annual average precipitation ranges from 1200 to 3000 mm across the region. The wet season occurs between December and May with ∼70 % of the annual precipitation falling in this period.

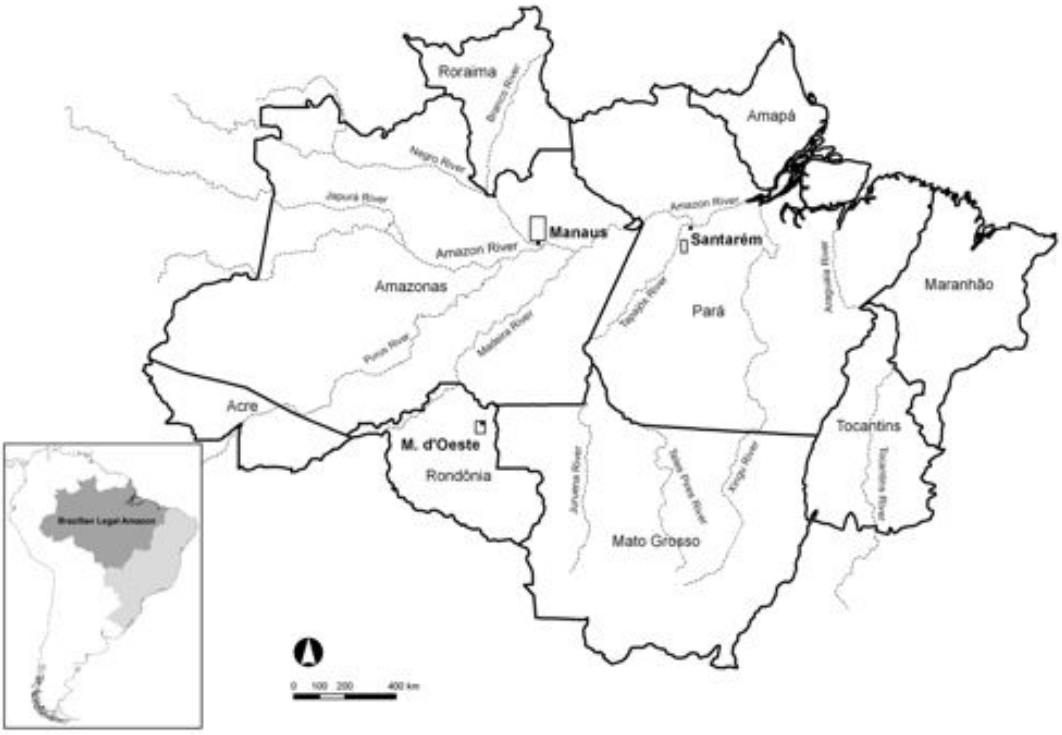

Figure 3.1: Brazilian Legal Amazon (dark grey area in bottom left insertion) in comparison to the whole of Brazil (light grey). The locations of the three study sites; Manaus, Santarém and Machadinho d'Oeste (M. d'Oeste), and major rivers within the Brazilian Legal Amazon are shown in the main figure.

Solar radiation is one of the main drivers of vegetative growth (Dong et al., 2012). Insolation, the amount of solar radiation reaching a given area, is dependant on latitude and cloud cover in the Amazon basin (Myneni et al., 2007). The equatorial latitudes of the study sites results in a similar number of daylight hours throughout the year. The lowest insolation (15.9 MJ^{-2} day^{-1}) occurs in the wetter months from December to May when cloud cover is greater. Santarém has consistently higher levels of solar radiation (from 16.3 to 22.0 MJ^{-2} day^{-1}) than Machadinho d'Oeste and Manaus. Peak solar radiation occurs in September at Manaus and Santarém whilst Machadinho d'Oeste experiences peak radiation in July (Figure 3.2).

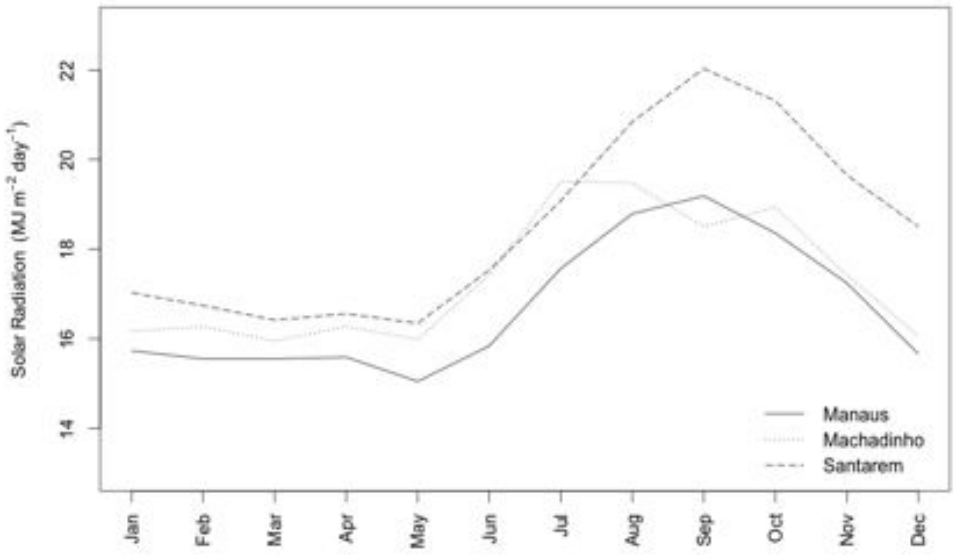

Figure 3.2: Incident global solar radiation measured at the three study sites located across the Brazilian Amazon (Stackhouse, 2015).

Geology and soils of the region determine the distribution of forest types (Feldpausch et al., 2012). The BLA is comprised of a Precambrian basement of igneous and metamorphic rocks overlain by Tertiary to Quaternary sedimentary sequences deposited by the Amazon River. The sedimentary deposits are primarily sand and clay (Negreiros et al., 2009). The erosion of these rocks has produced a diverse range of soils, predominantly of low fertility (e.g. Oxisols) (ISRIC, 2013).

The topography is predominantly controlled by the geology of the region although its evolution is due to an interplay of the regions river systems. Topography then influences forest type distribution through variations in slope and aspect. Dense lowland rainforest dominates the Amazon basin covering 65.8 % (Carreiras et al., 2006b) of the region followed by wetland forests (10.8 %) (Hess et al., 2015).

The following sections contain content from Carreiras et al. (2014) of which the PhD candidate is second author.

3.2 Manaus study area

The first study site, covers an area of 5,042 km^2 and is located to the north of Manaus, the capital city of the Amazonas state (6°5'7.33"W, 2°33'10.59"S, Figure 3.1). Within the region are two research sites set up by the Instituto Nacional de Pesquisas da

Amaznia (INPA) and the Smithsonian Institution (SI) Biological Dynamics of Forest Fragments Project (BDFFP), both established in 1979 (Laurance et al., 2011), and the forest reserves of Ducke and Egler where INPA conduct the majority of their research (INPA, 2015). Significant deforestation began in this region following construction of the BR-174 in the early 1970s which connects the capitals of Amazonas and Roraima. Most deforestation activity occurred either side of the highway and was primarily fuelled by agricultural expansion to form pasture land for grazing of cattle (Carvalho et al., 2002). The opportunity to study the impacts of clearance and forest fragmentation on biodiversity, as well as of ecosystem services, was recognised and spurred on the preservation of small fragments (typically less than 2 km^2) of primary tropical forest (Laurance et al., 2011). Many of these fragments became reconnected through rapid regrowth of forests as these clearances were abandoned from the mid 1980s onwards. The establishment of new pastures is now, rare and active pastures are a diminishing, short-lived feature of the region (Carreiras et al., 2014).

In the Manaus region the dry season falls between June and October (Laurance et al., 2011) when air temperatures reach a maximum of 33 ℃. During the dry season precipitation is 57 mm per month, increasing to 312 mm per month in the wet season (Figure 3.3a). During the rest of the year the minimum air temperature is 23 ℃. Average annual precipitation ranges from 1258 to 3157 mm (Silver et al., 2000b) and is concentrated between November and May.

Manaus is moderately flat, reaching a maximum elevation of 209 m to a minimum of 15 m. It consists primarily of nutrient poor soils (e.g. Oxisols) (Malhi and Wright, 2004) which are predominantly composed of clay and sand (ISRIC, 2013). Prior to disturbance in the 1970s vegetation was dominated by primarily dense tropical terra firme forest (Figure 3.4). The canopy of these forests averaged between 30 and 37 m in height with emergents reaching heights of up to 55 m, with the understory dominated by stemless plants (Scariot, 1999). A high diversity of tree species is found in the area, often exceeding 280 species ha^{-1} (Laurance et al., 2010; De Oliveira and Mori, 1999) and above ground biomass ranging from 180–425 Mg ha^{-1} (Laurance et al., 1999; Vieira et al., 2003).

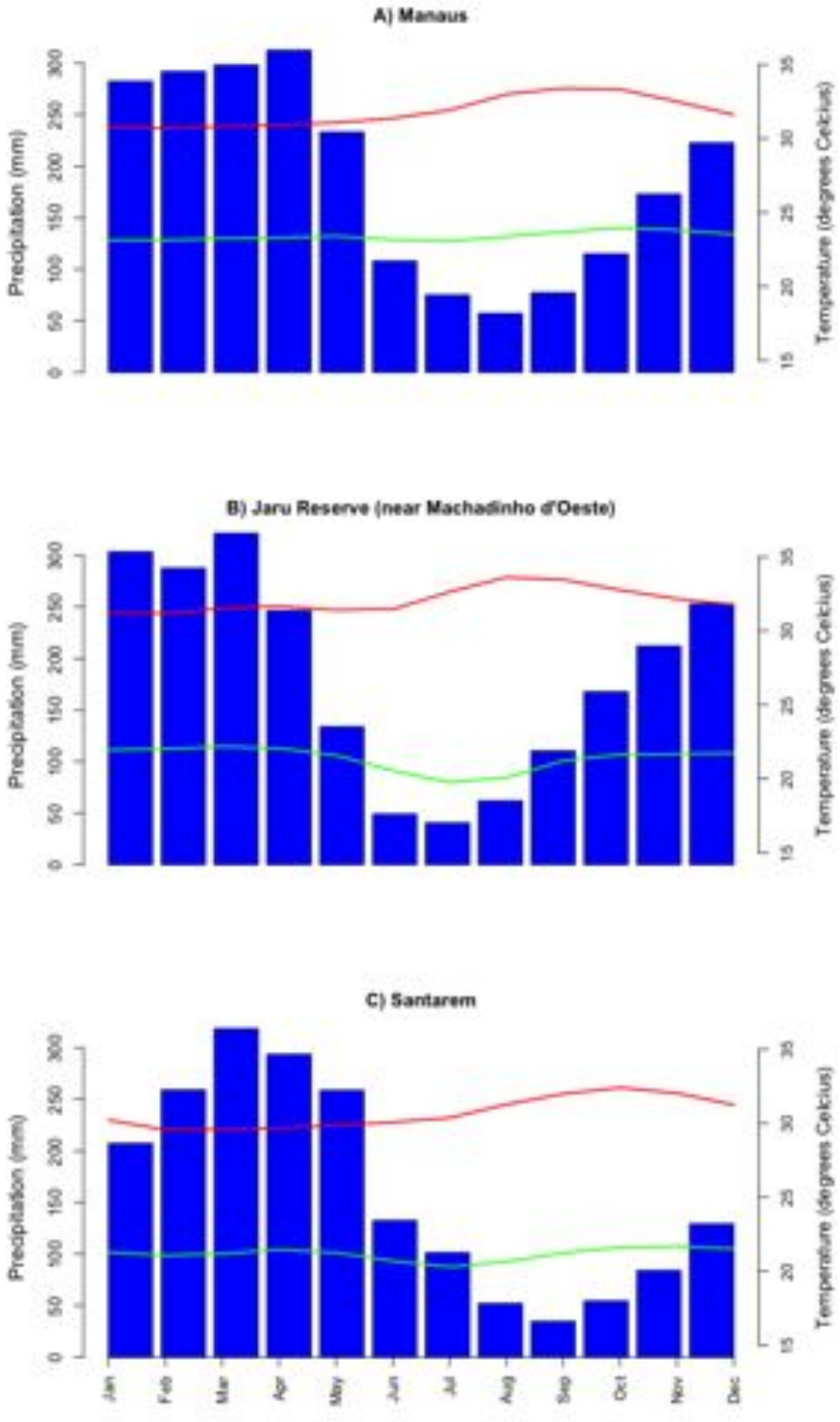

Figure 3.3: Average precipitation (blue), average maximum air temperature (red) and average minimum air temperature (green) for (a) Manaus, (b) Machadinho d'Oeste and (c) Santarém from 1974–2014 (BDMEP, 2014).

Figure 3.4: Typical dense tropical terra firme forest canopy north of Manaus.

3.3 Santarém study area

To the east of the Manaus region is the Santarém study site (54°55'42.32"W, 3°10'4.54"S, Figure 3.1) covering an area of 1118 km^2 and is located approximately 80 km to the south of Santarém, the second largest city in Pará state. The study area is within the Tapajós National Forest, between the Tapajós River and the BR-163 highway connecting Santarém to the state capital of Mato Grosso. The Tapajós National Forest conservation area was created in 1974 and is now used as a model for sustainable forest management, including logging activities (van Gardingen et al., 2006; Bacha and Rodriguez, 2007).

In the Santarém region the dry season falls between July and October (Varner et al., 2010) when air temperatures reach a maximum of 32 ℃. For the rest of the year air temperatures remains above 20 ℃. Average annual precipitation, which is concentrated between December and May, ranges from 1187 to 2057 mm (Bierregaard, 2001). During the dry season precipitation is 34 mm per month, increasing to 318 mm per month in the wet season (Figure 3.3b).

The elevation at Santarém ranges from 50–240 m. The region has similarly nutrient poor soils to the Manaus region, with soil type dominated by Ultisol and Oxisols (Keller et al., 2005; Silver et al., 2000b). Forests are less dense than in the Manaus region, with a mixture of broadleaf and palm tree species inclduing Acaí (Euterpe oleraceae) and Babau (Orbignya phalerata) (Espírito-Santo et al., 2005) (Figure 3.5). Canopy height ranges from 30 to 40 m, with emergent trees reaching 50 m. In most cases tree species

Figure 3.5: Typical forest canopy south of Santarém in the Tapajós National Forest (Sean McMahon, http://www.nature.org).

diversity exceeds 230 species per hectare (Silva et al., 1985).

3.4 Machadinho d'Oeste study area

The third site, Machadinho d'Oeste, (62°6'27.15"W, 9°32'55.73"S, Figure 3.1) covers an area of 1,780 km^2 and is located within the Machadinho d'Oeste municipality, Rondônia state. The Machadinho d'Oeste municipality was a settlement project initially set up by the Brazilian government in 1982, as part of the national development program Northwest Region Integrated Development Program (POLONORDESTE), however, rapid development and population growth lead to its autonomy in 1988 (Miranda, 2013). The majority of people in the municipality are dependent on agriculture for subsistence and less than half of the population live in urban areas (Miranda, 2013). With such dependency on the surroundings from a rural community it is not surprising that this municipality has been undergoing severe deforestation since the settlement was created in 1982.

The dry season falls between June and September in the region, during which air temperatures reach a maximum of 33 ℃. Temperatures in the region are above 19 ℃ throughout the year. Average annual precipitation is between 1057 to 3003 mm and is concentrated between October and May (Bierregaard, 2001). During the dry season precipitation is 40 mm per month, increasing to 321 mm per month in the wet season (Figure 3.3c).

Figure 3.6: Typical open ombrophylous forest south of Machadinho d'Oeste in the Jaru Biological Reserve (http://www.ecoamazonia.org.br).

Machadinho d'Oeste has an elevation of between 370 m and 90 m. The dominant soil types found in the region are Alfisols, Oxisols, Ultisols and alluvial deposits (Miranda, 2013). The predominant forest type, prior to any disturbance and regrowth of secondary forest species, was open ombrophylous forest (floresta aberta), palm trees and lianas (Departamento Nacional da Produço Mineral, 1978). Canopy heights range between 25 m and 35 m, with emergents trees reaching 45 m. Although biodiversity studies have not been undertaken in this specific area, similar field sites in the northern and central areas of Rondônia State have been found to contain approximately 220 species per hectare (Salomão and Lisboa, 1988; Brown et al., 1995).

Chapter 4

Remote Sensing of Land Cover Dynamics

This chapter was published in a scientific journal article, Carreiras et al. (2014), of which the PhD candidate is the second author.

4.1 Introduction

Humans are increasingly changing the dynamics of the Earth system, affecting processes at various scales (e.g., biosphere, hydrosphere, atmosphere). Climate change is now considered to be a reality and it would be occurring at a faster rate if several ecosystem services at the global scale were absent (Falkowski et al., 2000). For example, less than half of the total amount of carbon dioxide (CO_2) released to the atmosphere each year remains there as it is removed by the terrestrial and ocean carbon (C) sinks (Raupach, 2011). These removal processes, which are basically regulated by ecosystem structure and function, constitute important environmental services at the global scale.

The role of terrestrial ecosystems in the global C cycle and in determining biodiversity distributions have been widely recognized in the literature (e.g. Heimann and Reichstein, 2008), with particularly recognition given to the pan-tropical belt (Pan et al., 2011; Gibson et al., 2011). In the past two decades, two main international conventions have sought to establish mechanisms aimed at stabilizing greenhouse gas (GHG) concentrations in the atmosphere (the United Nations Framework Convention on Climate

Change; UNFCCC) and protecting biological diversity (Convention on Biological Diversity; CBD). Specifically, the alarmingly high rate of tropical land use and land cover change (LULCC) (Achard et al., 2002) and resulting biodiversity loss with further severe consequences for ecosystem function and structure (Hooper et al., 2012) has driven the UNFCCC to establish several investment mechanisms and market based C transactions. These are related to the enhancement of forest C stocks and the decrease of deforestation and forest degradation, while promoting sustainable development in developing countries (UNFCCC Non-Annex I countries). Such mechanisms include the UNFCCC Clean Development Mechanism (CDM) initiative and the post-Kyoto Protocol Reduced Emissions from Deforestation and Degradation (REDD+) program (e.g. Lederer, 2011). These efforts are proving successful in many regions leading to greater conservation of the intact forests of the Neotropical, Afrotropical, Australasia and Indo-Malay biogeographical regions (Olson et al., 2001). However, many of the deforested and degraded lands of the tropics are also capable of supporting forests and hence, in addition, there is potential to restore some of the ecosystem values (e.g., carbon amounts and biodiversity) lost through previous disturbances (Chazdon, 2003; Cardinale et al., 2012). This capacity depends in part, however, on the history of forest clearance and land use that has occurred and hence a clearer understanding of the potential of deforested areas to recover ecosystems is needed.

Brazils National Institute for Space Research (Instituto Nacional de Pesquisas Espaciais, INPE) has, since 1988, undertaken annual mapping of deforestation within the BLA using remote sensing data (INPE, 2013), which has been highly variable across the region. For example, an average deforestation rate of 21,050 km^2 yr^{-1} was reported between 1977 and 1988, which decreased subsequently to 11,030 km^2 yr^{-1} up to 1991; from 1991 to 2004 the deforestation rate increased to 27,772 km^2 yr^{-1} (reaching a record high of 29,059 km^2 yr^{-1} from 1994 to 1995), which followed a decrease to a record low of 4,571 km^2 yr^{-1} in 2012 (INPE, 2013). Currently, most of the deforested area is under agricultural use (following disturbance mainly with 'slash and burn' practices) but in many areas, this land has been abandoned and frequently supports forests at different stages of regeneration (Davidson et al., 2012).

Several estimates of the deforested land occupied with regeneration have been generated, mainly from interpretation of remote sensing data, but also using transition modelling.

Data from the National Oceanic and Atmospheric Administration (NOAA) Advanced Very High Resolution Radiometer (AVHRR) from 1988 – 1991 were used by Stone et al. (1994) to generate a land cover map of South America, and subsequently Schroeder and Winjum (1995) used this dataset to estimate the extent of forest regeneration in the BLA at $\sim 151 \times 10^3$ km^2. Fearnside and Guimarases (1996), using a matrix of annual transition probabilities, estimated that approximately 48% ($\sim 195 \times 103$ km^2) of the deforested landscape in 1990 supported forest regeneration. Lucas et al. (2000) using NOAA AVHRRR data estimated that $\sim 158 \times 103$ km^2 supported some type of forest regeneration in the period 1991 – 1994. Cardille and Foley (2003) used a matrix of annual transition probabilities to estimate that 36% ($\sim 91 \times 10^3$ km^2) of the area deforested between 1980 and 1995 in the entire Amazon river drainage basin was in some stage of secondary succession forest. Carreiras et al. (2006b) exploited a time-series of 12 monthly composite images of the year 2000, derived from the Satellite Pour l'Observation de la Terre (SPOT-4) VEGETATION sensor, and estimated that, in 2000, $\sim 140 \times ^3$ km^2 of land was occupied by regenerating forests. Neeff et al. (2006) used large-area land cover maps derived from remote sensing datasets to generate estimates of the distribution of regeneration within the BLA between 1978 and 2002 and concluded that regrowth increased from $\sim 29 \times 10^3$ km^2 in 1978 to $\sim 161 \times 10^3$ km^2 in 2002. Using the Landsat archive, INPE (2011) estimated that SF occupied 21% (740,000 km^2) of clear-cut areas in 2010 by identifying the current land use in previously deforested areas in the annual PRODES deforestation estimates. Whilst providing information on the extent of regenerating forests at certain points in time, the dynamics of regenerating forests and the land on which they occupy has only been attempted using remote sensing by a few studies (e.g. Lucas and Honzak, 2002). However, such information is needed across large areas as regenerating forests may represent one of the prime mechanisms by which biomass, biological diversity and ecosystem services can be restored (Fearnside, 2000; Houghton, 2005; Silva et al., 2011).

In other studies of secondary forest recovery land use history is determined from questionnaires and interviews with land owners (Mesquita et al., 2001; Uhl et al., 1988; Jakovac et al., 2015). This approach is applicable in studies where the landowner is available, as landowners do not always live near their properties. However, this approach is not an appropriate method for studies of extensive spatial extent where a

wide diversity of land use histories are present. Frequent satellite observations such as those provided by Landsat cover a large spatial extent and do not rely on the availability of landowners or managers. The aim of this chapter was to establish the extent to which the age class distribution of regenerating forests was determined by the history of deforestation and subsequent use and management of the land, thereby giving insight into the potential for forest restoration and conservation into the future. This was achieved by comparing Landsat sensor data classified into the broad amalgamated categories of mature forest, non-forest (i.e., agriculture, pasture) and secondary forest over decadal periods and time-separated by a maximum of four years.

Several measures were used to compare the three areas since the inception of widespread agricultural practices in the region (1970s for Manaus and Santarém and 1980s for Machadinho d'Oeste) up to the present. Deforestation (conversion from mature forest to non-forest or from secondary forest to non-forest) and regrowth rates (conversion from non-forest to regeneration), as well as the age of secondary forest, period of active land use prior to abandonment to regeneration, and the frequency of clearance were used to assess differences among these regions. The chapter builds on the work of Prates-Clark et al. (2009) in that the time-series was extended from 2003 to 2011 for Manaus and Santarém and a new time-series was generated for Machadinho d'Oeste.

4.2 Data

This chapter utilised existing land cover maps generated by Prates-Clark et al. (2009) and Carreiras et al. (2014) to expand the time-series spatially and temporally. Figure 4.1 highlights the original research and analysis carried out for this Ph.D, and what data from other research was utilised.

4.2.1 Existing land cover maps

4.2.1.1 Data

At Manaus, Prates-Clark et al. (2009) used Landsat Multi-spectral Scanner (MSS), Thematic Mapper (TM) and Enhanced Thematic Mapper Plus (ETM+). This data was acquired between 1973 and 2003 (path 231, row 62; Table 4.1). The Landsat MSS data acquired between 1973 and 1983 were only available as hard-copy prints. The

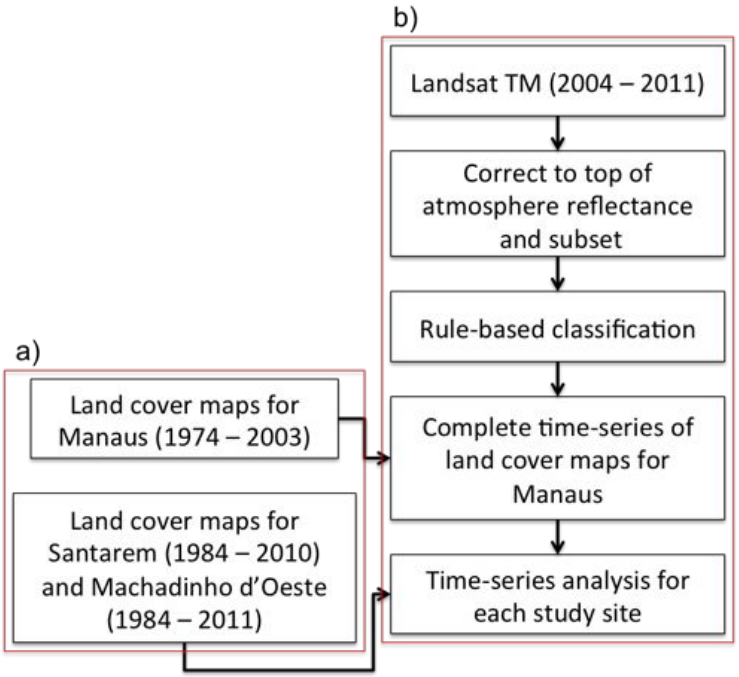

Figure 4.1: Summary of analysis undertaken for this Ph.D and research undertaken else where. a) Carreiras et al. (2014) and Prates-Clark et al. (2009) b) this Ph.D.

remaining Landsat TM and ETM+ scenes (1985 onwards) were provided in digital format from both INPE and the United States Geological Service (USGS).

For Santarém, Prates-Clark et al. (2009) used Landsat TM and ETM+ imagery acquired between 1984 and 2003 (path 227, row 62). The time-series was extended using Landsat TM data acquired for each year from 2005 to 2010. Coverage for 2011 was actively sought but no data with minimal cloud coverage was available.

The time-series classification for Machadinho d'Oeste had not been undertaken previously. 21 Landsat TM digital images, acquired between 1984 and 2011, were obtained from the USGS. At all sites, most scenes were unaffected by substantive cloud cover. Gaps in the time series ranged between one (70 %) and four years (3 %). A summary of the Landsat data used is presented in Table 4.1.

Most changes at all three study sites were associated with deforestation for agriculture and pasture. In addition at Santarém, extensive wildfires damaged the surrounding forests in 1992 and 1997. The last fire episode was associated with the 1997–1998 El Niño Southern Oscillation (ENSO) event.

4.2.2 Image pre-processing

Landsat images acquired by the USGS were orthorectified and calibrated to units of spectral radiance (W m^{-2} sr^{-1} m^{-1}) and then calibrated to top of atmosphere (TOA) reflectance using calibration factors and equations provided by Chander et al. (2009). Images acquired by INPE were processed to TOA reflectance and geometrically corrected using a third order polynomial and nearest neighbour transformation (Prates-Clark et al., 2009; Carreiras et al., 2014) in Environment for Visualizing Images (ENVI) software (Exelis Visual Information Solutions, Boulder, CO, USA). Each Landsat image was then subsetted to encompass the main area of deforestation and the intersection of all images in the time series.

4.2.2.1 Image classification

Several classification algorithms were used to generate the best possible discrimination between mature forest; non-forest and secondary forest at the three sites. At Manaus, Prates-Clark et al. (2009) used both minimum distance and maximum likelihood supervised classification algorithms (Lillesand et al., 2014) to generate the time series of three-class land cover maps for each image up to 2003. Training samples, representing the main cover types, were defined within a number of target areas identified by field observations and reference to very high resolution data.

In Santarém, the Landsat data acquired between 1984 and 2003 was classified using a fuzzy logic approach that was applied to the original Landsat bands supplemented by fractional images (shade/moisture, vegetation and soil). Each pixel of the Landsat data acquired between 2005 and 2010 was classified as one of the three main land cover classes (described above) using a machine learning classification algorithm, random forests (e.g. Hastie et al., 2009). As in the case of Manaus, regions of interest of a given class were drawn over each date when accurate expert knowledge was available to identify it as belonging to that class. The resulting training dataset was then used by the random forests algorithm to classify each pixel as MF, NF or SF (Carreiras et al., 2014).

In Machadinho d'Oeste, all Landsat TM dates were classified using the random forests algorithm, and the approach that was followed mimicked the one for Santarém between

2005 and 2010.

4.2.3 Data used in this chapter

This chapter extended the time-series for Manaus using Landsat TM data acquired for each year from 2006 to 2011. There were no cloud free images available for 2004 and 2005 (Table 4.1).

4.3 Methods

4.3.1 Image classification

Image pre-processing for data used in this chapter followed the same procedure as Prates-Clark et al. (2009) and Carreiras et al. (2014). As with the previous two studies, each digital image within the time-series for each site was classified into mature forest (MF), non-forest (NF), and secondary forest (SF), with the second including crops (herbaceous and woody) and pasture. Areas of water were also mapped and a common mask was applied to all dates in the time-series.

An object oriented classification (e.g. Johansen et al., 2007) was followed and involved a decision-rule classification applied within the eCognition software (Trimble Geospatial Imaging, Munich, Germany). The rule base method used data from the available Landsat sensor bands as well as data layers derived from spectral indices, namely the Normalized Difference Vegetation Index (NDVI) and Normalized Difference Water Index (NDWI). A schematic of the rule set used to classify images aquired for Manaus between 2006 and 2011 is shown in Figure 4.2.

The classification of MF was refined with a cloud-free mask of the MF area obtained through classification of the most-cloud-free and recent image in the time-series for each study site. Images acquired on the 31st August, 2011, 29th June, 2010 and 12th June 2011, for Manaus, Santarém and Machadinho d'Oeste respectively, were used to generate the MF mask, on the assumption that the land cover type had remained as MF for the whole of the time-series. If MF was covered by cloud in earlier images of the time-series, this was subsequently classified as MF. Table 4.2 summaries the classification technique used for each image and study site.

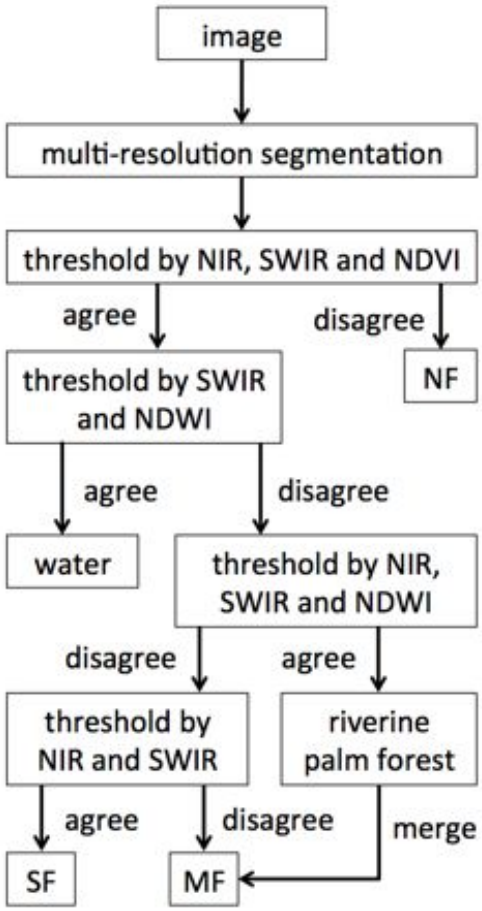

Figure 4.2: Rule structure for classifying Landsat imagery into secondary forest (SF) or nonforest (NF) back to mature forest (MF).Thresholds were derived on a scene by scene basis.

Table 4.1: Cloud free Landsat MSS, TM and ETM+ data used in the classification of the three Amazonian sites by Prates-Clark et al. (2009); Carreiras et al. (2014) and this chapter. Date format is yyyymmdd.

Manaus (Path 231, Row 62)		**Santarém (Path 227, Row 62)**		**Machadinho d'Oeste (Path 231, Row 67)**	
Date	Sensor	Date	Sensor	Date	Sensor
19730707	MSS				
19770731	MSS				
19780822	MSS				
19790703	MSS				
19830709	MSS				
		19840824	TM	19840617	TM
19850604	TM	19850726	TM		
		19860729	TM	19860810	TM
		19870716	TM	19870712	TM
19880815	TM	19880803	TM		
19890802	TM	19890822	TM	19890717	TM
		19900809	TM	19900618	TM
19910808	TM	19910711	TM	19910925	TM
19920607	TM				
		19931020	TM		
19941019	TM			19940816	TM
19950920	TM	19951010	TM	19950803	TM
19960720	TM	19960825	TM	19960704	TM
		19970727	TM	19970723	TM
		19980815	TM	19980624	TM
19990713	TM	19990903	TM	19990729	TM
		20000905	TM		
20010827	ETM+	20010916	ETM+	20010803	TM
20020830	ETM+				
20030809	TM	20030829	TM	20030724	TM
		20050701	TM	20050713	TM
20060716	TM	20060805	TM	20060716	TM
20070804	TM	20070621	TM	20070703	TM
20080806	TM	20081130	TM	20080806	TM
20090910	TM	20090712	TM	20090809	TM
20100727	TM	20100629	TM	20100625	TM
20110831	TM			20110612	TM

4.3.2 Post-classification

The comparison of the time-series of classified images (as MF, NF, or SF) identified several cases where some pixels classified as SF or NF in a given date were classified as MF in the following date. As this sequence is not plausible, in-house Interactive Data Language (IDL) code (Exelis Visual Information Solutions, Boulder, CO, USA)

Table 4.2: Three different classification schemes were implemented in the classification of the Landsat MSS, TM and ETM+ data available for the three Amazonian sites. The classification techniques are: M = maximum likelihood or minimum distance, RB = rule based, FL = fuzzy logic and RF = random forests.

Manaus		**Santarém**		**Machadinho d'Oeste**	
Date	**Classification method**	**Date**	**Classification method**	**Date**	**Classification method**
19730707	M	19840824	FL	19840617	RF
19770731	M	19850726	FL	19860810	RF
19780822	M	19860729	FL	19870712	RF
19790703	M	19870716	FL	19890717	RF
19830709	M	19880803	FL	19900618	RF
19850604	M	19890822	FL	19910925	RF
19880815	M	19900809	FL	19940816	RF
19890802	M	19910711	FL	19950803	RF
19910808	M	19931020	FL	19960704	RF
19920607	M	19951010	FL	19970723	RF
19941019	M	19960825	FL	19980624	RF
19950920	M	19970727	FL	19990729	RF
19960720	M	19980815	FL	20010803	RF
19990713	M	19990903	FL	20030724	RF
20010827	M	20000905	FL	20050713	RF
20020830	M	20010916	FL	20060716	RF
20030809	M	20030829	FL	20070703	RF
20060716	RB	20050701	RF	20080806	RF
20070804	RB	20060805	RF	20090809	RF
20080806	RB	20070621	RF	20100625	RF
20090910	RB	20081130	RF	20110612	RF
20100727	RB	20090712	RF		
20110831	RB	20100629	RF		

was written to identify these cases by comparing the classification over two consecutive dates. Where SF or NF areas were classified as such in one year and as MF in the next, the MF class was reallocated to SF. These areas were not reclassified as NF because it was assumed that spectral confusion between NF and MF was unlikely (Figure 4.3). This procedure was similar to that undertaken by Roberts (2002), who also considered disallowed transitions between cover types.

4.3.3 Deforestation and regrowth rates

Annual rates of change from MF (or SF) to NF (deforestation) and from NF to SF (regeneration) were calculated for consecutive dates in the time-series using equations 4.1 and 4.2 (Puyravaud, 2003).

$$r = \frac{1}{t_2 - t_1} \ln \frac{A_2}{A_1} \tag{4.1}$$

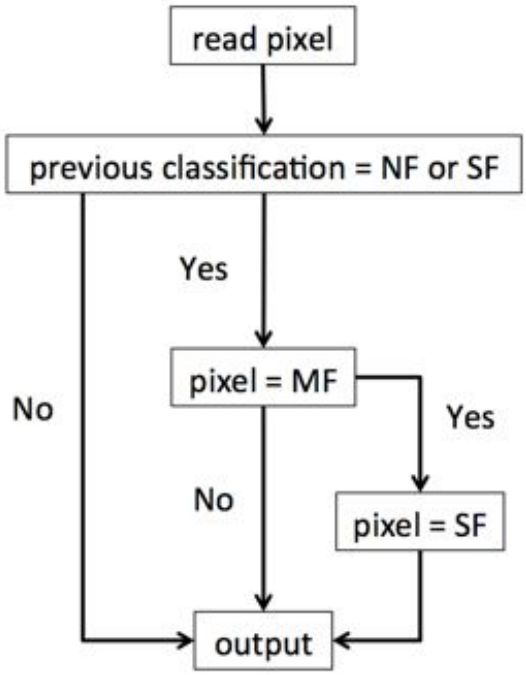

Figure 4.3: Process for correcting unlikely transitions from secondary forest (SF) or nonforest (NF) back to mature forest (MF).

$$R = \frac{A_1 - A_2}{t_2 - t_1} \tag{4.2}$$

where r and R are the annual rate of change expressed in percentage per year and hectares per year respectively; A1 and A2 are the MF (or SF, in the case of deforestation occurring in regeneration areas) or NF cover areas (ha) at time t1 and t2 respectively (time period). These rates were used to characterize the temporal evolution of change across the three sites, to detect events (primarily clearance) and describe general trends.

4.3.4 Age of secondary forest, period of active land use, and frequency of clearance

Algorithms were written and implemented in IDL to compare the classifications of MF, NF, and SF between dates. Subsequently, datasets relating to the history and dynamics of land use, namely the age of secondary forest (ASF), the period of active land use (PALU) prior to abandonment, and the frequency of clearance (FC) were generated

for each site and for each year in which an image had been acquired. The ASF was estimated by summing the time (in years) that each pixel was occupied by SF since the last clearance event. The PALU was defined as the difference (in years) between the time of initial forest clearance and the onset of regeneration. However, where reclearance of regenerating forest had occurred, the PALU was calculated by summing the period since the last reclearance event until the forest cover had re-established. The FC was estimated by summing the frequency of transitions from MF (or SF) to NF. For both the Manaus and Santarém study areas, fire scars were evident within some clearances by the lower near and shortwave infrared reflectance compared to the original vegetated surface (Pereira and Setzer, 1993). However, many burned areas acquired a vegetated cover quite rapidly (Cochrane, 1998), and so only a partial fire history could be retained.

To better spatially represent and discuss the main results, classes of ASF, PALU, and FC were generated and used to assess their temporal evolution. ASF classes were defined as initial ($\leq$5 years), intermediate (6–15 years) and advanced ($\geq$16 years). PALU classes were defined as short ($\leq$2 years), medium (3–4 years) and long ($\geq$5 years). FC classes were defined as low (1 time), medium (2 times) and high ($\geq$3 times).

4.3.5 Accuracy assessment and area calibration of the time-series of classified images

The most recent very high resolution (VHR) imagery was used to carry out the accuracy assessment of the time-series classifications at each site. As VHR data were not available to perform the accuracy assessment for all the classified images in the time-series, the accuracy in the classification of the image that was closest in time was assumed to be similar for the remaining images. To quantify the accuracy of the 2010 classification for Santarém, reference was made to 5 m SPOT-5 panchromatic data from 2009 and 2011 whilst the 2007 and 2010 classifications for Manaus and Machadinho d'Oeste respectively were validated using GeoEye imagery available on Google EarthTM.

At each site, 200 random points (greater than the minimum suggested by Congalton and Green, 1999; Lillesand et al., 2014) at the centre of polygons greater than 6 ha were generated for each class. The points on the classification were compared with the

VHR imagery from the same date. At Santarém, it was assumed that if the same land cover was present in both the 2011 and 2009 image, the land cover in 2010 would be the same. The accuracy assessment was reported as a standard error matrix, including the overall accuracy and omission and commission errors (Foody, 2009).

From the same VHR imagery and past field studies of the study sites (e.g. Prates-Clark et al., 2009; Miranda, 2013), woody agriculture crops established on the deforested areas were visible. At Manaus, a large area of oil palm was progressively planted in the north west of the site from the 1983 to 1989, whilst at Machadinho d'Oeste, perennial crops (mainly coffee plantations) were more common. To assess how well the areas of MF, NF and SF were discriminated using the classification, these areas were delineated manually from the VHR imagery and used in the generation of the error matrices.

The most straightforward way of estimating total areas for each class is to count the number of pixels in the MF, NF and SF classes with respect to the ground truth data. This is called naïve estimation in the remote sensing literature (Gallego, 2004). As a matter of fact, areal estimates obtained this way are biased (e.g. Walsh and Burk, 1993). Some post-classification methods have been used to improve these estimates, namely the so-called calibration techniques, which are divided into classical and inverse methods. The information contained in the error matrix was used to correct for misclassification bias (Walsh and Burk, 1993). Walsh and Burk (1993) carried out a simulation study and concluded that the inverse method consistently performed better than the classical method and lead to unbiased estimates for total areas. The idea behind this calibration technique was to use the misclassification probabilities among classes to revise the proportions given by pixel counting (pi) (Tenenbein, 1972). According to Tenenbein (1972) and Walsh and Burk (1993), the revised (calibrated) proportion of the total area occupied by class i (πi) can be estimated with equation (4.3):

$$\pi_i = \sum_{j=1}^{k} [f_i + n_j)/N] \, (n_{ij}/n_j) \tag{4.3}$$

where i represents the observed class, j the predicted class, k the number of classes, n the number of observations in the validation sample, N the combined number of observations in the validation and satellite datasets, f_i the (N-n) in class j, n_{ij} the

number of observations in class i that were classified as j, and n_j the sum of all training observations predicted as class j. This method was applied to calibrate the area estimates obtained from each date of classified images using the error matrices that were produced for the three sites.

4.4 Results

4.4.1 Accuracy assessment of land cover classification

The error matrices resulting from the accuracy assessment over Manaus, Santarém, and Machadinho d'Oeste are presented in Table 4.3, 4.4 and 4.5 respectively. For all three sites the overall accuracy was high (above 0.90), although some relatively high omission and commission errors were identified, especially in Santarém and Machadinho d'Oeste. For Manaus, the omission and commission errors were always below 10 %. For Santarém, a higher omission error in the SF class was detected (17.0 %), mainly due to misclassification as MF (11.5 %), which reflects also in the high commission error in the MF class (10.5%); At Machadinho d'Oeste, a major source of error also comes from a high omission error in the SF class (28%), with this mainly being a consequence of misclassification as NF (18.5 %) and to a lesser extent as MF (9.5%); a high commission error was also observed in the NF class (15.8%), with this being due to due to misclassification with SF.

Table 4.3: Error matrix obtained from the accuracy assessment of the 2007 land cover map of the Manaus site (MF mature forest, NF non-forest, SF secondary forest). The overall accuracy was 0.93.

	Classified				
Reference	**MF**	**NF**	**SF**	**Total**	**Omission error**
MF	186	4	10	200	0.070
NF	8	185	7	200	0.075
SF	11	2	187	200	0.065
Total	205	191	204	600	
Commission error	0.093	0.031	0.083		

In Manaus, tree crops (TC, 4,774 ha) was mostly incorrectly classified as SF (89%), illustrating the similarity in their spectral signatures, but accounted only for 4.4% of the SF area in 2007 (Table 4.6). However, most of the TC classified as SF in Manaus was associated with the oil palm plantation situated in the north west of the study site.

Table 4.4: Error matrix obtained from the accuracy assessment of the 2010 land cover map of the Santarém site (MF mature forest, NF non-forest, SF secondary forest). The overall accuracy was 0.93.

	Classified				
Reference	**MF**	**NF**	**SF**	**Total**	**Omission error**
MF	196	0	4	200	0.020
NF	0	198	2	200	0.010
SF	23	11	166	200	0.170
Total	219	209	172	600	
Commission error	**0.105**	**0.053**	**0.035**		

Table 4.5: Error matrix obtained from the accuracy assessment of the 2010 land cover map of the Machadinho dOeste site (MF mature forest, NF non-forest, SF secondary forest). The overall accuracy was 0.90.

	Classified				
Reference	**MF**	**NF**	**SF**	**Total**	**Omission error**
MF	200	0	0	200	0.000
NF	0	197	3	200	0.015
SF	19	37	144	200	0.280
Total	219	234	147	600	
Commission error	0.087	0.158	0.020		

The majority of TC in Machadinho d'Oeste was correctly classified as NF, although the overall area was very small (17 ha). Conversely, 70% of the perenially crops (PC, mainly coffee plantations) at Machadinho d'Oeste was misclassified as SF, although this only accounted for 2.1% the entire SF area in 2010. No woody crops were found in Santarém, only annual crops which were correctly classified as NF.

Table 4.6: Area (ha) and relative incidence (RI, %) of perennial (PC) and tree (TC) crops with the mapped area of mature forest (MF), non-forest (NF) and secondary forest (SF). Estimates were based on the land cover map closest to the date that was used to delineate crop types using very high resolution (VHR) imagery. There were no perenial or tree crops visible at Santarem at the time of publication.

	Manaus (2007)		**Machadinho d'Oeste** (2010)			
	TC		PC		TC	
Classified	Area (ha)	RI (%)	Area (ha)	RI (%)	Area (ha)	RI (%)
MF	139	0.0	31	0.1	0	0.0
NF	398	1.0	540	0.9	14	0.0
SF	4,237	4.4	1,323	2.1	3	0.0
Total	4,774		1,894		18	

4.4.2 Land cover change

North of Manaus, the percentage of MF decreased from 91% in 1973 to 72% in 2011. NF (4% in 1973) increased to 9% in 2011 whilst SF, which occupied an area of 5% in 1973, constituted 19% of the area in 2011 (Figure 4.4A). At the time of the first Landsat observation of the area south of Santarém (1984), MF occupied 79% of the area with the remainder composed of NF (2%) and SF (19%) (Figure 4.4B). By 2010, only 46% of MF was remaining and the extent of NF and SF had increased to 10% and 44%, respectively. For Machadinho d'Oeste, extensive loss (∼60%) of MF occurred between 1984 and 2011, from 91% to 32%. The percentage area of NF increased from 1% to 33% over the same period, suggesting that large areas of deforestation were actively sought for agriculture and/or pasture. SF caused by prior clearance of primary forests was around 9% in 1984 and increased to 36% of the total area in 2011 (Figure 4.4C).

For all sites, there was a strong correspondence between the land cover percentage and time for the MF class, with the rate of MF change as a function of the year decreasing by an average of 0.54% in Manaus to 1.39% in Santarém and 2.33% in Machadinho d'Oeste. At Santarém (Figure 4.4B), the abrupt decrease in the MF extent between 1997 and 1998 and the associated increase in NF were attributed to the large-area wildfire in 1997. As this area was then left to regenerate, a rapid increase in the SF extent was observed between 1999 and 2000 with a corresponding decrease in the NF proportion. For all sites, a corresponding increase in the area deforested occurred, with the land cover alternating between NF and SF in all cases. The change rate in the NF class increased from 0.09% (Manaus) and 0.38% (Santarém) to 1.29% (Machadinho d'Oeste) whilst the SF change rate progressively increased from Manaus (0.45%) to Santarém (1.02%) and Machadinho d'Oeste (1.04%).

4.4.3 Deforestation and regrowth rates

A summary of deforestation and regeneration rates is given in Table 4.7. The highest annual rate of deforestation of MF was observed at Santarém, with a 15.6% yr^{-1} loss between 1997 and 1998, with this associated with extensive wildfires in 1997. The largest single set of deforestation events occurred in Manaus, with 2.9% yr^{-1} (13,451 ha) cleared between 1983 and 1985. The highest average annual rate of deforestation of

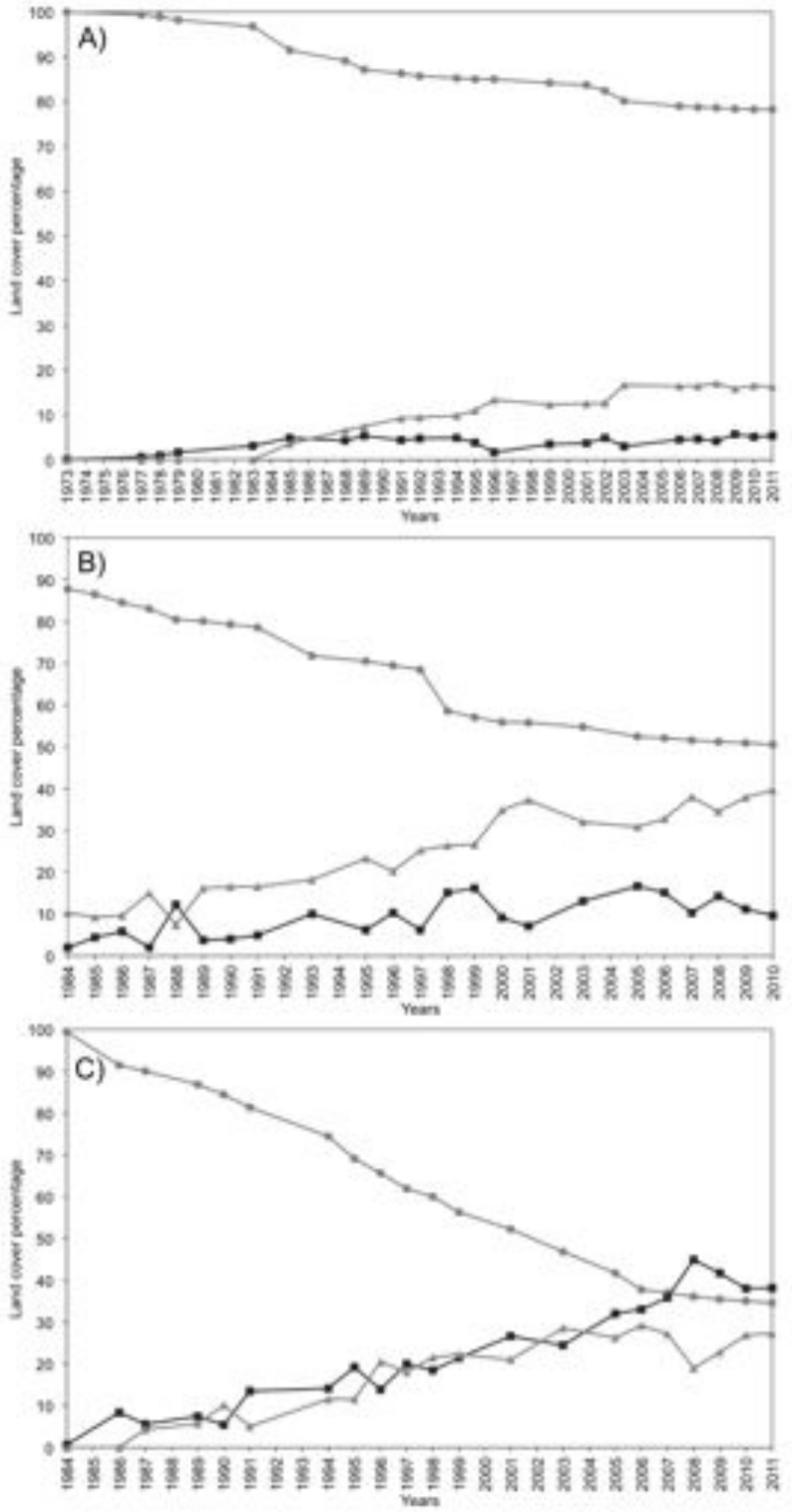

Figure 4.4: Land cover change (%) across the three selected sites; A) Manaus (1973–2011), B) Santarém (1984–2010), and C) Machadinho d'Oeste (1984–2011). Each dashed line represent the linear fit of the proportion of each land cover class as a function of the year; also showing are the corresponding equations and coefficient of determination (r^2).(◯ - mature forest, □ - non-forest, △ - secondary forest).

MF was in Machadinho d'Oeste (3.9% yr^{-1}), with an average of 4,142 ha yr^{-1} cleared. The highest maximum rates of SF clearance were in Machadinho d'Oeste (88.1% yr^{-1}, 1990-1991) and Santarém (82.3% yr^{-1}, 1987-1988), with average rates being 19.5% and 16.7% for these sites respectively. The largest area of SF cleared at each site in a single year was 16,711 ha (Machadinho d'Oeste; 2007-2008), 11,352 ha (Santarém; 1998-1999) and 8,453 ha (Manaus, 2008-2009). The highest rates of regeneration were observed at Santarém, averaging 78.5% yr^{-1} with the maximum absolute regrowth expansion following the 1997 wildfires occurring between 1998 and 1999 (11,726 ha yr^{-1}) and 1999 and 2000 (12,257 ha yr^{-1}). The highest absolute rates of regrowth occurred at Manaus, with a maximum of 24,738 ha between 2002 and 2003. The lowest rates of regrowth were at Machadinho d'Oeste, with these averaging 25.82% yr^{-1}. The highest overall deforestation rates (for both MF and SF) were greatest for Machadinho d'Oeste (7.2% yr^{-1}), followed by Santarém (4.9% yr^{-1}) and Manaus (1.4% yr^{-1}). Where high mean deforestation rates were coupled with a high standard deviation, significant events (e.g., fires, deforestation) or processes (regeneration) were indicated. On average, however, deforestation rates of SF were higher than those of MF, indicating reclearance at all sites and particularly Machadinho d'Oeste (averaging 19.5% yr^{-1}) and Santarém (averaging 16.7% yr^{-1}).

Absolute areas (annual or based on periods of observation) are useful when comparing deforestation and regeneration rates between sites and the processes of change. Several key indicators are then listed in Table 4.8 together with the dates for each site to which these apply. For all sites, a trend from indicators a) to f) was observed with the majority being cleared initially, regenerating forests progressively establishing with these then recleared to varying degrees, and, of these, several are then abandoned to regrowth again.

Table 4.7: Summary of deforestation and regrowth rates between consecutive dates in the Manaus, Santarém and Machdinho d'Oeste time-series (MF mature forest; SF secondary forest). Detailed deforestation and regeneration rates between consecutive dates for Manaus, Santarém and Machadinho d'Oeste are presented in the Appendix (Tables A.1, A.2, A.3)

		MF annual rate of deforestation		**SF annual rate of deforestation**		**Annual rate of deforestation**		**Annual rate of regrowth**	
		(% yr^{-1})	**(ha yr^{-1})**	**(% yr^{-1})**	**(ha yr^{-1})**	**(% yr^{-1})**	**(ha yr^{-1})**	**(% yr^{-1})**	**(ha yr^{-1})**
Manaus	Minimum	0.1	277	0.0	0	0.1	691	0.0	0
	Maximum	2.9	13,451	27.7	8,453	3.8	17,936	133.9	24,738
	Mean	0.7	3,123	6.4	3,231	1.4	6,355	34.1	6,017
	Standard deviation	0.9	3,726	6.5	2,699	1.1	4,905	33.7	5,756
Santarém	Minimum	0.4	235	0.5	194	0.5	448	10.5	832
	Maximum	15.6	11,046	82.3	11,352	17.7	16,952	261.5	12,257
	Mean	2.1	1,598	16.7	3,189	4.9	4,787	78.5	4,675
	Standard deviation	3.2	2,292	18.7	2,849	4.4	4,188	61.5	3,332
Machadinho	Minimum	1.2	748	0.0	17	1.5	2,386	3.7	103
	Maximum	10	9,223	88.1	16,711	17.7	18,202	84.2	17,389
	Mean	3.9	4,142	19.5	5,289	7.2	9,286	25.8	6,804
	Standard deviation	2.3	2,394	19.5	4,467	4.4	5,248	21.5	4,141

Table 4.8: An assessment of the dynamics of land use at Manaus, Santarém and Machadinho d'Oeste (figures in brackets represent the number of years).

Indicators	**Impact**	**Manaus**	**Santarém**	**Machadinho d'Oeste**
a) Clearance of MF only with little or no deforestation over SF	High pressure for new land	1973–1985 (12)	Pre-1984	1984–1987 (3)
		1985–1989 (4)	1986–1987 (1)	1987–1990 (3)
		2002-2003 (1)	1991–1993 (2)	1991–1996 (5)
b) Area of MF cleared >SF cleared.	Pressure for new land with some contained re-use of the existing deforested area (through reclearance)		1997–1998 (1)	1997–1998 (1)
			2006–2007 (1)	2001–2003 (2)
			2008–2009 (1)	
		1989–2002 (13)	1984–1986 (2)	1990–1991 (1)
		2003–2011 (11)	1987–1991 (4)	1996–1997 (1)
			1993–1997 (4)	1998–2001 (3)
c) Area of MF cleared <SF cleared			1998–2006 (8)	2003–2011 (8)
			2007–2008 (1)	
			2009–2010 (1)	
	Greater re-use of existing deforested land but still requirement for more land	1973–1985 (12)	1984–1986 (2)	1984–1986 (2)
		1988–1989 (1)	1987–1988 (1)	1987–1989 (2)
		1991–1994 (3)	1989–1993 (4)	1990–1995 (5)
d) Area of MF and SF cleared >area of SF regenerating		1996–2002 (6)	1995–1996 (1)	1996–1997 (1)
		2003–2007 (4)	1997–1999 (2)	1998–2001 (3)
		2008–2009 (1)	2001–2005 (4)	2003–2008 (5)
		2010–2011 (1)	2007–2008 (1)	2010–2011 (1)
e) Reclearance of SF but no clearance of MF	Contained re-use of area already deforested	No years	No years	No years
		1985–1988 (3)	1986–1987 (1)	1986–1987 (1)
		1989–1991 (2)	1988–1989 (1)	1989–1990 (1)
		1994–1996 (2)	1993–1995 (2)	1995–1996 (1)
f) Area of SF regeneration >MF and SF deforestation	Net abandonment of land to regenerating forests	2002–2003 (1)	1996–1997 (1)	1997–1998 (1)
		2007–2008 (1)	1999–2001 (2)	2001–2003 (2)
		2009–2010 (1)	2005–2007 (2)	2008–2010 (2)
			2008–2010 (2)	

4.4.4 Age of secondary forest (ASF), period of active land use (PALU), and frequency of clearance (FC)

Maps of the ASF, PALU, and FC for the last date of the time-series are presented in Figures 4.5, 4.6 and 4.7 for Manaus (2011), Santarém (2010) and Machadinho d'Oeste (2011) respectively and the proportion of areas with respect to these classes is indicated in Figure 4.8. At Manaus, regrowth forests were comparatively older, with 50% occupied by forests $\geq$ 16 years; 37% were between 6–15 years and 13% were $\leq$ 5 years (Figure 4.8A). At Santarém, 57% of forests were aged 6–15 years, with 28% being $\leq$ 5 years and 15% being $\geq$ 16 years. At Machadinho d'Oeste, the area occupied by SF aged $\leq$ 5 years, 6–15 years and $\geq$ 16 years was 46%, 41% and 13% respectively. Hence, the three sites contain different distributions of age classes, with this attributable to differences in the time since deforestation but also the PALU and the frequency of clearance events.

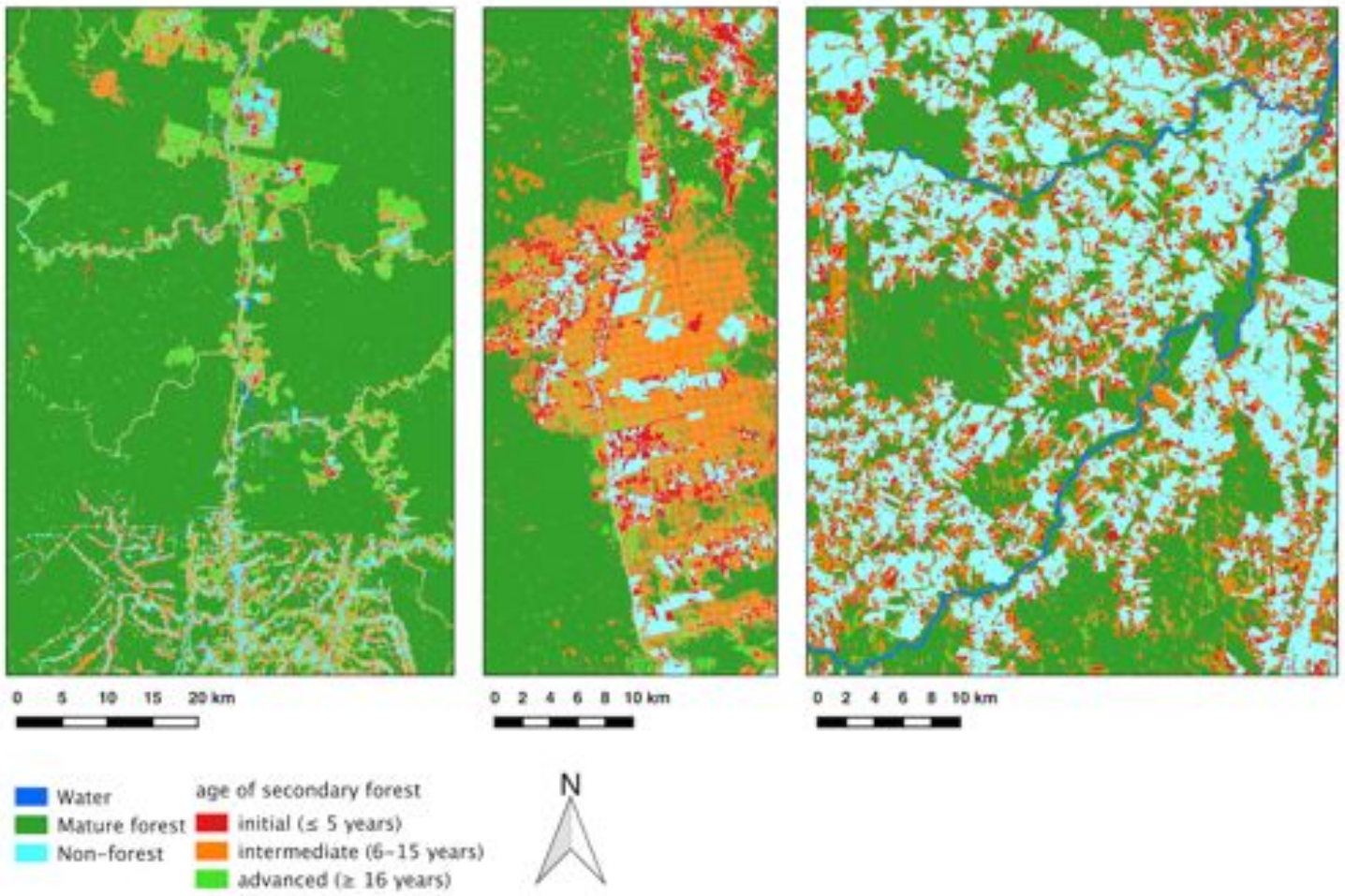

Figure 4.5: Maps displaying the age of secondary forest (ASF) across the three selected sites for areas undergoing secondary forest (SF) in the last year of the corresponding time-series; A) Manaus (2011), B) Santarém (2010), and C) Machadinho dOeste (2011).

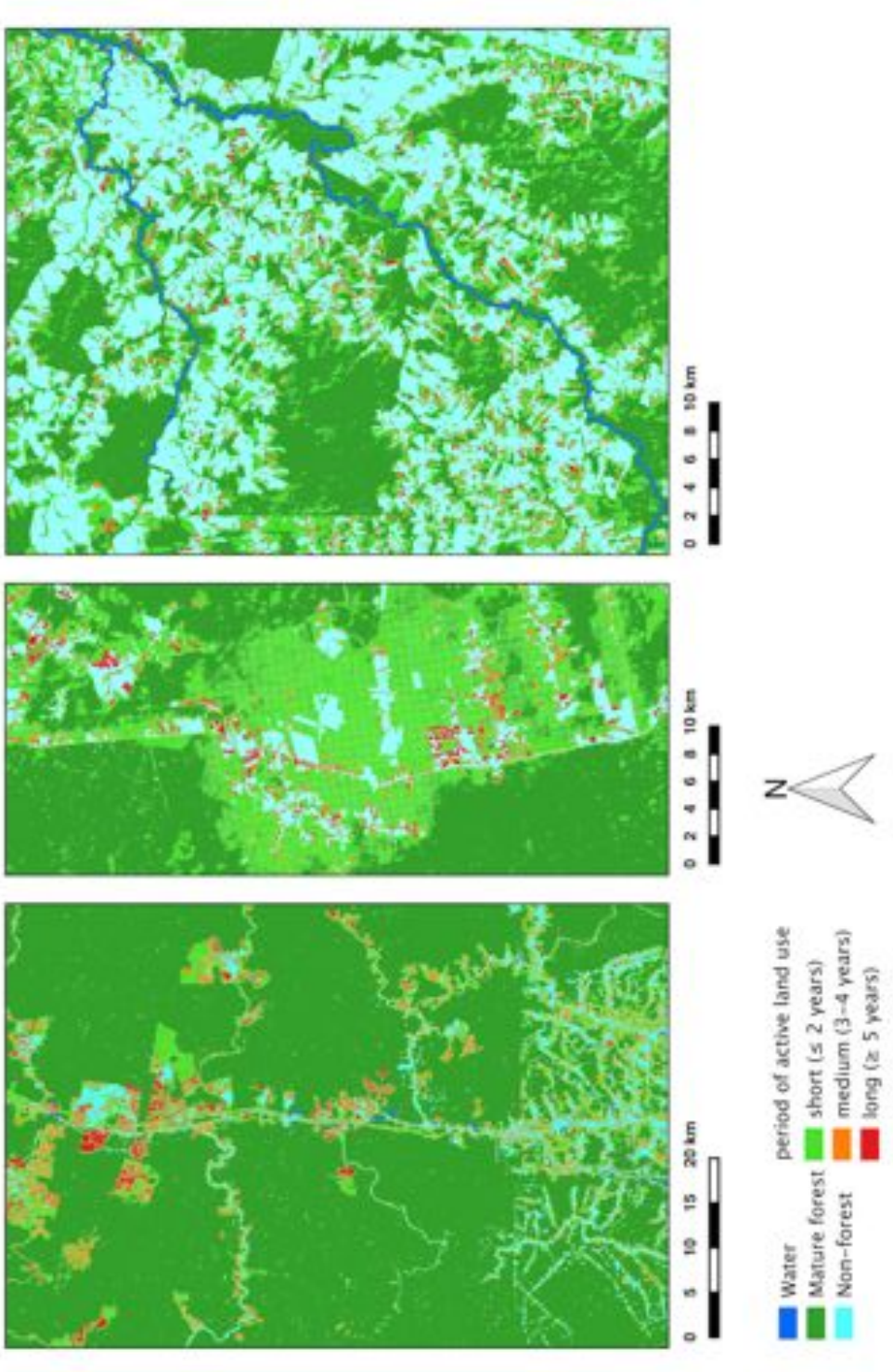

Figure 4.6: Maps displaying the period of active land use (PALU, years) across the three selected sites for areas undergoing secondary forest (SF) in the last year of the corresponding time- series; A) Manaus (2011), B) Santarém (2010), and C) Machadinho d'Oeste (2011). An area of 667 ha (1.5%) with a PALU of zero in the Santarém site was included in the short PALU class ($\leq$ 2 years) and corresponds to areas that were SF from 1984 to 2010.

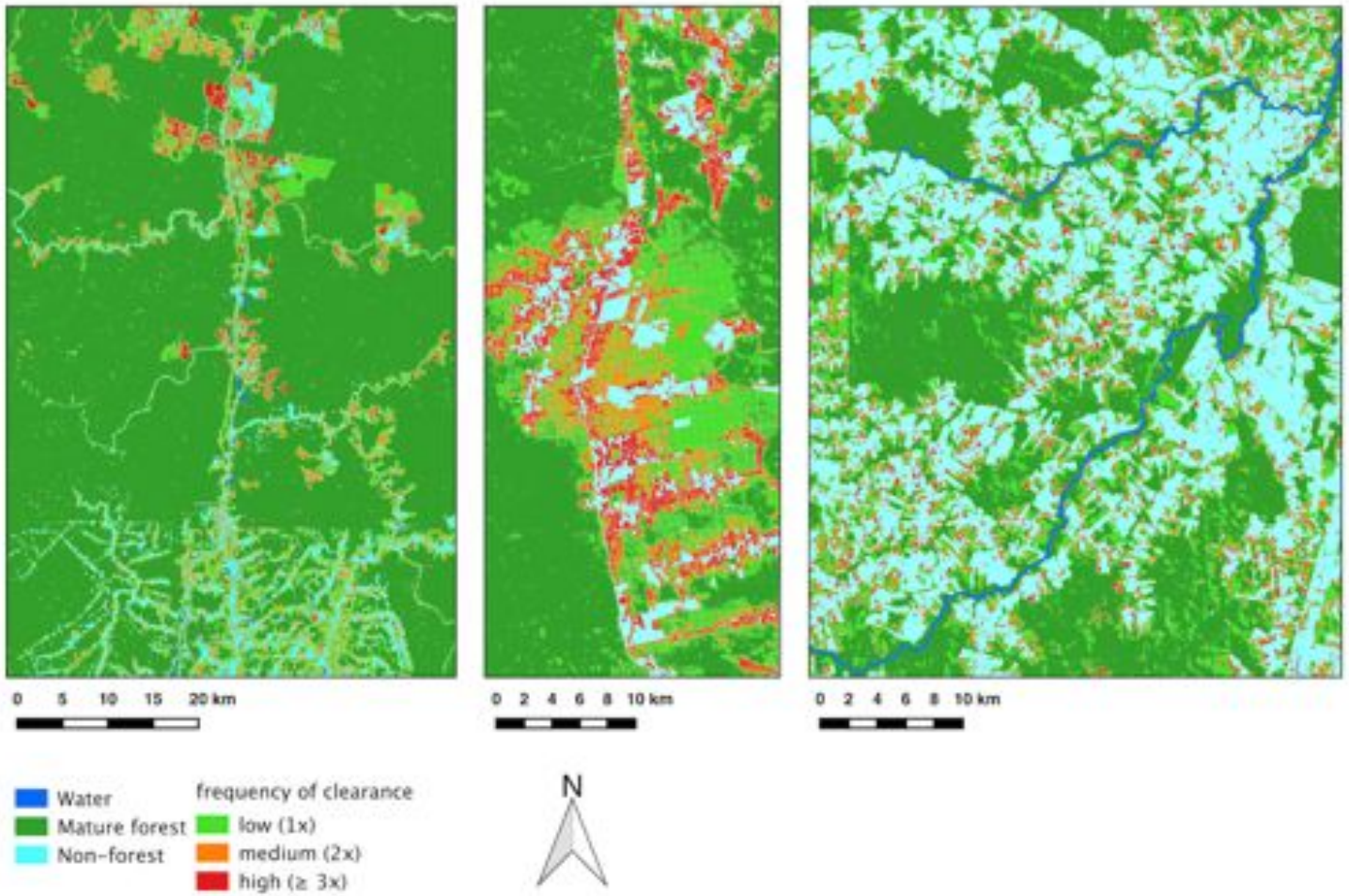

Figure 4.7: Maps displaying the frequency of clearance (FC) across the three selected sites for areas undergoing secondary forest (SF) in the last year of the corresponding time-series; A) Manaus (2011), B) Santare m (2010), and C) Machadinho dOeste (2011). In Manaus, Santarém and Machadinho d'Oeste an area of 103 ha (0.1%), 726 ha (1.6%), and 55 ha (0.1%), respectively, with a PALU of zero was included in the low FC class (1 time) and corresponded to areas that were non-forest (NF) in the first date of the time-series and no clearance has occurred in the secondary forest (SF) that persisted until the end of the time-series. In Santarém, the 726 ha also included areas that were already SF in 1984 that persisted until 2010.

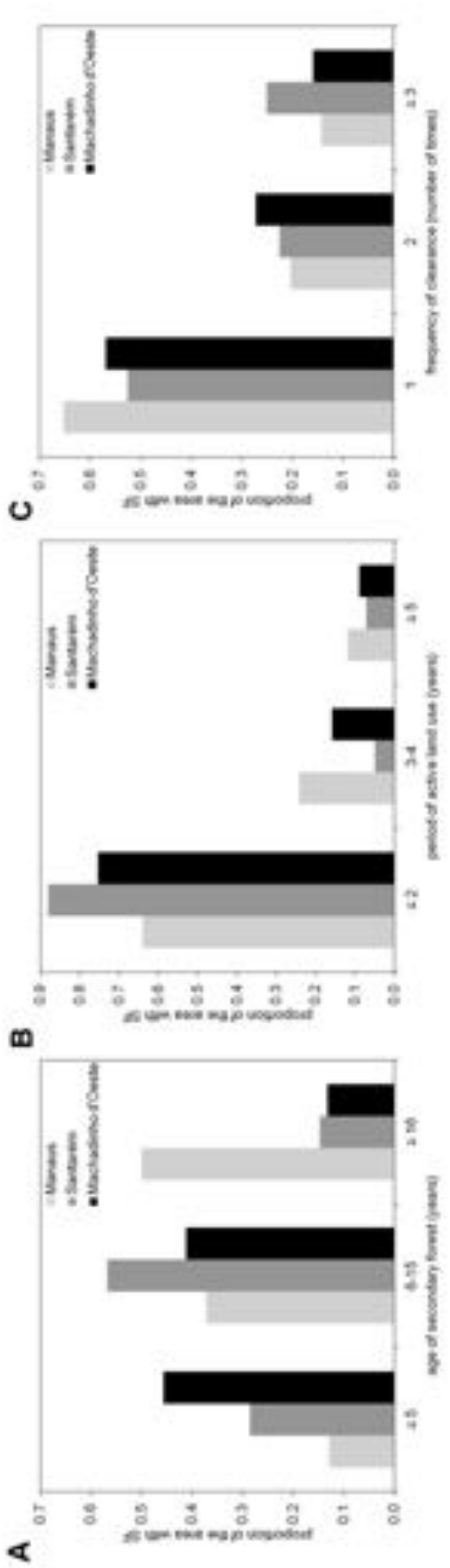

Figure 4.8: Classes of A) age of secondary forest (ASF), B) period of active land use (PALU), and C) frequency of clearance (FC) for the three sites, as a proportion of the area with secondary forest (SF) in the last date of the time-series. The proportion of the area with SF in the first class of PALU ($\leq$2 years) in the Santarém site includes a small proportion (1.5%) corresponding to areas of SF persisting in all dates of the time-series. The proportion of the area with SF in the first class of FC (1$\times$) in Manaus, Santarém and Machadinho dOeste includes a small percentage (0.1%, 1.6%, 0.1%, respectively) corresponding to those cases where non-forest (NF) was observed in the first date of the time-series and no clearance has occurred (i.e., the only transition was from NF to SF).

At all sites, the majority of land has been used actively for ≤ 2 years, either following the initial clearance of the primary forest or subsequent reclearance events, but the deforestation had commenced at different times. At Manaus, the PALU was also ≤ 2 years for over 64% of the area and many of the forests had been able to regenerate undisturbed, with some approaching 40 years in 2011. Some areas had nevertheless been used for 3-4 years (24%) and ≥ 5 years (12%) and had been cleared on one (65%), two (20%) or three or more (14%) occasions.

At Santarém, 88% of the deforested area had been used actively for ≤ 2 years prior to the last abandonment, with 5% and 7% used for 3–4 years and ≥ 5 years respectively. This lower age class distribution was attributed to the later date of initial deforestation, termed here as clearance, but also reclearance of forests, with 53%, 22% and 25% cleared on one, two or three or more occasions respectively. At Machadinho d'Oeste, the PALU was typically <2 years (75%) but 16% and 9% of clearances experienced a PALU of 3–4 and ≥ 5 years respectively. Again, forests were relatively young because of reclearance of the vegetation on one (57%), two (27%) and three or more (16%) occasions. Hence, different typologies of SF were observed at each site.

To investigate whether the typologies were dependent on the last date of the time-series, the same analysis was performed for all of the dates in the time-series for the ASF (Figure 4.9), PALU (Figure 4.10), and FC (Figure 4.11) classes. At Manaus, the proportion of the area with SF in the ≤ 5 year ASF class decreased irregularly from 100% with the onset of regeneration up to approximately 15% in the last date of the time-series (Figure 4.9A). This pattern was mirrored for the 6–15 year ASF class, which stabilized around 40% at the end of the time-series. The ≥ 16 year ASF class steadily increased from 23 years after the onset of SF up to around 50% in 2011. At Santarém (Figure 4.9B), the proportion of the area with SF in the ≤ 5 year ASF class decreased to around 30% in 2010. This decrease was, however, mirrored by an overall increase to about 60% in the 6–15 year ASF class. As at Manaus, the proportion of the area with SF in the ≥ 16 year ASF class increased from 15 years following the onset of regeneration covering approximately 15% in 2010. In Machadinho d'Oeste (Figure 4.9C), the proportion of SF in the ≤ 5 year ASF class systematically decreased from the onset of regeneration (100%) leveling at around 45% in 2011; an opposite pattern was observed in the 6–15 year ASF class, with a systematic increase since the onset of

regeneration up to approximately 40% in the last date of the time-series. As in Manaus and Santarém, a steady increase in the proportion of area with regeneration in the ≥ 16 year ASF class was observed, from 17 years after the onset of regeneration up to around 15% in 2011. By combining the ≤ 5 year and 6–15 year ASF classes, a more consistent but asymptotic increase in the area of SF was observed, with this compensating for the interplay between these ASF classes which occurs because of reclearance. The general trend across all sites is a decrease in the proportion of the area with SF in the ≤ 5 year ASF class up to the present, with a simultaneous increase in the proportion of the 6–10 and ≥ 16 year ASF classes. No asymptotic pattern is visible in the relationship between the proportion of the area with SF and the number of years following the onset of regeneration for this variable in the three selected sites.

Accordingly, and as a result of combining the 3-class PALU and FC maps for the last date of the time-series, a proxy for land use intensity in each site was generated (Table 4.9). At Manaus, of the 65% of land occupied by SF in 2011 that was subjected to only one clearing event, 41% had 2 or less years of PALU but a significant proportion (16% and 9%) had a medium and long PALU (3–4 years and ≥ 5 years) respectively. Santarém is paradigmatic, as almost all land with SF in 2010 that was cleared only once was subjected to short PALU (≤ 2 years). Assuming that high FC (≥ 3 times) and short (≤ 2 years) and medium (3–4 years) PALU will represent a higher land use intensity, then Manaus had 13% of the area undergoing SF in 2011 in these conditions, while Santarém and Machadinho d'Oeste had 20% and 15% in 2010 and 2011 respectively. In fact, a substantial amount of SF in Manaus established on land that was subjected to less severe land use management practices, bringing potential benefits for biomass accumulation and biodiversity restoration.

At Manaus, the proportion of areas where the PALU was ≤ 2 years was initially high (100%) but over time, this area decreased to about 40% but then increased subsequently to 60%, where it remained constant 32 years from the onset of regeneration (Figure 4.10A). This decrease was associated with an increase in the area that had been used for 3–4 year and ≥ 5 years (14–16 years after the onset of SF regeneration). At Santarém (Figure 4.10B), the proportion of the area where the PALU was ≤ 2 years remained high, with this suggesting clearance of SF was common practice. The areas where the PALU was between 3–4 years and ≥ 5 years remained relatively low (<5–10%)

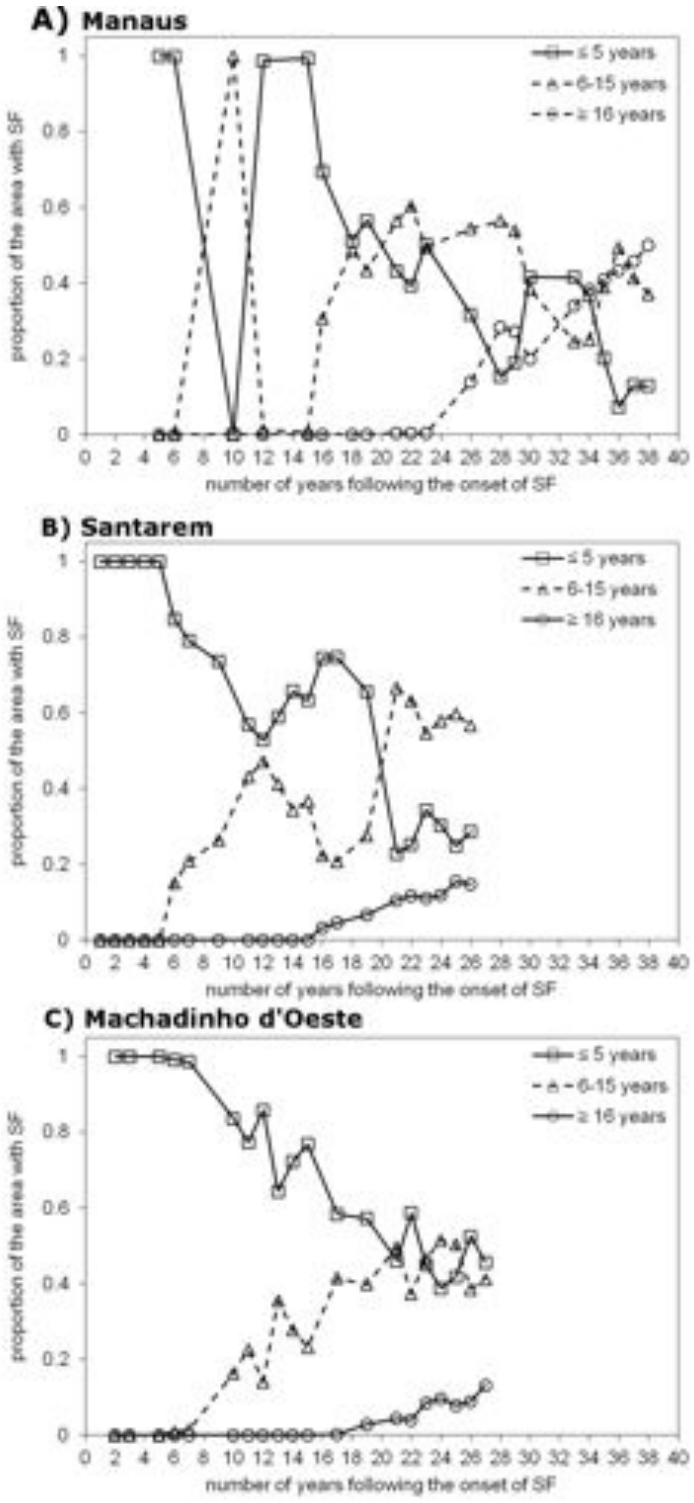

Figure 4.9: Proportion of the area with secondary forest (SF) as a function of the number of years following the onset of SF for the three classes of age of secondary forest (ASF) in A) Manaus, B) Santarém, and C) Machadinho d'Oeste: initial, 5 years; intermediate, 6–15 years; advanced, 16 years.

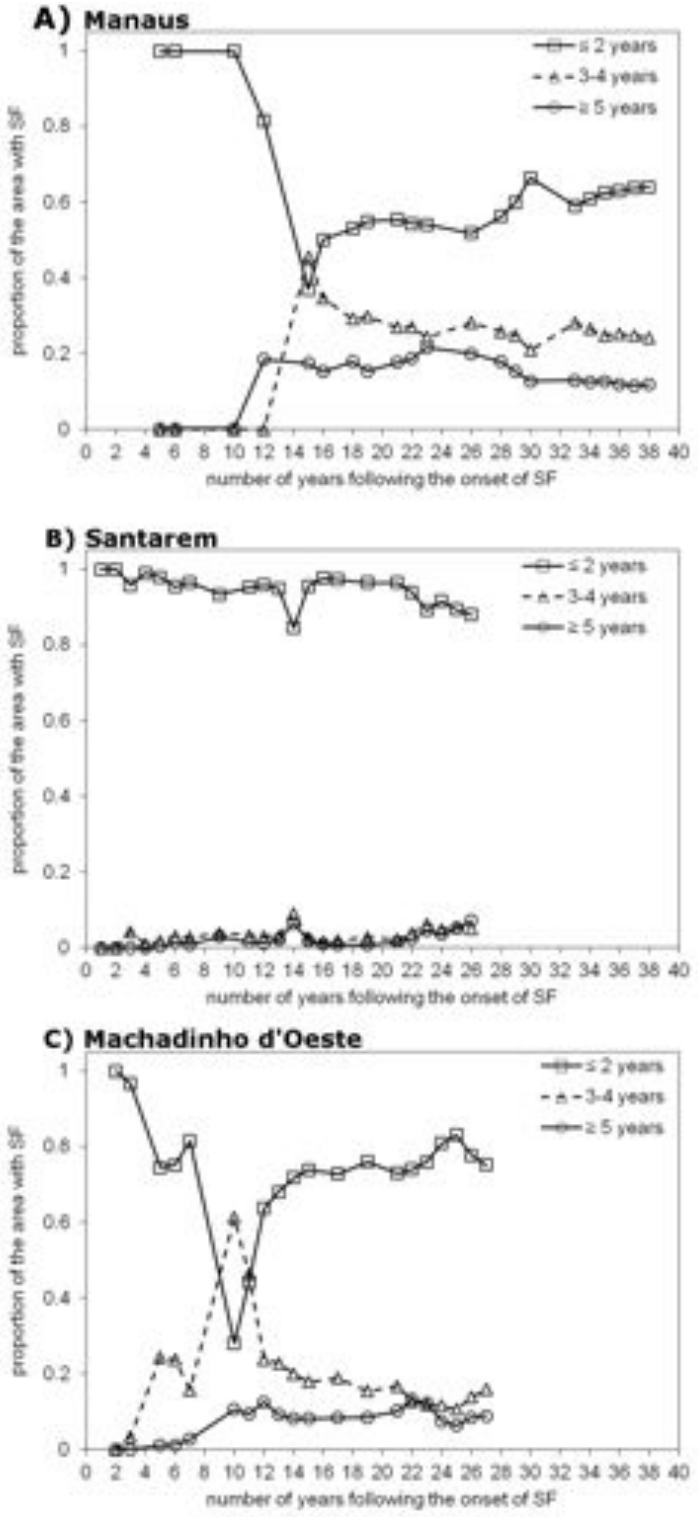

Figure 4.10: Proportion of the area with secondary forest (SF) as a function of the number of years following the onset of SF for the three classes of period of active land use (PALU) in A) Manaus, B) Santarém, and C) Machadinho d'Oeste: short, 2 years; medium, 3–4 years; long, 5 years.

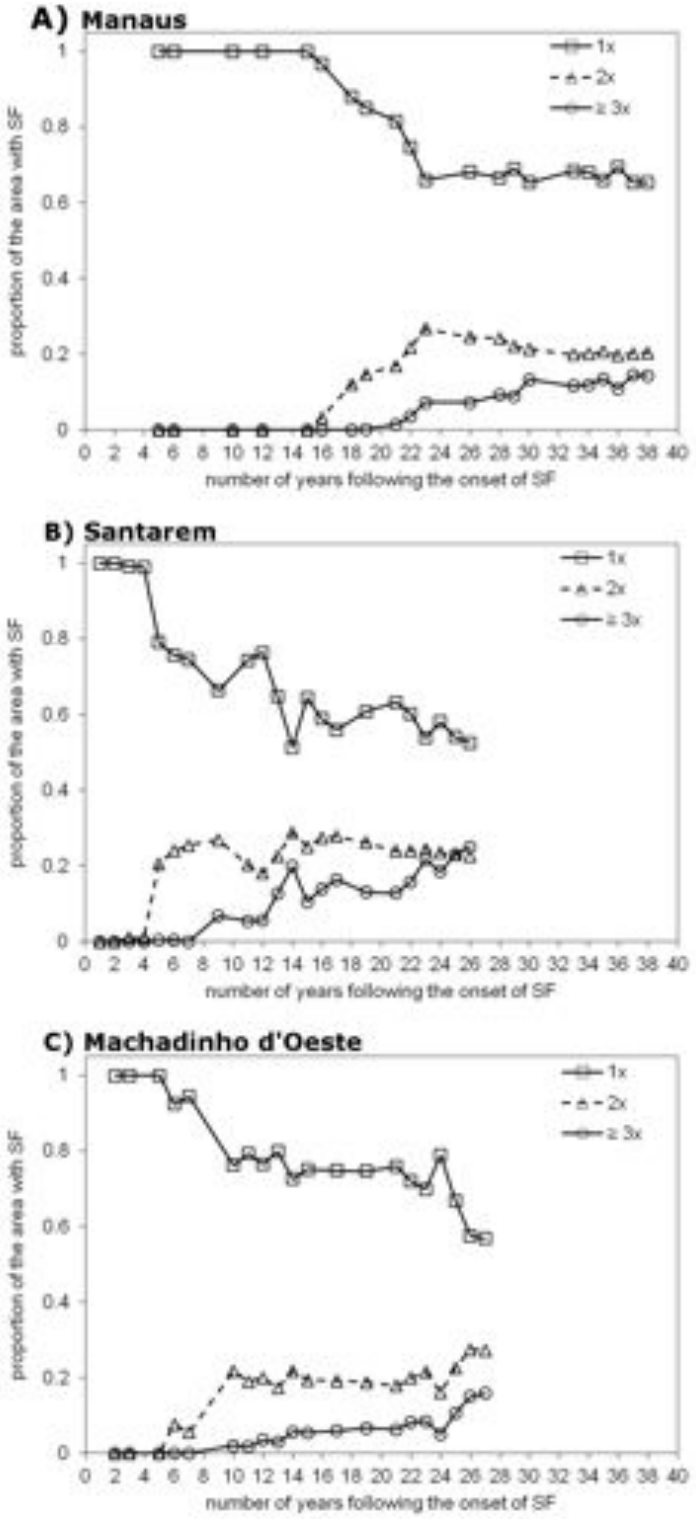

Figure 4.11: Proportion of the area with secondary forest (SF) as a function of the number of years following the onset of SF for the three classes of frequency of clearance (FC) in A) Manaus, B) Santarém, and C) Machadinho d'Oeste: low, 1 time; medium, 2 times; high, 3 times.

Table 4.9: Percentage of area with SF in the last date of the time-series, per combination of PALU and FC classes.

PALU (classes)	**FC (classes)**			**Total**
Manaus	**Low (1×)**	**Medium (2×)**	**High (≥3×)**	
Short (≤ 2 years)	41	13	10	64
Medium (3–4 years)	16	5	3	24
Long (≥ 5 years)	9	2	1	12
Total	65	20	14	
Santarém	**Low (1×)**	**Medium (2×)**	**High (≥3×)**	
Short (≤ 2 years)	51	20	17	88
Medium (3–4 years)	1	1	3	5
Long (≥ 5 years)	0	2	5	7
Total	53	22	25	
Machadinho dOeste	**Low (1×)**	**Medium (2×)**	**High (≥3×)**	
Short (≤2 years)	48	17	11	75
Medium (3–4 years)	5	7	4	16
Long (≥ 5 years)	4	4	1	9
Total	57	27	16	

but increased slightly towards the end of the time-series. At Machadinho d'Oeste, the temporal pattern was similar to that observed at Manaus: a decrease in the ≤ 2 year PALU class followed by a subsequent increase after 10 years following onset of SF with this corresponding to an increase in the 3–4 year PALU class. After 12–14 years, the proportion of the area of the ≤ 2, 3–4 and ≥ 5 years stabilized around 75%, 15% and 10% respectively.

The FC of SF also varied between sites (Figure 4.11). At Manaus, the SF had been cleared only once until about 14 years after the onset of SF but this proportion decreased, stabilizing at approximately 65% at the end of the time-series (2011). This occurred because SF began to be cleared again 15 years after the onset of regeneration and again after 19 years (i.e., 3 FC events), with these areas stabilizing at approximately 20% and 15% of the area respectively. At Santarém, SF was cleared within 2–4 years from the onset of regeneration and continually thereafter. This was reflected in the increase in the proportion of SF areas cleared twice (after 4 years) and three times (after 7 years) with these both stabilizing at approximately 20% of the area. At Machadinho d'Oeste, the proportion of areas with only a clearing event decreased to 55% 28 years after the onset of regeneration. The second and third FC classes commenced after 4 years and 7 years respectively with the proportions of these remaining relatively constant (25% and 15% of the area).

4.5 Discussion

4.5.1 Accuracy assessment of the land cover time-series

Several studies carried out in the Amazon have acknowledged some issues in discriminating SF from MF and, sometimes, NF. Lucas et al. (2000), when assessing the accuracy of mapping these same three classes in four areas across the BLA with NOAA AVHRR data, reported omission and commission errors ranging from 55–75% and 51–76%, respectively. These higher errors were associated with a greater confusion between NF and SF rather than between MF and SF. Carreiras et al. (2006b) used SPOT 4 VEGETATION data to generate a 5-class land cover map of the entire BLA and reported an omission and commission error in the SF class of 66% and 43%, respectively. This was due to confusion between the SF, MF and NF classes. The authors concluded that the misclassification among SF, MF, and NF was understandable, since from a spectral standpoint, SF is a transitional class between NF (i.e., agriculture/pasture) and MF; after deforestation, and following land abandonment. The initial stages of regeneration are spectrally similar to agriculture/pasture. Conversely, final stages of regrowth are more related to MF. Although the values reported in Carreiras et al. (2006b) and Lucas et al. (2000) are much higher than those from this study, the spatial resolution of the datasets that were used in the two studies (i.e., ∼1 km SPOT 4 VEGETATION and NOAA AVHRR) was much smaller than the 30 m spatial resolution Landsat TM and ETM+ data. The spatial arrangement of SF in the BLA, dominated by small previously abandoned areas, especially in Rondônia (de Barros Ferraz et al., 2005), creates an additional difficulty when trying to discriminate these from the surrounding land cover classes with coarse spatial resolution data. Kimes et al. (1999) used 20 m spatial resolution SPOT High Resolution Visible (HRV) data between 1986 and 1994 to discriminate MF, NF and SF over a study area located in Rondônia between Porto Velho and Ariquemes (BR-364 highway) and reported an accuracy of 95% in the SF class with misclassification happening mostly with the MF class. Metzger (2002) used Landsat TM data over the Bragantina region (Pará state) in 1996 to identify agricultural areas, SF stages (initial and developed) and MF; the reported omission and commission errors in the SF classes ranged from 8–11% and 7–10%, respectively, with misclassification occurring mainly from confusion with MF. Vieira et al. (2003) used Landsat 7 ETM+

data to map different stages of SF and other land cover classes in São Francisco do Pará (northeastern Pará state) and reported omission and commission errors between 17–25% and 22–40%, respectively, due mainly to misclassification among SF stages. Kuplich (2006) used Landsat TM and SAR data to discriminate SF stages, MF and pasture in an area north of Manaus (included in our Manaus site) and reported omission and commission errors in the SF stage classes of 10–99% and 32–80%, respectively, but those errors decreased when the SF stages were aggregated into a unique class (78% and 25%, respectively). Although errors are still high in some studies (Lucas et al., 2000; Carreiras et al., 2006a; Kuplich, 2006), others have been able to discriminate SF from MF and NF with a high degree of accuracy (Kimes et al., 1999; Metzger, 2002; Vieira et al., 2003).

A major limitation of this assessment it that only one date (classification) of each time-series per study area was validated with very high spatial resolution data. Nevertheless, those dates classified with the random forests algorithm, the 21 Landsat TM images of the Machadinho d'Oeste time-series (1984–2011) and the post 2003 Santarém Landsat TM images (2005–2010), were assessed with a 10-fold cross-validation procedure. In Machadinho d'Oeste, the average overall accuracy was ∼98%, the omission errors of the MF, NF and SF classes ranged from 0.0–4.4%, 0.0–2.1%, 0.7–7.6% respectively, and the commission errors of the same classes between 0.0–4.2%, 0.0–0.3%, 1.7–7.1% respectively. At Santarém, the 2005–2010 time-series of classified Landsat TM data had an average overall accuracy of 95%, the omission errors of the MF, NF and SF classes ranged between 1.8–6.7%, 0.0–0.9%, 8.1–16.7%, respectively, and the commission errors between 3.7–7.5%, 0.0–0.6%, 4.1–13.2%, respectively. Both the omission and commission errors of the NF class were very low, thus indicating that the major source of error of the SF class was misclassification as MF.

Prates-Clark et al. (2009) validated the 1995 and the 2001 land cover maps over Manaus and Santarém respectively using field-based reference data. For the validation of the 1995 land cover map over Manaus, field data collected in 1995 were used (Lucas et al., 2002; Lucas and Honzak, 2002) and the authors reported an overall accuracy of ∼99%, with omission errors in the MF, NF and SF classes of 0.3%, 3.5%, 1.9%, respectively, and commission errors of 0.5%, 7.0%, 9.5%, respectively. The major source of error in the SF class (higher commission error) was misclassification as MF class. At Santarém,

field data collected in 2002 (Prates-Clark, 2004) were used to validate the 2001 land cover map. The overall accuracy was 88%, the omission errors were 2.2%, 1.1% and 4.2% for the MF, NF and SF classes respectively, and the commission errors were 0.6%, 28.8% and 71.9% for the same classes respectively. As SF ages the complexity of the canopy structure increases (Lucas et al., 2002). This results in the spectral signature of each forest type to converge as SF ages (Lucas et al., 2002; Carreiras et al., 2016) and therefore misclassification as MF. The NF class displayed a high commission error that was related both as misclassification as MF and SF. Higher errors indicated in Prates-Clark et al. (2009) for the Santarém site were also depicted in our accuracy assessment of the 2010 land cover map, although of much lower magnitude.

4.5.2 Differences of land cover change patterns among sites

Extensive deforestation across the BLA started in the 1970s and concentrated along the southern and eastern rims of the region (Fearnside, 2005). The main deforestation drivers were conversion of forest to cropland and/or cattle ranches, which were carried out both by small farmers and large landholders (Kirby et al., 2006). According to the data provided by INPE, 2013 (INPE, 2013), the states where the three study sites are located displayed different deforestation rates (Figure 4.12). Deforestation rates were always higher in Pará, followed by Rondônia and Amazonas. However, since 2003–2005, deforestation rates have been decreasing, with Rondônia experiencing a rapid decrease leading to values closer to those observed in the Amazonas state. According to Nepstad et al. (2011) several factors contributed to this decline, namely the improvement of market-driven environmental governance (e.g., exclusion of activities leading to illegal deforestation and/or selective logging, widespread implementation of international certification systems), federal and state intervention through law enforcement campaigns and enlargement of protected areas; and raising awareness among small farmers and large-scale landowners to the potential financial compensation gained from activities leading to avoided deforestation and forest degradation in the Amazon region. Pará experienced the highest number of settled families by agrarian reform in the nine states composing the BLA (∼31,000 settled families per year in the period 2003–2006), and the number has been increasing since the 1960s (Pacheco,

2009). Although the vast majority of deforestation in the BLA can be tracked to large landholders occupying the land for cattle ranching, the implementation of planned settlements is not negligible, especially in Rondônia which is known by its small farmers radial, fishbone and watershed deforestation patterns (Fearnside, 2005). For example, up to the mid 1990s, the number of settled families in Rondônia was only second to Pará, with 1,423 settled families per year against 1,462 settled families per year in Pará (Pacheco, 2009).

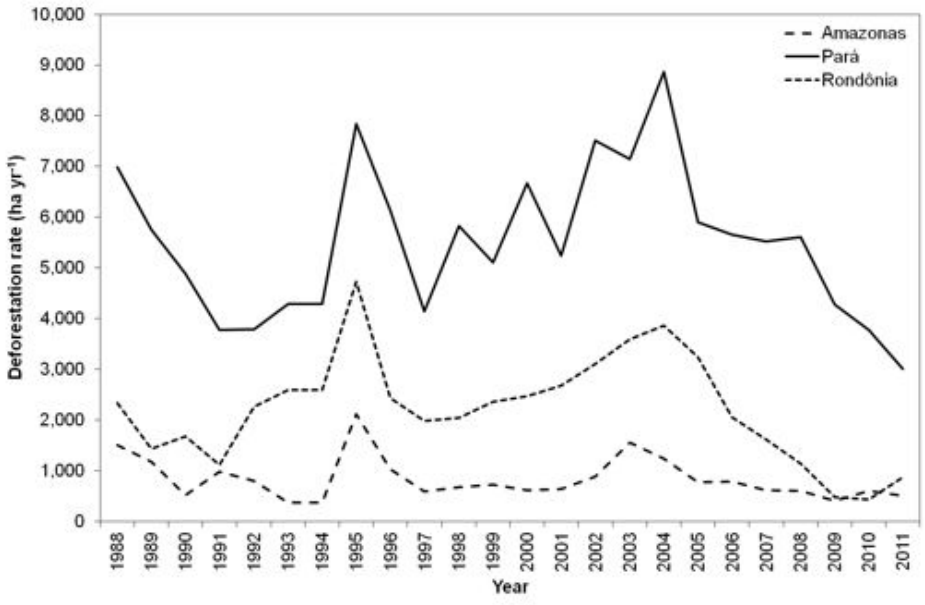

Figure 4.12: Deforestation rates since 1988 (ha yr^{-1}) in the Amazonas, Pará and Rondônia states according to the data reported by INPE (2013).

The three study areas have different socio-economic drivers leading to deforestation, different land uses and subsequent regeneration. The Manaus site is mostly included in the Manaus municipality, although 24% is also included in the Rio Preto da Eva municipality. This study area basically encompasses an area north of Manaus that is 30 km wide and 90 km long centered on the BR-174 highway, including the BDFFP and the Adolfo Ducke and Walter Egler forest reserves, as well as some other environmental protection areas. Started in 1979, the BDFFP is the single most important and enduring research project assessing habitat fragmentation (Laurance et al., 2011). As such, it seems that these conservation areas have been critical at preserving most of the forest in the region. The conservation units (CUs) limits accessed from the Brazilian Ministry of the Environment (MMA, available at http://mapas.mma.gov.br/i3geo/datadownload.htm) were used to estimate the ratio of relative incidence of deforestation (NF + SF) outside

and inside the CUs in the last date of the time-series for each site. The three sites had a significant proportion of the area included in the CUs: 43% in Manaus, 37% in Santarém and 23% in Machadinho d'Oeste. In Manaus, the relative incidence of deforestation outside the CUs was twice that inside CUs and in Santarém and Machadinho d'Oeste that value increased to five times. In fact, several studies have concluded that protected areas in the Amazon region are indeed effective at reducing deforestation rates (Nepstad et al., 2011; Rosa et al., 2013; Nolte et al., 2013). Figure 4.4A illustrates the lower amount of land cover change in Manaus, with approximately 20% of MF lost between 1973 and 2011, when compared with Santarém (more than 30% of MF lost between 1984 and 2010) and Machadinho d'Oeste (∼40% of MF lost between 1984 and 2011). Deforestation in the Manaus study area started long time ago, in the 1970s, with the construction of the BR-174 highway connecting Manaus and Boa Vista (the capital of the Roraima state). Early deforestation is traceable along this highway, many of which was abandoned as a result of poor soil fertility; indeed, many small farmers moved to Roraima which was considered to have younger fertile soils (Fearnside and de Alencastro Graça, 2006). The area of forest in 2011 was approximately 69% and 81% of the territory of the Manaus and Rio Preto da Eva municipalities respectively INPE (2013). Figure 4.4A shows that the proportion of MF in the Manaus site decreased from approximately 90% in 1973 to 71% in 2011, which compares well with the value reported by (INPE, 2013) for the Manaus municipality.

The Santarém site is located south of the city of Santarém, in the Belterra municipality, along the BR-163 highway, and including part of the Tapajós National Forest. This highway links Santarém and Cuiab in the south, the state capital of Mato Grosso. According to Scatena et al. (1996); Brondizio and Moran (2012), this region has a tradition of agriculture and agroforestry since the early 1900s, which has further escalated as a consequence of the construction of the BR-163 in the 1970s. In fact, of the three sites Santarém had the lowest proportion of MF at the beginning of the time-series (∼80%) and the highest proportion of SF (∼20%), thus suggesting that deforestation was commonplace in the area in the early 1980s. According to INPE (2013), approximately 68% of the forest area in the Belterra municipality was remaining in 2011, which compares with our estimate of 46% of MF in 2010. A vast majority of the Belterra municipality is included in the Tapajós National Forest, mainly the

part that is west of the BR-163 highway. So, it is not surprising that the proportion of remaining forest in this municipality is higher than the proportion of remaining forest in the study area that includes the fraction east of the BR-163 highway that is not a protected area. The Machadinho d'Oeste (Rondônia state) site is included mostly in the Machadinho d'Oeste municipality, although 20% overlaps the Vale do Anari municipality. Of the three sites, this was the one with the highest degree of land cover change, with a reduction of ∼60% in the MF cover from 1984 (91%) to 2011 (32%). Deforestation in this region started in the 1980s with the implementation of settlements by INCRA, of which Machadinho d'Oeste and Vale do Anari are just two examples (Batistella and Moran, 2005). According to Batistella and Moran (2005), the proportion of MF in 1988 and 1998 in Machadinho d'Oeste was around 80% and 66% respectively, which compares with our values of 82% in 1987 (1988 was not mapped) and 55% in 1998. INPE, 2013 (INPE, 2013) reports an area of MF in the Machadinho d'Oeste municipality in 2011 of approximately 61%, which compares with our value of 32%. Google Earth^{TM} data from 2013 shows that the areas of the Machadinho d'Oeste municipality to the east and north of the study area have much less deforestation and so this is a possible explanation for the higher proportion of MF detected by INPE (2013) up to 2011 and Batistella and Moran (2005) in 1998. Also, Batistella and Moran (2005) identified the land cover types occurring in the deforested areas of Machadinho. In 1988, approximately 2% was covered by SF, the value increasing to approximately 13% in 1998; our study mapped SF in 1987 and 1998 and the proportion was ∼13% and ∼29%, respectively. Our site is located in the Machadinho d'Oeste municipality that has experienced the most dramatic land cover change since the settlement was implemented. Therefore, when considering the entire Machadinho d'Oeste municipality, there are extensive areas to the north and east of the study area that remained intact, with these covered by MF. Nevertheless, there is a coincident temporal trend that is the increase of SF from 1988 to 1998.

4.5.3 Land abandonment and the emergence of secondary forest

Land abandonment in the BLA is a consequence of a range of factors that have changed across the last decades since the inception of large scale deforestation in the region.

Namely these are; reduced crop productivity as a consequence of poor soil fertility; lack of financial incentives, migratory patterns; non-traditional land uses and market fluctuations (Perz and Skole, 2003). At Manaus, in 2011, land abandonment resulted in SF that was comprised mainly of areas with advanced ASF (50% ≥16 years), although large areas of intermediate ASF (37% between 6–15 years) were also present (Figure 4.5A and Figure 4.8). This suggests that the conservation areas (BDFFP, forests reserves of Adolfo Ducke and Walter Egler, and several other environmental protection areas) were not only effective at preserving MF but also SF areas. As mentioned before, deforested areas in this study area were abandoned mainly because of poor soil fertility, with settlers moving to the nearby state of Roraima (Fearnside and de Alencastro Graça, 2006). It is clear from Figure 4.5A that the higher proportion of advanced ASF in the study area is in the northern half of the site. These areas undergoing regeneration in 2011 had mostly short PALU (64%) as a consequence of intensification of land use and requirement for new land, 24% of the area with a PALU of 3–4 years and low and medium FC (65% deforested 1 time and 20% deforested 2 times, respectively). In comparison, the study area south of Santarém, which included parts of the Tapajós National Forest, had regrowth dominated by areas with 6–15 year ASF classes in 2010. Those areas experienced essentially short PALU (88% ≤2 years) and low (52% deforested 1 time), medium (22% deforested 2 times) and high (25% deforested 3 or more times) FC. According to Brondizio and Moran (2012), land abandonment in the region, and associated regeneration, was high until 1999. At this point, large-scale soybean cultivation started, mainly because of the decay of primary and secondary roads, lack of social services, and limited access to water. On the other hand, land abandonment in Machadinho d'Oeste resulted in SF that was mainly in the ≤5 year (46%) and 6–15 year (41%) ASF classes, with these areas experiencing mostly (75%) ≤2 years of PALU and a FC of 1 (57%) or 2 (27%) occasions. This was a planned settlement and most of the deforested area is under agriculture and or pasture use, suggesting that a vast majority of the area undergoing SF could be indeed forest fallow that might be under cattle ranching use or being subjected to subsistence agriculture in a crop/fallow cycle (Brondizio and Moran, 2012).

One important aspect worth mentioning is the large proportion of SF in the Santarém site that resulted from the 1997 wildfires. This area of regeneration was not the consequence

of land abandonment but a natural process following fire-induced disturbance. This wildfire was just one among many others that occurred in the BLA as a consequence of the 1997-1998 El Niño Southern Oscillation (ENSO) event (Nepstad et al., 1999). In fact, the proportion of NF in 1997 (prior to the wildfire) was around 6% and in 1998 had increased to approximately 15%, mainly as a consequence of that large wildfire, perfectly visible in Figure 4.5B as the orange irregular zone of intermediate ASF in the centre of the study area. As a consequence of the natural regeneration process, the SF proportion increased to approximately 40% in 2000 (∼32% in 1997). Therefore, approximately 20% of the area of SF in 2010 was estimated as resulting from natural regeneration following that wildfire event. The proportion of the area with SF in 2010 resulting from land abandonment was approximately 36% (the overall value is around 44%).

4.5.4 Implications of prior land use for biomass accumulation and biodiversity restoration in secondary forests

Regenerating forests in the three selected sites have been classified in terms of ASF, PALU prior to abandonment and FC. Prior LULCC practices (e.g., 'slash and burn' agriculture and pasture) have a fundamental influence on the vegetation regenerating following land abandonment in the Amazon (Uhl and Jordan, 1984; Uhl, 1987; Uhl et al., 1988; Buschbacher et al., 1988; Saldarriaga et al., 1988; Mesquita et al., 2001; Lucas and Honzak, 2002; Chazdon, 2003; Chazdon et al., 2007). Vegetation structure, species composition and dominance are just some of the parameters of the regenerating vegetation that have been studied to identify the impact of prior land use practices (Uhl et al., 1981). As such, these have an impact on the capability of these forests to accumulate biomass (and to act as a C sink at a greater or lesser extent) and to restore biodiversity (Zarin et al., 2001).

Uhl et al. (1988) studied areas undergoing secondary succession following pasture abandonment in Pará (Paragominas municipality) and identified major patterns related to prior land use intensity. The authors identified three major pathways related to species composition, structure and biomass accumulation. Light use sites were characterized by a lower PALU (0–4 years) and with no reclearance or just one 'slash and burn' episode;

moderate and heavy use sites had higher PALU (6–12 years) and with 1–5 clearing episodes; in addition, heavy use sites have been subjected to large-scale mechanized operations (e.g., to remove woody debris and control of weeds). Light use sites had high species richness, with more than 20 species per 100 m^2, dominated by pioneer species of the genus *Cecropia, Cordia, Croton, Inga, Solanum, Trema and Xanthoxylum*, which could also be found in the MFs of the region. 8-year old sites had a ∼13 m closed canopy and an AGB accumulation rate of 10 Mg ha^{-1} yr^{-1}, mainly composed of trees (70%), although vines represented the second major vegetation type. Comparatively, moderate use sites had lower species richness, although many of the dominant species were the same (e.g., *Solanum* spp., *Cecropia* spp.). Whilst at the 8-year old sites, only a 7–8 m partially developed canopy dominated by *Vismia* spp. was observed and the AGB accumulation rate was only 5 Mg ha^{-1} yr^{-1}. At the heavy use sites species richness was poor (less than one tree per 100 m^2), mainly composed by scattered trees of the genus *Solanum* and *Cecropia*. The 8-year old sites were mainly composed by forb, grass and sedge species, and the AGB accumulation rate was only 0.6 Mg ha-1 yr^{-1}, around 17 and 8 times less than in light and moderate use sites respectively.

Mesquita et al. (2001) studied regeneration pathways in a region north of Manaus that is included in our Manaus site (BDFFP) and identified major differences related to prior land use. Basically, areas that were deforested and abandoned immediately were dominated by *Cecropia* spp. trees, whereas those that were abandoned after some years of pasture use were dominated by *Vismia* spp. trees. Lucas and Honzak (2002), also identified two distinct regeneration pathways in a region north of Manaus and in the same way as Mesquita et al. (2001); the authors identified *Vismia* spp. dominated regeneration associated to sites with more intensive land use and those dominated by *Cecropia* spp. to less intensive land use. According to Chazdon et al. (2007), in terms of AGB accumulation, tropical secondary forests are characterized by a rapid growth rates in the first years after land (agriculture or pasture) abandonment. Zarin et al. (2001) showed that there is a strong correlation between the AGB of secondary forests and the number of years following abandonment (i.e., ASF), soil texture and climate data in the Amazon region. On this pretext, the secondary forests in Manaus have the potential to accumulate more AGB, followed by Santarém and Machadinho d'Oeste. In 2011 (the last date of the time-series), Machadinho d'Oeste had approximately 45%

of the area of secondary forest with less than five years of age, and around 40% with less than three years of age. Machadinho d'Oeste was initially a settlement project implemented by the Brazilian government and today most of its people are dependent on subsistence agriculture (Miranda, 2013). Therefore, it is possible that some of the area mapped as SF was indeed forest fallow, part of a crop/fallow system of subsistence agriculture, which have been acknowledged by several studies (Brown and Lugo, 1990; Lu et al., 2003).

4.6 Conclusions

An accurate assessment of large-scale land use and land cover change dynamics over remote areas (e.g., Amazon) can only be carried out with an adequate monitoring system. Remote sensing data, in this case annual or quasi-annual time-series of high spatial resolution optical data (Landsat program), has proven its ability to accurately discriminate MF, SF and NF over three sites in the BLA experiencing several decades of deforestation. Lower deforestation rates and a greater proportion of 6–15 and $\geq$16 year ASF classes were characteristic of the Manaus site. On the other hand, Machadinho d'Oeste had the highest deforestation rates and lower regrowth rates, with most of its regeneration occurring in areas abandoned over the past 5 years. LULCC at Santarém displayed an intermediate behaviour, with intermediate deforestation rates and the highest regrowth rates, which lead to regeneration dominated by areas of 6–15 year ASF class forests. Conservation units were effective at reducing deforestation at all three sites. The temporal evolution of the spatial arrangement of the various parcels of land identified as one of the three classes could provide new insights about the fragmentation patterns in the region (Ewers et al., 2013).

Although several generalizations about the type and composition of secondary forest occurring in each of the three sites can be made, a correct assessment can only be made after an in situ assessment. Therefore, the research presented here will provide the opportunity to assess the influence of previous LULCC dynamics on the biomass accumulation and biodiversity restoration and further investigate hypotheses related to differences among the three sites. This work provides the basis for a field campaign to collect forest inventory data. This will be used to study the influence of prior LULCC

on the capability of regrowth areas to accumulate AGB in Chapter 5.

Chapter 5

Field data analysis

5.1 Introduction

To determine the effects of prior land use history on above ground biomass (AGB) accumulation, field based measurements of secondary forests (SF) that have undergone different treatments are required. AGB can be determined from diameter at breast height (DBH, 1.3 m) alone (e.g. Brown et al., 1989) or any combination of DBH with height or specific wood density (ρ) (e.g. Nelson et al., 1999; Chave et al., 2014). These parameters can be measured in the field. Basal area (BA) and stem density (stems ha^{-1}) are useful metrics in understanding secondary forest succession (e.g. Letcher and Chazdon, 2009; Mesquita et al., 2015). BA is derived from DBH and the total number of trees measured in the plot.

Variability in sampling design and data collection methods followed by studies investigating SF dynamics is demonstrated in Table 5.1. Forest plot position and size is often limited in secondary forest studies in the tropics by reliable information on land use history, soils and accessibility (Table 5.1). A reduction in bias of plot selection and placement of vegetation inventory plots is important when determining if spatial and temporal differences are real (Phillips et al., 2002b). Forest plots are commonly 0.2–100 ha in size (Houghton et al., 2001). However, Chave et al. (2004) demonstrated that the minimum plot size required to provide a significant representation of biomass per unit area (usually 1 ha) is 0.25 ha. However, there is often a trade-off between the need to represent the range of forest types or land use histories present and the number of

individual plots at an appropriate scale that can be measured in single field campaigns. These constraints can lead to the clustering of plots in accessible locations close to roads (Phillips et al., 2015). These areas are often subject to greater disturbance frequencies due to their proximity to roads and linear clearings (Olander et al., 1998; Laurance et al., 2009).

Table 5.1: Methods of data collection in secondary forests (SF) for studies in changes above ground biomass (AGB) and floristic composition.

Source	**Sampling strategy**	**Plot dimensions**	**DBH sampled**	**Method of data collection**	**Primary metric**
Saldarriaga et al. (1988)	Complete information on land use history, soils and topography	10 m × 30 m and 50 m × 50 m	≥1 cm and >10 cm	non-destructive	AGB
Aide et al. (1995)	Unknown, centre SF patch	45 m transect with 1 m × 1 m	≥1 cm	non-destructive	AGB
Alves et al. (1997)	Complete information on land use history	10 m × 100 m	≥5 cm	non-destructive	AGB
Feldpausch et al. (2007)	Stratified and accessibility	60 m × 3 m to 225 m × 3 m	≥1 cm	non-destructive	AGB
Letcher and Chazdon (2009)	Stratified - Complete information on land use history	five 2 m × 100 m - Gentry transect (Phillips et al., 2002a)	≥2.5 cm	non-destructive	AGB
Jakovac et al. (2015)	Stratified, centre SF patch	10 m × 50 m	≥5 cm	non-destructive	Floristics
Mesquita et al. (2015)	Stratified-random	100 m × 100 m	≥3 cm	non-destructive	Floristics
Wandelli and Fearnside (2015)	Complete information on land use history	10 m × 10 m	≥1 cm	destructive	AGB

Stand properties, such as average diameter at breast height (avDBH), basal area (BA), stem density and above ground biomass (AGB) increase with secondary forest age (Buschbacher et al., 1988; Saldarriaga et al., 1988; Uhl et al., 1982; Uhl, 1987; Uhl et al., 1988; Brown and Lugo, 1990; Nepstad et al., 1990; Alves et al., 1997; Silver et al., 2000b; Steininger, 2000; Lucas and Honzak, 2002; Feldpausch et al., 2004, 2005, 2007; Williamson et al., 2014). The growth rates of these properties vary in response to a number of factors (Cardille and Foley, 2003), as outlined in Chapter 2. Whilst, stem density can be altered through stem mortality or self-thinning (Mesquita et al., 2015). Unsustainable stem density is caused by resource deficit such as drought stress (Phillips et al., 2010). This can result in a change in other stand properties such as DBH and BA (e.g. Barlow et al., 2003; Feldpausch et al., 2007).

Secondary forest age can be determined through long term field observations, e.g. in chronosequences; interviews with land owners or analysis of time series remote sensing data (Chazdon et al., 2007; DeVries et al., 2015; Wandelli and Fearnside, 2015). However there is a discrepancy between the start date of SF regrowth between these methods. Ground based assessments and interviews are complicated by the definition of the commencement of SF regrowth as woody species begin to emerge whilst a pasture is still active (Feldpausch et al., 2007). The removal of cattle is used to define age 0 in these instances. In remote sensing estimates of SF age sufficient canopy closure is required for the detection of woody vegetation with a deviation from spectral indicies values associated with non forest land cover types (DeVries et al., 2015). This may not be congressant with the cesation of grazing however it is consistant and repeatable.

Allometric equations for determining AGB are the product of destructive sampling of each aboveground component of a tree. A relationship is produced between AGB and measurable parameters such as DBH, specific wood density (ρ) and height. To conduct destructive sampling of an entire stand is time consuming and logistically problematic, therefore these relationships are applied using readily available tree parameters. These are commonly: DBH, height, environmental conditions, such as precipitation and soil type, and ρ. Table 5.2 presents models derived from destructive sampling of trees found in the tropical rainforests of the Neotropics, Africa and Indonesia, demonstrating the range of parameters used in parameterisation of these allometric models.

Table 5.2: A comparison of data used to parameterise allometric models commonly used for AGB estimation in the tropical forests of Amazonia.

		Forest type		Data			Size range (cm)				
Biomass model	**Location**	**Mature**	**Secondary**	**DBH**	**H**	ρ	**0–20**	**20–50**	**50–100**	**>100**	***n***
Chave et al. (2014)	Pan-tropical	•	•	•	•	•	•	•	•	•	4004
Chave et al. (2005)	Pan-tropical	•	•	•	•	•	•	•	•	•	2410
Overman et al. (1994)	Colombia	•		•	•	•	•	•			54
Chambers et al. (2001)	Manaus, Amazonas	•		•			•	•	•		315
Higuchi et al. (1998)	Amazonas	•		•			•	•	•		315
Brown (1997)	Moist tropics	•		•			•	•	•		168
Nelson et al. (1999)	Manaus, Amazonas		•	•	•		•	•			132
Uhl et al. (1988)	Paragominas, Para		•	•	•		•	•	•		30

Allometric model selection is fundamental to reducing error and uncertainty in forest resource studies. Henry et al. (2013) developed "GlobAllomeTree", an open access international platform and database for tree allometric equations. This was to facilitate development of new models; improve the evaluation of tree and forest resources and improve knowledge on tree allometric equations through comparison with existing models. This ensures that the correct models are used in estimating AGB at a national level. It is agreed throughout the literature that locally derived models of AGB should be used where available (van Breugel et al., 2011; Molto et al., 2013; Chave et al., 2004, 2005, 2014). It is also agreed that DBH, H and ρ should be included in such calculations (Baker et al., 2004; Chave et al., 2004, 2005, 2014; Nogueira et al., 2008; Mitchard et al., 2014; Feldpausch et al., 2011, 2012). The DBH size range and number (n) of trees used to derive the model is a major source of variation in the AGB output and models should not be used beyond their range of validity for DBH (Chave et al., 2004, 2005).

Quantifying the error of AGB estimates is fundamental in forest inventory studies such as United Nations Framework Convention on Climate Change (UNFCCC) Reducing Emissions from Deforestation and Degradation (REDD+) measuring, reporting and verifying (MRV) activities to provide accurate estimates of forest AGB (Wertz-Kanounnikoff et al., 2008). It can be estimated through comparisons of repeat measurements (Chave et al., 2004), or by comparison of destructive sampling data and AGB derived from allometric equations (van Breugel et al., 2011; Wandelli and Fearnside, 2015). Error can be classed as either uncertainty, caused by the lack of knowledge of the true value, or systematic error, which is caused by a lack of accuracy (Gierlinski, 2016). The latter can be reduced by identifying the causes of this systematic error. Table 5.3 defines the different sources of error which propagate through the process of AGB estimation from parameter measurements to averaging AGB over a plot.

Table 5.3: Sources of error inherent in estimating AGB from allometric equations. Adapted from Chave et al. (2004) and Molto et al. (2013).

Step in AGB estimation	**Data**	**Error source**	**Percentage error**
Measure	DBH, H and ρ of 1 tree	quality of data	31% (Chave et al., 2004)
Height model	H of 1 tree	quality of model	N/A
Allometric model	AGB of 1 tree	quality of model	15.8–57.5% (Chave et al., 2004; Saatchi et al., 2011a; Wandelli and Fearnside, 2015)
Sum over trees	AGB of 1 plot	size of sampled area	5–20% in 1 to 0.1 ha plots (Keller et al., 2001; Chave et al., 2004)
Average over plots	AGB of the forest	representative of the plots	N/A

Chave et al. (2004) estimated the total error (47 %) associated with estimating AGB. This error was a combination of parameters used in allometric equations (31 %) and the type of allometric equation used (16 %) based on its input parameters, i.e. DBH, H and ρ. The error of AGB estimated from allometric equations compared to AGB derived from destructive sampling gave errors ranging from 18.9 % to 57.5 % north west of Manaus (Wandelli and Fearnside, 2015).

5.1.1 Outline and objectives

The focus of this chapter was to determine the influence of land use history on the above ground biomass accumulation and structural properties of secondary forests (SF) in central Amazonia. This work presents the application of allometric equations to determine tree height and above ground biomass in SF. The results will be utilised further in Chapter 6 to parameterise a forest growth model.

5.2 Data

The field data available for this research was collected from the Biological Dynamics of Forest Fragments Project (BDFFP) and fazendas north of Manaus during 1993, 1995 and 2014 as part of two separate projects.

5.2.1 The NERC TIGER Project

As part of the Natural Environment Research Councils (NERC) Terrestrial Initiative in Global Environmental Research (TIGER) project (Lucas et al., 2002), data was collected in 1993 from 14 10 m × 100 m plots located within regenerating forests primarily at Fazendas Porto Alegre, Esteio, Maringa and Agroman (Figure 5.2). 14 plots of equivalent size were sampled in 1995 (7 of which had been sampled in 1993). In total, 21 forests were sampled. In both years, the DBH (cm, at 1.3 m above ground level) for trees ≥ 5 cm was recorded and each tree measured was identified to genus and where possible to species. Where stilts (e.g. as typical to *Cecropia* species), buttress roots or deformities occurred at 1.3 m above the ground, DBH was measured at the first point where the tree cross-sectional outline was regular. Height (m) was estimated for every 10th tree, measured for DBH, using a SUUNTO clinometer together with distance measurements (Phillips et al., 1994). The height measurements were limited to 20–30 trees per plot so that in total, 481 trees selected from all plots were measured for both DBH and H.

A sampling strategy was not implemented during these field campaigns owing to a lack of data pertaining to age of secondary forest and extent prior to undertaking fieldwork. For the purposes of this study, plots which were <50 m from the SF edge or within areas of MF, as identified in Chapter 4, were removed from the dataset.

5.2.2 Regrowth-BR

Field data was collected from 23 sites for which the period of active land use (PALU) ranged from <1 year to >6 years and the frequency of clearance (FC) was up to 3 times. These were stratified by PALU and FC. Several forest plots measured in 1993 and 1995 were remeasured in 2014 as closely as GPS error and clearing between measurements would allow. The plot size was 20 m × 100 m. These plots were divided into two 10 m × 100 m plots with trees with DBH ≥5 cm included in one half and only those with a DBH ≥10 cm included in the other (Figure 5.1). Trees were identified to the genus and species level where possible. Height was measured for selected trees and all palm species in each plot using a Vertex hypsometer (Vertex Laser VL400 Ultrasonic-Laser Hypsometer III, Haglöf Sweden) and a laser range-finder (Leica Disto-5). In total 696

trees selected from all plots in 2014 were measured for both DBH and height. Sites were located >50 m from the SF edge to account for edge effects (Lopez-Gonzalez et al., 2011). Sampling followed the procedure detailed by the RAINFOR project (Phillips et al., 2015). Locations visited in more than one field campaign, within GPS error and the limits of accessibility, were assigned letters to indicate repeated measurements in addition to their plot number.

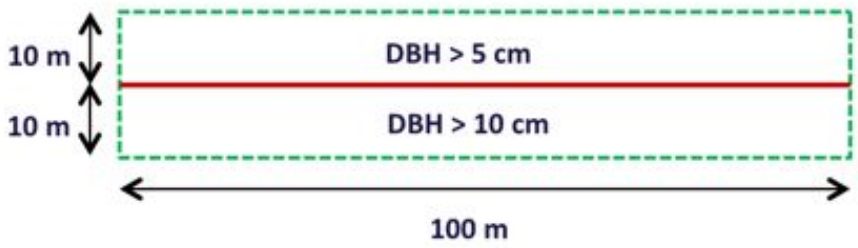

Figure 5.1: Nested plot design used to sample standing live and dead trees north of Manaus in the Regrowth-BR field campaign, 2014.

Figure 5.2: Areas of secondary forest located north of Manaus in 2011. Inventory plots sampled in 1993, 1995 and 2014.

5.3 Methods

5.3.1 Structural properties

Mean DBH (avDBH), basal area (BA) and stem density were calculated for each plot in addition to AGB for parameterisation of a forest growth model in Chapter 6. BA and stem density were calculated from the transect including trees with a DBH ≥5 cm. The stem density (stems ha^{-1}) is calculated by summing the number of individual trees (DBH >5 cm) in each plot and scaling up to 1 hectare. BA (m^2 ha^{-1}), defined as the sum of the cross section area of all tree trunks in a plot. BA (m^2), was calculated using:

$$BA = 0.00007854 \times D^2 \tag{5.1}$$

where, D is the diameter at breast height. This was summed in each plot and scaled to 1 hectare using a scaling factor (sf) of 10 for trees with a DBH 5–10 cm and 5 for DBH ≥ 10.

$$BA_{(m^2 ha^{-1})} = BA_{(m^2)} \times sf \tag{5.2}$$

5.3.2 Height modelling

The height (m) of a tree is required to determine its volume and therefore the biomass contained within it. To measure the height of every tree in a plot would be very time consuming and problematic in dense stands as the highest point of the crown is often not visible. Allometric relationships have therefore been defined between DBH (cm) and height. This is achieved by the collection of height and DBH from a representative subset of the trees in a sample. The relationship derived from these data is then applied to estimate the height of the entire forest inventory for the purpose of above ground biomass (AGB) estimations. Many site and environmental effects influence height modelling (Feldpausch et al., 2012; Lines et al., 2012). Feldpausch et al. (2012) derived a set of pan-Amazonia height models sub divided into regions by geography and substrate origin. The region Eastern and Central (E & C) Amazonia encompasses

the study site and is comprised of old sedimentary substrates derived from the other three regions from the study.

Tree height was predicted for those trees which weren't measured in the field using allometric models of height from regression of observed DBH and height measurements. Height allometry derived from the Regrowth-BR field campaign DBH vs H relationship excluded palms and dead standing trees. This model was compared with species specific allometry (Prates-Clark, 2004) and a model derived from field data collected in Central (E & C) Amazonia (Feldpausch et al., 2012) (Table 5.4). Prates-Clark (2004) used DBH and H data from 1993, 1994 and an additional field campaign in 2001 north of Manaus in the same secondary forests measured by this study. The DBH range of trees observed in advanced growth stage SF near Manaus often exceeded 40 cm. This is outside the range of DBH values used by (Prates-Clark, 2004) but not the model derived by Feldpausch et al. (2012). Using a model that is derived from a dataset of trees whose DBH range encompasses the entire dataset under investigation, will avoid the introduction of any inconsistency when switching between the different models to account for DBH exceeding the range of the first model. The tree height model which gave the best representation of the observed tree heights was determined by comparison with observed data and regression statistics.

Table 5.4: Allometric equations for estimating tree height (H, m) from DBH (D, cm) measurements tested in this study.

Region	**Genera**	**Equation**	DBH range (cm)	H range (m)	*n*	**Source**
	Cecropia, Pourama	$H = exp(1.233 + 0.594 \times ln(D))$	2.8–33.7	4.7–30.2	86	Prates-Clark (2004)
	Vismia	$H = exp(1.695 + 0.455 \times ln(D))$	3.8–39.2	10.1–30.9	130	Prates-Clark (2004)
	Miconia, Bellucia	$H = exp(1.971 + 0.312 \times ln(D))$	4.5–24.5	9.6–23.0	67	Prates-Clark (2004)
	Goupia	$H = exp(1.489 + 0.544 \times ln(D))$	3.2 - 21.6	7.7–24.3	23	Prates-Clark (2004)
	Laetia	$H = exp(1.039 + 0.737 \times ln(D))$	3.5–22.0	7.3–31.3	49	Prates-Clark (2004)
	Byrsonima	$H = exp(1.107 + 0.662 \times ln(D))$	41.1–36.6	7.7–36.8	6	Prates-Clark (2004)
	Mixed	$H = exp(1.275 + 0.593 \times ln(D))$	2.8–48.0	4.65–36.8	481	Prates-Clark (2004)
East and Central Amazonia	Mixed	$H = 48 \times (1 - exp(-0.038 * D^{0.82}))$	10.0–200.0	2.0–55.0	6588	Feldpausch et al. (2012)

5.3.3 Above ground biomass estimation

The Chave et al. (2014) pan-tropical biomass model (Equation 5.3) was selected to estimate the AGB of each individual tree. This allowed consistent estimates of AGB, as opposed to applying several locally derived models based on differing DBH ranges in comparison to the pan-tropical model which used a larger DBH range (Figure 5.3). The AGB of palm species was calculated using Equation 5.4 (Goodman et al., 2013):

$$AGB_{est} = 0.0673 \times (\rho \times D^2 \times H)^{0.976} \tag{5.3}$$

$$AGB_{est}^{0.25} = 0.55512 \times (DMF \times D^2 \times H)^{0.25} \tag{5.4}$$

where D is diameter at breast height (1.3 m above the ground, cm); H is tree height (m), AGB_{est} is the estimated above ground biomass for one tree (kg), ρ is the species specific wood density (Zanne et al., 2009) and DMF is the dry mass fraction (dry mass/fresh mass) with an average value for the *Arecaceae* family of 0.388 (Goodman et al., 2013). This was summed in each plot and scaled to 1 hectare using a scaling factor (sf) of 10 for trees with a DBH 5–10 cm and 5 for DBH $\geq$ 10 cm (Equation 5.5).

$$AGB_{(Mgha^{-1})} = AGB_{(kg)} \times sf \tag{5.5}$$

Data analysis was carried out using linear and multi-linear regressions (Zar, 1999) to evaluate the effects of land use history on estimated AGB and forest stand properties, avDBH, BA and stem density. To aid comparison with other studies of SF stand properties, annual increments of avDBH, BA and AGB were calculated as the rate of increase using the best fit regression models from 0–5 years, 0–10 years, 0–20 years and 0–37 years. To evaluate the differences over time, confidence intervals were applied to the data after subsetting it into broad land use classes. These were PALU $\leq$2 and $\geq$3 and FC 1 $\times$ and $\geq$2$\times$. These analyses were performed in R (Team, 2015).

5.3.4 Outlier removal

Plots were removed from the dataset if they were not representative of secondary forests. Plots 49 and 53 were removed because of their location in the palm plantation in the north of the study site and their relative abundance, 20 individuals in each plot, of the commercial oil palm species *Elaeis oleifera* (Hartley, 1967) compared to other plots located in the study site all of which contained zero individuals and were therefore not representative of naturally occurring SF. Plots 26h and 27h, the same stand measured twice, contained remnant mature forest trees and was <50 m from mature forest. Plots

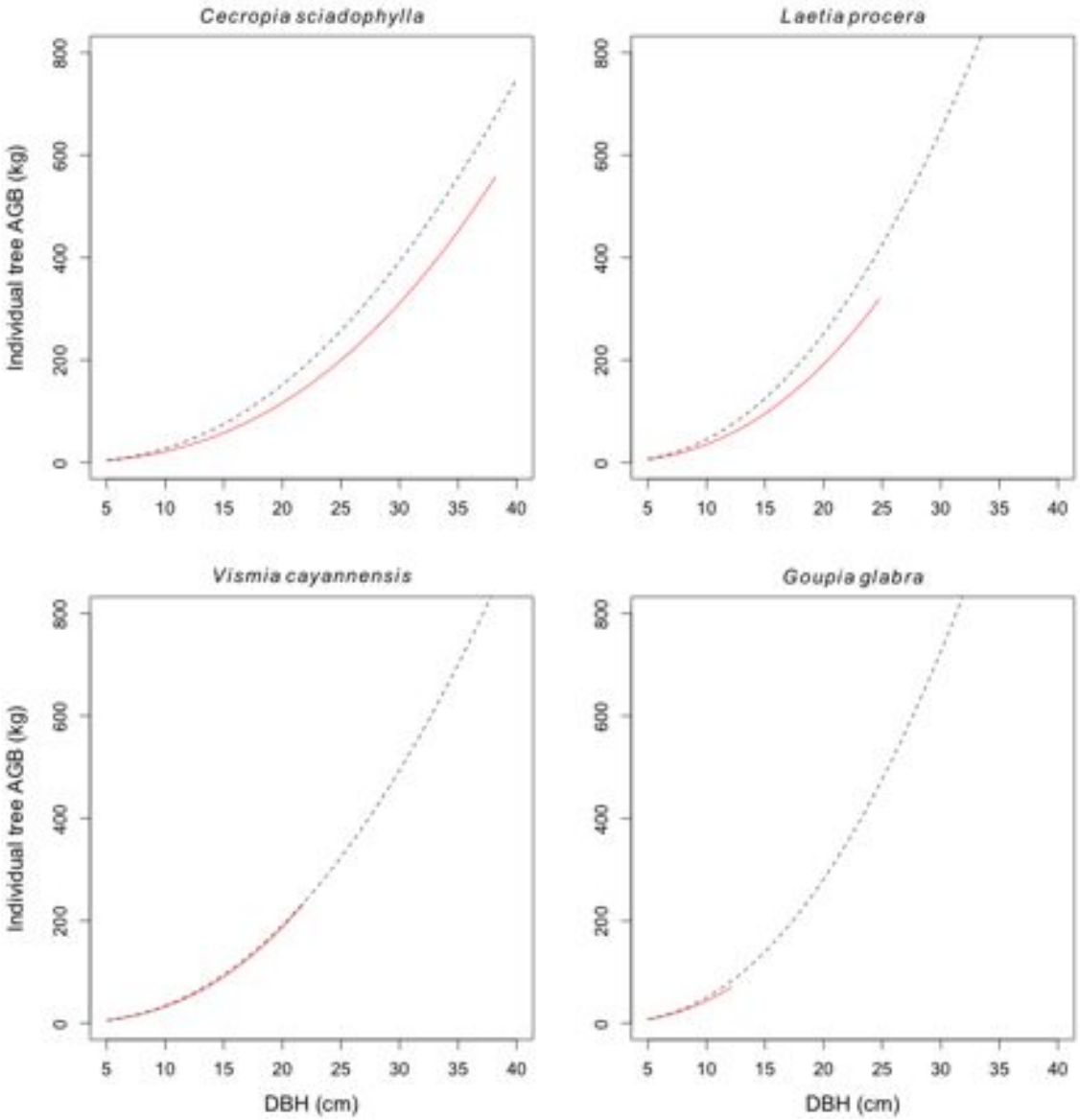

Figure 5.3: Comparison between the locally derived species specific allometric models for trees found north of Manaus (red line, Nelson et al. (1999)) and the pan-tropical allometric model (dotted line, Chave et al. (2014)). The locally derived model was only applied to the DBH range from which it was parameterised. Where height is used to calculate AGB it is calculated as a function of DBH in the E & C Amazonia model proposed by Feldpausch et al. (2012).

5 and 29 were on the perimeter of an INPA BDFFP fragmentation study site and as a result plot 29 was classified as mature forest in Chapter 4. Plot 5 was <50 m from the SF edge and as a result contained remnant mature forest trees when compared to DBH growth rates in the area (da Silva et al., 2002). Plot 45, measured in 1995, was not encompassed by the area classified in Chapter 4.

5.4 Results

Table 5.5 summaries the age; land use histories derived in chapter 4; sampling year and estimated structural properties for each plot. Stand age was between 2 and 37 years (mean = 17, median = 12). Density of stems >5 cm ranged from 880 to 4380 stems ha^{-1} (mean = 2012 stems ha^{-1}, median = 1930 stems ha^{-1}). Mean DBH (avDBH) per plot ranged from 6.3 to 16.6 cm (mean = 11.4 cm, median = 11.4 cm). Basal area ranged from 2.1 to 58.0 m^2 ha^{-1} (mean = 24.6 m^2 ha^{-1}, median = 20.3 m^2 ha^{-1}). Above ground biomass (AGB) ranged from 15.0 to 235.3 Mg ha^{-1} (mean = 132.1 Mg ha^{-1}, median = 128 Mg ha^{-1}).

Table 5.5: Summary of field data gathered from secondary forests located north of Manaus. Age, PALU and FC are derived in Chapter 4. Stem density, avDBH and BA only included the transect measuring stems with a DBH ≥5 cm. Plot 45 was outside the area classified in Chapter 4. Letters next to plot numbers indicate repeated measurements of the same plot within GPS error and the limits of accessibility.

Plot ID	Year sampled	Age (years)	PALU (years)	FC	Stem density (stems ha^1)	avDBH (cm)	BA (m^2 ha^{-1})	AGB (Mg ha^{-1})
1	1993	10	1	1	1750	12.4	27.7	174.1
2a	1993	10	1	1	1250	14.3	26.5	181.4
3a	2014	31	1	1	1400	14.3	22.74	171.9
4	1993	10	1	1	1620	11.6	22.7	138.5
5	1993	1	1	1	1630	12.0	24.4	158.2
6b	1993	10	1	1	1520	12.4	24.5	157.8
7b	1995	12	2	1	1570	12.0	24.6	161.7
8	1993	4	2	2	1330	6.3	4.2	15.0
9	1995	6	2	2	3070	7.9	16.5	59.6
10	1993	10	2	1	2010	10.1	20.2	98.7
11	1993	10	2	1	2660	10.2	26.1	139.2
12c	1993	10	2	1	2350	9.9	23.2	116.7
13c	1995		2	1	2140	10.5	25.22	132.6
14d	1993	8	11	1	2020	10.4	19.9	80.2
15d	1995	10	11	1	1920	10.7	20.6	84.1
16d	2014	29	11	1	1590	14.8	26.1	205.9
17e	1993	16	1	1	2010	10.8	23.7	139.0
18e	1995	18	1	1	1940	10.9	23.1	130.9
19e	2014	37	2	1	1590	14.8	35.5	235.3
20f	1993	8	9	2	2510	8.9	17.6	99.6
21f	1995	10	9	2	2320	9.4	18.7	101.1
22f	2014	29	3	1	1420	15.2	25.1	226.2
23g	1993	10	2	1	2010	10.5	22.2	120.0
24g	1995	12	2	1	1980	10.4	21.5	117.0
25	1993	2	1	1	880	8.7	5.7	32.5
26h	1993	2	3	4	1570	13.0	30.9	174.0
27h	1995	4	3	4	1600	13.9	35.7	208.5
28	1993		7	2	1690	12.9	37.3	216.2
29	1995	1	7	1	2590	9.2	18.7	107.5
30	1995	12	2	1	2030	10.5	22.3	107.1
31	1995	12	7	1	2370	9.7	22.5	114.8
32i	1995	12	6	1	4310	7.8	23.2	88.4
33i	2014	31	6	1	2450	12.5	30.0	195.5
34j	1995	12	7	1	4380	7.9	23.5	86.1
35j	2014	31	7	1	2030	13.3	26.7	179.4
36	1995	12	6	1	2160	10.6	23.8	137.1
37k	1995	12	2	1	2490	9.6	24.1	123.8
38k	2014	31	2	1	1950	12.8	27.5	170.6
39	1995	10	1	2	1570	12.4	23.3	142.0
40	1995	10	5	1	2320	9.5	19.1	77.1
41	1995	12	1	1	1700	10.8	18.9	81.3
42	1995	10	4	2	1490	7.0	6.2	28.8
43	1995	12	4	2	1850	11.9	31.1	174.0
44	1995	12	2	1	1520	11.2	20.8	103.7
45	1995	outside study area			2180	9.8	19.4	83.8
46	2014	31	1	1	2300	13.5	36.8	188.6
47	2014	37	2	1	1600	14.4	28.1	232.6
48	2014	23	1	2	1600	13.1	20.6	149.2
49	2014	19	2	3	1850	16.6	62.7	150.3
50	2014	22	1	2	3370	10.3	28.1	121.8
51	2014	25	2	2	1650	13.5	23.0	163.4
52	2014	25	2	2	1710	10.8	14.8	84.6
53	2014	20	1	2	2370	9.2	15.1	71.3
54	2014	29	9	1	1240	14.9	23.3	162.5
55	2014	22	6	2	1800	12.3	21.8	116.93
56	2014	19	7	2	2470	11.4	25.1	167.67
57	2014	19	4	2	1510	15.2	29.6	185.74
58	2014	29	6	2	1690	12.4	18.6	118.16
59	2014	22	4	2	2550	11.0	22.7	126.87
60	2014	15	2	3	2020	10.7	16.7	89.05
61	2014	22	3	2	1780	12.3	19.4	123.09

5.4.1 Height modelling

Perfomance of allometric regression moels for estimating tree height was analysed through comparisons between the observed and predicted tree heights (Figure 5.4). The species specific height models ($R = 0.66$, $RMSE = 8.3$ m) consistently overestimated the observed data and showed the greatest error when simulating height below 15 m. The height model derived from the Regrowth-BR data (DBH range = 5.0–84.0 cm, H range = 2.0–36.0 m, $n = 699$, Equation 5.6) and the Eastern and Central height model (Feldpausch et al., 2012) gave better R (0.77 and 0.77, respectively) and $RMSE$ (3.3 m and 3.5 m, respectively). Therefore, the height model derived from the Regrowth-BR data was used to estimate the height of trees that had not been measured in the field:

$$H = exp(0.33724 + 1.24032 \times ln(D) - 0.13187 \times ln(D)^2) \tag{5.6}$$

where H is tree height (m) and D is diameter at breast height (cm).

5.4.2 Land use history as a determinant of forest recovery

Changes in stand properties with increasing SF age are illustrated in Figure 5.5. As PALU and FC were not correlated to each other, they were used as additional independent variables along with secondary forest age for estimating avDBH, BA and AGB. In SF stands with ages between 2–37 years, regenerating on abandoned pasture and agriculture, increases in avDBH were best explained with a linear multiple regression ($r = 0.74$, error = 13.2%) using age, PALU and FC as independent variables. However the mean error of the estimator was the same as the model that only included age as an independent variable (Table 5.6). Increases in BA and AGB accumulation were best explained by a log-linear multiple regression ($r = 0.70$, error = 19.8 % and $r = 0.77$, error = 24.8 %, respectively) using age with FC for BA and age with PALU and FC for AGB as the independent variables. Figure 5.6 demonstrates the improved estimation of AGB by the multiple regression model as independent variables PALU and FC are added. Age was the most significant predictor in all the models, followed by FC. PALU was not a significant predictor (Table 5.6). The rate of increase of each parameter is

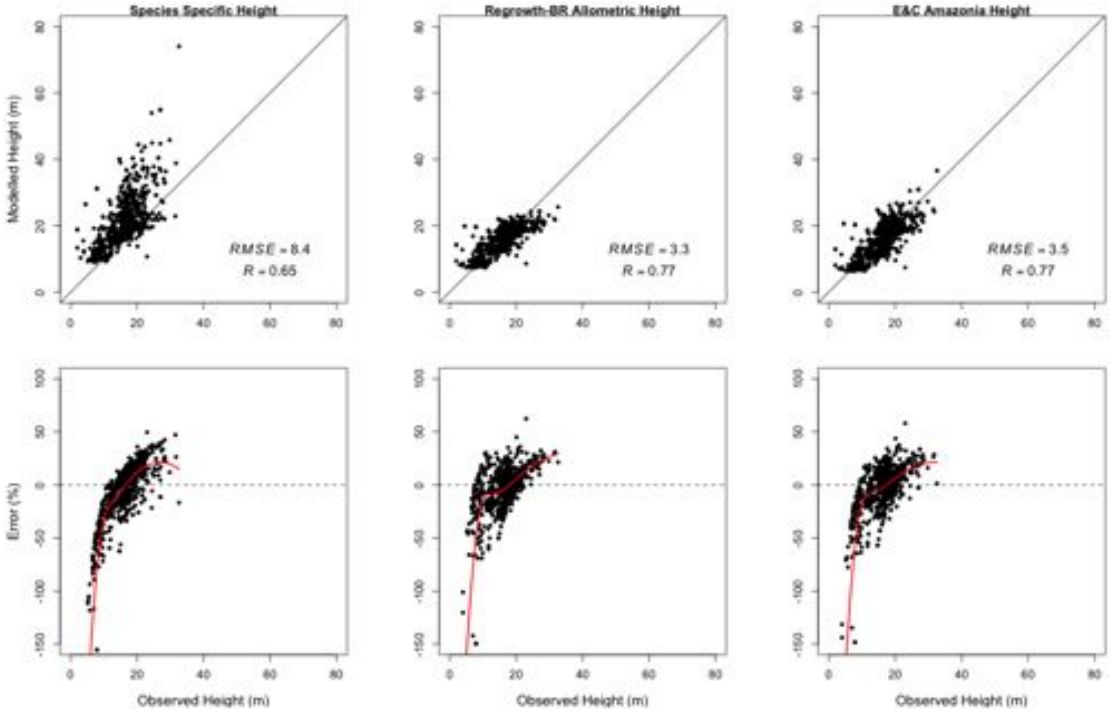

Figure 5.4: Goodness-of-fit for the allometric height (H) models. (First row) H as estimated from each model vs. observed H (n = 696), compared with the 1:1 line (solid line). (Second row) Relative error (estimated minus observed H, divided by observed H, in %); the thick red line represents a locally weighted scatterplot smoothing (LOWES) regression of the data points, illustrating a negative bias for H values <15 m in the species specfic models and <10 m in the other models tested.

shown in Table 5.7. No appropriate model could be fitted to stem density.

Table 5.6: Regression models for indirect estimates of mean diameter at breast height (avDBH, cm), basal area (BA, m^2 ha^{-1}) and above ground biomass (AGB, Mg ha^{-1}) of trees with DBH ≥5 cm in secondary-forest plots with the following independent variables: age of secondary forest (years), period of active land use prior to abandonment (PALU, years) and frequency of vegetation clearance (FC). Bold indicates the regression models that produced the best fit for each forest variable.

Independent variable	Regression equation for mean diameter at breast height (cm)	r	Standard error of the regression	Significance level (p value) Age	PALU	FC
Age	$avDBH = 8.43177 + (0.17212 \times age)$	0.73	13.2 %	<0.0001	-	-
Age and PALU	$avDBH = 8.64933 + (0.17292 \times age) - (0.06258 \times PALU)$	0.73	13.3 %	<0.0001	>0.1	-
Age and FC	$avDBH = 9.1399 + (0.1716 \times age) - (0.5116 \times FC)$	0.74	13.2 %	<0.0001	-	>0.01
Age, PALU and FC	$\boldsymbol{avDBH = 9.34847 + (0.17235 \times age) - (0.06158 \times PALU) - (0.50766 \times FC)}$	**0.74**	**13.2 %**	**<0.0001**	**>0.01**	**>0.01**
	Regression equation for basal area (m^2 ha^{-1})					
Age	$BA = 5.517 + 6.338 \times ln(age)$	0.61	21.6 %	<0.0001	-	-
Age and PALU	$BA = 5.9198 + (6.3872 \times ln(age)) - (0.1444 \times PALU)$	0.62	21.7 %	<0.0001	>0.1	-
Age and FC	$\boldsymbol{BA = 10.669 + (6.415 \times ln(age)) - (3.923 \times FC)}$	**0.70**	**19.7 %**	**<0.0001**	**-**	**<0.01**
Age, PALU and FC	$BA = 11.0447 + (6.4613 \times ln(age)) - (0.1382 \times PALU) - (3.9159 \times FC)$	0.70	19.8 %	<0.0001	>0.1	<0.01
	Regression equation for above ground biomass (Mg ha^{-1})					
Age	$AGB = -31.17096 + (60.61249 \times ln(age))$	0.71	26.8 %	<0.0001	-	-
Age and PALU	$AGB = -25.893 + (61.251 \times ln(age)) - (1.893 \times PALU)$	0.72	26.7 %	<0.0001	>0.1	-
Age and FC	$AGB = 2.398 + (61.110 \times ln(age)) - (25.563 \times FC)$	0.76	25.0 %	<0.0001	-	<0.01
Age, PALU and FC	$\boldsymbol{AGB = 7.436 + (61.733 \times ln(age)) - (1.852 \times PALU) - (25.467 \times FC)}$	**0.77**	**24.8 %**	**<0.0001**	**>0.1**	**<0.01**

The best model for indirectly estimating avDBH overestimated the avDBH for all forests with an avDBH ≤9 cm ($RMSE$ = 2.7 cm). BA was overestimated below 14 m^2 ha^{-1} ($RMSE$ = 7.3 m^2 ha^{-1}). AGB was distributed evenly either side of the 1:1 line ($RMSE$

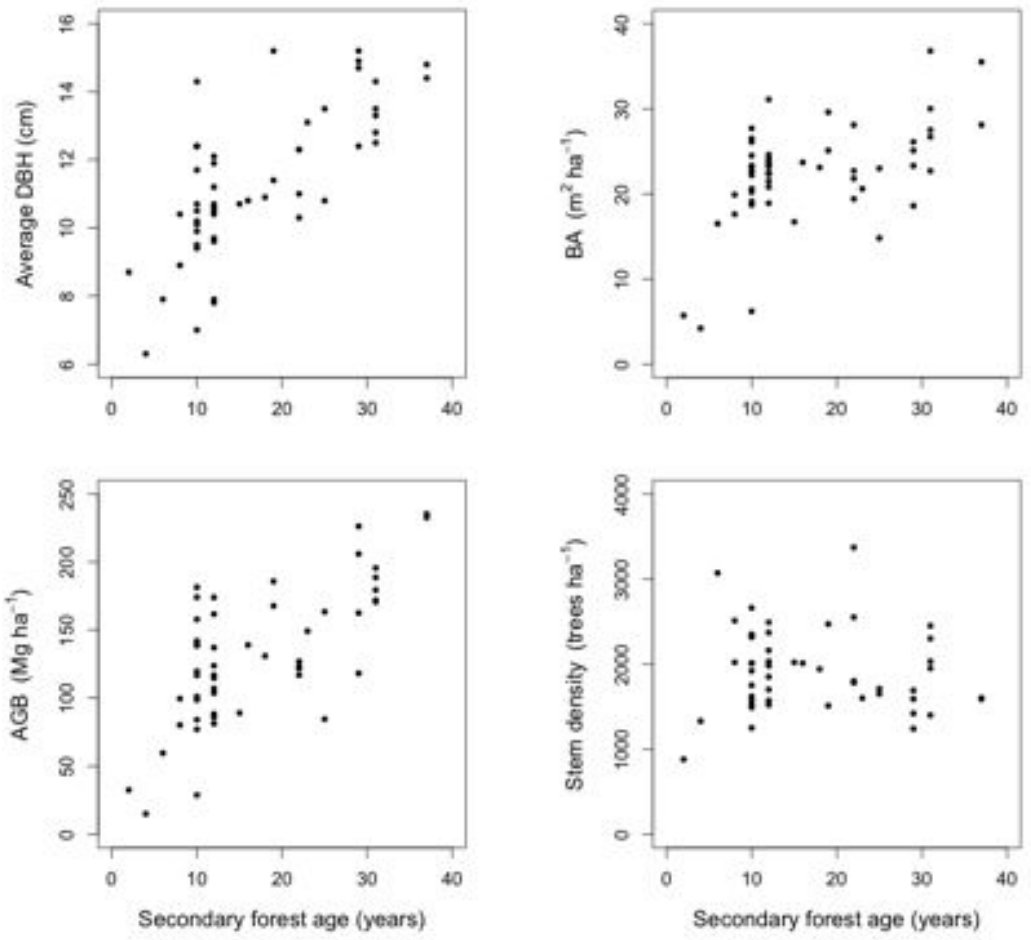

Figure 5.5: Relationship between the estimated stand parameters from trees with a DBH ≥5cm DBH and secondary forest (SF) age in 55 SF plots north of Manaus.

Table 5.7: Growth rates of avDBH, BA and AGB estimated from the best fit regression models (Table 5.6).

Increase per year	**0–5 years**	**0–10 years**	**0–20 years**	**0–37 years**
avDBH (cm y^{-1})	0.138	0.158	0.163	0.167
BA (m^2 ha^{-1} y^{-1})	2.04	1.46	0.95	0.62
AGB (Mg ha^{-1} y^{-1})	13.3	10.8	6.4	5.05

= 61.7 Mg ha^{-1}). Poor estimation of the forest stand parameters was inferred when the residual from the modelled estimate was outside the *RMSE* range. This occurred in plots 2 and 57, whose avDBH was greater than others of the same age, and plot 42, whose avDBH was smaller than others of the same age. For BA and AGB this occurred in plots 43 and 52, whose BA and AGB were greater than others of the same age, and plot 42, whose BA and AGB were smaller than others of the same age. All regression models showed the greatest errors in the lower ranges of their distributions (Figure

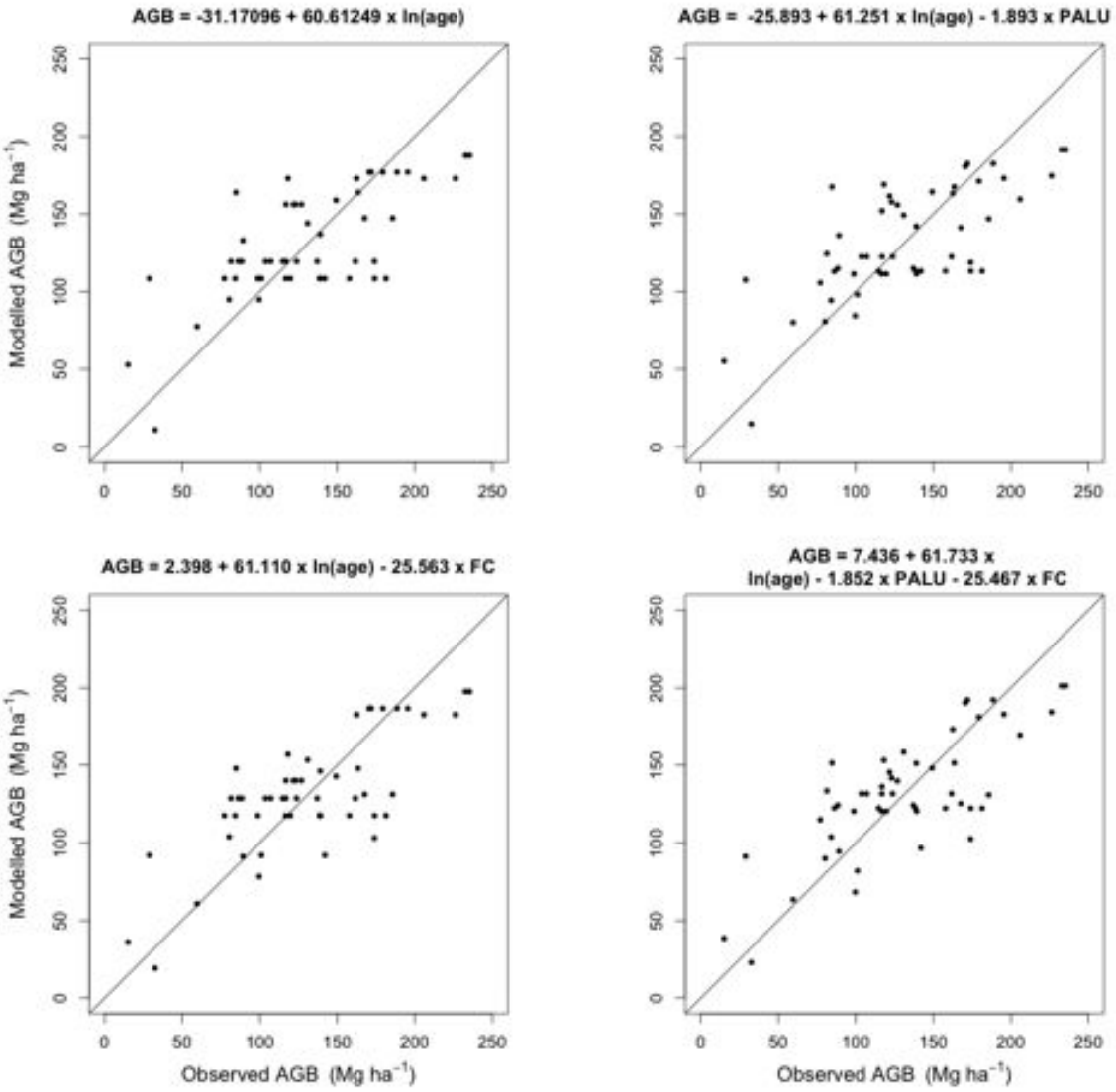

Figure 5.6: Comparison of log-linear regressions for the indirect estimation of AGB in secondary forests using different combinations of age and land use history metrics as independent variables.

5.7).

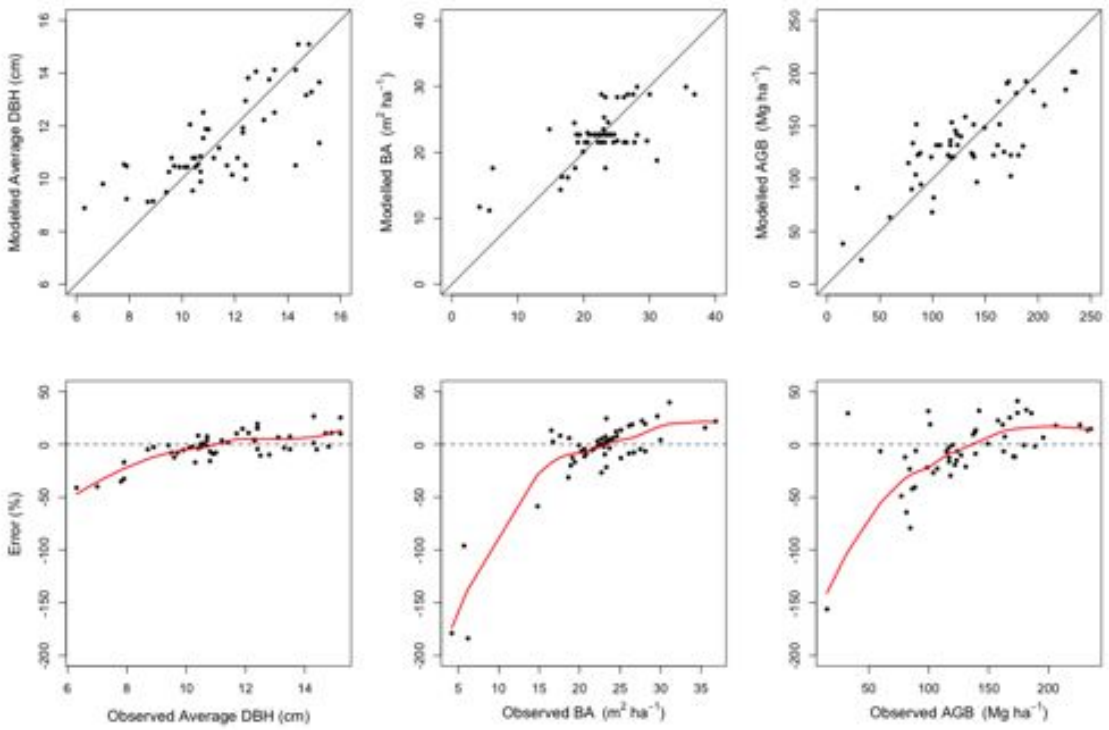

Figure 5.7: Comparison of observed avDBH, BA and AGB with data predicted using the best fit regression models.

When subsetting the data by FC a greater r value is achieved between age and BA than subsetting by PALU. However, avDBH and age have a higher correlation coefficient when PALU is ≥3. Subsetting the data by PALU provides the best prediction for stem density (Table 5.8).

Table 5.8: Comparison in subsetting the data by frequency of clearance (FC) and period of active land use (PALU, years) on the correlation of independent variables with secondary forest age using the best fit models regression models. The best r values for each variable are in bold.

Independent variable	**Correlation coefficient (r) for variable in relation to secondary forest age**			
	FC = 1x	**FC ≥2x**	**PALU ≤2 years**	**PALU ≥3 years**
avDBH	0.72	0.75	0.72	**0.78**
BA	**0.77**	0.51	0.69	0.48
AGB	**0.80**	0.61	0.73	0.74
Stem density	0.02	0.05	**0.15**	**0.34**

Despite these differences in r between the two subsets Figure 5.8 illustrates that there is no statistical difference in estimated AGB between either method of subsetting the data as evidenced by the overlapping 95 % confidence intervals. This lack in separability was evident in avDBH, BA and stem density (Appendix Figures A.2 and A.1).

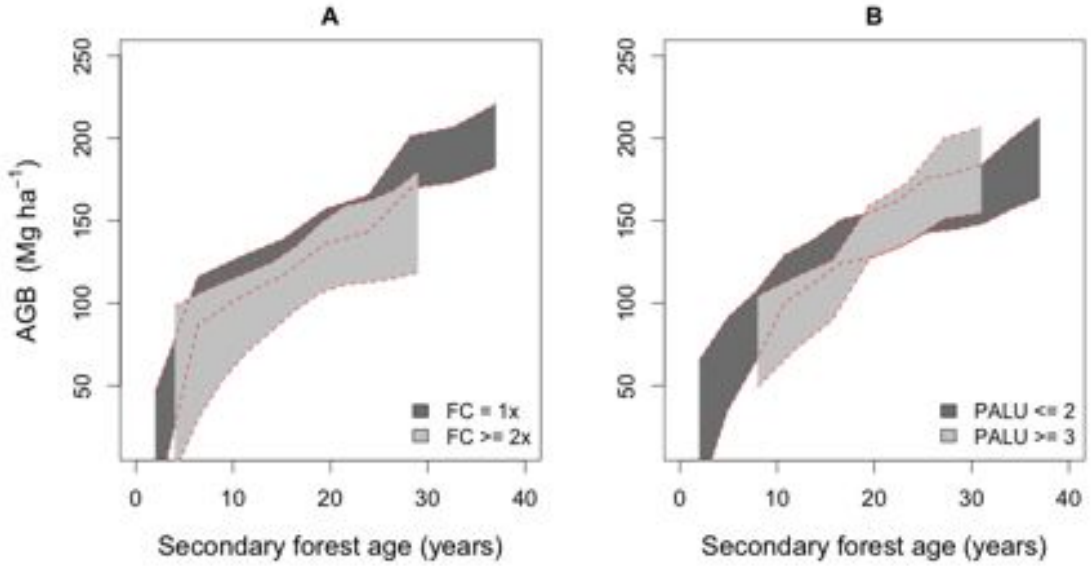

Figure 5.8: Lack of separability of AGB between different land use history subsets A) frequency of clearance (FC) and B) period of active land use (PALU). Illustrated by the overlapping 95% confidence intervals of a linear-log regression.

5.5 Discussion

The rate of AGB accumulation was in agreement with the majority of other studies into SFs. The only exception occurred in the first 5 years where the rate of accumulation in this study and Feldpausch et al. (2004) (16.4 Mg ha^{-1} y^{-1}) was more than double that found in SF regenerating on pasture (5.2 Mg ha^{-1} y^{-1}) and almost double that found in SF regenerating on 'slash and burn' (8.4 Mg ha^{-1} y^{-1}) north of Manaus (Wandelli and Fearnside, 2015). Whilst this chapter and Feldpausch et al. (2004) sampled 0.2 ha and 0.03 ha, respectively and used allometric relationships based on other datasets to derive AGB, Wandelli and Fearnside (2015) used destructive methods to create local allometric equations from which AGB could be estimated for 1 ha plots. In addition, the land use history for each plot studied by Wandelli and Fearnside (2015) was obtained from interviews of land owners and their neighbours, although a common technique (e.g. Uhl et al., 1988; Moran et al., 2000; Kong et al., 2009; Jakovac et al., 2015) this information is subjective and potentially vulnerable to human error. Land use history gathered from optical satellite data cannot provide information on land use type and clearance method as it is limited by the lack of continuous cloud free observations in the tropics. However, these data are objective and their accuracy can be quantified. AGB accumulation rates were derived from regression models. In these models under and over prediction of stand parameters occurred in the tails of the secondary forest age distribution where there were fewer data points. These errors come as a result of the plot sampling and stratification. Whilst there was a sampling scheme in place for the Regrowth-BR field campaign (2014) the initial data collection in 1993 and 1994 was done without prior knowledge of forest age and land use history. This resulted in clustering of points in intermediate age (10–20 yr) stands. This under sampling of the extremes of the secondary forest age present may cause misrepresentation of growth rates in younger and more mature forests.

The rate of AGB accumulation in the first 10 years in this chapter (10.8 Mg ha^{-1} y^{-1}) was similar to that observed in SF, with similar light to moderate land use histories, after 8–12 years of regrowth near Manaus and elsewhere in the BLA (9.1–11 Mg ha^{-1} y^{-1}) (Uhl et al., 1988; Brown and Lugo, 1990; Steininger, 2000; Feldpausch et al., 2004). AGB accumulation for the first 20 years (6.4 Mg ha^{-1} y^{-1}) was similar to SF of similar

ages (16–20 years) in Rondônia (6.4–7.9 Mg ha^{-1} y^{-1}, Alves et al., 1997) and two reviews of SF AGB accumulation up to 20 years (6.17 Mg ha^{-1} y^{-1} and 6.1 Mg ha^{-1} y^{-1}, Silver et al., 2000b; Poorter et al., 2016, respectively).

The rate of AGB accumulation declined over the 37 years of regrowth studied, this plateauing occurs when the mortality of pioneer trees is balanced by the recruitment of new trees and higher fractions of the total biomass are invested in non-productive tissues (Chazdon, 2012). However, after 37 years AGB accumulation (5.05 Mg ha^{-1} y^{-1}) was still greater than that found in mature forests (3.8 Mg ha^{-1} y^{-1}) in the study site (Vieira et al., 2004). Final estimates of AGB after 37 years of regrowth (up to 235.3 Mg ha^{-1}) were 66% of the mean AGB (355.8 ± 47.0 Mg ha^{-1}) of mature forests near Manaus (Laurance et al., 1999). This is in contrast to Houghton (2010) and Ramankutty et al. (2007) who suggested that these secondary forests recover 70 % of their original biomass in the first 25 years. Forests studied in this chapter could take more than 250 years to reach similar mature forest values of AGB with current growth rate trajectories.

Stems with DBH 0.1 – 4.9 cm were exclded from this study to allow for complete sampling of the land use history distribution in the time available. Carreiras (upublished) showed a consistent (across plot size) between AGB calculated for DBH ≥10 cm and ≥5 cm and DBH and AGB calculated for DBH ≥20 cm and ≥5 cm. The slope of the relationship was similar to the 1:1 line. Not including DBH 5–10 cm gave AGB <≈15 % of the mean AGB when including DBH 5–10 cm. The impact of not including DBH 5–20 cm reduced estimated AGB by ≈55 % compared to the mean AGB of DBH calculated from BDH ≥5 cm. Given these differences it is likely that including DBH ≥1 cmwould increase mean AGB by >15 %. Stem size distribution at this size would be required to provide a more accurate estimate of the imapct of excluding stems <5 cm.

The land use history derived in Chapter 4 only provided minor improvements in the correlation coefficient explaining the increase of AGB with secondary forest age (Table 5.6). The forest plots described in Uhl et al. (1988) and Wandelli and Fearnside (2015) which showed a significant decrease in AGB accumulation, compared with ‘light use or agricultural use sites, were subjected to an average of 6 years PALU and 4 burning events. The highest intensity of land use in this chapter was represented by an average

of 6 years PALU and FC of 1–2× in the moderate to long term use (PALU ≥3) plots. No information on burning or initial clearance technique (e.g. bulldozed in the heavy use sites in Uhl et al. (1988)) was available to this chapter, as mentioned previously. This indicates the importance of information regarding the FC and burning, as this is the main difference between the land use intensity in this chapter and those in Uhl et al. (1988), Wandelli and Fearnside (2015) and Jakovac et al. (2015, 2016).

The final avDBH increment after 37 years of growth (0.167 cm y^{-1}) was similar to the value for mature forests (0.164–0.175 cm y^{-1}) in the study area (da Silva et al., 2002; Vieira et al., 2004). The stem density (1590–1600 stems ha^{-1}) of the oldest plots (19e and 47, 37 years) was more than twice that of mature forest in the study site, 626 stems ha^{-1} (Vieira et al., 2004). This further demonstrates that the oldest secondary forests studied in this chapter are far from resembling local mature forests.

The absence of a relationship between stem density (DBH ≥5 cm) and secondary forest age in this chapter is in opposition to the positive correlation observed for the first 6–10 years of regrowth noted by Lucas and Honzak (2002); Feldpausch et al. (2005, 2007) and Mesquita et al. (2015) north of Manaus. This chapter sampled trees with a DBH ≥5 cm whilst the opposing studies sampled trees with a DBH ≥1 cm and ≥3 cm and thus included higher numbers of saplings in these young secondary forests (Montgomery and Chazdon, 2001). This may explain the differences between stem densities of plots with 31 years of regrowth (38k and 33i, 1950–2300 stems ha^{-1}) to that observed by Mesquita et al. (2015) in abandoned clearcuts of the same age and land use history (∼3200 stems ha^{-1}).

5.6 Conclusions

This chapter demonstrated that light to medium land use intensity causes no significant differences in secondary forest regrowth rates north of Manaus. Despite this, frequency of vegetation clearance was highlighted as an important remote senisng derived metric which can be used to aid the prediction of biomass recovery. Biomass and structural components require more than 37 years of regrowth before secondary forest resembles mature forest stands in the area. This data will be utilised in parameterisation and validation of a forest growth model in the following chapter.

Chapter 6

Parameterisation and Validation of 3-PG$_2$

6.1 Introduction

Secondary forests accumulate biomass rapidly and their rate of sequestration is an important variable for future land use management and planning. To date the pan-tropical, remote sensing based (Saatchi et al., 2011a; Baccini et al., 2012; Avitabile et al., 2015), and regional (Nogueira et al., 2008) Amazon biomass studies have not explicitly considered secondary forests. This is often because inventory data is not available as there is little monitoring of secondary forests within the Amazon. For example Mitchard et al. (2014) masked secondary forest from their above ground biomass (AGB) estimates, owing to a lack of data for these forest types, by using the extent of intact forest. Saatchi et al. (2011a) and Baccini et al. (2012) applied relationships between remnant forests and remote sensing datasets including optical; SAR and the Ice, Cloud and Land Elevation Satellite (ICESat) Geoscience Laser Altimeter System (GLAS) across the whole of the region. The only property from which to distinguish secondary forests in these datasets would be their height although older secondary forests often exhibit the same height as mature forest (Prates-Clark et al., 2009; Helmer et al., 2009).

Optical datasets show similar reflectance between secondary and primary forests after 16 years of regrowth (Lucas et al., 2000) and relationships between optical radiation

and AGB are weak and limited by near constant cloud cover in the tropics (Kuplich et al., 2005). Airborne L-band SAR data, with 5 m resolution, can predict AGB up to 150 ± 23.8 Mg ha^{-1} in dense tropical rainforest however it loses sensitivity beyond this (Saatchi et al., 2011b). Whilst in combination with X-band data it can detect AGB to 307 ± 50 Mg ha^{-1} (Englhart et al., 2011). It has been demonstrated that airborne P-band SAR, with 10 m resolution, is sensitive to higher levels of AGB, <300 ± 22.6 Mg ha^{-1} (Saatchi et al., 2011b). These airborne sensors cannot, however, be used to monitor the entire tropics continously. The P-band sensor onboard the European Space Agencys (ESA) BIOMASS mission will provide greater spatial coverage, however its 200 m resolution is insufficient for characterising small patches of secondary forest. Analysis of SAR texture metrics has produced strong relationships with AGB, although further investigation is needed for remote sensing to reach its full potential as a source of useful information demanded by programmes such as UN REDD+ (Cutler et al., 2012). A modelling approach is well placed to address this knowledge gap through the study of changes in secondary forest biomass derived from field observations and physiological process understanding. In addition, modelling provides the opportunity to forecast changes in biomass accumulation whereas remote sensing and interpolation techniques can only provide estimates of past AGB.

This study is focused on modelling forest growth at the stand scale to best understand the biomass accumulation of individual secondary forest stands. There are many physiologically process-based forest growth models that have been parameterised for temperate and tropical forests which operate at this scale (Nightingale et al., 2004). Of these models the majority have been parameterised for, and applied to, forests and plantations within temperate broadleaf and boreal coniferous forests (Potithep and Yasuoka, 2011; White et al., 2000). With work also focusing on pine and *Eucalyptus* in New Zealand, Australia, Africa, South America, Europe (Landsberg et al., 2001; Rodríguez et al., 2002; Sands and Landsberg, 2002; Almeida et al., 2004b; Dye et al., 2004; Rodríguez-Suárez et al., 2010). The majority of applications to tropical forest using this type of model has been in Asia (Dislich et al., 2009; Kammesheidt et al., 2011; Dislich and Huth, 2012; Hartig et al., 2014; Pütz et al., 2014) with fewer studies focusing on the tropical rainforests of South America (Hirsch et al., 2004; White et al., 2006).

Process-based forest growth models are designed to investigate the effects of climate; soil water; air pollutants; rooting characteristics and nutrient uptake on stand growth. Importantly for this study they calculate the carbon balance of the stand as a result of photosynthesis and respiration i.e. net primary productivity (NPP). This is added to through the simulation of community dynamics such as recruitment and mortality; growth parameters; biomass accumulation and calculation of the hydrological balance to understand water stresses. This thesis is focused on the potential biomass accumulation in secondary forests and as such will seek to utilise a scalable model which encompasses one of the main processes of regrowth in tropical rainforests, rapid biomass accumulation (Brown and Lugo, 1990). Table 6.1 provides a summary of models which have been implemented in tropical forest to estimate above ground biomass and structural properties.

Table 6.1: Forest growth models which have been implemented in the tropics to study biomass and/or structural changes during succession.

Model name	Distance dependent	Empirical	Gap model	Succession model	Mixed-species	Process based	Single species	Stand level	Tree-based	Source
3-PG						•	•	•		Landsberg and Waring (1997)
FORMIX3			•		•				•	Köhler and Huth (1998)
JABOWA			•							Botkin et al. (1972)
OUTENIQUA			•		•	•			•	Van Daalen and Shugart (1989)
SYMFOR	•	•		•						Phillips and van Gardingen (2001)
TROLL	•				•	•				Chave (1999)

Gap models simulate the process of natural succession that occurs in tree fall gaps after the mortality of a large canopy dominating tree produces gaps in the forest canopy. This leads to the release of suppressed trees and increased tree recruitment rates, both of which drive succession. The JABOWA model (named after the initials of its authors) (Botkin et al., 1972) is the parent model of all forest gap models (Bugmann, 2001). In JABOWA the forest is assumed to be a composite of many small stands, each of a different age and successional stage. These patches are vertically homogeneous and all tree crowns extend horizontally across the entire patch. The distribution of leaves is also considered homogeneous and are located in an indefinitely thin layer at the top of the stem. The processes of succession can be described separately as the forest is a mosaic

of independent patches with no interaction between patches (Bugmann, 2001).

The individual-based mixed rainforest growth simulator (FORMIX3) (Bossel and Krieger, 1991), and the later FORMIND (Köhler and Huth, 1998), models simulate forest dynamics on an individual tree-by-tree basis. The rainforest model FORMIX3 (Huth et al., 1998) aggregates tree species in functional groups on the basis of their potential height and light demands. These are: fast growing light demanding pioneers; shade tolerant intermediate successional species and tall, slow growing mature forest species. These gap models describe individual tree growth; competition between neighbouring trees and the whole forest's dynamic within the context of a carbon balance model. The model constrains forest growth by the effect of varying light conditions in the different canopy layers and location in the forest, and through biomass consumption and losses. Whilst each individual tree in the model competes for light and space (Huth et al., 1998). In much the same way as the JABOWA model, the shifting stand mosaic of natural forests, created by tree fall gaps, is represented explicitly within the model. To perform these estimates for individual trees in forest stands of 1 ha, the model requires data on stem number distribution for species in each of the functional groups for parameterisation. These distributions will change in a secondary forest as succession progresses (Uhl et al., 1988). Therefore the distribution of stem numbers in each functional group will vary depending on the time of sampling. As these models considered each individual tree they require intensive parameterisation owing to their representation of multiple functional groups, and are computationally intensive when applied over multiple stands. FORMIX3 has been extensively tested and applied to tropical forests in Panama, Malaysia, French Guyana, Venezuela, Mexico, Brazil (Atlantic Forest), Madagascar and Paraguay. The majority of these studies have focused on natural succession following disturbances such as selective logging or similar harvesting and impacts of fragmentation on the carbon and hydrological balances (Rüger et al., 2007; Groeneveld et al., 2009; Pütz et al., 2011, 2014; de Paula et al., 2015). Whilst others focus on its use for the study of structural changes (Fischer et al., 2015) and the effects of disturbance on biodiversity (Köhler and Huth, 2007).

The physiological principles predicting growth (3-PG) model was developed by Landsberg and Waring (1997) for use in *Eucalyptus globulus* plantations. It is a stand-level model that requires readily available site and climate data as inputs and predicts stand

development at a monthly-time step. An important aspect of the 3-PG model is that it is point based, representing a homogeneous 1 ha forest stand, and it is therefore more computationally viable to process large areas using 3-PG than gap models such as FORMIX3 during which each individual tree is modelled.

Since its inception it has been utilised to model *Eucalyptus* plantations across the globe. Originally developed in plantations in Australia and New Zealand (Landsberg and Waring, 1997), it has since been used throughout countries in Africa (Dye et al., 2004), South America (Almeida et al., 2004b) and Europe (Tomé et al., 2004; Rodríguez-Suárez et al., 2010) to estimate *Eucalyptus* plantation growth. It has also been used to estimate forest properties in other fast-growing forests and forest plantations such as *Picea sitchensis* and *Salix* in Great Britain (Waring, 2000; Surendran Nair et al., 2012), *Pinus radiata* in Australia (Coops et al., 1998), *Pinus contorta* and *Pinus taeda* in the United States (Landsberg et al., 2001).

Although 3-PG has been used extensively in Brazil to simulated the growth of *Eucalyptus* plantations (e.g. Almeida et al., 2003, 2004a,b, 2007a,b), there has only been one study that seeks to model the productivity of tropical rainforest in Brazil. White et al. (2006) estimated the NPP of forested and deforested areas in the basin using 3-PG. This produced estimates that were comparable with NPP derived from the 1 km MODIS photosynthetically active radiation (fPAR) product. This study covered a large area however, in which typically small secondary forest patches are not well characterised in 1 km MODIS data (Lucas et al., 2002).

3-PGS (3-PG Satellites) is a simplified version of 3-PG which derives NPP estimates from monthly estimates of fPAR absorption. This is calculated from the red and near infrared (NIR) reflectance bands of remotely sensed data. To acquire this data at the appropriate time scale a sensor with a high temporal resolution is required such as Advanced Very High Resolution Radiometer (AVHRR) normalised vegetation index (NDVI), MODIS fPAR product, Landsat, SPOT or Sentinel 2. Secondary forest plots are commonly <100 ha and are therefore badly characterised by the coarse resolution (1 km) of the AVHRR NDVI and MODIS fPAR products. The finer spatial resolution of the Landsat, Sentinel 2 and SPOT sensors (30 m, 20 m and 25 m respectively) have been shown to be applicable in characterising the extent of small areas of secondary

forests (e.g. Carreiras et al., 2014). Landsat data has been gathered for >30 years whilst the SPOT archive only begins in 1986. However, cloud free observations in Brazil's wet season (October and March) are highly unlikely (Sano et al., 2007). Thus preventing monthly or annual estimates of NPP.

Nightingale et al. (2008b) parameterised and calibrated 3-PG and 3-PGS to estimate the NPP of mixed species restoration, plantation and old-growth rainforests in Queensland, Australia achieving an R^2 >0.95 for all of modelled outputs when compared to field measurements. These versions of 3-PG were chosen for this application because of their flexibility, relative simplicity and reasonable requirements in terms of parameter values (Almeida et al., 2004b). In 3-PGS, if NDVI (0.0–1.0) $\leq$0.2, fPAR = 0 and if NDVI $\geq$0.75 then fPAR = 0.95 (Nightingale et al., 2008b). Regenerating forests attain a leaf area index (LAI) >4 after nine years of regrowth (Lucas et al., 2002), this results in an NDVI >0.75 (Zarco-Tejada and Ustin, 2001). This makes the simplified 3-PGS unsuitable for modelling secondary forest growth in the Brazilian Amazon.

Despite few examples of the use of 3-PG in tropical rainforests this type of model can be applied to various environments and species (Potithep and Yasuoka, 2011). Furthermore, Landsberg et al. (2003) showed that the 3-PG model is robust and reliable and can be used with confidence to predict growth in areas where trees have not been grown recently. This is relevant in the context of abandoned agricultural sites in the Brazilian Amazon. The flexibility of 3-PG was demonstrated by Bryars et al. (2013), who showed that fixed physiological parameters in 3-PG can produce accurate estimates for single species pine plantations in different geographic regions. This flexibility allows for application of the model at large spatial scales providing forest types are similar in each location.

3-PG$_2$ is an updated version of 3-PG. The main changes in 3-PG$_2$ are to the model's water balance sub model, particularly the rainfall interception; soil evaporation and water movement in the soil sub-models. Several studies have shown that the water balance model in 3-PG required improvement to provide more realistic results (e.g. Almeida et al., 2003; Feikema et al., 2007). Water movement in the 'root zone' and 'non-root zone' is modelled by considering root system development and distribution in the soil profile (Almeida et al., 2007a). In 3-PG$_2$ it is possible to take into account

possible effects from changes in ambient CO_2 on production and transpiration. This is an important development that may allow the model to be used to estimate responses in forest growth to increased concentrations of anthropogenic atmospheric CO_2. Although it has been hypothesized that enhanced growth rates through CO_2 fertilisation may be the cause of increased mortality rates in tropical rainforests through poor structural maintenance alongside rapid growth (Brienen et al., 2015).

6.1.1 Sensitivity Analysis

Before adjusting the parameters of 3-PG$_2$, the application of a sensitivity analysis (SA) will identify those parameters which are most important and therefore require the most precise estimation. Model sensitivity is defined as the standard deviation of output X (σ_{Xp}) with respect to parameter(p) as:

$$\sigma_{Xp} = \frac{\delta X}{X} / \frac{\delta p}{p} \tag{6.1}$$

i.e. the ratio of fractional change in output to fractional change in the parameter (σ_{Xp}) is calculated by running the model for a range of δp for each p (Saltelli et al., 2004). The use of positive and negative values for δp are used to capture possible non-linearity in the model outputs. The process can be repeated for sites with radically different environmental (climactic and physical) conditions to capture any variability introduced through interaction of these variables with p.

σ_{Xp} can be divided into main effects and joint effects. Main, or primary, effects are those direct interactions between δp and δX. Joint effects are caused by interactions between two or more parameters which can cause a greater δX than through varying each parameter individually.

A sensitivity analysis is capable of providing information on a model's sensitivity on several layers. Structural sensitivity is defined by how sensitive the performance of the model is to structural assumptions, or processes, it includes. Parameter sensitivity is the response shown in the model's performance to the values of parameters that characterise relationships included in the model. Finally, the sensitivity of the model's performance to variations in the data required to drive the model, such as climatic and

environmental variables, is known as the input sensitivity.

Sensitivity analyses are vital for the validation model structure. A SA that indicates that the majority of parameter sensitivity lies within the primary interactions demonstrates a good model structure (Sobol, 2001). Performing a SA is a key step in refining parameter selection (Landsberg and Sands, 2010). In the case of PROMOD, a process based forest growth model, the results of multiple sensitivity analyses have been invaluable in strengthening the acceptance of the model's structure an enhancing understanding of it's behaviour. Sensitivity analyses have been used to facilitate adaptation of the model to novel situations or species e.g. PROMOD for *Eucalyptus nitens* and *P. radiata* (Sands et al., 2000).

There are two methods of SA. Local SA test the model output sensitivity by varying one parameter at a time whilst the others remain at their central values ('one factor-at-a-time', OAT). Several local SA have been carried out on 3-PG (Battaglia and Sands, 1997; Sands and Landsberg, 2002; Almeida et al., 2004b; Esprey et al., 2004; Almeida et al., 2007a). The combination of these studies does not cover the full parameter space of 3-PG as each individual study only tested the effect of varying 9–27 of the model's 60 parameters. These parameters were selected for their contribution to specific aspects of 3-PG, namely those characterising canopy structure and canopy quantum efficiency; allometric relationships and biomass partitioning; branch and bark fractions; basic wood density; litterfall and root turnover rates and various environmental modifiers. These affect 3-PG$_2$ outputs in various ways. Some parameters only influence a subset of outputs, whilst many affect most outputs and, in some cases, combinations of parameters interact in their effects. These OAT methods are only informative at the central point where the calculation is executed and does not cover the whole input parameter space (Song et al., 2012). Therefore, they are unsuitable for analysing complex biophysical process models comprised of several dimensions and non-linear responses (Saltelli and Annoni, 2010) as they cannot quantify the effects of parameter interaction.

The elementary effects method or 'Morris Method' (Morris, 1991) determines which input factors may be considered to have effects which are (a) negligible, (b) linear and additive, or (c) non-linear or involved in interactions with other factors (feedbacks). It is used to reduce the number of parameters to be analysed in a more detailed SA

of a computationally costly model, or a model such as 3-PG$_2$ with a large number of inputs.

A preferable SA technique is a model-independent global SA. In a global SA the effect of each parameter within the full parameter space is considered. This is achieved by changing the value of all input parameters in each simulation. This captures the variation in outputs with respect to the multiple input variation. These methods also allow examination of interactions between parameters when varied simultaneously. Common variance based global SA techniques include: Fourier amplitude sensitivity analysis (FAST) (Cukier et al., 1975; Saltelli et al., 1999), the Sobol method (Sobol, 2001; Saltelli, 2002; Saltelli and Annoni, 2010), Saltelli's method (Saltelli et al., 1999), the Derivative-based Global Sensitivity Measure (DGSM) (Sobol and Kucherenko, 2010) and the Bayesian Analysis of Computer Code Outputs (BACCO) sensitivity analysis, which creates a model emulation (Oakley and O'Hagan, 2004). These variance based techniques work within a probabilistic framework by decomposing the variance of the model output into fractions that can be attributed to individual inputs or groups of inputs. The percentages by which each input affects the output, can be used as a measure of sensitivity. In these methods importance of a model input is based on the expected reduction in the model output variance provoked by knowing the value of the model input with certainty.

In a Sobol SA these measures of sensitivity are expressed as (Sobol) sensitivity indices (SIs). This method utilises Monte Carlo (or quasi-Monte Carlo) to sample the entire parameter space requiring thousands of model simulations. Despite these high computational demands, this powerful SA technique has recently become more popular in forest growth modelling (e.g. Wu et al., 2012; Wang et al., 2013a), because of its ability to incorporate parameter interactions and its relatively straightforward interpretation (Nossent et al., 2011).

Although computationally different, the FAST method uses the same measure of sensitivity as Sobol'. The main advantages of FAST is its robustness, especially at low sample size, and its capability in ascribing the output variance to individual inputs in the model. FAST and Sobol are both independent of the model structure. However, FAST is computationally complex for a model with a large number of inputs (Christopher

Frey and Patil, 2002) such as 3-PG$_2$.

The DGSM method relies on averaging local derivatives, the effects of one variable whilst holding others constant, using Monte Carlo or preferably quasi-Monte Carlo sampling methods. This technique is more accurate than the Morris method in computing the elementary effects as each derivative is evaluated as strict local derivatives with small increments in comparison to the variable uncertainty ranges used by the Morris method (Kucherenko et al., 2009). The computational time required for numerical evaluation of DGSM is many orders of magnitude lower than that for estimation of the Sobol sensitivity indices, as the method benefits from much higher convergence rate if quasi-Monte Carlo sampling methods are used. It becomes especially efficient if automatic calculation of derivatives is used (Sobol and Kucherenko, 2010).

These methods require Monte Carlo simulations to sample the entire range of the parameter space. This high computational cost has been a barrier to using these techniques in the past (Verbeeck et al., 2006), however the availability of high-performance computing (HPC) resources have lowered this barrier (Dietze et al., 2013). In the absence of a HPC, a screening technique, e.g. the Morris method, can be applied to reduce the number of parameters under consideration.

The BACCO method uses a Bayesian analysis approach. It builds a statistically based representation of the model from a set of training data points derived from runs of the model of interest. A space-filling algorithm is used to fill in the gaps not sampled in the input parameter space. This model emulation is used to compute the sensitivity indices of interest. This method is designed to be faster, easier and more efficient to run across the entire parameter space than running the model under investigation thousands of times. However, this method requires information on the probability distribution function for each model input to provide a representational emulator designed from only a few hundred runs (Petropoulos et al., 2009).

The sensitivity of ten of the 3-PG$_2$'s outputs, namely: mean DBH (avDBH), basal area (BA), LAI, StandVol, evapotranspiration, fraction of available soil water (fASW) , transpiration and biomass pools, were assessed by Song et al. (2012). Using a variance-based global sensitivity analysis to calculate the elementary effects, this study assessed the impact of key parameters linked to the allocation of biomass in different parts of a

tree; stand volume; leaf area; photosynthesis and water availability; biomass removal and turnover rates in above ground components and root growth. Whilst the majority of SA carried out on 3-PG involve simple regression analysis (Esprey et al., 2004; Zhao et al., 2009; Rodríguez-Suárez et al., 2010) which follow the same procedure as local SA in their 'OAT' sampling and share it's limitations.

6.1.2 Model parameterisation

Parameterisation is the assignment of parameter values from independent data or estimation by adjusting them to optimise fit of the model output to observed data (Almeida et al., 2004a). This process operates directly on the model. It should not be confused with calibration in which an empirical relationship is developed to improve the match of the model output to observed data. It does not affect the model, but operates on its outputs.

To assign species specific or, in the case of mixed regrowth forests, mixed species forest parameter values, a thorough understanding of 3-PG$_2$; the meaning of its parameters and a knowledge of the sensitivity of its outputs to each parameter, is required. This understanding will support the parameterisation of 3-PG$_2$, or any other PBM, to novel species and environments.

Assigning parameter values through mensuration produces a more realistic representation of the system being simulated and should be carried out wherever possible in favour of parameter estimation. For example, 3-PG$_2$ uses an allometric (power) relationship between mean stem mass and mean stem diameter. Supporting data pertaining to this relationship is readily available in the form of published allometric relationships between DBH and AGB (e.g. Brown et al., 1989; Chave et al., 2014). Therefore parameter values can be assigned based on this data, rather than by fitting 3-PG output to observed stand data to estimate the parameters used in the relationship.

Parameter estimation for PBMs can be performed using a technique that minimises the merit function, the residual sum-of-squares. This is achieved by adjusting the values of nominated parameters. These methods include the simplex optimization method (Walters, 1999) and the Marquardt algorithm (Finsterle and Kowalsky, 2011).

Bayesian parameter estimation allows the probability distribution of a parameter to

represent subjective uncertainty or belief. This approach does not require much of the data to be modelled as it is only interested in how particular parts of the data depend on the other parts (Spiegelhalter et al., 2002). Bayesian parameterisation of complex PBMs is essentially more efficient that iterating over the entire parameter space because it targets key areas. This method of model parameterisation is suited to deal with interactions between parameters, which is shown to occur in complex parameter rich PBMs (Hartig et al., 2014) such as FORMIX3 and 3-PG.

A Bayesian calibration was undertaken of six models including 3-PG and FORMIX3 by van Oijen et al. (2013). This technique performs well as long as the probability of the parameter range distribution was known. As the application of 3-PG and similar models in tropical forests is limited, and therefore the distribution of their parameters is unknown, this approach is not appropriate for this study.

Monte Carlo, or stochastic simulation, estimation techniques involve the repeated random sampling of parameter values to obtain a fit between the model outputs and observed data (Rubinstein and Kroese, 2011). The method is robust and easy to implement and has the ability to provide estimates of output uncertainty and can handle different distribution types (Verbeeck et al., 2006).

A similar approach is the simple iterative process that is often used to parameterise 3-PG when field observations of parameters are not available (Sands and Landsberg, 2002; Landsberg et al., 2003; Almeida et al., 2004a; Potithep and Yasuoka, 2011). This involves running the model and comparing the output with observed values. Parameter values are then adjusted to improve the fit and the model is re-run. Multiple iterations of this process results in good fits between observed and simulated values (Nightingale et al., 2008b). This process is improved when more observed data is available to test the model output (Landsberg et al., 2003). Beyond this description, details, especially those of how model fit is measured, are often lacking with regards to the parameterisation of 3-PG.

Lehmann and Huth (2015) demonstrated that indirect stand attributes such as stem count; basal area (BA) and biomass were sufficient to parameterise a model of tropical forests to calculate the LAI, an important factor in deriving NPP, and subsequently other outputs. These properties are commonly collected data in forest inventory studies

making model parameterisation more straight forward. Such as the method used for determining a good model fit.

6.1.3 Overview of 3-PG$_2$

6.1.3.1 Structure

3-PG$_2$ estimates biomass production and partitioning to the main structural components of the tree stems, roots and foliage. Biomass production is calculated as a direct linear relationship with intercepted solar radiation. The slope of this regression is the light use efficiency (LUE) (ξ, g_{DM} MJ^{-1}). LUE is calculated from the canopy quantum efficiency (α_c, mol mol^{-1}) which is in turn determined by canopy conductance, air temperature, frost, vapour pressure deficit (VPD), available soil water (ASW), soil nutrient status and stand age. The proportion of intercepted radiation (Q_{int}) is determined by Beer's law. These two factors, Q_{int} and α_c, allow the calculation of gross primary productivity (GPP). A constant ratio between NPP and GPP is assumed in place of dynamically calculating respiration. Partitioning of NPP to the below and above ground components, stem (WS), foliage (WF) and root (WF), is governed by a series of growth modifiers representing stand age, soil fertility and environmental variables. Mean diameter at breast height (avDBH) is calculated through an allometric relationship with WS. BA is calculated from DBH and the stem density (StemNo). Stem density in turn is reduced through self-thinning on a basis of the mean WS for the current StemNo. A full mathematical description of 3-PG$_2$ is detailed in the section A.4 of the Appendix.

6.1.3.2 Inputs and Outputs

The model operates on a monthly time step. Monthly averages of short wave radiation, mean maximum and minimum air temperature, VPD, frost days and rainfall are required to drive 3-PG$_2$ (Table 6.3). Site specific factors representing the physical characteristic of the site being modelled include latitude, soil fertility, CO_2 concentration, ASW, initial biomass pools, stem density, salinity, soil stone percentage, edge trees, tree cover, starting age and end age (Table 6.4). Species parameter values (Table 6.2) describe the physiological characteristic for the trees being simulated. Model outputs can be generated annually or monthly. This study focused on monthly predictions for avDBH

(cm), BA (m^2 ha^{-1}) and WS (Mg ha^{-1}) (a full list of outputs is detailed in Table A.5 of the Appendix).

Table 6.2: 3-PG$_2$ parameter ranges and resulting values after parameterisation.

Description	Symbol	Units	Rainforest range	Source
Biomass partitioning and turnover				
Allometric relationships & partitioning				
Foliage:stem partitioning ratio at D=2 cm	*pFS2*	-	0.6 – 1	White et al. (2006); Nightingale et al. (2008b)
Foliage:stem partitioning ratio at D=20 cm	*pFS20*	-	0.15 – 0.9	White et al. (2006); Nightingale et al. (2008b)
Constant in the stem mass v. diam. relationship	a_S	-	0.0917 – 0.22	White et al. (2006); Nightingale et al. (2008b)
Power in the stem mass v. diam. relationship	n_S	-	2 – 2.7	White et al. (2006); Nightingale et al. (2008b), Observed
Maximum fraction of NPP to roots	*pRx*	-	0.8	Default
Minimum fraction of NPP to roots	*pRn*	-	0.25	Default
Volume of soil accessed by 1 kg of root dry matter	*spRootVol*	$m^3\ kg^{-1}$	3.8	Default
Litterfall & root turnover				
Maximum litterfall rate	*gammaFx*	$month^{-1}$	0.005 – 0.072	Klinge and Rodrigues (1968); Franken et al. (1979); Dantas and Phillipson (1989); Scott et al. (1992); Smith et al. (1998); Hirsch et al. (2004); Rowland et al. (2014a)
Litterfall rate at t = 0	*gammaF0*	$month^{-1}$	0.001	Default
Age at which litterfall rate has median value	*tgammaF*	months	10 – 12	White et al. (2006); Nightingale et al. (2008b),
Average monthly root turnover rate	*gammaR*	$month^{-1}$	0.0428	Rowland et al. (2014a)
NPP & conductance modifiers				
Temperature modifier (fT)				
Minimum temperature for growth	*Tmin*	℃	2 – 10	Xiao et al. (2005)
Optimum temperature for growth	*Topt*	℃	25 – 30	Xiao et al. (2005)
Maximum temperature for growth	*Tmax*	℃	35 – 48	Xiao et al. (2005)
Frost modifier (fFRost)				
Days production lost per frost day	*kF*	days	0	Default
Atmospheric CO2 modifier (fCO_2)				
Assimilation enhancement factor at 700 ppm	*fCalphax*	-	1.4	Default
Canopy conductance enhancement factor at 700 ppm	*fCgx*	-	0.7	Default
Fertitlity effects				
Value of 'm' when FR = 0	*m0*	-	0	Default
Value of 'fNutr' when FR = 0	*fN0*	-	1	Default
Power of (1-FR) in 'fNutr'	*fNn*	-	0	Default
Salinity effects				
Upper threshold for salinity modifier	*EC0*	-	999	Default
Lower threshold for salinity modifier	*EC0*	-	999	Default
Power for salinity modifier	*ECn*	-	1	Default
Age modifier (fAge)				
Maximum stand age used in age modifier	*MaxAge*	years	50 – 500	White et al. (2006); Nightingale et al. (2008b)
Power of relative age in function for fAge	*nAge*	-	4	Default
Relative age to give fAge = 0.5	*rAge*	-	0.95	Default
Stem mortality & self-thinning				

Continued on next page

Table 6.2 – *Continued from previous page*

Description	Symbol	Units	Rainforest range	Source
Mortality rate for large t	$gammaNx$	% year^{-1}	0 – 1.48	Laurance et al. (1998, 2000); Williamson et al. (2000)
Seedling mortality rate (t = 0)	$gammaN0$	% year^{-1}	0 – 0.15	Kitajima (1994)
Age at which mortality rate has median value	$tgammaN$	years	0	Default
Shape of mortality response	$ngammaN$	-	1	Default
Max. stem mass per tree @ 1000 trees/hectare	$wSx1000$	kg tree^{-1}	80 – 500	White et al. (2006); Nightingale et al. (2008b)
Power in self-thinning rule	$thinPower$	-	0.9 – 2	White et al. (2006); Nightingale et al. (2008b)
Fraction mean single-tree foliage biomass lost per dead tree	mF	-	0	Default
Fraction mean single-tree root biomass lost per dead tree	mR	-	0.2 – 0.2037	White et al. (2006); Nightingale et al. (2008b)
Fraction mean single-tree stem biomass lost per dead tree	mS	-	0.2 – 0.2038	White et al. (2006); Nightingale et al. (2008b)
Canopy structure and processes				
Specific leaf area				
Specific leaf area at age 0	$SLA0$	m^2 kg^{-1}	2 – 22.772	Asner et al. (2004); Selaya et al. (2007)
Specific leaf area for mature leaves	$SLA1$	m^2 kg^{-1}	2 – 20	Medina and Klinge (1983); Fittkau and Klinge (1973); Carswell et al. (2000); Hirsch et al. (2004); Hoffmann et al. (2005); Selaya et al. (2007); Verbeeck et al. (2011)
Age at which specific leaf area = (SLA0+SLA1)/2	$tSLA$	years	2.5 – 5	White et al. (2006); Nightingale et al. (2008b)
Light interception and VPD attenuation				
Extinction coefficient for absorption of PAR by canopy	k	-	0.5 – 0.78	Shuttleworth (1988); Wirth et al. (2001); Saldarriaga and Luxmoore (1991)
Age at canopy cover	$fullCanAge$	years	3 – 5	Guariguata and Ostertag (2001)
LAI at which VPD in canopy reduced to 50%	$cVPD$	m^2 m^{-2}	5	Default
Rainfall interception				
Max thickness of water retained on leaf	$tWaterMax$	mm	0.25	Default
Maximum proportion of rainfall evaporated from canopy	$MaxIntcp$	-	0.25 – 0.22	White et al. (2006); Nightingale et al. (2008b)
LAI for maximum rainfall interception	$LAIxIntcp$	-	0.15 – 3	White et al. (2006); Nightingale et al. (2008b)
Production and respiration				
Maximum canopy quantum efficiency	$alphaCx$	$molCmolPAR$	0.0033 – 0.08	Hui et al. (2001); Harris et al. (2004)
Ratio NPP/GPP	Y	-	0.29 – 0.46	Malhi et al. (2009b)
Percentage growth enhancement of edge trees	$edgeEffect$	-	20	Default
Conductance				
Soil aerodynamic conductance	g_{As}	m s^{-1}	0.2	Default
Canopy aerodynamic conductance	g_{Ac}	m s^{-1}	0.0428 – 0.1564	Vourlitis et al. (2002)
Maximum canopy conductance	$MaxCond$	m s^{-1}	0.0016 – 0.0353	Kumagai et al. (2004); Aylett (1985); Körner (1995); Motzer et al. (2005); Vourlitis et al. (2001); Roberts et al. (1990)
LAI for maximum canopy conductance	LAI_{gcx}	-	3 – 3.33	White et al. (2006); Nightingale et al. (2008b)
Defines stomatal response to VPD	$CoeffCond$	mBar^{-1}	0.0125 – 0.080	White et al. (2006); Nightingale et al. (2008b)
Wood and stand properties				
Branch and bark fraction (fracBB)				
Branch and bark fraction at age 0	$fracBB0$	-	0.15 – 0.75	White et al. (2006); Nightingale et al. (2008b)
Branch and bark fraction for mature stands	$fracBB1$	-	0.15	Default
Age at which fracBB = (fracBB0+fracBB1)/2	tBB	years	2 – 10	White et al. (2006); Nightingale et al. (2008b)

Continued on next page

Table 6.2 – *Continued from previous page*

Description	Symbol	Units	Rainforest range	Source
Basic Density				
Minimum basic density - for young trees	*rhoMin*	Mg m^{-3}	0.52	Zanne et al. (2009)
Maximum basic density - for older trees	*rhoMax*	Mg m^{-3}	0.87	Zanne et al. (2009)
Age at which rho = (rhoMin+rhoMax)/2	*tRho*	years	4	Default
Stem height				
Constant in the stem height relationship	*aH*	-	0	Default
Power of DBH in the stem height relationship	*nHB*	-	0	Default
Power of stocking in the stem height relationship	*nHN*	-	0	Default
Stem volume				
Constant in the stem volume relationship	*aV*	-	0	Default
Power of DBH in the stem volume relationship	*nVB*	-	0	Default
Power of stocking in the stem volume relationship	*nVN*	-	0	Default
Conversion factors				
Intercept of net v. solar radiation relationship	*Qa*	W m^{-2}	-8 – -90	Almeida and Sands (2015)
Slope of net v. solar radiation relationship	*Qb*	-	0.8	Default
Molecular weight of dry matter	*gDM_mol*	gDM mol^{-2}	24	Default
Conversion of solar radiation to PAR	*molPAR_MJ*	mol MJ^{-2}	2.3	Default

6.1.4 Outline and objectives

The focus of this chapter was to develop a model based approach to study the forest growth and above ground carbon accumulation of secondary forest (SF) in central Amazonia. This work presents the sensitivity analysis, parameterisation and validation the forest growth model Physiological Principles Predicting Growth (3-PG$_2$) using time series plot data from SF near Manaus in the Brazilian Amazon. The work will be utilised in Chapter 7 to produce site wide above ground biomass (AGB) maps to compare with existing pan-tropical AGB products.

6.2 Methods

6.2.1 Field data

This study utilizes the remaining 52 secondary forest field plots, after outlier removal, near Manaus described in Chapter 5. The stocking density of these forests ranged from 880 to 4380 trees per ha at the various stages of growth. This data includes a mix of 212 species found in secondary and mature forests. Measurements of interest for this research included stand stocking, basal area (BA), diameter at breast height (DBH) and above ground biomass (AGB) (Chapter 5, Table 5.5). The outliers removed from the analysis in Chapter 5 were also excluded here.

6.2.2 Climate and soils data

Climate data required by 3-PG$_2$ is detailed in Table 6.3. Monthly average climate data including maximum and minimum air temperature and precipitation were obtained from the beginning of regrowth north of Manaus (1977, Chapter 4) from the meteorological station in Manaus (BDMEP, 2014). Monthly estimates of total incoming short-wave solar radiation were obtained from the NASA Global Modelling and Assimilation Office (Global Modeling and Assimilation Office (GMAO), 2015). Soil information, including texture (Table A.6) and water holding capacity in the A and B horizon were obtained from the Soil and Terrain Database (SOTER) (ISRIC, 2013) and Dunne and Willmott (1996). The soil texture at Manaus is sandy clay (ISRIC, 2013). These attributes were considered uniform across the study site. The soil information did not contain

Table 6.3: Climate data required by 3-PG$_2$

Description	Symbol	Units
Monthly mean daily maximum temperature	Tmax	℃
Monthly mean daily minimum temperature	Tmin	℃
Monthly mean vapour pressure deficit	VPD	mBar
Monthly rainfall	Rain	mm month^{-1}
Monthly mean daily solar radiation	Solar Rad	MJ m^{-2} d^{-1}
Monthly mean daily pan evaporation	Evap	mm d^{-1}
Rainy days per month	Rain days	-
Rainfall intensity	Typical rain intensity during rainfall events	mm hr^{-1}
Frost days per month	d_F	-

details relating to soil nitrogen content, and given that soils across the moist tropics are considered to be infertile (Serrao et al., 1979), the soil fertility growth modifier was set at a low constant value of 0.3 (Nightingale et al., 2008b). A soil fertility rating of 0.3 corresponds to the low LUE (0.0033 molC molPAR^{-1}) measured near these sites (Fluxnet tower ZF2) (Carswell et al., 2000).

Where observed VPD is not available it is possible to calculate it from the maximum (T$_x$) and minimum (T$_n$) air temperature (Landsberg and Waring, 1997).

$$VPD_x = 6.1078 \times Exp(17.269 \times Tx/(237.3 + Tx)), \tag{6.2a}$$

$$VPD_n = 6.1078 \times Exp(17.269 \times Tn/(237.3 + Tn)), \tag{6.2b}$$

$$VPD = (VPDx - VPDn)/2 \tag{6.2c}$$

A mean climate dataset calculated from 1970 to 2011 was used in the sensitivity analysis and parameterisation of the model. This limits the variation in model output to seasonal differences in climate, rather than variation between years.

6.2.3 Sensitivity analysis

A Morris (Morris, 1991) screening analysis was conducted on 3-PG$_2$. Each parameter was varied separately 140 times (total of 9660 runs), a multiple of D+1 where D is the number of parameters (Morris, 1991), whilst the others remained constant using a script written in Python. As there is limited information about the prior probability distributions for each parameter (Song et al., 2012), an independent uniform distribution was assumed for each parameter with bounds varying 30% either side of its default value (Esprey et al., 2004; Song et al., 2012). The output of each run was stored if StemNo was

greater than the mean number of trees across the 52 field plots, >2000 ha^{-1}, and the leaf area index (LAI) was lower than the mean MODIS Leaf Area Index 8-day composite of 6.6. These constraints helped to ensure that the parameter values used were realistic and didn't cause uncharacteristic growth responses. The coefficient of variation (CV), calculated as the standard deviation divided by the mean, standardises the variance allowing comparison between outputs whose ranges have different scales. The CV for each output of interest, avDBH, BA and WS, was calculated after each parameter was varied. The CV was then ranked from highest to lowest for each output of interest. The results were compared to the SA conducted by Song et al. (2012) of the model to confirm the validity of the results. The 20 parameters with the highest CV for each parameter were then assigned species specific values through model parameterisation as in Esprey et al. (2004) and Song et al. (2012). The remaining parameters were assigned default values of *E. globulus* (Landsberg et al., 2002) if values for tropical secondary forest were not available through mensuration or observation.

6.2.4 Parameterisation

The 3-PG$_2$ parameterisation procedure involved running the model and quantitatively comparing BA, avDBH and ABG with the field-measured values at the corresponding measurement date. 3-PG$_2$ requires initial data pertaining to site factors (Table 6.4) and stand data (Table 6.4). Initial biomass pools were arbitrarily set at 0.01 Mg ha^{-1} (Nightingale et al., 2008b), partitioned as 2% for foliage (iWF), 82% for stems (iWS) and 16% for root biomass (iWR) (Poorter et al., 2012), regardless of tree stocking density at each site. The iStocking (Table 6.4) was taken as the mean stocking of each field plot at the time of observation. This was carried out to make the parameter set applicable across different forest stands. These initial stand parameters values were used for each of the field plots.

A full parameter set, shown in Table 6.2, for use in 3-PG$_2$ does not exist for secondary forests in the Brazilian Amazon. The most important parameters defined in the sensitivity analysis above, for determining the outputs of interest, were varied across their known range for tropical forests (Table 6.2). These ranges were derived from studies that had directly measured the parameter; where the same parameter is used in a model or where local forest experts had defined the value (Nightingale et al., 2008b).

Table 6.4: Names and description of initial stand parameters and site factors that can be set during model initialisation for each site. * In the context of this research the PlantedDate is the date each site is abandoned.

Variable name	**Description of site factor**	**Unit**
Latitude	Latitude of site centre (negative for S hemisphere)	degrees
FR	Fertility rating (0 to 1)	-
CO2	Atmospheric CO_2 concentration	ppm
MaxASW	Maximum plant-available soil water capacity	mm
MinASW	Minimum plant-available soil water capacity	mm
SoilClass	Soil class as per Table A.6	-
WFi	Initial foliage biomass	Mg ha^{-1}
WRi	Initial root biomass	Mg ha^{-1}
WSi	Initial stem biomass	Mg ha^{-1}
iStocking	Initial stand stocking	trees ha^{-}1
Salinity	Salinity of soil = electric conductivity	dS m^{-1}
%Stones	% of soil profile volume occupied by stones	-
Soil depth	Depth of soil profile, i.e. maximum rooting depth	m
%treeCover	% of ground area devoted to forest, rest is nominally called pasture	%
edgeTrees	Number trees on edges of strip or block plantings	trees ha^{-1}
PlantedDate	Date that seedlings were planted*	-
initialAge	Stand age at the start of the simulation	years
endAge	Stand age at the end of the simulation	years

Where no published values were available for tropical forests or if the parameter had little or no impact on the model output, as determined by the sensitivity analysis, the default value was used. Default values related to *E. globulus* were defined by Sands and Landsberg (2002). If parameter values were observed at the study site, these values were used to provide realistic physiological representation of the forests being modelled. Values for soil water modifiers (*Swconst; Swpower*) were determined by the soil texture class (Table A.6).

The constant (a_S) and the power(n_S) were calculated in the allometric relationship between avDBH observed in the field and the estimated AGB (Potithep and Yasuoka, 2011) (Equation 6.3).

$$W_S = a_S DBH^{n_S} \tag{6.3}$$

From this relationships, a_S and n_S were calculated as 0.1204 and 2.5232 respectively ($r^2 = 0.97$ for DBH *vs.* stem biomass).

The following parameters were assigned directly (Table 6.2). The age at which full canopy cover is reach (*fullCanAge*) was assigned a value of 4 years (Lucas and Honzak, 2002). The exponential coefficient (k) determines the model sensitivity to VPD. In this

parameterisation of 3-PG$_2$ k was assigned a value 0.0125 per kilopascal, or one-quarter of the default value of 0.05 (Landsberg and Waring, 1997), similar to values measured for tropical trees (Granier et al., 1996). This lower VPD coefficient alters the dominance of physiological control of growth to soil moisture (White et al., 2006). The optimum temperature was assigned a nominal value such that it was similar to the long-term mean temperature of the study area (Almeida et al., 2004a).The minimum and maximum density (*rho0* and *rho1*) were taken as the minimum (0.111 gcm^{-3}) and maximum (1.054 gcm^{-3}) values of specific wood density of trees sampled in the field plots (Zanne et al., 2009). However ,these density measurements are only used for calculating stem volume in 3-PG$_2$ so they are not required in determining avDBH, BA and AGB.

The edge effect parameter was introduced in 3-PG$_2$ by Almeida et al. (2007a) to empirically simulate the enhanced growth rate of *E. globulus* when a wide spacing pattern is implemented in plantations with very low stocking rates (<150 stems ha^{-1}). In this study it was set to 0 as mature tropical rainforests have a typical stand density >500 stems ha^{-1} (Phillips et al., 1994) whilst the secondary forests in the study area had an average stem density >2000 stems ha^{-1}. Edge effects negatively impact on tropical forest growth (Denslow, 1987; Bierregaard Jr. et al., 1992) through perturbation of environmental stresses such as increased temperature (Didham and Lawton, 1999) and increased susceptibility to wind and fire damage (Mesquita et al., 1999; Cochrane, 2003). However, the edge effects parameter is not able to replicate this.

To carry out the parameter estimation of the remaining inputs the total residual error was calculated. This involved implementing a Monte Carlo simulation in which the model was run 20,000 times in which forest growth was simulated for 37 years, the age of the oldest field plots in this study site. The number of model runs needed to capture the total variation in the model outputs is determined by separately plotting the variance of the simulated BA, DBH and AGB after every simulation. Converging variance values indicate the optimum number of simulations has been reached (Verbeeck et al., 2006). Using a script written in Python the value of each important parameter was randomly sampled across its range whilst assuming a uniform distribution. This method was chosen because parameter value distributions were often unknown owing to a small number of published values for each parameter. This avoids making any assumptions about the parameter distribution as the published ranges may not cover

the entire distribution. Each parameter set was implemented in the model and the resulting outputs and corresponding parameter set were stored. The residual error was calculated between the model outputs at 37 years and the field data. The final output values generated from the best fit linear and log-linear models (Table 5.6, Chapter 5), where secondary forest age was the only independent variable, were used to calculate the residual error. The residual errors were totalled as a percentage error for each parameter set. The parameter set that achieved the lowest residual error was selected as the optimum parameter set.

The 95th percentile confidence intervals were calculated from the 1500 parameter sets (Campling et al., 2002) that gave the lowest residual error for each output of interest. This provided an estimate of model uncertainty for the outputs of interest.

6.2.5 Validation

The fit between modelled and observed data from the field sites was assessed through regression statistics including the calculation of residual error. The root mean squared error (RMSE) was calculated using leave one out cross validation (LOOCV). In LOOCV a linear model is fitted to the n-1 of the field sites were n is the total number of field sites. This was done until each site had been excluded once. Each of the linear models generated by this exclusion was compared to the outputs from the parameter set with the lowest total residual error. The residual errors were calculated for the fitted avDBH, BA and AGB between the observed outputs and the modelled data (observed - modelled). These provide an indication of model performance across the output ranges included in the parameterisation dataset. Although AGB was the main output of interest, avDBH and BA were included so that a more realistic parameter set was generated through improved simulation of forest structure.

6.3 Results

6.3.1 Sensitivity Analysis

The coefficient of variation of input parameters corresponding to each model output are presented in Figure 6.1. The influential parameters and their rankings (as measured by

the coefficient of variation) for the model outputs avDBH and BA were very similar. 3-PG$_2$ was sensitive to parameters relating to limiting growth and mortality (e.g. fN0, Tmax, gammaR and thinPower), canopy parameters (e.g. alphaCx, MaxCond and CoeffCond) and biomass partitioning (e.g. pRx and pRn) when considering AGB. Parameters relating to the water balance (e.g. gAs, tWaterMax and cVPD0) had less of an effect on the variance of model outputs (Figure 6.1).

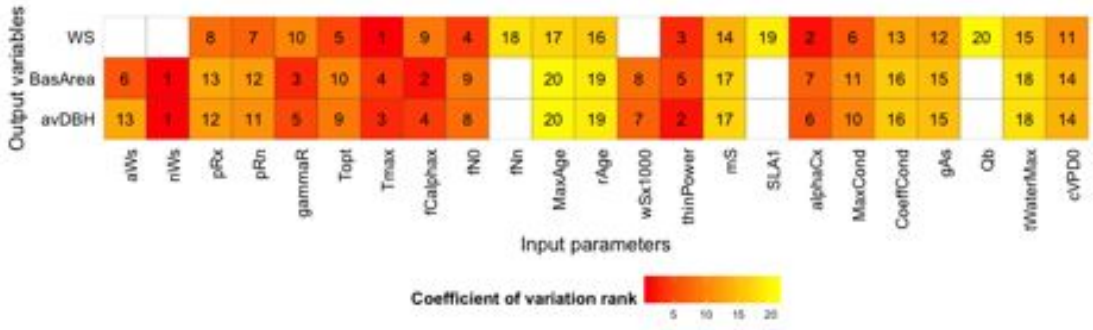

Figure 6.1: Coefficient of variation of 3-PG$_2$ input parameters on output variables. The 20 most influential input parameters are shown for each output of interest. Numbers indicate the rank of coefficient of variation for each input parameter on each output variable from highest (1) to lowest (20) by descending order of CV value. Colour shading is used to symbolize elementary effects using normalized values of variance.

6.3.2 Parameterisation

After 400 iterations the variance of the modelled avDBH, BA and WS converges (Figure 6.2). After 2000 simulations the variance of in the modelled LAI converged.

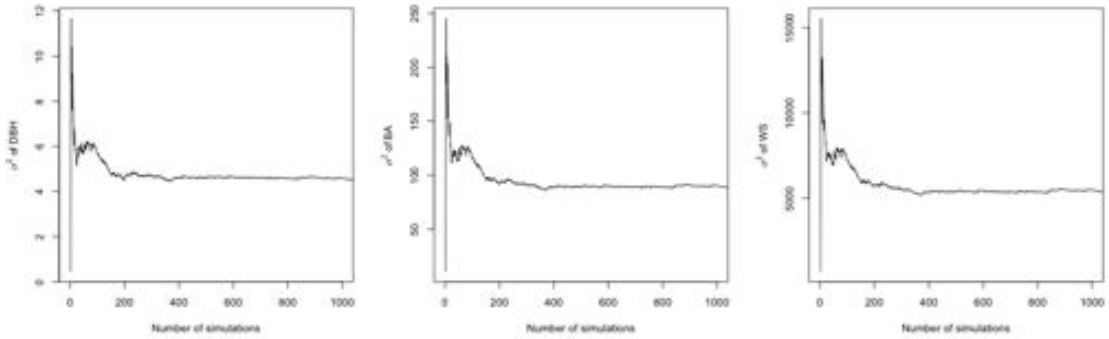

Figure 6.2: The variance of 3-PG$_2$ outputs; average diameter at breast height (DBH, cm) basal area (BA, m^2 ha^{-1}), and above ground biomass (AGB, Mg ha^{-1}) for the secondary forests located north of Manaus plotted as a function of the number of Monte Carlo simulations. For these simulations only the 24 most influential parameters, as identified by the sensitivity analysis, were taken into account.

The parameter values in Table 6.5 produced the best fit with a total residual error, for a 37 year old forest, of 13.9 % after 20,000 runs. This parameter set predicted avDBH, BA and AGB with 5.5 %, 8.4% and 0.004% residual error, respectively. This is in comparison to the mean estimates for strucutral properties of a 37 year old forest north of Manaus. The cumulative difference between outputs from this parameter set and observed data over the entire simulation period was 2179 %. Lower values were achieve for the entire growth curve however this occured due to a cesation in NPP.

Table 6.5: 3-PG$_2$ parameter values for secondary forest north of Manaus estimated from mensuration, observation and a Monte Carlo parameterisation. Only the most important parameters, as shown by the sensitivity analysis were estimated using a Monte Carlo simulation. The remaining parameters were set to their default values (Landsberg et al., 2002).

Parameter	**Rainforest Range**	**Result**
Foliage:stem partitioning ratio at D=2 cm (no units)	0.6 – 1	1.0
Foliage:stem partitioning ratio at D=20 cm (no units)	0.15 – 0.9	0.20
Constant in the stem mass v. diam. relationship (no units)	0.0917 – 0.22	0.1204
Power in the stem mass v. diam. relationship (no units)	2 – 2.7	2.5232
Maximum fraction of NPP to roots (no units)	0.8	0.7108
Minimum fraction of NPP to roots (no units)	0.25	0.1846
Average monthly root turnover rate (month^{-1})	0.015 – 0.0428	0.039
Optimum temperature for growth (°C)	25 – 30	27.6
Maximum temperature for growth (°C)	35 – 48	38.9
Assimilation enhancement factor at 700 ppm (no units)	1.4	1.4
Value of 'fNutr' when FR = 0 (no units)	1	0.65
Power of (1-FR) in 'fNutr' (no units)	0	0.46
Maximum stand age used in age modifier (years)	50 – 500	328
Relative age to give fAge = 0.5 (no units)	0.95	0.69
Max. stem mass per tree @ 1000 trees/hectare (kg tree^{-1})	80 – 500	259.8
Power in self-thinning rule (no units)	0.9 – 2	1.43
Fraction mean single-tree stem biomass lost per dead tree (no units)	0.2 – 0.2038	0.2
Specific leaf area for mature leaves (m^2 kg^{-1})	2 - 20	14
LAI at which VPD in canopy reduced to 50% (m^2 m^{-2})	5	6.7
Max thickness of water retained on leaf (mm)	0.25 ±30 %	0.34
Maximum canopy quantum efficiency ($molCmolPAR^{-1}$)	0.0033 - 0.08	0.049
Soil aerodynamic conductance (m s^{-1})	0.2 ±30 %	0.2
Maximum canopy conductance (m s^{-1})	0.0016 - 0.0353	0.032
Defines stomatal response to VPD (mBar^{-1})	0.0125–0.0800	0.024
Slope of net v. solar radiation relationship (no units)	0.8	0.8

6.3.3 Validation

Statistically highly significant p values (<0.001) exist between the 3-PG$_2$ modelled predictions and field measured estimates of AGB, average DBH and BA (Figure 6.3). Despite low r values avDBH was the most accurately predicted stand output followed by AGB, then BA. The LOOCV produced RMSE equivalent of 5-10 % of the mean output values for avDBH, BA and AGB. avDBH and BA were consistantly underestimated below 6 cm and 10 m^2 ha^{-1}, respectively (Table 6.6 and Figure 6.3). AGB was underestimated at the majority of sites whilst the greatest residual error occured in sites with <50 Mg ha^{-1}.

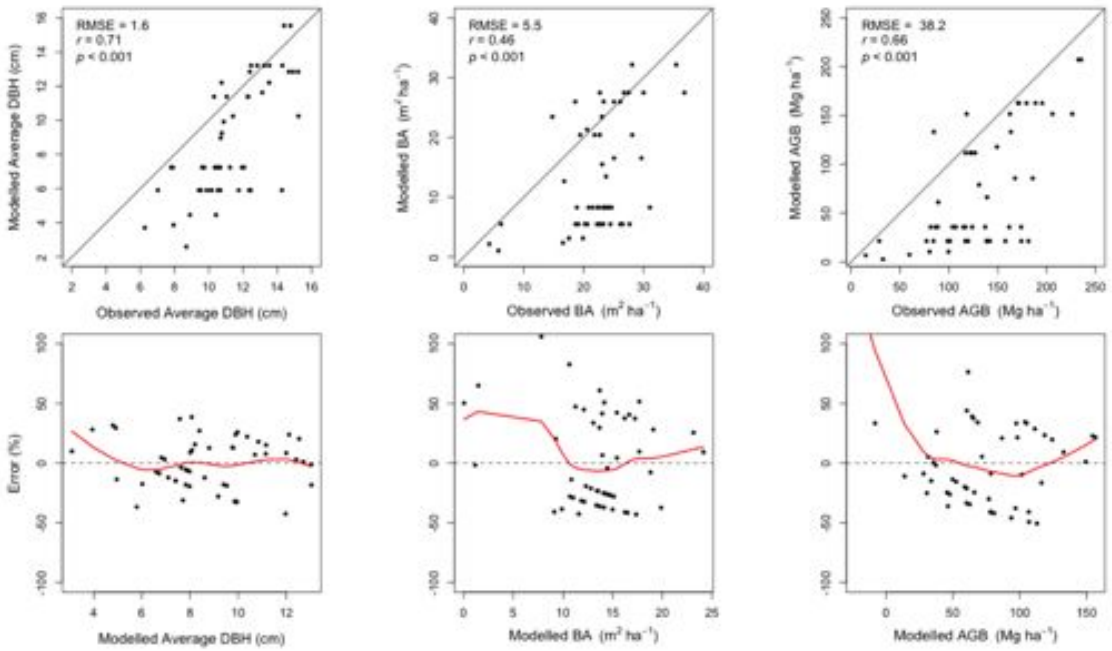

Figure 6.3: Relationship between 3-PG$_2$ modelled and field measured estimates of basal area (m^2 ha^{-1}), average diameter at breast height (DBH) (cm) and above ground biomass (AGB) (Mg ha^{-1}) for the secondary forests located north of Manaus. The solid black line represents the 1:1 relationship. The solid red line represents the mean residual error.

Table 6.6: Model prediction errors for three key model outputs: basal area, diameter at breast height and above ground biomass, based on simulations within secondary forests in central Amazonia, Brazil.

Residuals (observed - modelled)						
Plot	**avDBH (cm)**	**%**	**BA (m^2 ha^{-1})**	**%**	**AGB (Mg ha^{-1})**	**%**
1	6.5	52.2	22.2	80.2	152.8	87.8
2a	8.4	58.6	21.0	79.3	160.1	88.2
3a	1.1	7.6	-4.8	-21.1	9.3	5.4
4	5.8	49.7	17.2	75.8	117.2	84.6
6b	6.5	52.4	19.0	77.5	136.5	86.5
7b	4.8	40.0	16.4	66.4	126.0	77.9
8	2.6	40.8	2.1	48.9	8.4	55.9
9	4.1	51.2	14.2	85.7	52.2	87.6
10	4.2	41.8	14.7	72.8	77.4	78.4
11	4.3	41.9	20.6	79.0	117.9	84.7
12c	4.0	40.2	17.7	76.4	95.3	81.7
14d	6.0	57.2	16.7	84.2	69.7	86.9
15d	4.8	44.7	15.1	73.4	62.8	74.7
16d	1.8	12.5	0.1	0.4	54.4	26.4
17e	1.5	14.1	10.3	43.2	72.9	52.4
18e	1.0	8.8	7.6	32.9	52.0	39.8
19e	-0.8	-5.2	3.3	9.3	28.2	12.0
20f	4.4	49.9	14.4	82.2	89.1	89.5
21f	3.5	37.4	13.2	70.6	79.8	78.9
22f	2.4	15.6	-0.9	-3.7	74.7	33.0
23g	4.6	43.9	16.8	75.3	98.4	82.2
24g	3.1	30.0	13.2	61.6	81.2	69.5
25	6.1	70.2	4.7	81.6	29.8	91.8
30	3.3	31.1	14.1	63.0	71.4	66.7

Continued on next page

Table 6.6 – *Continued from previous page*

Plot	**avDBH (cm)**	**%**	**BA (m^2 ha^{-1})**	**%**	**AGB (Mg ha^{-1})**	**%**
31	2.5	25.6	14.2	63.2	79.1	68.9
32i	0.5	7.0	15.0	64.4	52.7	59.6
33i	-0.7	-5.9	2.5	8.4	32.9	16.8
34j	0.7	8.4	15.2	64.8	50.4	58.5
35j	0.0	0.3	-0.8	-2.9	16.8	9.4
37k	2.4	24.6	15.9	65.8	88.1	71.2
38k	-0.4	-2.9	0.0	0.0	8.0	4.7
36	3.3	31.6	15.6	65.3	101.4	74.0
39	6.5	52.6	17.8	76.4	120.6	85.0
40	3.6	38.1	13.6	71.2	55.8	72.4
41	3.4	32.1	10.6	56.2	45.6	56.1
42	1.1	15.9	0.7	11.2	7.4	25.9
43	4.7	39.3	22.8	73.4	138.3	79.5
44	4.0	35.5	12.5	60.3	68.0	65.6
46	0.3	2.4	9.3	25.4	26.0	13.8
47	-1.1	-7.9	-4.1	-14.5	25.5	11.0
48	1.5	11.4	-0.7	-3.6	31.4	21.1
50	-1.1	-10.4	7.7	27.4	10.1	8.3
51	1.3	9.8	-0.4	-1.8	30.2	18.5
52	-1.5	-13.5	-8.7	-58.8	-48.5	-57.3
54	2.1	14.0	-2.7	-11.4	10.9	6.7
55	0.9	7.3	1.4	6.6	5.3	4.5
56	1.2	10.2	8.5	34.1	82.1	48.9
57	5.0	32.8	13.1	44.2	100.1	53.9
58	-0.4	-3.6	-7.4	-39.8	-33.4	-28.2
59	-0.3	-3.1	2.3	10.0	15.2	12.0
60	1.7	16.2	4.1	24.3	27.9	31.3
61	0.9	7.5	-1.0	-5.1	11.4	9.3

Continued on next page

Table 6.6 – *Continued from previous page*

Plot	**avDBH (cm)**	%	**BA (m^2 ha^{-1})**	%	**AGB (Mg ha^{-1})**	%
Max	**8.4**	**70.2**	**22.8**	**85.7**	**160.1**	**91.8**
Min	**-1.5**	**-13.5**	**-8.7**	**-58.8**	**-48.5**	**-57.3**

Viva suggestions

The under and over estimation of outputs results from the inability of 3-PG$_2$ to replicate the logarithmic growth curves noted in Chapter 5 and the selection of a parameter set which replicated outputs after 37 years of growth only. A possible solution to this, as discussed with examiners during the viva for this thesis (Boyd and Clifton-Brown, 2017), is in the implementation of a hierarchical sequence of model runs that succeed one another. Each model run is individually parameterised for a particular age range, including a suitable maximum age parameter to reduce stem density through time (Mesquita et al., 2015). It is hoped that this modification will produce greater similarity to the field data used in model validation by simulating rapid initial growth followed by a shift towards asymptotic growth rates.

Annual NPP increased rapidly in the first 11 years of growth (Figure 6.4) before reaching an asymptote between 5 and 12 Mg ha^{-1} for the remainder of the growth period. The final annual NPP was 7.4 Mg ha^{-1}.

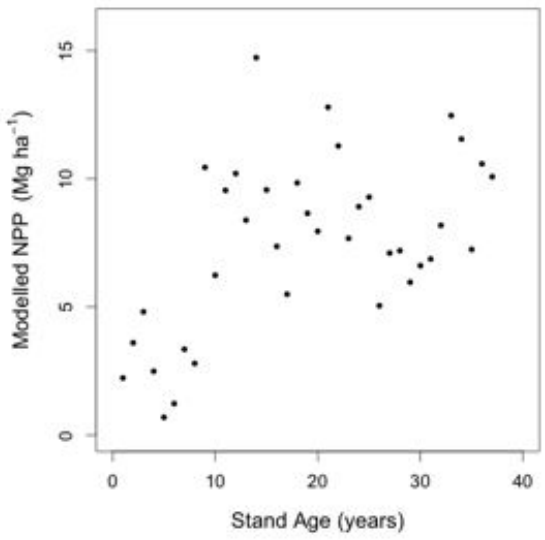

Figure 6.4: Annual NPP (Mg C ha^{-1}) simulated by by 3-PG$_2$ for secondary forests north of Manaus.

6.3.4 Parameter suitability

The distribution of simulated avDBH, BA and AGB for a 37 year old secondary forest are shown in Figure 6.5. This distribution is based on the 400 Monte Carlo simulations closest to the observed data. The mean simulated avDBH, BA, AGB values were 13.6 cm, 30.0 m^2 ha^{-1} and 184.9 Mg ha^{-1} respectively. The standard deviation of the avDBH, BA, AGB distributions were 2.1 cm, 9.4 m^2 ha^{-1} and 73.1 Mg ha^{-1} respectively. The regression models derived from the field data gave avDBH, BA and AGB as 13.8 cm, 28.4 m^2 ha^{-1} and 187.7 Mg ha^{-1} respectively after 37 years of growth. The observed outputs all differed from the mean simulated value, but fall within the range of one standard deviation of their simulated output distribution.

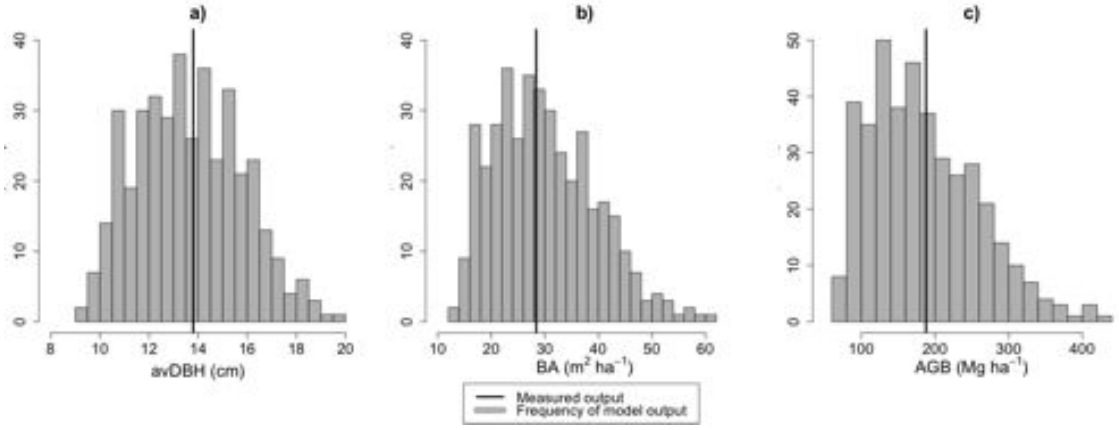

Figure 6.5: Distribution of a) average diameter at breast height (avDBH, cm); b) basal (BA, m^2 ha^{-1}) and c) above ground biomass (AGB, Mg ha^{-1}) of a 37 year old secondary forest north of Manaus. The calculation of these distributions are based on 400 Monte Carlo simulations. Only the 24 most influential parameters, as identified by the sensitivity analysis, were varied. The black bars show the observed avDBH, BA and ABG values and is not representative of frequency.

6.4 Discussion

6.4.1 Model sensitivity

The model was sensitive to parameters relating to biomass partitioning, canopy processes and conductance for the outputs considered. These operate at the core of the model (Landsberg and Waring, 1997) and reflect the findings of Song et al. (2012) who implemented a more detailed variance based global sensitivity analysis on 3-PG$_2$. High sensitivity to aWs and nWs was evident in avDBH and BA (Almeida et al., 2004a; Potithep and Yasuoka, 2011; Song et al., 2012). These parameters are directly involved in the calculation of these outputs from the NPP that is partitioned to stem biomass (WS). Maximum canopy quantum efficiency, the maximum yield of photosynthesis, was sensitive for all outputs as NPP in 3-PG$_2$ is directly driven by incident solar radiation.

All three outputs were highly sensitive to parameters involved in the calculation of the temperature growth modifier (White et al., 2000; Sands and Landsberg, 2002; Nightingale et al., 2008b; Song et al., 2012). The mean air temperature in Manaus was 27.6 ℃ with little variation in Tmin and Tmax annually. Tropical trees operate in an environment where their optimum temperature is already met, unlike the temperate and boreal trees, for which 3-PG has been extensively tested, that exist below their

optimum (Way and Oren, 2010). This validates the use of the long term mean annual air temperature as the optimum growth temperature in the model.

All outputs were sensitive to thinPower, whilst avDBH and BA were sensitive to wSx1000. These parameters interact with the stem density of a stand, a well understood process of density-dependent competition in forests (Chazdon et al., 2010; Toledo et al., 2013; Stark et al., 2015; da Cunha et al., 2016). This demonstrates that the processes of competition are appropriately represented, which is especially important in unmanaged forests.

Hirsch et al. (2004) did not use the fertility rating (FR) in their implementation of 3-PG, as part of an ecosystem model in the Brazilian Amazon, owing to uncertainty in the effects of low soil fertility (Malhi and Wright, 2004). Whilst this chapter showed that changes in fertility modifier parameters (fN0 and fNn) and root partitioning parameters (pRx and pRn), resulted in variations in stem growth in this low fertility soil. The fertility modifier operates directly on the calculation of GPP whilst pRx and pRn determine the magnitude of NPP partitioned to roots, which increases in low fertility soils in the Brazilian Amazon (Malhi et al., 2009b). These findings support the use of the FR in 3-PG$_2$. However, this representation of fertility by a single parameter (FR) in 3-PG$_2$, that does not change during the simulation, is recognised as an over simplification of such a dynamic element (Landsberg and Sands, 2010). Dynamics of this model parameter can be addressed through the coupling of 3-PG with biogeochemical models such as CERES-N (Godwin et al., 1991). High output sensitivity to core model functions, reinforces the choice of 3-PG$_2$ as a robust process based model that is transferable to different environments outside of it's original bounds of development.

Owing to the recognised importance in tree growth physiology of these core parameters, they are well documented in the literature (Appendix Table 6.2). This resulted in the important parameters identified by the SA being those for which a range of values already existed for tropical forests. Correlation of the output distribution for the best parameter-sets closest to the observed data demonstrates the stability of the parameter ranges sourced from the literature for estimating these forest properties (Verbeeck et al., 2006) .

The parameter-set defined here is, to the authors knowledge, the first definition of

these values for secondary forest in the Brazilian Amazon. This parameter-set is only validated for up to 37 years of growth as that was the age of the oldest SF stand north of Manaus. Fischer et al. (2014) and Fischer et al. (2015) simulated forest growth from 0 to 600–1000 years in tropical forests using an individual tree growth model (FORMIX3) however, validation data was unavailable for such an extended period of growth.

6.4.2 Model performance

The final model estimate for annual NPP was within the range of NPP measured in mature forest (5.6 to 10.1 Mg ha^{-1}) north of Manaus on BDFFP sites (Chambers et al., 2001; Clark et al., 2001; Piedade and Junk, 2001; Malhi et al., 2009b). This demonstrates that the physiological processes driving productivity in 3-PG$_2$ are applicable to secondary forests in Brazil in addition to the range of environments in which 3-PG has been successfully implemented e.g. temperate rainforest (Bryars et al., 2013) and plantations in dry Mediterranean and temperate environments (Dye et al., 2004; Potithep and Yasuoka, 2011).

Within 3-PG$_2$ mean DBH was the most accurately predicted stand property, followed by BA and AGB. The error (RMSE) calculated for the mean DBH was 0.28 cm greater than that noted by Nightingale et al. (2008b) using 3-PG, however in the same study 3-PGS gave an error 0.16 cm greater than this chapter for mean DBH. Errors for estimating BA and AGB were both greater than those in Nightingale et al. (2008b) who derived an individual parameter set for each of the mixed species tropical forest plots being simulated including known intial stocking. This chapter aimed to derive one parameter-set for all SF north of Manaus, whilst Nightingale et al. (2008b) created a parameter-set for each forest being investigated. In any forest stand BA estimates should reflect processes of mortality. Stem density was kept constant over the simulation period in keeping with the mean stem density of field study sites (Chapter 5). Therefore, the BA output in 3-PG does not provide a true representation of BA in unmanaged forests. 3-PGS was shown to perform similarly well ($R^2 = 0.77$) when simulating NPP for mature Amazonian forests (White et al., 2006). After 20 years of growth this chapter predicted 128 Mg ha^{-1} a similar value (120 Mg ha^{-1}) was predicted by Hirsch et al. (2004) for SF north of Manaus. Error in the estimation of AGB is driven by variation in the observed field data as discussed in Chapter 5.

The under and over estimation of outputs was largely due to the inability of 3-PG$_2$ to replicate the logarithmic growth curves noted in Chapter 5. An unmanaged forest, secondary succession or old-growth, undergoes a constant process of mortality and recruitment (Chambers et al., 2013; Plourde et al., 2015; Rozendaal and Chazdon, 2015). In addition to an age related decline in growth, these processes dictate the structural properties of a naturally occurring forest through mortality. The maximum age and self-thinning parameters in 3-PG$_2$ are capable of reproducing this growth curve, however they eventually cause a decline in the values of outputs such as WS or avDBH. Logarithmic growth curves were achieved by some of the parameter sets during the Monte Carlo parameterisation, however they were deemed unrealistic as this growth curve was achieved through a reduction in NPP <1 Mg ha^{-1}. The current model structure does not include the recruitment of new individuals to the stand or sprouting from stumps and roots, and is therefore unable to reproduce the initial rapid recovery of biomass (Brown and Lugo, 1990; Hirsch et al., 2004). This limitation also impacts on the models ability to simulate dynamics in stem density, which has to be set in the model initialisation.

A possible solution to this is in the implementation of a hierarchical sequence of model runs that succeed one another. Each model run is individually parameterised for a particular age range, including a suitable maximum age parameter to reduce stem density through time (Mesquita et al., 2015). The addition of recruitment to this implementation would potentially improve the models ability to mimic the dynamics of a successional forest such as the individual based model FORMIX3 (Huth et al., 1998). This aims to provide a more realistic representation of stand dynamics in SF and thus provide better estimates of stem density, mean DBH, BA and AGB.

Repeat chronosequence measurements are invaluable in describing the successional dynamics of SF. Such data does exist within the tropics (Ruiz et al., 2005; Letcher and Chazdon, 2009; Williamson et al., 2014; Mesquita et al., 2015; Norden et al., 2015) however it was unavailable to this study. In addition to a lack of detail at a fine resolution, this study was unable to validate the additional outputs generated by 3-PG$_2$. Confidence in the model's ability to accurately represent the system would be enhanced if it were possible to validate the model and parameter-set against these data (Nightingale et al., 2008b).

6.5 Conclusions

This chapter sought to test the applicability of 3-PG$_2$ to predict the accumulation of above ground biomass in secondary forests in central Amazonia. It was demonstrated that the physiological process basis of the forest growth model 3-PG$_2$ is transferable to mixed secondary forest in the Brazilian Amazon through the use of a generic parameterisation. This applicability was illustrated through various variance based Monte Carlo techniques for studying model output sensitivity and parameter-set stability. The majority of difficulties of modelling such a system were due to the nature of a natural system compared to the intensively managed plantations for which 3-PG$_2$ was developed. The parameter-set defined here, validated for up to 37 years of secondary forest growth, provides the opportunity to assess the contribution of secondary forests to the carbon budget of the Brazilian Amazon. The application of this parameter-set to estimate secondary forest above ground biomass is presented in the following chapter including model sensitivity to changes in climate.

Chapter 7

Application of 3-PG to Mixed Secondary Forests

7.1 Introduction

Secondary forests accumulate biomass rapidly and their rate of sequestration is an important variable for the global carbon cycle (GCC) and future land use management and planning (Chazdon et al., 2016). Espírito-Santo et al. (2014) considered the role of the Brazilian Legal Amazon (BLA) as part of the missing carbon sink through sequestration by regenerating tree fall gaps. Secondary forests are estimated to have a similarly large extent to these natural disturbances with ≈21–35% of deforested areas in the Amazon supporting regenerating forests (Lucas et al., 2000; Carreiras et al., 2006b; Hansen et al., 2013; de Almeida et al., 2016). The above ground biomass (AGB) content of these forests is primarily determined by their age, thus AGB estimates range from 15 to 232.6 Mg ha^{-1} in Manaus over 37 years of growth (Chapter 5). These regrowth forests have the potential to attain an AGB equivalent to mature forests ranging from 252–356 Mg ha^{-1} (Laurance et al., 1999; Avitabile et al., 2015). Owing to these differences, uncertainty of AGB fluxes for regrowth forests in the Americas is high, approximately 50 % (Pan et al., 2011). Therefore, quantifying this biomass pool will aid in the understanding of the role that these forests play in the regional carbon budget.

7.2 Regional biomass estimates

To date there has been no direct consideration of secondary forest, particularly on the basis of its age and distribution in regional AGB estimates(Table 7.1). Two of the most recent estimates of AGB across the tropics, that include areas of secondary forest, are derived from a combination of field and remotely sensed data (Saatchi et al., 2011a; Baccini et al., 2012). Both estimates (Saatchi and Baccini respectively herein) utilise similar methods and datasets. This includes discrete canopy height estimates from the ICESat GLAS LiDAR sensor which is converted to AGB through empirical relationships between LiDAR variables and field estimates of AGB in the same footprint. These estimates are extrapolated using non-linear models in MaxEnt (Saatchi) and Random Forests (Baccini) across the landscape. Variables used in these models include: visual and infra red reflectance from Moderate Resolution Imaging Spectroradiometer (MODIS) sensors; elevation data from the Shuttle Radar Topography Mission (SRTM) and QuickSCAT radar scatterometer data (Saatchi only).

Table 7.1: Estimates of above ground biomass for the Brazilian Amazon and Pan-tropical rainforests. *potential cover. **also included field measurement interpolation. Table adapted and updated from Houghton et al. (2001). Studies which included 'some' secondary forests did not consider them seperately from mature forests.

Extent	Method and source	Spatial resolution	Secondary forests
Amazon	**Multiplying mean biomass density**		
	Olson et al. (1983)	1°	included
	Fearnside (1997)*	1 km	some
	Houghton et al. (2000)**	30m	included
	Field measurement interpolation		
	Gillespie et al. (1992)*	1 km	some
	Houghton et al. (2001)	5 km	avoided
	Malhi et al. (2006)	0.5°	avoided
	Nogueira et al. (2008)	1 km	some
	MCT (Ministry of Science and Technology) (2016)	1 km	included
	Mitchard et al. (2014)	500 m	avoided
	Methods based on environmental gradients		
	Brown (unpublished)	5 km	avoided
	U.S. Agency for International Development, 2012	-	-
	Forest growth modelling		
	Potter et al. (2001)	1°	some
	Hirsch et al. (2004)	63 km	included
	White et al. (2006)	0.5°	some
Pan-tropical	**Remote sensing**		
	DeFries and Belward (2000)	1 km	some
	Saatchi et al. (2007)	1 km	included
	Saatchi et al. (2011a)	1 km	some
	Baccini et al. (2012)	500 m	some
	Avitabile et al. (2015)	1 km	some

Differences in these estimates comes, in part, as a result of their respective nominal

dates, Saatchi is 2000–2001 whilst Baccini is 2007–2008. Both estimates used allometric equations from the same source (Chave et al., 2005). However, Baccini did not include wood density whilst Saatchi did. Uncertainty of Saatchi ranges from ±6 % to ±53 % for each pixel (Saatchi et al., 2011a) whilst Baccini has an overall uncertainty of ±7 % for Amazonia (Baccini et al., 2012). Avitabile et al. (2015) (Avitabile herein) sought to refine these estimates through the use of independent field data and high-resolution local or national AGB maps as reference datasets. This fused data approach used bias removal and weighted linear averaging to incorporate and spatialise biomass patterns indicated by the reference data. This was applied to areas with homogeneous error patterns in Saatchi and Baccini. AGB estimates in Avitabile were lower than both Saatchi (9 %) and Baccini (18 %) over their common area across the tropics. However, Avitabile estimated higher AGB than Saatchi and lower estimates than Baccini in the central Amazon basin in the fused map (Avitabile et al., 2015).

Information on secondary forest AGB was included in the field data utilised by Saatchi, Baccini and Avitabile (Saatchi et al., 2011a). However, none of the AGB estimates considered forests as separate classes e.g. old-growth, secondary, degraded and savannah. Structural differences between old-growth and secondary forest such as multiple canopy layering vs. single canopies (Steininger, 2000; Peña-Claros, 2003) are not detectable using metrics of canopy height and near infra red reflectance. Therefore the same relationships applied to mature forests cannot necessarily be applied to secondary forests.

7.3 Climate change

Increasing concentrations in atmospheric CO_2 have contributed to estimates of changes in mean air temperature and precipitation in Amazonia ranging from 1.7 to 5.6 ℃ and -13 to 21 % this century, respectively (Alexander et al., 2013). In addition, increased temporal and spatial variability in the climate of Latin America is expected e.g. >70% of climate models predict an annual rainfall reduction in the Eastern Amazon during the dry season (Alexander et al., 2013). Disruption of the El Nino Southern Oscillation (ENSO) has the potential to increase the severity of droughts in the region, especially when coupled with seasonal reductions in rainfall (Cochrane and Barber,

2009). Increases in drought frequency and severity (Lewis et al., 2011) are already causing: persistent changes in canopy structure and moisture content (Saatchi et al., 2013a; Hilker et al., 2014); increased tree mortality (Williamson et al., 2000; Rolim et al., 2005; Doughty et al., 2015); reductions in soil water and increased fire activity (Aragão et al., 2007; Zeng et al., 2008; Malhi et al., 2008). These heightened mortality rates and the subsequent loss of biomass demonstrates the vulnerability of the Amazon forests to moisture stress through hydraulic failure (Phillips et al., 2009; Choat et al., 2012; Corlett, 2016). The release of carbon from tropical forests as a result of these effects may exacerbate future climate perturbations, although their magnitude is uncertain (Bonan, 2008; Malhi et al., 2008). CO_2 fertilisation, although common in other biomes (e.g. Donohue et al., 2013), has not been proven to occur in tropical forests where increased concentrations of atmospheric CO_2 have increased water-use efficiency, a response often associated with severe soil water deficits (Cernusak et al., 2013; Groenendijk et al., 2014; van der Sleen et al., 2015). In 3-PG_2, CO_2 is used in the calculation of a growth modifier which influences the efficiency with which a stand can utilise the incident solar radiation (canopy quantum efficiency). However this parameter is as yet undeveloped and has little bearing on the final model output.

The majority of climate change sensitivity studies incorporating forest growth modelling in the tropics have been carried out using Dynamic Global Vegetation Models (DGVM) whilst only a few examples investigate impacts at site specific scales (Table 7.2).

Table 7.2: Forest growth model sensitivity to future climate change and climate perturbations in the tropics. DGVM - Dynamic Global Vegetation Model. ENSO - El Nino Southern Oscillation

Source	**Location**	**Model type/scale**	**Climate parameter being tested**	**Main findings**
White et al. (2006)	Amazon	Stand level	1997 ENSO climate	ENSO induced drought effects not present in SW and NW Amazon although total NPP for the basin is reduced
Ahlström et al. (2012)	Global	DGVM	Sensitivity to 18 climate models	Tropics will become source of carbon by the end of the 21^{st} century
Good et al. (2012)	Amazon	DGVM	Sensitivity to two Hadley Centre climate models	Amazon dieback remains a possibility under a business as usual emissions scenario
Wang et al. (2013b)	Tropics	DGVM	Sensitivity to global climate perturbations	Temperature and CO_2 coupling driven by heterotrophic respiration and NPP changes linked to temperature variations
Huntingford et al. (2013)	Tropics	DGVM	Sensitivity to 22 climate models	AGB gains for the 21st century
Fischer et al. (2014)	Madagascar	Tree-based	Precipitation	0 %–30 % decline in precipitation has minor impact on AGB. Decline below 30 % would cause considerable decrease in AGB
Castanho et al. (2014)	Amazon	DGVM	Atmospheric CO_2	DGVMs underestimate drought events and unable to predict growth dynamics at individual sites
Guan et al. (2014)	Africa	DGVM	Seasonal rainfall	Radiation limits further gains to productivity in the wet tropics
Slot et al. (2014)	Panama	DGVM	Canopy air temperature	Warming increases respiration and creates additional feedback loop between climate change and carbon
Schippers et al. (2015)	Thailand	Individual tree	Max air temperature, precipitation and atmospheric CO_2	Maximum temperature has a strong negative impact of stem growth

7.4 Outline and objectives

This chapter focuses on the implementation of a process based model approach to study the forest growth and above ground biomass accumulation of secondary forest (SF) in the central and western Brazilian Amazon. This work presents the estimation of secondary forest biomass using the forest growth model previously parameterised in Chapter 6, Physiological Principles Predicting Growth (3-PG_2). Modelling estimates are compared to existing pan-tropical AGB maps. Model sensitivity to climate change is studied to inform on applicability of the use of 3-PG_2 for modelling patterns of biomass accumulation in the future.

7.5 Methods

7.5.1 Data

This study utilises the parameter-set derived for 3-PG_2 in Chapter 6 for Manaus. However, the parameter-set derived in Chapter 6 is only validated for SF north of Manaus so estimates for Santarém and Machdinho d'Oeste should be treated as unvalidated.The initial site factors used for each site are detailed in Table 7.3. Default values for parameters are used when unknown, whilst others were assumed (e.g. initial biomass pools, Chapter 6).

Aboveground biomass was simulated up to 2011 for Manaus and Machadinho d'Oeste and 2010 for Santarém by simulating SF growth in each pixel. The PlantedDate was determined as:

$$\text{PlantedDate} = \text{Final Year Of Prediction} - \text{ASF} \tag{7.1}$$

where ASF is the age of the secondary forest patch determined for each year of simulation in Chapter 4. This was used to select the appropriate climate data for driving each model run and endAge, equal to the ASF, for determining the runtime of each model run.

The climate data required by 3-PG_2 is detailed in Chapter 6, Table 6.3. Monthly average climate data including maximum and minimum air temperature and total

Table 7.3: Names and description of initial stand parameters and site factors used in model initialisation for simulating the growth of secondary forest near Manaus, Santarém and Machadinho d'Oeste. * In the context of this research the PlantedDate is the date each site is abandoned.

Variable	Manaus	Santarém	Machadinho d'Oeste	Source
Latitude (degrees)	-2.33	-3.1	-9.3	–
FR (0–1)	0.3	0.3	0.3	Nightingale et al. (2008b)
CO2 (ppm)	395	395	395	Keeling et al. (2005)
MaxASW (mm)	1000	1250	1000	Nepstad et al. (2004)
MinASW (mm)	250	250	250	Nepstad et al. (2004)
iASW (mm)	500	500	500	Default
SoilClass	Clay	Sandy clay	Sandy clay	ISRIC (2013)
WFi (Mg ha^{-1})	0.0002	0.0002	0.0002	Nightingale et al. (2008b)
WRi (Mg ha^{-1})	0.0016	0.0016	0.0016	Nightingale et al. (2008b)
WSi (Mg ha^{-1})	0.0082	0.0082	0.0082	Nightingale et al. (2008b)
iStocking (trees ha⁻1)	2005	2005	2005	Chapter 5
Salinity (dS m^{-1})	0	0	0	Default
%Stones (%)	0	0	0	Default
Soil depth (m)	5	5	5	Default
%treeCover (%)	100	100	100	Default
edgeTrees (trees ha^{-1})	0	0	0	Default
PlantedDate (Year/month)	Times-series classification dependant			–
initialAge (years)	0.1	0.1	0.1	–
endAge (years)	Times-series classification dependant			–

precipitation were obtained from the beginning of regrowth at each study site (Manaus – 1977, Santarém – 1984 and Machadinho d'Oeste – 1984, Chapter 4). Climate data for Manaus was collected at Manaus Banco de Dados Meteorológicos para Ensino e Pesquisa (BDMEP) meteorological station, Santarém BDMEP station for Santarém and Jaru reserve, the nearest (35 km) BDMEP station, for Machadinho d'Oeste (BDMEP, 2014). Gaps in the meteorological data were filled with the mean value for that month from the dataset. Monthly estimates of total incoming short-wave solar radiation were obtained from the NASA Global Modelling and Assimilation Office (Global Modeling and Assimilation Office (GMAO), 2015). Soil information, including texture (Appendix, Table A.6) and water holding capacity in the A and B horizon were obtained from the Soil and Terrain Database (ISRIC, 2013) and Dunne and Willmott (1996). The soil fertility growth modifier was set at 0.3 for all sites (Nightingale et al., 2008b). These attributes were considered uniform across each SF patch and study site.

Remote sensing derived estimates of AGB by Saatchi et al. (2011a), Baccini et al. (2012) and Avitabile et al. (2015) were downloaded via *pers. comms.* with Saatchi et al. (2011a), http://www.whrc.org and http://www.wageningenur.nl/, respectively. These data were subset to the same extent of each study site. Following this each was resampled to 30 m and projected to the corresponding universal transverse mercator

zone for each site using a nearest neighbour transformation algorithm (Prates-Clark et al., 2009; Cutler et al., 2012; Carreiras et al., 2014) for comparison with the outputs of this chapter. Each estimate was masked to the area of SF delineated in Chapter 4, at the appropriate year.

7.5.2 Above ground biomass simulations

Above ground biomass was simulated for each site up to the same year as the latest available Landsat imagery in Chapter 4. Following a model run for each pixel, the final AGB was stored and all AGB values were written to the attribute table in a raster file upon completion. This was implemented using a script written in Python and the open source KEA raster file format that supports raster attribute tables (Bunting and Gillingham, 2013).

Forest growth was simulated up to the years 2000, 2007 and 2009 for comparison with the remote sensing (RS) derived estimates of Saatchi, Baccini and Avitabile, respectively. The difference between each RS estimate and that produced by 3-PG$_2$ was calculated for each study site for the area of SF delineated in Chapter 4. Summary statistics of each estimate were derived for the area of SF delineated in Chapter 4, at the appropriate year, at each site for comparison. Boxplots provided an overall comparison between 3-PG$_2$ and the RS estimate whilst 2D histograms provided a comparison of the distributions of AGB. These analyses were carried out in the open source RSGISLib (Bunting et al., 2014) and R (Team, 2015) software packages.

7.5.3 Climate sensitivity

Sensitivity to variations in climate was assessed using individual model runs driven by the initial conditions and parameter-set for Manaus only. The effect of alternative climate scenarios on AGB accumulation was investigated through five mean annual precipitation scenarios and five mean annual air temperature scenarios by varying monthly precipitation and (minimum and maximum) air temperature separately. Quarterly differences within years, in air temperature and precipitation were used to reflect seasonal differences (Table 7.4). These scenarios represent the regional climate change estimates in Amazonia (68°80'0" W, 19°55'0" S to 50°00'0" W, 11°43'9" N) between

the periods 1980 to 1999 and 2080 to 2099 for IPCC scenario A1B (Alexander et al., 2013) which represents energy systems with a balance between fossil and non-fossil fuels. These scenarios were compared to results derived from the climatic conditions between 1980 and 1999. Each model run simulated 37 years of growth, the maximum age for which the parameter-set in 3-PG$_2$ is validated. Climate sensitivity was assessed through comparison of AGB growth curves and final AGB attained for each climate scenario.

Scenarios in which precipitation and air temperature varied simultaneously were not included in this study as they were not readily available (Alexander et al., 2013). Combining the separate distributions of precipitation and air temperature scenarios would not overcome this as the individual models making up these two sets of scenarios do not make up the same distribution i.e. lower quartile predictions for air temperature may not correspond to the same quartile of precipitation predictions.

Table 7.4: Distribution statistics of changes to mean air temperature and precipitation in the 21 model predictions from 1980–1999 mean to 2080–2099 mean (Alexander et al., 2013). DJF - December, January February; MAM - March, April, May; JJA - June, July, August; SON - September, October, November

	Temperature Response (℃)					**Precipitation Response (%)**				
Season	Min	Lower quartile	Median	Upper quartile	Max	Min	Lower quartile	Median	Upper quartile	Max
DJF	1.7	2.4	3	3.7	4.6	-13	0	4	11	17
MAM	1.7	2.5	3	3.7	4.6	-13	-1	1	4	14
JJA	2	2.7	3.5	3.9	5.6	-38	-10	-3	2	13
SON	1.8	2.8	3.5	4.1	5.4	-35	-12	-2	8	21
Annual	1.8	2.6	3.3	3.7	5.1	-21	-3	0	6	14

7.6 Results

7.6.1 Above ground biomass simulations

Figure 7.1 shows AGB estimates for the three study sites in 2010 for Santarém and 2011 for Manaus and Machadinho d'Oeste. Manaus had the highest estimates of AGB in SF areas followed by Santarém then Machadinho d'Oeste (Table 7.5).

Distributions of 3-PG$_2$ estimates of AGB are consistently lower than those derived from remote sensing data at Manaus (Figure 7.2). Median values for the remote sensing estimates were always greater than the maximum predictions for the corresponding 3-PG$_2$ estimates at Manaus with a mean difference of 59.9 %. However, this is not the

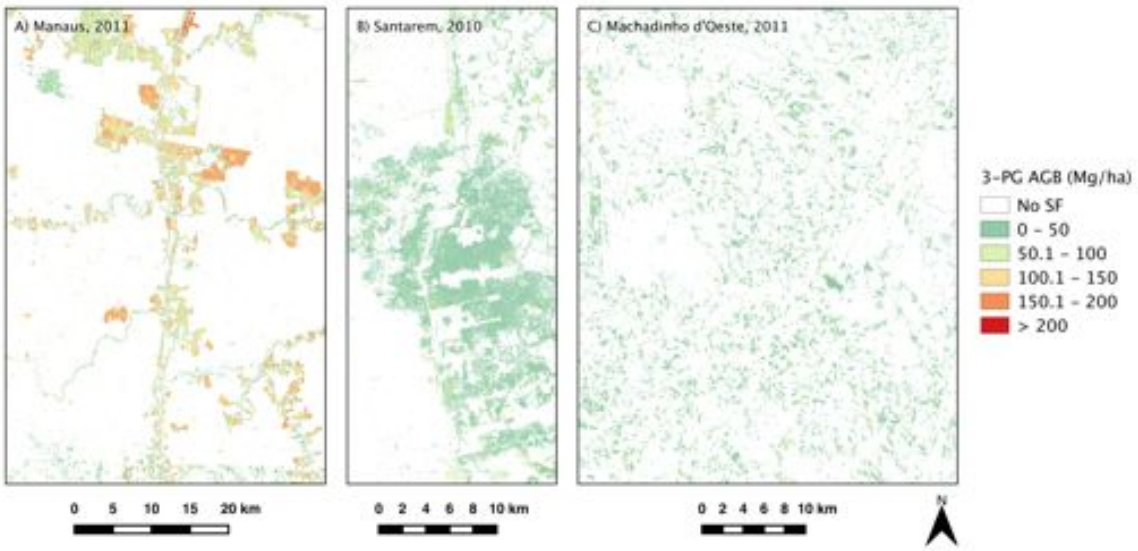

Figure 7.1: Distribution of estimated total live woody aboveground biomass (AGB) from 3-PG$_2$ for secondary forests at 30 m resolution for the Manaus, Santarém and Machadinho d'Oeste.

case when considering the addition of uncertainty (38.2 Mg ha^{-1}) to the 3-PG$_2$ estimates (Table 7.5). There was an overlap of the upper quartiles of the 3-PG$_2$ estimates with the lower quartiles of the Baccini and Avitabile estimates when including the uncertainty in the 3-PG$_2$ estimate. Remote sensing estimates were consistently higher than the corresponding 3-PG$_2$ AGB estimate by a factor of 3.6.

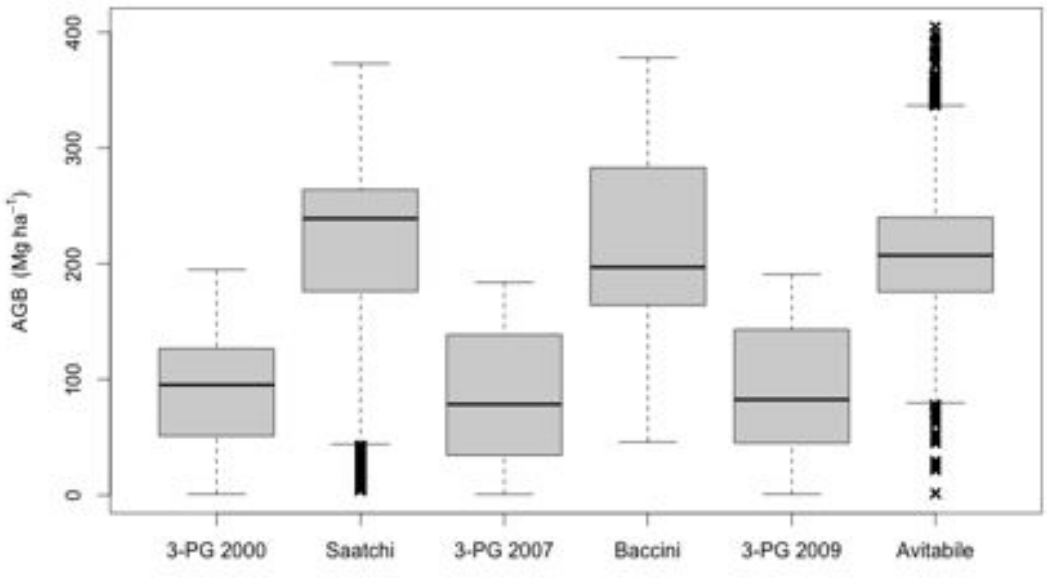

Figure 7.2: Comparison of above ground biomass (AGB) for each remote sensing derived estimate and 3-PG$_2$ simulated AGB for corresponding year at Manaus.

The summary statistics for Santarém and Machadinho d'Oeste demonstrate the same differences between the 3-PG$_2$ and remote sensing estimates of AGB (Table 7.5). However there is overlap of the upper quartile for 3-PG$_2$ and lower quartile for Saatchi at Machadinho d'Oeste. Differences between estimates hold when uncertainty is considered for Santarém. Whilst all estimates of AGB for Machadinho d'Oeste are within the uncertainty bounds of 3-PG$_2$.

Table 7.5: Summary of above ground biomass estimates for secondary forest near Manaus, Santarém and Machadinho d'Oeste from remote sensing data and the forest growth model 3-PG$_2$. * Mean uncertainty of pixels covering SF. **Relative error for Latin America, 27.8% of SF mean.

Above ground biomass estimate (Mg ha^{-1})								
Manaus								
	Min	Lower quartile	Median	Mean	Upper quartile	Max	Uncertainty	Total (Pg)
3-PG 2000	0.8	51.2	95.3	86.0	126.7	194.8	±36.5	0.0777
Saatchi	4.0	176.0	239.0	211.1	264.0	373.0	±57.6**	0.1908
3-PG 2007	0.7	34.5	78.5	80.7	138.6	183.9	±36.5	0.0729
Baccini	46	164	197	218.7	283	378	±25	0.1963
3-PG 2009	0.8	45.0	82.6	88.5	143.1	190.8	±36.5	0.0800
Avitabile	1.4	175.6	207.3	207.3	240.1	404.7	±26.6	0.1860
Santarém								
	Min	Lower quartile	Median	Mean	Upper quartile	Max	Uncertainty	Total (Pg)
3-PG 2000	0.9	12.9	30.6	28.9	32.9	80.2	±36.5	0.0143
Saatchi	4.0	94.0	219.0	183.6	258.0	376.0	±51.0**	0.0904
3-PG 2007	0.7	17.7	41.2	35.9	43.8	98.7	±36.5	0.0178
Baccini	35.0	152.0	183.0	196.1	235.0	367.0	±25	0.0965
3-PG 2009	0.7	21.7	47.7	41.6	53.4	106.8	±36.5	0.0205
Avitabile	7.7	145.8	198.3	225	317.7	477.7	±39.4	0.1109
Machadinho d'Oeste								
	Min	Lower quartile	Median	Mean	Upper quartile	Max	Uncertainty	Total (Pg)
3-PG 2000	0.8	4.7	23.1	35.2	58.5	138.5	±36.5	0.0187
Saatchi	3.0	24.0	56.0	94.6	155.0	411.0	±43.1**	0.0499
3-PG 2007	0.8	5.5	20.6	34.6	58.6	150.9	±36.5	0.0184
Baccini	29.0	98.0	120.0	125.3	151.0	296.0	±25	0.0659
3-PG 2009	0.7	3.0	18.7	30.4	54.1	145.7	±36.5	0.0166
Avitabile	0.1	99.7	121.8	135.8	164.3	358.2	±20.2 *	0.0719

Histograms of the AGB distributions of the remote sensing derived estimates (x-axis) and corresponding 3-PG$_2$ estimates (y-axis) were compared using 2D histograms (Figure 7.3). Estimated AGB values with a high frequency in both histograms are shown in red and areas of low frequency in blue. Areas of highest frequency concordance between Saatchi and it's related 3-PG$_2$ estimate occurred at 240–270 Mg ha^{-1} and 40–60 Mg ha^{-1}, respectively, followed by 125–155 Mg ha^{-1} in the 3-PG$_2$ estimate (Figure 7.3A).

The highest frequency concordance between Baccini and 3-PG$_2$ was 155–170 Mg ha^{-1} and 40 Mg ha^{-1}, respectively (Figure 7.3B). The greatest concordance between Avitabile and 3-PG$_2$ was greater than Saatchi and Baccini. However, frequency concordance was less concentrated than the other comparisons resulting in fewer high frequency areas in the comparison (Figure 7.3C). All comparisons had an r^2 <0.1 for the correlations between the pixels values of the outputs from this chapter and the respective remote sensing estimate.

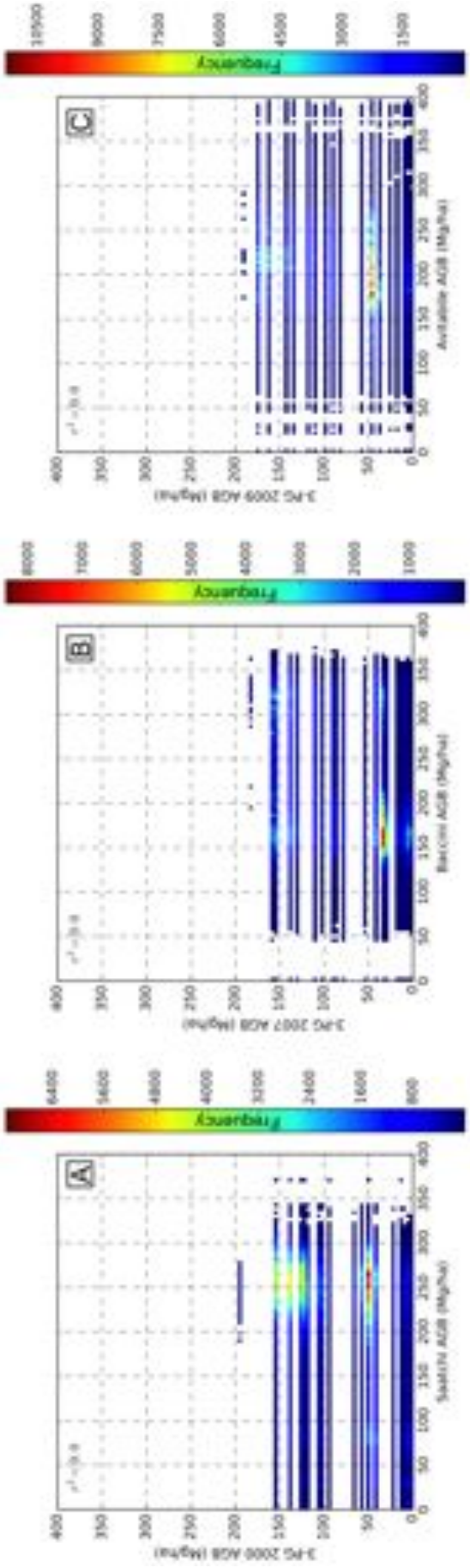

Figure 7.3: 2D histograms showing comparison between the histogram distributions of the Saatchi estimate (a), Baccini estimate (b) and Avitabile estimate (c) of above ground biomass (AGB) and 3-PG_2 simulated AGB for corresponding year at Manaus. Red areas indicate high concordance between AGB estimates with high frequencies in the two histograms. Blue areas indicate low concordance in the frequencies of each axes.

In comparison to Saatchi, the majority of 3-PG$_2$ estimates with a difference <100 Mg ha^{-1} are distributed in the large continuous blocks of SF (Figure 7.4A). Differences >300 Mg ha^{-1} are isolated to small patches throughout the study site. Negative differences occur in the small SF stands in the south of the study site and at the boundaries between SF and non-forest (NF). Positive differences of AGB in Baccini compared to 3-PG$_2$ are greatest along roads; SF and mature forest boundaries and blow downs (Figure 7.4B). There is little negative difference between Baccini and 3-PG$_2$.

The distribution of higher estimates by Avitabile, compared to 3-PG$_2$ in Manaus, is evenly distributed across the study site with less of a pattern in its spatial heterogeneity (Figure 7.4C). Negative differences occur predominantly in the south of the study site. Continuous blocks of SF covered by multiple 0.5–1 km pixels in the RS estimates show lower differences to the 3-PG$_2$ estimates in the comparisons with Baccini, and Avitabile particularly.

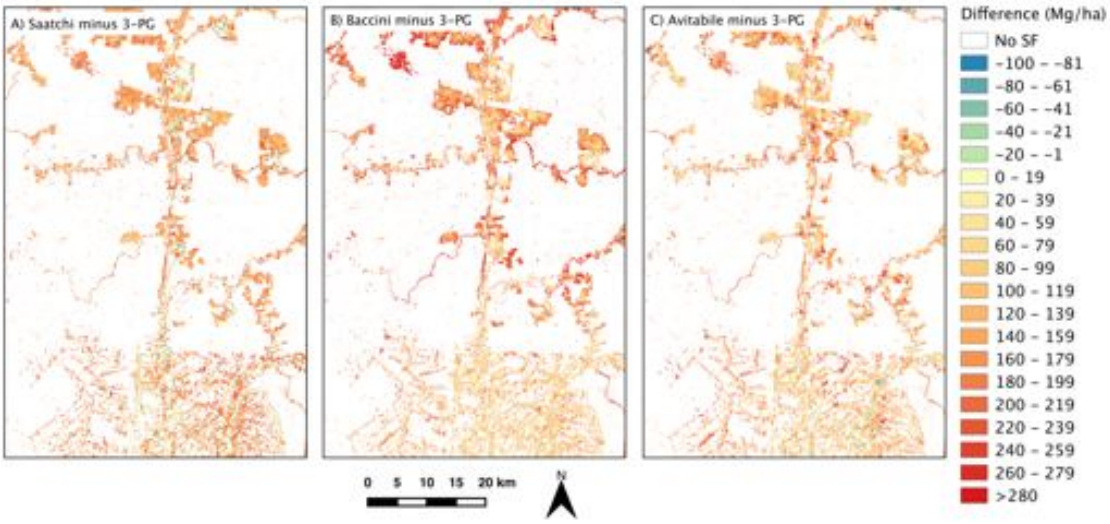

Figure 7.4: Difference maps obtained by subtracting the AGB estimates of 3-PG$_2$ from Saatchi (a), Baccini (b) and Avitabile (c) at Manaus.

7.6.2 Climate sensitivity

Increases in mean annual air temperature above a mean of 1.8 ℃ resulted in a decrease of final AGB after 37 years of growth in comparison with current conditions (Figure 7.5A). Increases in annual precipitation of ≥6 % caused final AGB to increase. Whilst the median IPCC prediction for annual precipitation remained the same as present day levels, the distribution of precipitation changed seasonally with a shift to more

extreme wet seasons and dry seasons causing final AGB to increase by 23 Mg ha^{-1}. Decreases in annual precipitation ≥3 % resulted in a decrease of 0.22 Mg ha^{-1} mm^{-1} in final AGB after 37 years of growth (Figure 7.5B). After 4–5 years of growth the AGB accumulation rates in the air temperature scenarios diverged whilst this occurred in <4 years when altering the annual precipitation (Figure 7.5C & D). Across the range of predicted scenarios, changes in precipitation caused the greatest absolute differences in final AGB in comparison to mean annual air temperature, 221.7 Mg ha^{-1} and 50.6 Mg ha^{-1}, respectively.

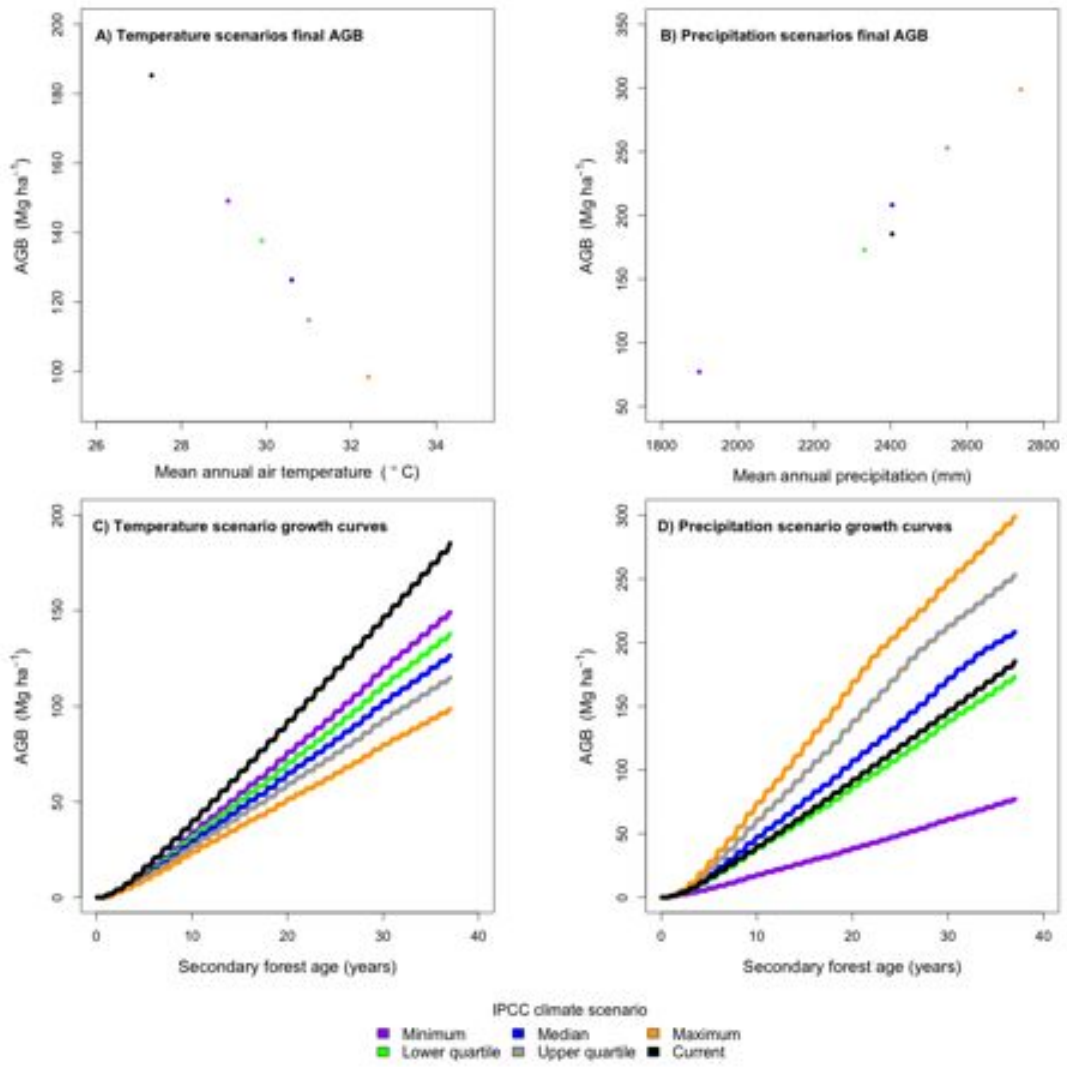

Figure 7.5: A) Final AGB estimates as a function of mean annual air temperature. B) Final AGB estimates as a function of mean annual precipitation. C) Estimated pattern of AGB accumulation for different mean annual air temperatures. D) Estimated pattern of AGB accumulation for different mean annual precipitation. Each mean annual air temperature and mean annual precipitation is derived from the IPCC A1B scenario for Amazonia.

7.7 Discussion

7.7.1 Differences in above ground biomass

The highest mean and median AGB were estimated in Manaus by 3-PG$_2$ in comparison to Santarém and Machadinho d'Oeste. This is a result of the difference in age distributions between each location (Chapter 4). This is supported by similar differences between sites when comparing mean and median AGB of each RS estimate. Mitchard et al. (2014) showed similar trends, at a regional scale, of increasing AGB with increasing latitude, longitude and distance along a SW–NE line (i.e. Machadinho d'Oeste–Santarém). However these findings are not significant when utilising a generalized least square method as they are spatially autocorrelated (Saatchi et al., 2015). Despite the similarity in overall trends between this study and the RS estimates, the difference in magnitude of estimates highlights the importance of considering SF age and distribution (Guariguata and Ostertag, 2001; Neeff et al., 2006; Wandelli and Fearnside, 2015; Jakovac et al., 2015; Poorter et al., 2016) as neither are considered in the RS estimates.

Areas of SF smaller than the coarse resolution (0.5–1 km) of the remote sensing datasets will be poorly represented in the RS studies compared here. Evidence for this can be seen in the distribution of the largest differences in AGB estimates between RS derived maps and this chapter, often occurring within small patches of SF and at the interface between SF and MF. Small patches of SF may be aggregated into larger pixels containing MF whilst the finer detail for SF edges will be lost at coarser resolutions.

Spatial differences arise as a result of heterogeneity in the forest structure within patches of the same ages. This variation across a stand is detectable in the remote sensing data sets used by Saatchi, Baccini and Avitabile (Varela et al., 2008; Lucas et al., 2011; Nagendra et al., 2013; Réjou-Méchain et al., 2014) provided that areas of SF are larger than the resolution of these data. Such variation will not be replicated by this chapter as stands are treated as homogeneous areas, and can be considered a limitation of implementing a stand based model in such an environment. This is evident in the gradient of differences between estimates, which neared 0 Mg ha^{-1} with greater distance from MF. Distance to MF edge has been demonstrated to influence SF recovery (Wijdeven and Kuzee, 2000; Cubiña and Mitchell Aide, 2001; ZermeñoHernández et al.,

2015; ArroyoRodríguez et al., 2015) as they are often the source of seeds and new propagules in areas where the seed bank has been denuded (Uhl et al., 1988). This highlights possible limitations of implementing a forest growth model with no spatial interaction between stands and surrounding land cover types in an unmanaged setting. Forest landscape models simulate interaction between stands, however their resolution is too coarse (>100 ha) to represent SF (Mladenoff, 2004). 3-PGSpatial (3-PG_2S) (Almeida et al., 2007a) includes spatially variable inputs for soil parameters and a species module which provides the ability to model more than one species, or in the case of this chapter, species groups, across the landscape. These modifications however, are still in development and the species module does not allow spatially variable inputs (Almeida et al., 2007a).

A constant value of 0.01 Mg ha^{-1} for the initial biomass pool is not representative of the spatial variability found in naturally regenerating forests landscapes where AGB varies between 0.4 and 8.4 Mg ha^{-1} within the first year (Anderson et al., 2006). Varying the initial biomass pool between simulations was shown to influence the final AGB estimates in 3-PGS (Nightingale et al., 2008a). This has the potential for RS derived estimates to be higher than to those by 3-PG_2 for SF regenerating in areas such as blow-downs and other natural disturbance, e.g. the large blow-down in the north west of the study site in Manaus. These areas often have higher tree species diversity in comparison to those areas subject to anthropogenic influences (Chambers et al., 2013; Baker et al., 2016) and a ready source of seedlings and saplings leading to rapid recovery for biomass (Turner et al., 1998). In this chapter, this was seen in the comparison of all RS estimates to 3-PG_2 with areas of AGB <50 Mg ha^{-1} in 3-PG_2 being shown to have higher AGB estimates in each corresponding RS estimate. It is important to understand this uncertainty in the AGB of natural disturbances such as blow-downs, ranging from 0.01 ha to 2,651 ha, covered a total of 92,656 ha from 1988 to 2001 in the BLA (Nelson et al., 1994; Espírito-Santo et al., 2010, 2014).

Higher estimates by 3-PG_2 than the remote sensing estimates occur at the edges of intensively used pastures and small fragments that are densely distributed north of Manaus. In such areas, AGB accumulation is often limited by edge effects, such as increased tree mortality or variation in seed rain with distance from forest sources in (Chaplin-Kramer et al., 2015). Additional biomass loss occurs at forest edges through

tree mortality of large trees within 300 m of the forest edge due to changes in the micro climate and elevated wind turbulence (Laurance et al., 1997, 2000). These are replaced by short-lived pioneers in high stem densities (Laurance et al., 2006) thus reducing AGB in these areas (Nascimento and Laurance, 2004). These forests would therefore have lower AGB than forests of a similar age as estimated by this chapter. Additional causes of the discrepancies seen between estimates include differences in parameterising sample plot measurements; weak allometric relationships for SF in the RS derived estimates (Ometto et al., 2014); sample plot size (Anderson et al., 2010); deforestation between remote sensing data acquisition dates and differences in height and specific wood density across biogeographic areas (Feldpausch et al., 2011).

7.7.2 Importance for Brazilian Amazon

INPE determined the area of land within the PRODES deforestation estimates under secondary vegetation to be 3.3 % (16.5 Mha) of the BLA in 2010 (de Almeida et al., 2016). The mean SF age distribution of the three areas studied in this thesis in 2010, the last common date, was 29 %, 45 % and 26 % for young (0–5 years), intermediate (6–15 years) and advanced (≥16 years) SF, respectively. Assuming this distribution is consistent across the BLA there was 4.8 Mha, 7.4 Mha, 4.3 Mha of young, intermediate and advanced SF present, respectively, in 2010. Using 3-PG_2, regionally variable growth rates can be used to estimate the mean above ground carbon (AGC) within each age class. This variation was achieved using the initial datasets outlined in Chapter 6 and 7. Mean simulated AGC across the three studies sites for these classes is 5.0±5.6 Mg C ha^{-1}, 39.8±18.2 Mg C ha^{-1} and 128±41.7 Mg C ha^{-1}, respectively, assuming the carbon content of AGB is 45 % (Fearnside, 2000). Estimated secondary forest carbon content for the Brazilian Amazon in 2010 is shown in Table 7.6.

Table 7.6: Estimated secondary forest age and above ground biomass distribution for the Brazilian Legal Amazon. Assumptions of age are based on the distributions see at Manaus, Santarém and Machadinho dOeste in Chapter 4. Above ground biomass estimates are derived from 3-PG_2.

	1–5 years	**6–15 years**	**≥16 years**	**Total**
Area (Mha)	4.8	7.4	4.3	16.5
Total biomass (Pg C)	0.0108	0.1334	0.2487	0.39
Total standard deviation (Pg C)	0.0120	0.0609	0.0806	0.15

The Brazilian Ministry of Science and Technology (MCT) estimated 18.1 $\times$ 10^6 Mg C yr^{-1} absorption by SF between 2002 and 2010 in their Third National Communication to the United Nations Framework Convention on Climate Change (UNFCC). Carbon (C) in AGB accumulated at a rate of 2.6 Mg C ha^{-1} yr^{-1} over 6,998,799 ha (MCT (Ministry of Science and Technology), 2016), using a carbon content of AGB as 45 % (Fearnside, 2000). Secondary forest age distribution for 2010 in Manaus, Machadinho d'Oeste and Santarém ranged from 1 to 33 years with 72 % $\leq$15 years old (Chapter 4). Mean AGC accumulation rate of these forests, as predicted by 3-PG_2 across the three sites, is shown in Table 7.7. Assuming these distributions and accumulation rates are representative of the BLA, the estimate of secondary forest carbon uptake is higher by a factor of 1.77 in Brazil's communication to the UNFCCC. The absolute difference is 7.9 $\times$ 10^6 Mg C yr^{-1} between 2002 and 2010.

Wandelli and Fearnside (2015) conducted a similar comparison for Brazil's Second National Communication to the UNFCC (1994–2002) using different accumulation rates for SF regenerating on pasture and SF regenerating on agriculture with an assumed mean SF age of four years in 2002. Wandelli and Fearnside (2015) estimated that carbon uptake estimated by MCT (Ministry of Science and Technology) (2010) was higher by a factor of 4.1 with an absolute difference of 6.8 $\times$ 10^6 Mg C yr^{-1}. However, this is owing to the use of the value of 9 $\times$ 10^6 Mg CO_2 yr^{-1}. Carbon dioxide has a molecular mass 3.67 times greater than carbon, therefore the true estimate of AGC accumulation for 1994–2002 was 2.5 $\times$ 10^6 Mg C yr^{-1}. Therefore a revised carbon uptake was higher by a factor of 1.14, with an absolute difference of 0.3 $\times$ 10^6 Mg C yr^{-1} according to Wandelli and Fearnside (2015). In addition, consideration of SF older than 8 years was limited owing to the field data on which the AGC accumulation rates were based. Where as in this thesis, all possible ages for SF, i.e. upto 37 years old, can be considered using the results of Chapter 4 (Table 7.7).

Chazdon et al. (2016) estimated SF age based on a regression, derived from extensive plot data, of AGB from Baccini et al. (2012) for Latin American countries including Brazil. Secondary forest was divided into three age classes: 0–20 years, 20–60 years and 60–100 years. This was achieved using the Michaelis-Menten (MM) equation:

$$AGB = (a \times Age)/(a_{50} + Age) \tag{7.2}$$

where a is an asymptote parameter that defines AGB of mature forests and a_{50} defines the age at which 50 % of mature forest AGB is reached. These were derived from intact forest reserves and a regression of total precipitation, climate water deficit and rainfall seasonality, respectively. Table 7.8 shows the a and a_{50} for the three study sites and the median AGB from Baccini et al. (2012) for the areas of SF identified in Chapter 4. These data were used to estimated SF *Age* from the Baccini SF AGB for each study site using the inverted MM equation, the same method as that used by Chazdon et al. (2016):

$$Age = (a_{50} \times AGB)/(a - AGB) \tag{7.3}$$

where age is in years and AGB (Mg ha^{-1}) is the median Baccini et al. (2012) for each

Table 7.7: Mean above ground carbon accumulation rates for secondary forest present between 2002-2010, estimated by 3-PG$_2$.

Age	% of SF area	AGC accumulation rate (Mg C yr^{-1})	Total area (ha)	Total accumlation rate (Mg C yr^{-1})
1	11.20%	0.33	783,764.38	261,306.84
2	6.80%	0.49	476,016.20	235,081.82
3	2.27%	0.52	158,637.11	81,782.62
4	3.45%	0.79	241,210.57	189,707.33
5	3.95%	1.04	276,378.07	288,740.82
7	8.92%	1.40	624,136.33	870,728.30
8	8.68%	1.46	607,228.88	886,893.55
9	6.11%	1.60	427,785.66	682,736.70
10	0.79%	1.68	55,138.18	92,484.66
11	6.45%	1.75	451,600.76	788,512.58
12	6.66%	1.80	466,316.57	841,595.33
13	1.29%	1.81	90,439.50	163,705.92
14	2.15%	1.85	150,698.74	279,118.58
15	3.45%	1.91	241,756.67	461,442.17
16	2.86%	1.95	200,126.37	390,775.74
17	1.14%	1.97	80,110.58	157,504.26
18	1.91%	1.93	133,328.37	256,717.20
19	3.35%	2.03	234,371.64	476,442.52
20	0.52%	2.11	36,632.21	77,255.50
21	3.15%	2.15	220,704.64	474,956.21
22	4.46%	2.19	312,442.48	683,784.59
23	0.23%	2.18	16,216.69	35,321.69
24	0.47%	2.16	32,943.31	71,316.10
25	4.87%	2.16	341,186.96	736,696.98
26	0.51%	2.17	35,380.88	76,677.59
27	4.24%	2.21	296,945.49	655,206.55
33	0.10%	2.27	7,301.85	16,603.28
		Total	6,998,799.10	10,233,095.41

study site.

Table 7.8: Michaelis-Menten equation parameters for Manaus, Santarém and Machadinho d'Oeste.

	3-PG$_2$ a_{50}	a (Mg ha^{-1})	Median Baccini et al. (2012) SF AGB (Mg ha^{-1})
Manaus	31	355 (Laurance et al., 1999)	197
Santarém	37	372 (Keller et al., 2001)	183
Machadinho d'Oeste	56	446 (Alves et al., 1997)	120

This resulted in a median SF age of 39, 36 and 21 for Manaus, Santarém and Machadinho d'Oeste, respectively. These ages for SF in 2008 are, on average, 3.4 times greater than those derived from the dense time series analysis in Chapter 4 from the same year. This indicates that SF 0–20 years would represent a greater proportion of the SF aged 60–100 years in moist tropical forests in the BLA than predicted by Chazdon et al. (2016). This increase would be mirrored by a reduction in SF between 20–60 years old as a portion of it would be categorised as younger forest. However this age class, and SF aged 60–100 years, has a mean AGB above that for which 3-PG$_2$ was parameterised in Chapter 6. These differences reflect the estimated mean difference in SF AGB shown in this Chapter by Baccini et al. (2012). If these differences in AGB are representative of the entire BLA this will alter the AGC held within the SF aged 0–60 years categorised by Chazdon et al. (2016), thus affecting their contribution to the carbon balance of the BLA. However, it is difficult to quantify the extent to which the estimates of Chazdon et al. (2016) will change in this discussion, due to a lack of data field and model parameter-sets for SF older than 37 years.

In addition, Chazdon et al. (2016) estimates that SF (0–20 years) represents 21 % of land cover in Brazil in 2007–2008 whilst INPE categorised only 3.31 % of the BLA as secondary vegetation in 2010 (Almeida Castanho et al., 2016). Hansen et al. (2013) showed that 0.9 % of forests across the entire extent of Brazil, and 0.4 % in the BLA, started regrowing after 2000. Hansen et al. (2013) used Landsat data from 2000–2012 limiting the maximum SF age to 11 years. de Almeida et al. (2016) mapped deforestation for 37 years (1973–2010) and has therefore potentially categorised SF up to 36 years old. Neither Hansen et al. (2013) or de Almeida et al. (2016) estimate forest age. Comparison between these values is difficult owing to differences in temporal and spatial scales of the data used for estimation of SF age and extent. This highlights the problems in deriving useful comparative estimates of secondary forest's contribution to the regional

and global carbon balance

7.7.3 Climate sensitivity of 3-PG$_2$

The findings of this chapter continue the downward trend in AGB accumulation rate with increasing air temperature seen previously in Amazonian forest plots across temperature gradients (Malhi et al., 2004), where rates of accumulation decreased from 8.2 Mg ha^{-1} yr^{-1} to 5 Mg ha^{-1} yr^{-1} from 23 ℃ to 28 ℃. This linear trend is continued in this chapter with accumulation rates of 4 Mg ha^{-1} yr^{-1} to 2.7 Mg ha^{-1} yr^{-1} from 29 ℃ to 32 ℃. Similarly, this chapter is in-line with other studies that showed a negative correlation between increasing air temperature and productivity (Zhao and Running, 2010; Vlam et al., 2014; Schippers et al., 2015).

In 3-PG$_2$, maximum air temperature is used to constrain productivity through the temperature growth modifier which reduces the canopy quantum efficiency. Increases in mean annual air temperature above this mean reduces AGB accumulation in tropical trees as they currently operate at their optimum temperature (Way and Oren, 2010). Each IPCC air temperature scenario raises the maximum air temperature. This elevates the mean annual air temperature above the optimum temperature for growth as defined by the long term mean (27.6 ℃). Increases in air temperature will increase vapour pressure deficit (VPD) (Ryan, 2011), particularly as evapotranspiration was not altered in this chapter. This will cause a decrease in the VPD growth modifier and cause a further reduction in productivity in 3-PG$_2$ (Landsberg and Waring, 1997).

Decreases in tree growth in the reduced precipitation simulations of this chapter show a similar trend to throughfall exclusion experiments across the tropics (Brando et al., 2008; Trumbore and Barbosa De Camargo, 2009; Metcalfe et al., 2010; Schuldt et al., 2011). Reductions in precipitation of 30–40 % caused a mean reduction in AGB accumulation of 0.7 Mg ha^{-1} yr^{-1} in throughfall experiments in Amazonia (Brando et al., 2008; Trumbore and Barbosa De Camargo, 2009; Metcalfe et al., 2010). In addition, Fischer et al. (2014) showed that a reduction >30 % in precipitation was required to impact above ground carbon stocks by use of a process based model. These findings however are in contrast to this chapter which indicated that a 21 % reduction in annual precipitation reduced AGB accumulation by 2.9 Mg ha^{-1} yr^{-1}. Phillips et al. (2009) showed that

mature forests subjected to a 100 mm increase in water deficit, lost 10.6 Mg ha^{-1}. Whilst the same reduction in precipitation caused the final AGB of secondary forests to decline by 27 Mg ha^{-1} in 3-PG$_2$. These comparisons highlight a possible limitation in using 3-PG$_2$ to simulate the effects of reduced precipitation on tropical forest growth.

In this chapter, a positive correlation between increasing precipitation and AGB accumulation is indicative of available soil water limitation on tree growth given current temperature conditions in 3-PG$_2$. The soil water growth modifier determines the overall effect of the volume of available soil water on productivity. It is derived from soil texture constants and available soil water which increases with increased precipitation in 3-PG$_2$ (Almeida et al., 2007a). Similarly to this chapter, Malhi et al. (2004) indicated a positive correlation between annual precipitation and AGB accumulation rates in Amazonia forest plots. However, the increase in AGB accumulation predicted by 3-PG$_2$ was six times greater than that shown by Malhi et al. (2004). Although it is likely that this is because they were unable to control mean annual air temperature in the field, this is important because it was shown to have a greater correlation with above ground coarse wood productivity than precipitation by Malhi et al. (2004).

These discrepancies in the prediction of responses by forest growth to changes in precipitation are related to processes in the canopy and below ground. Root and foliage components are key in determining the drought response of trees (McDowell, 2011). In 3-PG$_2$ root volume determines the area of the root zone from which water can be utilised and foliage mass is used in the simulation of canopy processes such as transpiration and conductance. Partitioning to these components is not validated in this parameterisation (Chapter 6) and may therefore require further parameterisation to effectively simulate the effects of reduced mean annual precipitation on AGB accumulation.

The combined effects of higher air temperature and lower precipitation are typical of droughts often initiated by El Nino Southern Oscialltions (ENSO) in the Amazon (Marengo et al., 2008; Zeng et al., 2008). These events have caused severe droughts in the Amazon in recent decades causing losses in above ground carbon from 1.6 Pg C to 2.2 Pg C (Lewis et al., 2011). Responses to climate change shown in this chapter and White et al. (2006) highlight the potential of 3-PG$_2$ to study the possible effects on individual secondary forest stands whilst considering greater stresses caused by

ENSO extremes. This is currently limited to yearly time steps as modelling of seasonal differences in the water balance sub model require responses of canopy conductance to temperature, VPD and soil water to be better understood (Almeida et al., 2007a). However, increases in AGB accumulation subject to the median rainfall scenario indicate that recent changes to the water use module of 3-PG in 3-PG$_2$ are able to account for seasonal variations in precipitation.

7.8 Conclusions

This chapter has presented an initial assessment of the process based forest growth model 3-PG$_2$ in estimating secondary forest above ground biomass in comparison to the most up to date estimates of above ground biomass in the tropics. The highest levels of above ground biomass in secondary forest were predicted for the Manaus site were the oldest forests were located. This was followed by estimates for Santarém and lastly Machadinho d'Oeste where secondary forests were younger. Remote sensing estimates of secondary forest above ground biomass up to 37 years old were higher by a factor of 3.6 at the Manaus site. These estimates were used to highlight the uncertainty in regional secondary forest biomass estimates owing to the unknown distribution of secondary forest age and extent across the Brazilian Amazon.

Long term decreases in precipitation and increase in temperature from current climate conditions will have a negative impact on secondary forest growth. Predicted changes in mean annual precipitation caused greater changes in final AGB of 37 year old secondary forests than predicted changes in temperature. Further parameterisation of 3-PG$_2$ is required however to provide an accurate representation of these processes.

Chapter 8

Discussion and Conclusions

8.1 Discussion

8.1.1 Does land use history derived from remote sensing influence secondary forest above ground biomass accumulation?

Secondary forest (SF) age derived from the remote sensing time-series analysis produced relationships with above ground biomass (AGB) accumulation comparable to studies which assessed SF age through interviews with land owners and field observations (e.g. Uhl et al., 1988; Alves et al., 1997; Feldpausch et al., 2004; Poorter et al., 2016). In addition to validating SF AGB estimates, this result validates SF age derived from dense time-series analysis of optical remote sensing imagery. Limitations of this approach are related to the intensive analysis required to categorise each image into land cover types and the classification accuracy assessment for years where validation data exist, prior to conducting a time series analysis.

The lack of distinction between the chosen land use intensity classes, i.e. frequency of clearance (FC) = 1× and ≥ 2× or period of active land use (PALU) ≤2 years and ≥3 years, highlights that the threshold of remote sensing derived land use intensity required to affect long term AGB accumulation is likely to be similar to studies where land was subject to 'heavy use. Studies which characterised land use as 'heavy use' were characterised by burning and high FC (e.g. Uhl et al., 1988; Wandelli and Fearnside,

2015; Jakovac et al., 2015). This importance of FC was mirrored in this thesis by the improvement of regression fitting to AGB and basal area when including FC, especially.

8.1.2 Can secondary forest growth be modelled using a process based forest growth model?

3-PG$_2$ simulated a realistic representation of net primary productivity in tropical rainforests. This demonstrates the robustness and applicability of the models core physiological processes in forests other than single species plantations. Strong sensitivity to temperature parameters was encouraging as similar controls are apparent in field studies of tropical tree physiological responses (Schippers et al., 2015). In addition, parameter sensitivity remained similar to studies of *E.globulus* plantations demonstrating parameter and model stability across stand types (Song et al., 2012).

The lack of a representation of succession within the 3-PG$_2$ structure led to limitations in the models ability to reproduce the logarithmic growth curves often observed in SF AGB accumulation (Poorter et al., 2016). This limitation is manifest in the model initialisation of a new stand as the model is designed to simulate the growth of a known number of planted trees which cannot increase with recruitment of new individuals. Implementation of a recruitment module may be the first step towards addressing this limitation as the current model structure already incorporates the processes of self-thinning and density dependent mortality needed to simulate the mortality of individual trees as succession progresses (Lohbeck et al., 2013; Lasky et al., 2014).

8.1.3 To what extent has the contribution of secondary forest to the regional carbon budget been over estimated?

The use of combinations of remote sensing data and their relationships with field data to estimate AGB of the tropics do not current consider SF separately from mature forests. Therefore SF age cannot be considered when estimating the AGB of these areas. Comparison of AGB estimates by Saatchi et al. (2011b); Baccini et al. (2012) and Avitabile et al. (2015) for Manaus, Santarém and Machadinho d'Oeste against estimates derived from 3-PG$_2$ highlight greater disagreement between remote sensing estimates

and 3-PG$_2$ at boundaries between SF and other land cover types in comparison to areas of continuous SF. This exposes limitations of employing 3-PG$_2$ to model natural regrowth forests subject to spatial interactions with adjacent land covers. In addition, owing to the fixed value for initial AGB (0.01 Mg ha^{-1}), 3-PG$_2$ estimates that AGB recovery following natural disturbances is lower than remote sensing derived estimates by >180 Mg ha^{-1}.

Estimates reported to the UNFCCC may be up to 1.77 times greater than those by 3-PG$_2$, assuming similar patterns of SF age and AGB across the BLA as seen here. This differences in SF AGB highlight the importance of understanding SF age and extent.

8.1.4 Is a parameterisation of 3-PG$_2$ for current climate conditions an appropriate tool for assessing the impact of future climate change on secondary forests?

Studies of site specific to global scale responses of forest growth to changes in temperature and precipitation highlight the potential negative impacts of future changes in climate (Brando et al., 2008; Phillips et al., 2009). 3-PG$_2$ estimated that forest growth responses to changes in precipitation and air temperature followed similar trends to those seen elsewhere (e.g. Schuldt et al., 2011; Fischer et al., 2014; Vlam et al., 2014). Differences in scale and locality make comparison between estimates difficult. However, AGB accumulation responses to decreases in precipitation were >5 times that seen in field based experiments in the tropics (Brando et al., 2008; Metcalfe et al., 2010). Potential causes of these discrepancies relate to incomplete validation of model outputs such as root and foliage mass. These components are key in determining stand growth responses to changes in air temperature and precipitation. Therefore, further parameterisation is required to simulate responses of these forests to changes in climate. Following this, consideration of the combined effects of changing air temperature, precipitation and evapotranspiration would potentially provide a more realistic forecast of SF responses to future climate conditions.

8.1.5 Wider importance

Globally, tropical forests cover 5816059.2 Mha (Hansen et al., 2013). Forest gain, natural regrowth and plantations, present in 2012, which started growing in 2001, made up 0.4 % of this. The age of these forests, and those that began regrowing before 2001 is still unknown. This study, and many others, show that SF age is the most significant predictor of SF AGB (e.g. Wandelli and Fearnside, 2015; Poorter et al., 2016). Therefore this is the most important parameter required to estimate SF contribution to the global carbon cycle still requiring estimation as many other contributing factors, such as extent, growth conditions and remote sensing measurements, are readily available.

Incorporation of spatially variable AGB estimates is an important next step in reporting the national and regional contributions of forests for climate change mitigation. Variables such as temperature, precipitation and radiation are key important drivers of forest growth and can be considered through a process based modelling approach, such as that described here. A modelling based approach, with the ability to forecast carbon absorption though forest growth, will be beneficial in submitting national adaptation programme of actions (NAPAs). NAPAs provide a process for Non-Annex I countries to identify priority activities responding to their urgent and immediate needs with regard to adaptation to climate change (Hardee and Mutunga, 2010). In Brazil and other Non Annex I countries with deforested tropical forests a process based modelling framework would allow the estimation of potential SF carbon sequestration in deforested areas yet to be abandoned.

Differences in land management have multiple implications for forest regrowth beyond AGB (e.g. Martin et al., 2013; Cram et al., 2015; Newbold et al., 2015; Jakovac et al., 2016). Land use-intensification, often resulting in high FC, explains more variation in species density than SF age (Williamson et al., 2014; Mesquita et al., 2015) and impedes SF height and BA increases (Jakovac et al., 2015). Areas with high land use intensity may be at risk of entering a state of arrested succession which reduces SF potential to provide environmental service to Amazonian people (Jakovac et al., 2015).

Knowledge of extent, condition and carbon content are key parameters for REDD+ monitoring and reporting. Along with the ability to forecast biomass accumulation, the implementation of a forest growth model has the potential to be a key step in allowing

more intelligent and active management of land to be achieved for meeting REDD+ targets and the role of regrowth in achieving those targets.

8.2 Main Findings

Using remote sensing and established field data analysis techniques this thesis investigated the impact of land use intensity on recovery of above ground biomass in areas undergoing regeneration. Land use intensity and age varied across the three sites studied here. Manaus experienced the lowest intensity of land use and had some of the oldest secondary forests. This in contrast to Machadinho d'Oeste where the secondary forests exhibited the highest land use intensity and largest proportion of young forests of the three study sites. These differences are attributed to patterns in deforestation and regrowth rates at the three locations.

After >30 years of regrowth in secondary forests near Manaus, there was no significant difference in above ground biomass estimates between land use classes; (defined by the remote sensing metrics) frequency of clearance and period of active land use. After 37 years of regrowth secondary forests attained up to two thirds the above ground biomass of mature forests near Manaus. Light to medium land use intensity does not cause significant differences in above ground biomass accumulation of secondary forests up to 37 years.

Using Monte Carlo analysis techniques a variance based global sensitivity analysis and parameterisation was conducted for the process based forest growth model 3-PG_2. 3-PG_2 was demonstrated to be applicable outside of plantation forests, for which is was designed, through a similarly high sensitivity to parameters operating at the models core. This work presents the first 3-PG_2 parameter-set for predicting, to the authors knowledge, above ground biomass, basal area and diameter at breast height in moist tropical secondary forest in the Brazilian Amazon up to 37 years of age.

Using regionally specific initial site parameters and meteorological data, the process based forest growth model 3-PG_2 was used to scrutinise the performance of current remote sensing techniques in the estimation of tropical secondary forest above ground biomass. Remote sensing derived estimates of above ground biomass were significantly greater than those predicted by 3-PG_2, on average by a factor of 3.6. Applying

these adjusted biomass accumulation rates and assuming similar secondary forest age distributions, the carbon uptake calculated in Brazil's report to the UNFCCC was greater than this study with in estimates for secondary forest carbon absorption of up to 1.77 times greater. Furthermore, the use of these remote sensing above ground biomass estimates to derive secondary forests age has the potential to overestimate forest age by a factor of 3. Based on estimates of secondary forest extent and assumptions of the distributions of age and above ground carbon, the estimated carbon stored in secondary forest of the Brazilian Amazon was 0.39 Pg C ±0.15 Pg C in 2010.

Increases in annual air temperature ≥1.7 ℃ reduce above ground biomass accumulation by 0.4 Mg ha^{-1} yr^{-1} $℃^{-1}$. Whilst trends in the responses to changes in annual precipitation are similar to those indicated by field studies, their magnitude differs by a factor of up to six. Further investigation and parameterisation is required to validate the applicability of 3-PG_2 in forecasting forest growth in respect to future changes in precipitation and subsequent changes in evapotranspiration.

8.3 Conclusion

- The period of active land use and frequency of clearance required to significantly reduce above ground biomass accumulation in secondary forests is greater than three years and greater than one clearance, respectively.
- More than 37 years of regrowth is necessary to recover levels of above ground biomass comparable to primary forests north of Manaus.
- The forest growth model 3-PG_2 was adapted to mixed tropical secondary forests. Modelled simulations and in field estimates of above ground biomass could be related after 37 years of growth.
- Using 3-PG_2 forest growth was shown to respond negatively to future changes in climate, the magnitude of the response is uncertain.

8.4 Future work

8.4.1 Secondary forest age and extent

This thesis highlighted the uncertainty in secondary forest above ground biomass estimates owing to a lack of knowledge regarding the true distribution of secondary forest extent and age within the Brazilian Amazon. de Almeida et al. (2016) estimated the extent of secondary vegetation within the deforested areas mapped annually under the PRODES programme in 2008 and 2010.

Developments since the completion of Chapter 4 allow the estimation of secondary forest age using single date remote sensing imagery, with a combination of optical (Landsat Thematic Mapper) and radar (Advanced Land Observing Satellite Phased Arrayed L-band Synthetic Aperture Radar) (Carreiras et al., 2016). The combination of these outputs would allow the estimation of secondary forest age for the entire Brazilian Amazon.

8.4.2 Canopy and below ground processes in 3-PG$_2$

Assessments of model sensitivity to changes in air temperature and precipitation, given the current parameterisation for secondary forest, highlight potential areas where the model does not produce a representative simulation of moist tropical secondary forest. These areas include processes which govern water-use efficiency such as canopy and below ground processes. To improve the models performance in simulating these processes requires validation of model outputs such as leaf area index, root mass and foliage mass. Better parameterisation of the modules which govern these outputs requires collating secondary forest data from sources such as the RAINFOR network (Malhi et al., 2004) and TropForC (Anderson-Teixeira et al., 2016). Additional field work may be necessary when such data is unavailable. Specific attention will be given to collecting data on the parameters identified as having the highest sensitivity in 3-PG$_2$. This data will be used to create a single, or indeed multiple, parameter-set(s) that represent secondary forests across the basin.

8.4.3 Reproducing succession

Under estimation of stand properties in young secondary forest by 3-PG$_2$ is caused by a failure to replicate an asymptotic growth curve when the stem density remains constant. This growth curve often, observed in secondary forest (Poorter et al., 2016), is a characteristic of continual turnover of functional groups during succession as these forests move towards the dynamic equilibrium state of mature forests. 3-PG$_2$ has to date only considered plantation stands that do not have a process representative of succession, e.g. recruitment of new trees.

The implementation of a hierarchy of individual models will potentially simulate natural regrowth and succession by 3-PG$_2$. This will involve a hierarchical sequence of 3-PG$_2$ model runs that feed into one another that are individually parameterised for a particular age range. This will include a suitable maximum age parameter to reduce stem counts through time to more accurately represent outputs influenced by the turn over of trees within a stand such as basal area, mean diameter at breast height and stem biomass.

References

Achard, F., Eva, H. D., Stibig, H.-J., Mayaux, P., Gallego, J., Richards, T., Malingreau, J.-P., 2002. Determination of deforestation rates of the world's humid tropical forests. Science 297 (5583), 999–1002.

Affum-baffoe, K., Baker, T. R., Lewis, S. L., Lopez-gonzalez, G., Sonke, B., Djuikouo, K., Ojo, L. O., Phillips, O. L., Reitsma, J. M., White, L., Comiskey, J. A., Ewango, C. E. N., Feldpausch, T. R., Hamilton, A. C., Gloor, M., Hart, T., Hladik, A., Lloyd, J., Lovett, J. C., Makana, J.-r., Malhi, Y., Mbago, F. M., Ndangalasi, H. J., 2009. Increasing carbon storage in intact African tropical forests. Nature 457 (February).

Ahlström, A., Schurgers, G., Arneth, A., 2012. Robustness and uncertainty in terrestrial ecosystem carbon response to CMIP5 climate change projections. Environmental Research Letters 7 (4), 44008.
URL http://stacks.iop.org/1748-9326/7/i=4/a=044008

Aichi, 2011. Strategic Plan for Biodiversity 2011 2020 and the Aichi Targets.
URL www.cbd.int/sp2020

Aide, T., Zimmerman, J. K., Herrera, L., Rosario, M., Serrano, M., sep 1995. Forest recovery in abandoned tropical pastures in Puerto Rico. Forest Ecology and Management 77 (1-3), 77–86.
URL http://www.sciencedirect.com/science/article/pii/037811279503576V

Aide, T. M., Cavelier, J., 1994. Barriers to Lowland Tropical Forest Restoration in the Sierra Nevada de Santa Marta, Colombia. Restoration Ecology 2 (4), 219–229.
URL http://dx.doi.org/10.1111/j.1526-100X.1994.tb00054.x

Alder, D., 1996. Models for basal area dynamics of mixed tropical forest: Neo-tropical experience and prospects for application in Ghana. Growth studies in tropical moist forest in Africa, 93–105.

Alder, D., Silva, J. N. M., 2012. The cohort-empirical modelling strategy and its application to forest management for Tapajós Forest , Pará , Brazilian Amazon. CEP 314 (4), 17–23.
URL http://www.bio-met.co.uk/pdf/2Alder314.pdf

Alexander, L., Allen, S., Bindoff, N. L., Bréon, F.-M., Church, J., Cubasch, U., Emori, S., Forster, P., Friedlingstein, P., Nathan, Gillett, Gregory, J., Hartmann, D., Jansen, E., Ben, Kirtman, Knutti, R., Kanikicharla, K. K., Lemke, P., Marotzke, J., Masson-Delmotte, V., Meehl, G., Mokhov, I., Piao, S., Plattner, G.-K., Dahe, Q., Ramaswamy, V., Randall, D., Rhein, M., Rojas, M., Sabine, C., Shindell, D., Stocker, T. F., Talley, L., Vaughan, D., Xie, S.-P., 2013. Working Group 1 Contribution to the IPCC Fifth Assessment Report Climate Change 2013: The Physical Science Basis Summary for Policy Makers. Tech. Rep. September 2013, Intergovernmental Panel on Climate Change.

Almeida, A. C., Landsberg, J. J., Sands, P. J., may 2004a. Parameterisation of 3-PG model for fast-growing Eucalyptus grandis plantations. Forest Ecology and Management 193 (1-2), 179–195.
URL http://www.sciencedirect.com/science/article/pii/S037811270400057X

Almeida, A. C., Landsberg, J. J., Sands, P. J., Ambrogi, M. S., Fonseca, S., Barddal, S. M., Bertolucci, F. L., may 2004b. Needs and opportunities for using a process-based productivity model as a practical tool in Eucalyptus plantations. Forest Ecology and Management 193 (1-2), 167–177.
URL http://www.sciencedirect.com/science/article/pii/S0378112704000568

Almeida, A. C., Maestri, R., Landsberg, J. J., Scolforo, J. R. S., 2003. Linking process-based and empirical forest models in Eucalyptus plantations in Brazil. Modelling Forest Systems. CABI, Wallingford, UK, 63–74.

Almeida, A. C., Paul, K. I., Siggins, A., Sands, P. J., Polglase, P., Marcar, N. E., Jovanovic, T., Theiveyanathan, S., Crawford, D. F., England, J. R., Falkiner, R., Hawkins, C., White., D., 2007a. Development, calibration and validation of the forest growth model 3-PG with an improved water balance. Tech. rep., ensis.

Almeida, A. C., Sands, P. J., 2015. Improving the ability of 3PG to model the water balance of forest plantations in contrasting environments. Ecohydrology.

Almeida, A. C., Soares, J. V., Landsberg, J. J., Rezende, G. D., oct 2007b. Growth and water balance of Eucalyptus grandis hybrid plantations in Brazil during a rotation for pulp production. Forest Ecology and Management 251 (1-2), 10–21.
URL http://www.sciencedirect.com/science/article/pii/S037811270700463X

Almeida Castanho, A. D., Galbraith, D., Zhang, K., Coe, M. T., Costa, M. H., Moorcroft, P., 2016. Changing Amazon biomass and the role of atmospheric CO2 concentration, climate, and land use. Global Biogeochemical Cycles.

Alvarez-Clare, S., Mack, M. C., Brooks, M., jul 2013. A direct test of nitrogen and phosphorus limitation to net primary productivity in a lowland tropical wet forest. Ecology 94 (7), 1540–1551.
URL http://dx.doi.org/10.1890/12-2128.1

Alves, D., Soares, J. V., Amaral, S., Mello, E., Almeida, S., Da Silva, O. F., Silveira, A., 1997. Biomass of primary and secondary vegetation in Rondônia, Western Brazilian Amazon. Global Change Biology 3 (5), 451–461.

Alves, D. S., Morton, D. C., Batistella, M., Roberts, D. A., Souza, C., 2009. The Changing Rates and Patterns of Deforestation and Land Use in Brazilian Amazonia. In: Amazonia and Global Change. American Geophysical Union, pp. 11–23.
URL http://dx.doi.org/10.1029/2009GM000902

Anderson, K. J., Allen, A. P., Gillooly, J. F., Brown, J. H., 2006. Temperaturedependence of biomass accumulation rates during secondary succession. Ecology Letters 9 (6), 673–682.

Anderson, L. O., Malhi, Y., Aragão, L. E. O. C., Ladle, R., Arai, E., Barbier, N., Phillips, O., aug 2010. Remote sensing detection of droughts in Amazonian forest canopies. The New phytologist 187 (3), 733–750.
URL http://www.ncbi.nlm.nih.gov/pubmed/20659255

Anderson, M. C., Norman, J. M., Meyers, T. P., Diak, G. R., 2000. An analytical model for estimating canopy transpiration and carbon assimilation fluxes based on canopy light-use efficiency. Agricultural and Forest Meteorology 101 (4), 265–289.

Anderson-Teixeira, K. J., Wang, M. M. H., McGarvey, J. C., LeBauer, D. S., jan 2016. Carbon dynamics of mature and regrowth tropical forests derived from a pantropical database (TropForC-db). Global change biology.
URL http://www.ncbi.nlm.nih.gov/pubmed/26790568

Aragão, L. E. O. C., Malhi, Y., Roman-Cuesta, R. M., Saatchi, S., Anderson, L. O., Shimabukuro, Y. E., apr 2007. Spatial patterns and fire response of recent Amazonian droughts. Geophysical Research Letters 34 (7), n/a–n/a.
URL http://dx.doi.org/10.1029/2006GL028946

Aragão, L. E. O. C., Poulter, B., Barlow, J. B., Anderson, L. O., Malhi, Y., Saatchi, S., Phillips, O. L., Gloor, E., nov 2014. Environmental change and the carbon balance of Amazonian forests. Biological Reviews 89 (4), 913–931.
URL http://dx.doi.org/10.1111/brv.12088

ArroyoRodríguez, V., CavenderBares, J., Escobar, F., Melo, F. P. L., Tabarelli, M., Santos, B. A., 2012. Maintenance of tree phylogenetic diversity in a highly fragmented rain forest. Journal of ecology 100 (3), 702–711.

ArroyoRodríguez, V., Melo, F. P. L., MartínezRamos, M., Bongers, F., Chazdon, R. L., Meave, J. A., Norden, N., Santos, B. A., Leal, I. R., Tabarelli, M., 2015. Multiple successional pathways in humanmodified tropical landscapes: new insights from forest succession, forest fragmentation and landscape ecology research. Biological Reviews.

Asner, G. P., jun 2011. Painting the world REDD: addressing scientific barriers to monitoring emissions from tropical forests. Environmental Research Letters 6 (2), 21002.
URL http://stacks.iop.org/1748-9326/6/i=2/a=021002?key=crossref.21f477eee28606ba8f23aafc73162d95

Asner, G. P., Elmore, A. J., Olander, L. P., Martin, R. E., Harris, A. T., oct 2004. GRAZING SYSTEMS, ECOSYSTEM RESPONSES, AND GLOBAL CHANGE. Annual Review of Environment and Resources 29 (1), 261–299.
URL http://dx.doi.org/10.1146/annurev.energy.29.062403.102142

Asner, G. P., Knapp, D. E., Broadbent, E. N., Oliveira, P. J. C., Keller, M., Silva, J. N., oct 2005. Selective Logging in the Brazilian Amazon. Science 310 (5747), 480–482.
URL http://www.sciencemag.org/content/310/5747/480.abstract

Avitabile, V., Herold, M., Heuvelink, G. B. M., Lewis, S. L., Phillips, O. L., Asner, G. P., Armston, J., Asthon, P., Banin, L. F., Bayol, N., 2015. An integrated pantropical biomass map using multiple reference datasets. Global change biology.

Aweto, A. O., jul 1981. Secondary Succession and Soil Fertility Restoration in South-Western Nigeria: II. Soil Fertility Restoration. Journal of Ecology 69 (2), 609–614.
URL http://www.jstor.org/stable/2259687

Aylett, G. P., 1985. Irradiance interception, leaf conductance and photosynthesis in Jamaican upper montane rain forest trees. Photosynthetica.

Baccini, A., Goetz, S. J., Walker, W. S., Laporte, N. T., Sun, M., Sulla-Menashe, D., Hackler, J., Beck, P. S. a., Dubayah, R., Friedl, M. a., Samanta, S., Houghton, R. a., jan 2012. Estimated carbon dioxide emissions from tropical deforestation improved by carbon-density maps. Nature Climate Change 2 (3), 182–185.
URL http://www.nature.com/doifinder/10.1038/nclimate1354

Bacha, C. J. C., Rodriguez, L. C. E., 2007. Profitability and social impacts of reduced impact logging in the Tapajós National Forest, BrazilA case study. Ecological Economics 63 (1), 70–77.

Bagley, J. E., Desai, A. R., Harding, K. J., Snyder, P. K., Foley, J. A., aug 2013. Drought and Deforestation: Has Land Cover Change Influenced Recent Precipitation Extremes in the Amazon? Journal of Climate 27 (1), 345–361.
URL http://dx.doi.org/10.1175/JCLI-D-12-00369.1

Baker, T. R., Phillips, O. L., Malhi, Y., Almeida, S., Arroyo, L., Di Fiore, A., Erwin, T., Higuchi, N., Killeen, T. J., Laurance, S. G., 2004. Increasing biomass in Amazonian forest plots. Philosophical Transactions of the Royal Society of London: Biological Sciences 359 (1443), 353–365.

Baker, T. R., Vela Díaz, D. M., Chama Moscoso, V., Navarro, G., Monteagudo, A., Pinto, R., Cangani, K., Fyllas, N. M., Lopez Gonzalez, G., Laurance, W. F., 2016. Consistent, small effects of treefall disturbances on the composition and diversity of four Amazonian forests. Journal of Ecology.

Barber, C. P., Cochrane, M. A., Souza, C. M., Laurance, W. F., 2014. Roads, deforestation, and the mitigating effect of protected areas in the Amazon. Biological conservation 177, 203–209.

Barlow, J., Parry, L., Gardner, T. A., Ferreira, J., Aragão, L. E., Carmenta, R., Berenguer, E., Vieira, I. C., Souza, C., Cochrane, M. A., oct 2012. The critical importance of considering fire in REDD+ programs. Biological Conservation 154, 1–8.
URL http://www.sciencedirect.com/science/article/pii/S0006320712001772

Barlow, J., Peres, C. A., Lagan, B. O., Haugaasen, T., 2003. Large tree mortality and the decline of forest biomass following Amazonian wildfires. Ecology letters 6 (1), 6–8.

Barona, E., Ramankutty, N., Hyman, G., Coomes, O. T., apr 2010. The role of pasture and soybean in deforestation of the Brazilian Amazon. Environmental Research Letters 5 (2), 24002.
URL http://stacks.iop.org/1748-9326/5/i=2/a=024002?key=crossref.0915548e0da31af1f7accd6aaf06b3e3

Batistella, M., Moran, E. F., jun 2005. Dimensões humanas do uso e cobertura das terras na Amazônia: uma contribuição do LBA. Acta Amazonica 35 (2), 239–247.
URL http://www.scielo.br/scielo.php?script=sci{_}arttext{\&}pid=S0044-59672005000200014{\&}lng=pt{\&}nrm=iso{\&}tlng=pt

Battaglia, M., Sands, P., 1997. Modelling site productivity of Eucalyptus globulus in response to climatic and site factors. Functional Plant Biology 24 (6), 831–850.

Battaglia, M., Sands, P., White, D., Mummery, D., 2004. CABALA: a linked carbon, water and nitrogen model of forest growth for silvicultural decision support. Forest Ecology and Management 193 (1), 251–282.

BDMEP, 2014. Bank of Meteorological Data for Education and Research (BDMEP).
URL http://www.inmet.gov.br/projetos/rede/pesquisa/

Bierregaard, R. O., 2001. Lessons from Amazonia : the ecology and conservation of a fragmented forest. Yale University Press, New Haven.

Bierregaard Jr., R. O., Lovejoy, T. E., Kapos, V., dos Santos, A. A., Hutchings, R. W., dec 1992. The Biological Dynamics of Tropical Rainforest Fragments. BioScience 42 (11), 859—-866 CR —- Copyright © 1992 Oxford Univer.
URL http://www.jstor.org/stable/1312085

Bini, D., dos Santos, C. A., do Carmo, K. B., Kishino, N., Andrade, G., Zangaro, W., Nogueira, M. A., mar 2013. Effects of land use on soil organic carbon and microbial processes associated with soil health in southern Brazil. European Journal of Soil Biology 55, 117–123.
URL http://www.sciencedirect.com/science/article/pii/S1164556313000071

Blay, D., 2002. Tropical secondary forest management in humid Africa: reality and perspectives. In: Proceedings of the Workshop on Tropical Secondary Forest Management in Africa: Reality and Perspectives, Kenya. pp. 9–13.

Bonan, G. B., jun 2008. Forests and Climate Change: Forcings, Feedbacks, and the Climate Benefits of Forests. Science 320 (5882), 1444–1449.
URL http://science.sciencemag.org/content/320/5882/1444.abstract

Bossel, H., Krieger, H., dec 1991. Simulation model of natural tropical forest dynamics. Ecological Modelling 59 (1-2), 37–71.
URL http://www.sciencedirect.com/science/article/pii/030438009190127M

Bot, A., Benites, J., 2005. The importance of soil organic matter: key to drought-resistant soil and sustained food production. No. 80. Food & Agriculture Org.

Botkin, D. B., Janak, J. F., Wallis, J. R., 1972. Some ecological consequences of a computer model of forest growth. The Journal of Ecology, 849–872.

Bowman, M. S., Soares-Filho, B. S., Merry, F. D., Nepstad, D. C., Rodrigues, H., Almeida, O. T., jul 2012. Persistence of cattle ranching in the Brazilian Amazon: A spatial analysis of the rationale for beef production. Land Use Policy 29 (3), 558–568.
URL http://www.sciencedirect.com/science/article/pii/S0264837711001037

Brando, P. M., Nepstad, D. C., Davidson, E. A., Trumbore, S. E., Ray, D., Camargo, P., may 2008. Drought effects on litterfall, wood production and belowground carbon cycling in an Amazon forest: results of a throughfall reduction experiment. Philosophical Transactions of the Royal Society of London B: Biological Sciences 363 (1498), 1839–1848.

URL http://rstb.royalsocietypublishing.org/content/363/1498/1839.abstract

Bregman, T. P., Sekercioglu, C. H., Tobias, J. A., 2014. Global patterns and predictors of bird species responses to forest fragmentation: implications for ecosystem function and conservation. Biological Conservation 169, 372–383.

Brienen, R. J. W., Phillips, O. L., Feldpausch, T. R., Gloor, E., Baker, T. R., Lloyd, J., Lopez-Gonzalez, G., Monteagudo-Mendoza, A., Malhi, Y., Lewis, S. L., Vasquez Martinez, R., Alexiades, M., Alvarez Davila, E., Alvarez-Loayza, P., Andrade, A., Aragao, L. E. O. C., Araujo-Murakami, A., Arets, E. J. M. M., Arroyo, L., Aymard C., G. A., Banki, O. S., Baraloto, C., Barroso, J., Bonal, D., Boot, R. G. A., Camargo, J. L. C., Castilho, C. V., Chama, V., Chao, K. J., Chave, J., Comiskey, J. A., Cornejo Valverde, F., da Costa, L., de Oliveira, E. A., Di Fiore, A., Erwin, T. L., Fauset, S., Forsthofer, M., Galbraith, D. R., Grahame, E. S., Groot, N., Herault, B., Higuchi, N., Honorio Coronado, E. N., Keeling, H., Killeen, T. J., Laurance, W. F., Laurance, S., Licona, J., Magnussen, W. E., Marimon, B. S., Marimon-Junior, B. H., Mendoza, C., Neill, D. A., Nogueira, E. M., Nunez, P., Pallqui Camacho, N. C., Parada, A., Pardo-Molina, G., Peacock, J., Pena-Claros, M., Pickavance, G. C., Pitman, N. C. A., Poorter, L., Prieto, A., Quesada, C. A., Ramirez, F., Ramirez-Angulo, H., Restrepo, Z., Roopsind, A., Rudas, A., Salomao, R. P., Schwarz, M., Silva, N., Silva-Espejo, J. E., Silveira, M., Stropp, J., Talbot, J., ter Steege, H., Teran-Aguilar, J., Terborgh, J., Thomas-Caesar, R., Toledo, M., Torello-Raventos, M., Umetsu, R. K., van der Heijden, G. M. F., van der Hout, P., Guimaraes Vieira, I. C., Vieira, S. A., Vilanova, E., Vos, V. A., Zagt, R. J., mar 2015. Long-term decline of the Amazon carbon sink. Nature 519 (7543), 344–348.
URL http://dx.doi.org/10.1038/nature1428310.1038/nature14283http://www.nature.com/nature/journal/v519/n7543/abs/nature14283.html{\#}supplementary-information

Broich, M., Hansen, M., Stolle, F., Potapov, P., Margono, B. A., Adusei, B., 2011. Remotely sensed forest cover loss shows high spatial and temporal variation across Sumatera and Kalimantan, Indonesia 20002008. Environmental Research Letters 6 (1), 14010.

Brokaw, N. V. L., jun 1982. The Definition of Treefall Gap and Its Effect on Measures of Forest Dynamics. Biotropica 14 (2), 158—-160 CR —- Copyright © 1982 The Associati.
URL http://www.jstor.org/stable/2387750

Brondizio, E. S., Moran, E. F., jan 2012. Level-dependent deforestation trajectories in the Brazilian Amazon from 1970 to 2001. Population and Environment 34 (1), 69–85.
URL http://link.springer.com/10.1007/s11111-011-0159-8

Brown, I. F., Martinelli, L. A., Thomas, W. W., Moreira, M. Z., Cid Ferreira, C. A., Victoria, R. A., 1995. Uncertainty in the biomass of Amazonian forests: an example from Rondonia, Brazil. Forest Ecology and Management 75 (1), 175–189.

Brown, S., 1997. Estimating biomass and biomass change of tropical forests: a primer. Vol. 134. Food & Agriculture Org.

Brown, S., Gillespie, A. J. R., Lugo, A. E., 1989. Biomass Estimation Methods for Tropical Forests with Applications to Forest Inventory Data. Forest science.
URL http://www.ingentaconnect.com/content/saf/fs/1989/00000035/00000004/art00003

Brown, S., Lugo, A. E., 1990. Tropical secondary forests. Journal of tropical ecology.
URL http://journals.cambridge.org/production/action/cjoGetFulltext?fulltextid=5253132

Bryars, C., Maier, C., Zhao, D., Kane, M., Borders, B., Will, R., Teskey, R., 2013. Fixed physiological parameters in the 3-PG model produced accurate estimates of loblolly pine growth on sites in different geographic regions. Forest Ecology and Management 289, 501–514.

Budowski, G., 1965. The choice and classification of natural habitats in need of preservation in Central America. Tech. rep.

Budowski, G., 1970. The distinction between old secondary and climax species in tropical Central American lowlands. Tropical Ecology 11 (1), 44—-48+.

Bugmann, H., 2001. A review of forest gap models. Climatic Change 51 (3-4), 259–305.

Bunting, P., Clewley, D., Lucas, R. M., Gillingham, S., 2014. The remote sensing and GIS software library (RSGISLib). Computers & geosciences 62, 216–226.

Bunting, P., Gillingham, S., aug 2013. The KEA image file format. Computers & Geosciences 57, 54–58.
URL http://linkinghub.elsevier.com/retrieve/pii/S0098300413001015

Buschbacher, R., Uhl, C., Serrao, E. A. S., 1988. Abandoned Pastures in Eastern Amazonia. II. Nutrient Stocks in the Soil and Vegetation. The Journal of Ecology 76 (3), 682–699.
URL http://www.jstor.org/stable/10.2307/2260567

Buys, P., 2007. At loggerheads?: agricultural expansion, poverty reduction, and environment in the tropical forests. World Bank Publications.

Caccetta, P., Furby, S. L., O'Connell, J., Wallace, J. F., Wu, X., 2007. Continental monitoring: 34 years of land cover change using Landsat imagery. In: 32nd International symposium on remote sensing of environment. pp. 25–29.

Campbell, A., Dickson, B., Gibbs, H., Hansen, M., Kapos, V., Lysenko, I., Miles, L., Scharlemann, J., 2009. The role of protected areas in storing carbon and reducing emissions. In: IOP Conference Series: Earth and Environmental Science. Vol. 6. p. 2025.

Campling, P., Gobin, A., Beven, K., Feyen, J., feb 2002. Rainfall-runoff modelling of a humid tropical catchment: the TOPMODEL approach. Hydrological Processes 16 (2), 231–253.
URL http://dx.doi.org/10.1002/hyp.341

Cardille, J. A., Foley, J. A., 2003. Agricultural land-use change in Brazilian Amazonia between 1980 and 1995: Evidence from integrated satellite and census data. Remote Sensing of Environment 87 (4), 551–562.

Cardinale, B. J., Duffy, J. E., Gonzalez, A., Hooper, D. U., Perrings, C., Venail, P., Narwani, A., Mace, G. M., Tilman, D., Wardle, D. A., 2012. Biodiversity loss and its impact on humanity. Nature 486 (7401), 59–67.

Carpentier, J.-P., de la recherche Forestière, Q. P. D., 1996. Modélisation du rendement et de la production des bétulaies jaunes à résineux. Gouv. du Québec, Ministère des Fôrets, Direction de la Recherche.

Carreiras, J., Lucas, R., Jones, J., 2016. Mapping secondary forest dynamics in the Brazilian Amazon with Landsat TM and ALOS PALSAR. Remote Sensing of Environment.

Carreiras, J. M. B., Jones, J., Lucas, R. M., Gabriel, C., aug 2014. Land Use and Land Cover Change Dynamics across the Brazilian Amazon: Insights from Extensive Time-Series Analysis of Remote Sensing Data. PLoS ONE 9 (8), e104144.
URL http://dx.doi.org/10.1371/journal.pone.0104144

Carreiras, J. M. B., Pereira, J. M. C., Campagnolo, M. L., Shimabukuro, Y. E., apr 2006a. Assessing the extent of agriculture/pasture and secondary succession forest in the Brazilian Legal Amazon using SPOT VEGETATION data. Remote Sensing of Environment 101 (3), 283–298.
URL http://linkinghub.elsevier.com/retrieve/pii/S0034425706000204

Carreiras, J. M. B., Pereira, J. M. C., Shimabukuro, Y. E., 2006b. Land-cover mapping in the Brazilian Amazon using SPOT-4 Vegetation Data and Machine Learning Classification Methods. Photogrammetric Engineering & Remote Sensing 72 (8), 897–910.
URL http://asprs.org/a/publications/pers/2006journal/august/2006{_}aug{_}897-910.pdf

Carswell, F. E., Meir, P., Wandelli, E. V., Bonates, L. C. M., Kruijt, B., Barbosa, E. M.,

Nobre, A. D., Grace, J., Jarvis, P. G., 2000. Photosynthetic capacity in a central Amazonian rain forest. Tree Physiology 20 (3), 179–186.

Carvalho, G. O., Nepstad, D., McGrath, D., del Carmen Vera Diaz, M., Santilli, M., Barros, A. C., apr 2002. Frontier Expansion in the Amazon: Balancing Development and Sustainability. Environment: Science and Policy for Sustainable Development 44 (3), 34–44.
URL http://www.tandfonline.com/doi/abs/10.1080/00139150209605606{\#}.VjYaJliko2k.mendeley

Castanho, A., Galbraith, D., Zhang, K., Coe, M. T., Costa, M. H., Moorcroft, P. R., 2014. The Influence of Atmospheric CO2 Concentration and Climate Variability on Amazon Tropical Forest. In: AGU Fall Meeting Abstracts. Vol. 1. p. 4.

Cernusak, L. A., Winter, K., Dalling, J. W., Holtum, J. A. M., Jaramillo, C., Körner, C., Leakey, A. D. B., Norby, R. J., Poulter, B., Turner, B. L., Wright, S. J., 2013. Tropical forest responses to increasing atmospheric CO2: current knowledge and opportunities for future research.
URL http://dx.doi.org/10.1071/FP12309

Chambers, J. Q., Asner, G. P., Morton, D. C., Anderson, L. O., Saatchi, S. S., Espírito-Santo, F. D. B., Palace, M., Souza, C. M., aug 2007. Regional ecosystem structure and function: ecological insights from remote sensing of tropical forests. Trends in ecology & evolution 22 (8), 414–423.
URL http://www.ncbi.nlm.nih.gov/pubmed/17493704

Chambers, J. Q., Negron-Juarez, R. I., Marra, D. M., Di Vittorio, A., Tews, J., Roberts, D., Ribeiro, G. H. P. M., Trumbore, S. E., Higuchi, N., 2013. The steady-state mosaic of disturbance and succession across an old-growth Central Amazon forest landscape. Proceedings of the National Academy of Sciences 110 (10), 3949–3954.

Chambers, J. Q., Santos, J. D., Ribeiro, R. J., Higuchi, N., oct 2001. Tree damage, allometric relationships, and above-ground net primary production in central Amazon forest. Forest Ecology and Management 152 (1-3), 73–84.
URL http://linkinghub.elsevier.com/retrieve/pii/S0378112700005910

Chander, G., Markham, B. L., Helder, D. L., may 2009. Summary of current radiometric calibration coefficients for Landsat MSS, TM, ETM+, and EO-1 ALI sensors. Remote Sensing of Environment 113 (5), 893–903.
URL http://linkinghub.elsevier.com/retrieve/pii/S0034425709000169

Chanthorn, W., Ratanapongsai, Y., Brockelman, W. Y., Allen, M. A., Favier, C., Dubois, M. A., 2015. Viewing tropical forest succession as a three-dimensional dynamical system. Theoretical Ecology, 1–10.

Chaplin-Kramer, R., Ramler, I., Sharp, R., Haddad, N. M., Gerber, J. S., West, P. C., Mandle, L., Engstrom, P., Baccini, A., Sim, S., 2015. Degradation in carbon stocks near tropical forest edges. Nature communications 6.

Chave, J., 1999. Study of structural, successional and spatial patterns in tropical rain forests using TROLL, a spatially explicit forest model. Ecological modelling 124 (2), 233–254.

Chave, J., Andalo, C., Brown, S., Cairns, M. A., Chambers, J. Q., Eamus, D., Fölster, H., Fromard, F., Higuchi, N., Kira, T., 2005. Tree allometry and improved estimation of carbon stocks and balance in tropical forests. Oecologia 145 (1), 87–99.

Chave, J., Condit, R., Aguilar, S., Hernandez, A., Lao, S., Perez, R., 2004. Error propagation and scaling for tropical forest biomass estimates. Philosophical Transactions of the Royal Society B: Biological Sciences 359 (1443), 409–420.

Chave, J., RéjouMéchain, M., Búrquez, A., Chidumayo, E., Colgan, M. S., Delitti, W. B. C., Duque, A., Eid, T., Fearnside, P. M., Goodman, R. C., 2014. Improved allometric models to estimate the aboveground biomass of tropical trees. Global change biology 20 (10), 3177–3190.

Chazdon, R., 2012. Tropical forest regeneration.
URL `http://www.doaj.org/doaj?currentYear=2013{\&}id=1241595{\&}go=1{\&}func=abstract{\&}fromYear={\&}toYear=`

Chazdon, R. L., 2003. Tropical forest recovery: legacies of human impact and natural disturbances. Perspectives in Plant Ecology, evolution and systematics 6 (1), 51–71.

Chazdon, R. L., 2008. Chance and determinism in tropical forest succession. Tropical forest community ecology, 384–408.

Chazdon, R. L., 2014. Second Growth. The University of Chicago Press, Chicago and London.

Chazdon, R. L., Broadbent, E. N., Rozendaal, D. M. A., Bongers, F., Zambrano, A. M. A., Aide, T. M., Balvanera, P., Becknell, J. M., Boukili, V., Brancalion, P. H. S., Craven, D., Almeida-Cortez, J. S., Cabral, G. A. L., de Jong, B., Denslow, J. S., Dent, D. H., DeWalt, S. J., Dupuy, J. M., Durán, S. M., Espírito-Santo, M. M., Fandino, M. C., César, R. G., Hall, J. S., Hernández-Stefanoni, J. L., Jakovac, C. C., Junqueira, A. B., Kennard, D., Letcher, S. G., Lohbeck, M., Martínez-Ramos, M., Massoca, P., Meave, J. A., Mesquita, R., Mora, F., Muñoz, R., Muscarella, R., Nunes, Y. R. F., Ochoa-Gaona, S., Orihuela-Belmonte, E., Peña-Claros, M., Pérez-García, E. A., Piotto, D., Powers, J. S., Rodríguez-Velazquez, J., Romero-Pérez, I. E., Ruíz, J., Saldarriaga, J. G., Sanchez-Azofeifa, A., Schwartz, N. B., Steininger, M. K., Swenson, N. G., Uriarte, M., van Breugel, M., van der Wal, H., Veloso, M. D. M., Vester, H.,

Vieira, I. C. G., Bentos, T. V., Williamson, G. B., Poorter, L., may 2016. Carbon sequestration potential of second-growth forest regeneration in the Latin American tropics. Science Advances 2 (5).
URL http://advances.sciencemag.org/content/2/5/e1501639.abstract

Chazdon, R. L., Finegan, B., Capers, R. S., Salgado-Negret, B., Casanoves, F., Boukili, V., Norden, N., jan 2010. Composition and Dynamics of Functional Groups of Trees During Tropical Forest Succession in Northeastern Costa Rica. Biotropica 42 (1), 31–40.
URL http://dx.doi.org/10.1111/j.1744-7429.2009.00566.x

Chazdon, R. L., Letcher, S. G., van Breugel, M., Martinez-Ramos, M., Bongers, F., Finegan, B., 2007. Rates of change in tree communities of secondary Neotropical forests following major disturbances. Philosophical Transactions of the Royal Society 362, 273–289.
URL http://rstb.royalsocietypublishing.org/content/362/1478/273.short

Chazdon, R. L., Peres, C. A., Dent, D., Sheil, D., Lugo, A. E., Lamb, D., Stork, N. E., Miller, S. E., 2009. The potential for species conservation in tropical secondary forests. Conservation Biology 23 (6), 1406–1417.

Chen, J., Gong, P., He, C., Pu, R., Shi, P., 2003. Land-use/land-cover change detection using improved change-vector analysis. Photogrammetric Engineering & Remote Sensing 69 (4), 369–379.

Choat, B., Jansen, S., Brodribb, T. J., Cochard, H., Delzon, S., Bhaskar, R., Bucci, S. J., Feild, T. S., Gleason, S. M., Hacke, U. G., Jacobsen, A. L., Lens, F., Maherali, H., Martinez-Vilalta, J., Mayr, S., Mencuccini, M., Mitchell, P. J., Nardini, A., Pittermann, J., Pratt, R. B., Sperry, J. S., Westoby, M., Wright, I. J., Zanne, A. E., nov 2012. Global convergence in the vulnerability of forests to drought. Nature 491 (7426), 752–755.
URL http://dx.doi.org/10.1038/nature11688http://www.nature.com/nature/journal/v491/n7426/abs/nature11688.html{\#}supplementary-information

Chokkalingam, U., De Jong, W. I. L., 2001. Secondary forest: a working definition and typology. The International Forestry Review 3 (1), 19–26.
URL http://www.jstor.org/stable/42609342

Christopher Frey, H., Patil, S. R., 2002. Identification and review of sensitivity analysis methods. Risk analysis 22 (3), 553–578.

Clark, D. A., Brown, S., Kicklighter, D. W., Chambers, J. Q., Thomlinson, J. R., Ni, J., apr 2001. Measuring Net Primary Production in Forests: Concepts and Field

Methods. Ecological Applications 11 (2), 356–370.
URL http://www.jstor.org/stable/3060894

Clark, D. B., Kellner, J. R., dec 2012. Tropical forest biomass estimation and the fallacy of misplaced concreteness. Journal of Vegetation Science 23 (6), 1191–1196.
URL http://dx.doi.org/10.1111/j.1654-1103.2012.01471.x

Cleveland, C. C., Taylor, P., Chadwick, K. D., Dahlin, K., Doughty, C. E., Malhi, Y., Smith, W. K., 2015. A comparison of plot-based, satellite and Earth system model estimates of tropical forest net primary production Running Title: NPP in tropical forests.

Cleveland, C. C., Townsend, A. R., Taylor, P., Alvarez-Clare, S., Bustamante, M. M. C., Chuyong, G., Dobrowski, S. Z., Grierson, P., Harms, K. E., Houlton, B. Z., Marklein, A., Parton, W., Porder, S., Reed, S. C., Sierra, C. a., Silver, W. L., Tanner, E. V. J., Wieder, W. R., sep 2011. Relationships among net primary productivity, nutrients and climate in tropical rain forest: a pan-tropical analysis. Ecology letters 14 (9), 939–947.
URL http://www.ncbi.nlm.nih.gov/pubmed/21749602

Cochrane, M. A., 1998. Linear mixture model classification of burned forests in the eastern Amazon. International Journal of Remote Sensing 19 (17), 3433–3440.

Cochrane, M. a., feb 2003. Fire science for rainforests. Nature 421 (6926), 913–919.
URL http://www.ncbi.nlm.nih.gov/pubmed/12606992

Cochrane, M. A., Barber, C. P., 2009. Climate change, human land use and future fires in the Amazon. Global Change Biology 15 (3), 601–612.

Collingham, Y. C., Huntley, B., 2000. Impacts of habitat fragmentation and patch size upon migration rates. Ecological Applications 10 (1), 131–144.

Comita, L. S., Engelbrecht, B. M. J., 2009. Seasonal and spatial variation in water availability drive habitat associations in a tropical forest. Ecology 90 (10), 2755–2765.

Congalton, R. G., Green, K., 1999. Assessing the accuracy of remotely sensed data: principles and applications. Lewis Publishers, Boca Raton, Fla.

Coops, N. C., Waring, R. H., Landsberg, J. J., 1998. Assessing forest productivity in Australia and New Zealand using a physiologically-based model driven with averaged monthly weather data and satellite-derived estimates of canopy photosynthetic capacity. Forest Ecology and Management 104 (1), 113–127.

Coppin, P., Jonckheere, I., Nackaerts, K., Muys, B., Lambin, E., 2004. Review ArticleDigital change detection methods in ecosystem monitoring: a review. International journal of remote sensing 25 (9), 1565–1596.

Corlett, R., 2014. Classifying Tropical Forests. In: Köhl, M., Pancel, L. (Eds.), Tropical Forestry Handbook SE - 52-1. Springer Berlin Heidelberg, pp. 1–9.
URL http://dx.doi.org/10.1007/978-3-642-41554-8{_}52-1

Corlett, R. T., 2016. The Impacts of Droughts in Tropical Forests. Trends in Plant Science.
URL http://www.sciencedirect.com/science/article/pii/S1360138516000571

Cram, S., Sommer, I., Fernández, P., Galicia, L., Ríos, C., Barois, I., 2015. Soil natural capital modification through landuse and cover change in a tropical forest landscape: implications for management. Journal of Tropical Forest Science, 189–201.

Cramer, W., Kicklighter, D. W., Bondeau, A., Iii, B. M., Churkina, G., Nemry, B., Ruimy, A., Schloss, A. L., Intercomparison, T., Model, P. O. F. T. P. N., 1999. Comparing global models of terrestrial net primary productivity (NPP): overview and key results. Global change biology 5 (S1), 1–15.

Cubiña, A., Mitchell Aide, T., jun 2001. The Effect of Distance from Forest Edge on Seed Rain and Soil Seed Bank in a Tropical Pasture. BIOTROPICA 33 (2), 260–267.
URL http://dx.doi.org/10.1646/0006-3606(2001)033[0260:TEODFF]2.0.COhttp://2

Cukier, R. I., Schaibly, J. H., Shuler, K. E., 1975. Study of the sensitivity of coupled reaction systems to uncertainties in rate coefficients. III. Analysis of the approximations. The Journal of Chemical Physics 63 (3), 1140–1149.

Curtis, R. O., Clendenen, G. W., DeMars, D. J., Forest, P. N., 1981. A new stand simulator for coast Douglas-fir: DFSIM user's guide. US Department of Agriculture, Forest Service, Pacific Northwest Forest and Range Experiment Station.

Cutler, M. E. J., Boyd, D. S., Foody, G. M., Vetrivel, A., jun 2012. Estimating tropical forest biomass with a combination of SAR image texture and Landsat TM data: An assessment of predictions between regions. ISPRS Journal of Photogrammetry and Remote Sensing 70, 66–77.
URL http://linkinghub.elsevier.com/retrieve/pii/S0924271612000652

da Cunha, T. A., Finger, C. A. G., Hasenauer, H., 2016. Tree basal area increment models for Cedrela, Amburana, Copaifera and Swietenia growing in the Amazon rain forests. Forest Ecology and Management 365, 174–183.

da Silva, R. P., dos Santos, J., Tribuzy, E. S., Chambers, J. Q., Nakamura, S., Higuchi, N., aug 2002. Diameter increment and growth patterns for individual tree growing in Central Amazon, Brazil. Forest Ecology and Management 166 (1-3), 295–301.
URL http://linkinghub.elsevier.com/retrieve/pii/S0378112701006788

Dantas, M., Phillipson, J., 1989. Litterfall and litter nutrient content in primary and secondary Amazonian terra firme'rain forest. Journal of Tropical Ecology 5 (01), 27–36.

Davidson, E. A., Claudio, J. R. C., Vieira, I. C. G., Figueiredo, R. O., Ishida, F. Y., Santos, M. T. P., Guerrero, J. B., Kalif, K., Saba, R. T., 2004. Nitrogen and phosphorus limitation of biomass growth in a tropical secondary forest. Ecologica Applications 14 (4), 150–163.
URL http://www.esajournals.org/doi/abs/10.1890/01-6006

Davidson, E. A., de Araújo, A. C., Artaxo, P., Balch, J. K., Brown, I. F., Bustamante, M. M. C., Coe, M. T., DeFries, R. S., Keller, M., Longo, M., 2012. The Amazon basin in transition. Nature 481 (7381), 321–328.

de Almeida, C. A., Coutinho, A. C., Esquerdo, J. C. D. M., Adami, M., Venturieri, A., Diniz, C. G., Dessay, N., Durieux, L., Gomes, A. R., 2016. High spatial resolution land use and land cover mapping of the Brazilian Legal Amazon in 2008 using Landsat-5/TM and MODIS data.

de Barros Ferraz, S. F., Vettorazzi, C. A., Theobald, D. M., Ballester, M. V. R., 2005. Landscape dynamics of Amazonian deforestation between 1984 and 2002 in central Rondônia, Brazil: assessment and future scenarios. Forest Ecology and Management 204 (1), 69–85.

De Grandcourt, A., Epron, D., Montpied, P., Louisanna, E., Béreau, M., Garbaye, J., Guehl, J.-M., jan 2004. Contrasting responses to mycorrhizal inoculation and phosphorus availability in seedlings of two tropical rainforest tree species. New Phytologist 161 (3), 865–875.
URL http://doi.wiley.com/10.1046/j.1469-8137.2004.00978.x

De Melo, F. P. L., Dirzo, R., Tabarelli, M., 2006. Biased seed rain in forest edges: evidence from the Brazilian Atlantic forest. Biological Conservation 132 (1), 50–60.

de Moraes, J. F. L., Volkoff, B., Cerri, C. C., Bernoux, M., 1996. Soil properties under Amazon forest and changes due to pasture installation in Rondonia, Brazil. Geoderma 70, 63–81.
URL http://www.sciencedirect.com/science/article/pii/0016706195000720

De Oliveira, A. A., Mori, S. A., 1999. A central Amazonian terra firme forest. I. High tree species richness on poor soils. Biodiversity & Conservation 8 (9), 1219–1244.

de Paula, M. D., Groeneveld, J., Huth, A., 2015. Tropical forest degradation and recovery in fragmented landscapesSimulating changes in tree community, forest hydrology and carbon balance. Global Ecology and Conservation 3, 664–677.

De Rouw, A., 1995. The fallow period as a weed-break in shifting cultivation (tropical wet forests). Agriculture, ecosystems & environment 54 (1), 31–43.

DeFries, R. S., Belward, A. S., 2000. Global and regional land cover characterization from satellite data: an introduction to the Special Issue. International Journal of Remote Sensing 21 (6-7), 1083–1092.

Denslow, J. S., jan 1987. Tropical Rainforest Gaps and Tree Species Diversity. Annual Review of Ecology and Systematics 18, 431—-451 CR —- Copyright © 1987 Annual Review.
URL http://www.jstor.org/stable/2097139

Departamento Nacional da Produço Mineral, 1978. Projeto RADAMBRASIL. Folha SC.20 Porto Velho; geologia, geomorfologia, pedologia, vegetaço e uso potencial da terra. Tech. rep., DNPM, Rio de Janeiro, Brazil.

DeVries, B., Decuyper, M., Verbesselt, J., Zeileis, A., Herold, M., Joseph, S., nov 2015. Tracking disturbance-regrowth dynamics in tropical forests using structural change detection and Landsat time series. Remote Sensing of Environment 169, 320–334.
URL http://www.sciencedirect.com/science/article/pii/S0034425715301061

Dial, R., Bloodworth, B., Lee, A., Boyne, P., Heys, J., 2004. The distribution of free space and its relation to canopy composition at six forest sites. Forest Science 50 (3), 312–325.

Dick, C. W., Hardy, O. J., Jones, F. A., Petit, R. J., 2008. Spatial scales of pollen and seed-mediated gene flow in tropical rain forest trees. Tropical Plant Biology 1 (1), 20–33.

Didham, R. K., Lawton, J. H., 1999. Edge structure determines the magnitude of changes in microclimate and vegetation structure in tropical forest fragments1. Biotropica 31 (1), 17–30.

Dietze, M. C., Lebauer, D. S., Kooper, R. O. B., sep 2013. On improving the communication between models and data. Plant, Cell & Environment 36 (9), 1575–1585.
URL http://dx.doi.org/10.1111/pce.12043

Dinh, H. T. M., Rocca, F., Tebaldini, S., D'Alessandro, M. M., Le Toan, T., 2012. Linear and circular polarization P band SAR tomography for tropical forest biomass study. In: Synthetic Aperture Radar, 2012. EUSAR. 9th European Conference on. VDE, pp. 489–492.

Dislich, C., Günter, S., Homeier, J., Schröder, B., Huth, A., 2009. Simulating forest dynamics of a tropical montane forest in South Ecuador. Erdkunde, 347–364.

Dislich, C., Huth, A., jul 2012. Modelling the impact of shallow landslides on forest

structure in tropical montane forests. Ecological Modelling 239, 40–53.
URL http://www.sciencedirect.com/science/article/pii/S0304380012001822

Don, A., Schumacher, J., Freibauer, A., 2011. Impact of tropical landuse change on soil organic carbon stocksa metaanalysis. Global Change Biology 17 (4), 1658–1670.

Dong, S. X., Davies, S. J., Ashton, P. S., Bunyavejchewin, S., Supardi, M. N. N., Kassim, A. R., Tan, S., Moorcroft, P. R., 2012. Variability in solar radiation and temperature explains observed patterns and trends in tree growth rates across four tropical forests. Proceedings of the Royal Society of London B: Biological Sciences 279 (1744), 3923–3931.

Donohue, R. J., Roderick, M. L., McVicar, T. R., Farquhar, G. D., 2013. Impact of CO2 fertilization on maximum foliage cover across the globe's warm, arid environments. Geophysical Research Letters 40 (12), 3031–3035.

dos Santos, U. M., de Carvalho Gonçalves, J. F., Feldpausch, T. R., 2006. Growth, leaf nutrient concentration and photosynthetic nutrient use efficiency in tropical tree species planted in degraded areas in central Amazonia. Forest Ecology and Management 226 (1), 299–309.

Doughty, C. E., Metcalfe, D. B., Girardin, C. A. J., Amezquita, F. F., Cabrera, D. G., Huasco, W. H., Silva-Espejo, J. E., Araujo-Murakami, A., da Costa, M. C., Rocha, W., Feldpausch, T. R., Mendoza, A. L. M., da Costa, A. C. L., Meir, P., Phillips, O. L., Malhi, Y., mar 2015. Drought impact on forest carbon dynamics and fluxes in Amazonia. Nature 519 (7541), 78–82.
URL http://dx.doi.org/10.1038/nature1421310.1038/nature14213http://www.nature.com/nature/journal/v519/n7541/abs/nature14213.html{\#}supplementary-information

Doyle, T. W., 1981. The role of disturbance in the gap dynamics of a montane rain forest: an application of a tropical forest succession model. In: Forest succession. Springer, pp. 56–73.

Dubayah, R. O., Sheldon, S. L., Clark, D. B., Hofton, M. A., Blair, J. B., Hurtt, G. C., Chazdon, R. L., 2010. Estimation of tropical forest height and biomass dynamics using lidar remote sensing at La Selva, Costa Rica. Journal of Geophysical Research: Biogeosciences 115 (G2).

Dunne, K. A., Willmott, C. J., 1996. Global distribution of plantextractable water capacity of soil. International Journal of Climatology 16 (8), 841–859.

Dye, P. J., Jacobs, S., Drew, D., 2004. Verification of 3-PG growth and water-use

predictions in twelve Eucalyptus plantation stands in Zululand, South Africa. Forest Ecology and Management 193 (1), 197–218.

Eaton, J. M., Lawrence, D., sep 2009. Loss of carbon sequestration potential after several decades of shifting cultivation in the Southern Yucatán. Forest Ecology and Management 258 (6), 949–958.
URL http://www.sciencedirect.com/science/article/pii/S0378112708007895

Englhart, S., Keuck, V., Siegert, F., may 2011. Aboveground biomass retrieval in tropical forests The potential of combined X- and L-band SAR data use. Remote Sensing of Environment 115 (5), 1260–1271.
URL http://linkinghub.elsevier.com/retrieve/pii/S0034425711000216

Espírito-Santo, F. D. B., Gloor, M., Keller, M., Malhi, Y., Saatchi, S., Nelson, B., Junior, R. C. O., Pereira, C., Lloyd, J., Frolking, S., Palace, M., Shimabukuro, Y. E., Duarte, V., Mendoza, A. M., López-González, G., Baker, T. R., Feldpausch, T. R., Brienen, R. J. W., Asner, G. P., Boyd, D. S., Phillips, O. L., 2014. Size and frequency of natural forest disturbances and the Amazon forest carbon balance. Nature communications 5.

Espírito-Santo, F. D. B., Keller, M., Braswell, B., Nelson, B. W., Frolking, S., Vicente, G., jun 2010. Storm intensity and old-growth forest disturbances in the Amazon region. Geophysical Research Letters 37 (11), n/a–n/a.
URL http://doi.wiley.com/10.1029/2010GL043146

Espírito-Santo, F. D. B., Shimabukuro, Y. E., Aragão, L. E. O., Machado, E. L. M., 2005. Analysis of the floristic and phytosociologic composition of Tapajós national forest with geographic support of satellite images. Acta Amazonica 35 (2), 155–173.

Esprey, L. J., Sands, P. J., Smith, C. W., may 2004. Understanding 3-PG using a sensitivity analysis. Forest Ecology and Management 193 (1-2), 235–250.
URL http://www.sciencedirect.com/science/article/pii/S037811270400060X

Ewel, J. J., 1986. Designing agricultural ecosystems for the humid tropics. Annual Review of Ecology and Systematics, 245–271.

Ewers, R. M., Didham, R. K., Pearse, W. D., Lefebvre, V., Rosa, I., Carreiras, J., Lucas, R. M., Reuman, D. C., 2013. Using landscape history to predict biodiversity patterns in fragmented landscapes. Ecology letters 16 (10), 1221–1233.

Falkowski, P., Scholes, R. J., Boyle, E. e. a., Canadell, J., Canfield, D., Elser, J., Gruber, N., Hibbard, K., Högberg, P., Linder, S., 2000. The global carbon cycle: a test of our knowledge of earth as a system. science 290 (5490), 291–296.

Fearnside, P. M., 1997. Wood density for estimating forest biomass in Brazilian Amazonia. Forest ecology and management 90 (1), 59–87.

Fearnside, P. M., 2000. Global warming and tropical land-use change: greenhouse gas emissions from biomass burning, decomposition and soils in forest conversion, shifting cultivation and secondary vegetation. Climatic change 46 (1-2), 115–158.

Fearnside, P. M., jun 2005. Deforestation in Brazilian Amazonia: History, Rates, and Consequences. Conservation Biology 19 (3), 680–688.
URL `http://doi.wiley.com/10.1111/j.1523-1739.2005.00697.x`

Fearnside, P. M., de Alencastro Graça, P. M. L., nov 2006. BR-319: Brazil's Manaus-Porto Velho highway and the potential impact of linking the arc of deforestation to central amazonia. Environmental management 38 (5), 705–716.
URL `http://www.ncbi.nlm.nih.gov/pubmed/16990982`

Fearnside, P. M., Guimarases, W. M., 1996. Carbon uptake by secondary forests in Brazilian Amazonia. Forest Ecology and Management 80, 35–46.

Fedrigo, M., Meir, P., Sheil, D., Van Heist, M., Woodhouse, I. H., Mitchard, E. T. A., 2013. Fusing radar and optical remote sensing for biomass prediction in mountainous tropical forests. In: Geoscience and Remote Sensing Symposium (IGARSS), 2013 IEEE International. IEEE, pp. 975–978.

Feikema, P. M., Beverly, C. R., Morris, J. D., Collopy, J. J., Baker, T. G., Lane, P. N. J., 2007. Predicting the impacts of plantations on catchment water balances using the 3PG forest growth model. In: MODSIM 2007 International Congress on Modelling and Simulation. Modelling and Simulation Society of Australia and New Zealand. pp. 2237–2243.

Feldpausch, T. R., Banin, L., Phillips, O. L., Baker, T. R., Lewis, S. L., Quesada, C. A., Affum-Baffoe, K., Arets, E. J. M. M., Berry, N. J., Bird, M., 2011. Height-diameter allometry of tropical forest trees. Biogeosciences.

Feldpausch, T. R., Lloyd, J., Lewis, S. L., Brienen, R. J. W., Gloor, M., Monteagudo Mendoza, A., Lopez-Gonzalez, G., Banin, L., Abu Salim, K., Affum-Baffoe, K., 2012. Tree height integrated into pantropical forest biomass estimates. Biogeosciences, 3381–3403.

Feldpausch, T. R., Prates-Clark, C. C., Fernandes, E. C. M., Riha, S. J., 2007. Secondary forest growth deviation from chronosequence predictions in central Amazonia. Global Change Biology 13, 967–979.

Feldpausch, T. R., Riha, S. J., Fernandes, E. C. M., Wandelli, E. V., jan 2005. Development of Forest Structure and Leaf Area in Secondary Forests Regenerating on

Abandoned Pastures in Central Amazônia. Earth Interactions 9 (6), 1–22.
URL http://dx.doi.org/10.1175/EI140.1

Feldpausch, T. R., Rondon, M. A., Fernandes, E. C. M., Riha, S. J., Wandelli, E., 2004. Carbon and nutrient accumulation in secondary forests regenerating on pastures in central Amazonia. Ecological Applications 14 (4), 164–176.
URL http://www.esajournals.org/doi/abs/10.1890/01-6015

Ferreira, N. C., Ferreira, L. G., Miziara, F., jan 2007. Deforestation Hotspots in the Brazilian Amazon: Evidence and Causes as Assessed from Remote Sensing and Census Data. Earth Interactions 11 (1), 1–16.
URL http://journals.ametsoc.org/doi/abs/10.1175/EI201.1

Fickas, K. C., Cohen, W. B., Yang, Z., 2015. Landsat-based monitoring of annual wetland change in the Willamette Valley of Oregon, USA from 1972 to 2012. Wetlands Ecology and Management, 1–20.

Fine, P., 2015. Ecological and evolutionary drivers of geographic variation in species diversity. Annual Review of Ecology, Evolution, and Systematics 46 (1).

Finegan, B., mar 1996. Pattern and process in neotropical secondary rain forests: the first 100 years of succession. Trends in ecology & evolution 11 (3), 119–124.
URL http://www.sciencedirect.com/science/article/pii/0169534796810901

Finsterle, S., Kowalsky, M. B., 2011. A truncated LevenbergMarquardt algorithm for the calibration of highly parameterized nonlinear models. Computers & Geosciences 37 (6), 731–738.

Fischer, R., Armstrong, A., Shugart, H. H., Huth, A., feb 2014. Simulating the impacts of reduced rainfall on carbon stocks and net ecosystem exchange in a tropical forest. Environmental Modelling & Software 52, 200–206.
URL http://www.sciencedirect.com/science/article/pii/S1364815213002697

Fischer, R., Ensslin, A., Rutten, G., Fischer, M., Costa, D. S., Kleyer, M., Hemp, A., Paulick, S., Huth, A., 2015. Simulating Carbon Stocks and Fluxes of an African Tropical Montane Forest with an Individual-Based Forest Model. PloS one.

Fittkau, E. J., Klinge, H., 1973. On biomass and trophic structure of the central Amazonian rain forest ecosystem. Biotropica, 2–14.

Fleischman, J. G., Ayasli, S., Adams, E. M. t., Gosselin, D. R., 1996. Foliage attenuation and backscatter analysis of SAR imagery. IEEE Transactions on Aerospace and Electronic Systems 32 (1), 135–144.

Foley, J. A., DeFries, R., Asner, G. P., Barford, C., Bonan, G., Carpenter, S. R., Chapin,

F. S., Coe, M. T., Daily, G. C., Gibbs, H. K., 2005. Global consequences of land use. science 309 (5734), 570–574.

Foody, G. M., 2009. Sample size determination for image classification accuracy assessment and comparison. International Journal of Remote Sensing 30 (20), 5273–5291.

Franken, M., Irmler, U., Klinge, H., 1979. Litterfall in inundation, riverine and terra firme forests of central Amazonia. Tropical Ecology 20 (2), 225–235.

Franklin, J., 2003. Regeneration and growth of pioneer and shadetolerant rain forest trees in Tonga. New Zealand Journal of Botany 41 (4), 669–684.

Frelich, L. E., Calcote, R. R., Davis, M. B., Pastor, J., 1993. Patch formation and maintenance in an old-growth hemlock-hardwood forest. Ecology 74 (2), 513–527.

Gallego, F. J., 2004. Remote sensing and land cover area estimation. International Journal of Remote Sensing 25 (15), 3019–3047.

García, O., 2005. TADAM: A dynamic whole-stand approximation for the TASS growth model. The Forestry Chronicle 81 (4), 575–581.

Gehring, C., Denich, M., Vlek, P. L. G., jul 2005a. Resilience of secondary forest regrowth after slash-and-burn agriculture in central Amazonia. Journal of Tropical Ecology 21 (5), 519–527.
URL `http://www.journals.cambridge.org/abstract{\_}S0266467405002543`

Gehring, C., Vlek, P. L., de Souza, L. A., Denich, M., dec 2005b. Biological nitrogen fixation in secondary regrowth and mature rainforest of central Amazonia. Agriculture, Ecosystems & Environment 111 (1-4), 237–252.
URL `http://www.sciencedirect.com/science/article/pii/S0167880905002847`

Gibson, L., Lee, T. M., Koh, L. P., Brook, B. W., Gardner, T. a., Barlow, J., Peres, C. a., Bradshaw, C. J. a., Laurance, W. F., Lovejoy, T. E., Sodhi, N. S., oct 2011. Primary forests are irreplaceable for sustaining tropical biodiversity. Nature 478 (7369), 378–381.
URL `http://www.ncbi.nlm.nih.gov/pubmed/21918513`

Gierlinski, M., 2016. Understanding Statistical Error: A Primer for Biologists. John Wiley & Sons.

Gillespie, A. J. R., Brown, S., Lugo, A. E., 1992. Tropical forest biomass estimation from truncated stand tables. Forest Ecology and Management 48 (1), 69–87.

Gillooly, J. F., Brown, J. H., West, G. B., Savage, V. M., Charnov, E. L., 2001. Effects of size and temperature on metabolic rate. science 293 (5538), 2248–2251.

Girardin, C. A. J., Malhi, Y., Aragao, L., Mamani, M., Huaraca Huasco, W., Durand, L., Feeley, K. J., Rapp, J., SILVAESPEJO, J. E., Silman, M., 2010. Net primary productivity allocation and cycling of carbon along a tropical forest elevational transect in the Peruvian Andes. Global Change Biology 16 (12), 3176–3192.

Global Modeling and Assimilation Office (GMAO), 2015. tavg1_2d_rad_Nx: MERRA 2D IAU Diagnostic, Radiation Surface and TOA, Time Average 1-hourly.

Godwin, D. C., Jones, C. A., Hanks, J., Ritchie, J. T., 1991. Nitrogen dynamics in soil-plant systems. Modeling plant and soil systems., 287–321.

Gómez-Pompa, A., Vazquez-Yanes, C., 1974. Studies on the secondary succession of tropical lowlands: the life cycle of secondary species. In: Proceedings of the first international congress of ecology. pp. 336–342.

Gómez-Pompa, A., Vázquez-Yanes, C., 1985. Estudios sobre la regeneración de selvas en regiones cálido-húmedas de México. Investigaciones sobre la regeneración de selvas altas en Veracruz, México 2, 1–25.

Good, P., Jones, C., Lowe, J., Betts, R., Gedney, N., apr 2012. Comparing Tropical Forest Projections from Two Generations of Hadley Centre Earth System Models, HadGEM2-ES and HadCM3LC. Journal of Climate 26 (2), 495–511.
URL http://dx.doi.org/10.1175/JCLI-D-11-00366.1

Goodman, R. C., Phillips, O. L., del Castillo Torres, D., Freitas, L., Cortese, S. T., Monteagudo, A., Baker, T. R., dec 2013. Amazon palm biomass and allometry. Forest Ecology and Management 310, 994–1004.
URL http://www.sciencedirect.com/science/article/pii/S0378112713006592

Goulding, M., Barthem, R., Ferreira, E. J. G., 2003. The Smithsonian atlas of the Amazon. Smithsonian Books.

Granier, A., Huc, R., Barigah, S. T., 1996. Transpiration of natural rain forest and its dependence on climatic factors. Agricultural and forest meteorology 78 (1), 19–29.

Groenendijk, P., Zuidema, P., Sleen, P. V. D., Vlam, M., Ehlers, I., Schleucher, J., 2014. Long-term CO2 rise has increased photosynthetic efficiency and water use efficiency but did not stimulate diameter growth of tropical trees. In: AGU Fall Meeting Abstracts. Vol. 1. p. 3.

Groeneveld, J., Alves, L. F., Bernacci, L. C., Catharino, E. L. M., Knogge, C., Metzger, J. P., Pütz, S., Huth, a., oct 2009. The impact of fragmentation and density regulation on forest succession in the Atlantic rain forest. Ecological Modelling 220 (19), 2450–2459.
URL http://linkinghub.elsevier.com/retrieve/pii/S0304380009004153

Grover, K., Quegan, S., da Costa Freitas, C., 1999. Quantitative estimation of tropical forest cover by SAR. IEEE Transactions on Geoscience and Remote Sensing 37 (1), 479–490.
URL http://ieeexplore.ieee.org/lpdocs/epic03/wrapper.htm?arnumber=739096

Guan, K., Good, S. P., Caylor, K. K., Sato, H., Wood, E. F., Li, H., dec 2014. Continental-scale impacts of intra-seasonal rainfall variability on simulated ecosystem responses in Africa. Biogeosciences 11 (23), 6939–6954.
URL http://www.biogeosciences.net/11/6939/2014/http://www.biogeosciences.net/11/6939/2014/bg-11-6939-2014.pdf

Guariguata, M. R., Ostertag, R., jul 2001. Neotropical secondary forest succession: changes in structural and functional characteristics. Forest Ecology and Management 148 (1-3), 185–206.
URL http://linkinghub.elsevier.com/retrieve/pii/S0378112700005351

Hame, T., Rauste, Y., Antropov, O., Ahola, H. A., Kilpi, J., 2013. Improved mapping of tropical forests with optical and SAR imagery, Part II: Above ground biomass estimation. Selected Topics in Applied Earth Observations and Remote Sensing, IEEE Journal of 6 (1), 92–101.

Hamrick, J. L., Murawski, D. A., Nason, J. D., 1993. The influence of seed dispersal mechanisms on the genetic structure of tropical tree populations. In: Frugivory and seed dispersal: ecological and evolutionary aspects. Springer, pp. 281–297.

Hansen, M. C., Loveland, T. R., jul 2012. A review of large area monitoring of land cover change using Landsat data. Remote Sensing of Environment 122, 66–74.
URL http://www.sciencedirect.com/science/article/pii/S0034425712000314

Hansen, M. C., Potapov, P. V., Moore, R., Hancher, M., Turubanova, S. a., Tyukavina, a., Thau, D., Stehman, S. V., Goetz, S. J., Loveland, T. R., Kommareddy, a., Egorov, a., Chini, L., Justice, C. O., Townshend, J. R. G., nov 2013. High-Resolution Global Maps of 21st-Century Forest Cover Change. Science 342 (6160), 850–853.
URL http://www.sciencemag.org/cgi/doi/10.1126/science.1244693

Hansen, M. C., Stehman, S. V., Potapov, P. V., 2010. Quantification of global gross forest cover loss. Proceedings of the National Academy of Sciences of the United States of America 107 (19), 8650–8655.

Hardee, K., Mutunga, C., 2010. Strengthening the link between climate change adaptation and national development plans: lessons from the case of population in National Adaptation Programmes of Action (NAPAs). Mitigation and Adaptation Strategies for Global Change 15 (2), 113–126.

Harris, P. P., Huntingford, C., Gash, J. H. C., Hodnett, M. G., Cox, P. M., Malhi, Y., Araújo, A. C., 2004. Calibration of a land-surface model using data from primary forest sites in Amazonia. Theoretical and Applied Climatology 78 (1-3), 27–45.
URL http://dx.doi.org/10.1007/s00704-004-0042-y

Hartig, F., Dislich, C., Wiegand, T., Huth, A., 2014. Supplementary material for Technical Note: Approximate Bayesian parameterization of a process-based tropical forest model. Biogeosciences.

Hartley, C. W. S., 1967. The oil palm. The oil palm.

Hartshorn, G. S., 2013. Tropical Forest Ecosystems.

Hastie, T., Tibshirani, R., Friedman, J., 2009. Unsupervised learning. Springer.

Heimann, M., Reichstein, M., jan 2008. Terrestrial ecosystem carbon dynamics and climate feedbacks. Nature 451 (7176), 289–292.
URL http://www.ncbi.nlm.nih.gov/pubmed/18202646

Helmer, E. H., Lefsky, M. A., Roberts, D. A., 2009. Biomass accumulation rates of Amazonian secondary forest and biomass of old-growth forests from Landsat time series and the Geoscience Laser Altimeter System. Journal of Applied Remote Sensing 3 (1), 33505–33531.
URL http://dx.doi.org/10.1117/1.3082116

Henao-Gallego, N., Escobar-Ramírez, S., Calle, Z., Montoya-Lerma, J., Armbrecht, I., 2012. An artificial aril designed to induce seed hauling by ants for ecological rehabilitation purposes. Restoration Ecology 20 (5), 555–560.

Henry, M., Bombelli, A., Trotta, C., Alessandrini, A., Birigazzi, L., Sola, G., Vieilledent, G., Santenoise, P., Longuetaud, F., Valentini, R., Picard, N., Saint-Andr, L., 2013. GlobAllomeTree: international platform for tree allometric equations to support volume, biomass and carbon assessment. iForest - Biogeosciences and Forestry 6 (6), 326–330.
URL http://www.sisef.it/iforest/contents/?id=ifor0901-006http://www.sisef.it/iforest/pdf/?id=ifor0901-006

Hess, L. L., Melack, J. M., Affonso, A. G., Barbosa, C., Gastil-Buhl, M., Novo, E. M. L. M., 2015. Wetlands of the lowland Amazon basin: Extent, vegetative cover, and dual-season inundated area as mapped with JERS-1 Synthetic Aperture Radar. Wetlands 35 (4), 745–756.

Higuchi, N., dos Santos, J., Ribeiro, R. J., Minette, L., Biot, Y., 1998. Biomassa da parte aérea da vegetação da floresta tropical úmida de terra-firme da Amazônia brasileira. Acta Amazonica 28 (2), 153–165.

Hilker, T., Hall, F. G., Coops, N. C., Collatz, J. G., Black, T. A., Tucker, C. J., Sellers,

P. J., Grant, N., oct 2013. Remote sensing of transpiration and heat fluxes using multi-angle observations. Remote Sensing of Environment 137, 31–42.
URL http://www.sciencedirect.com/science/article/pii/S0034425713001776

Hilker, T., Lyapustin, A. I., Tucker, C. J., Hall, F. G., Myneni, R. B., Wang, Y., Bi, J., Mendes de Moura, Y., Sellers, P. J., nov 2014. Vegetation dynamics and rainfall sensitivity of the Amazon. Proceedings of the National Academy of Sciences 111 (45), 16041–16046.
URL http://www.pnas.org/content/111/45/16041.abstract

Hirsch, A. I., Little, W. S., Houghton, R. a., Scott, N. a., White, J. D., may 2004. The net carbon flux due to deforestation and forest re-growth in the Brazilian Amazon: analysis using a process-based model. Global Change Biology 10 (5), 908–924.
URL http://www.blackwell-synergy.com/links/doi/10.1111{\%}2Fj.1529-8817.2003.00765.x

Hoffmann, W. A., Franco, A. C., Moreira, M. Z., Haridasan, M., 2005. Specific leaf area explains differences in leaf traits between congeneric savanna and forest trees. Functional Ecology 19 (6), 932–940.

Hogg, E. H., Wein, R. W., 2005. Impacts of drought on forest growth and regeneration following fire in southwestern Yukon, Canada. Canadian Journal of Forest Research 35 (9), 2141–2150.

Hooper, D. U., Adair, E. C., Cardinale, B. J., Byrnes, J. E. K., Hungate, B. A., Matulich, K. L., Gonzalez, A., Duffy, J. E., Gamfeldt, L., O'Connor, M. I., 2012. A global synthesis reveals biodiversity loss as a major driver of ecosystem change. Nature 486 (7401), 105–108.

Houghton, R. A., 2005. Aboveground forest biomass and the global carbon balance. Global Change Biology 11 (6), 945–958.

Houghton, R. A., 2010. How well do we know the flux of CO2 from landuse change? Tellus B 62 (5), 337–351.

Houghton, R. A., Lawrence, K. T., Hackler, J. L., Brown, S., 2001. The spatial distribution of forest biomass in the Brazilian Amazon: a comparison of estimates. Global Change Biology 7 (7), 731–746.
URL http://dx.doi.org/10.1111/j.1365-2486.2001.00426.x

Houghton, R. a., Skole, D. L., Nobre, C. a., Hackler, J. L., Lawrence, K. T., Chomentowski, W. H., jan 2000. Annual fluxes of carbon from deforestation and regrowth in the Brazilian Amazon. Nature 403 (6767), 301–304.
URL http://www.ncbi.nlm.nih.gov/pubmed/10659847

Huete, A. R., Davies, K., Restrepo-Coupe, N., Ratana, P., Sun, Q., Saleska, S. R., Schaaf, C., 2014. Seasonal and Diurnal Tropical Forest Greenness Observed and Modeled Using MODIS Terra and Aqua Sensors. In: AGU Fall Meeting Abstracts. Vol. 1. p. 3.

Huete, A. R., Didan, K., Shimabukuro, Y. E., Ratana, P., Saleska, S. R., Hutyra, L. R., Yang, W., Nemani, R. R., Myneni, R., 2006. Amazon rainforests green-up with sunlight in dry season. Geophysical Research Letters 33 (6), L06405.
URL http://doi.wiley.com/10.1029/2005GL025583

Hughes, R. F., Kauffman, J. B., Cummings, D. L., sep 2000. Fire in the Brazilian Amazon. Oecologia 124 (4), 574–588.
URL http://link.springer.com/10.1007/s004420000416

Hughes, R. F., Kauffman, J. B., Jaramillo, V. J., sep 1999. BIOMASS, CARBON, AND NUTRIENT DYNAMICS OF SECONDARY FORESTS IN A HUMID TROPICAL REGION OF MÉXICO. Ecology 80 (6), 1892–1907.
URL http://dx.doi.org/10.1890/0012-9658(1999)080[1892:BCANDO]2.0.CO2

Hui, D., Luo, Y., Cheng, W., Coleman, J. S., Johnson, D. W., Sims, D. A., 2001. Canopy radiation- and water-use efficiencies as affected by elevated [CO2]. Global Change Biology 7 (1), 75–91.
URL http://dx.doi.org/10.1046/j.1365-2486.2001.00391.x

Humphries, S. W., Long, S. P., 1995. WIMOVAC: a software package for modelling the dynamics of plant leaf and canopy photosynthesis. Computer applications in the biosciences: CABIOS 11 (4), 361–371.

Huntingford, C., Zelazowski, P., Galbraith, D., Mercado, L. M., Sitch, S., Fisher, R., Lomas, M., Walker, A. P., Jones, C. D., Booth, B. B. B., Malhi, Y., Hemming, D., Kay, G., Good, P., Lewis, S. L., Phillips, O. L., Atkin, O. K., Lloyd, J., Gloor, E., Zaragoza-Castells, J., Meir, P., Betts, R., Harris, P. P., Nobre, C., Marengo, J., Cox, P. M., apr 2013. Simulated resilience of tropical rainforests to CO2-induced climate change. Nature Geosci 6 (4), 268–273.
URL http://dx.doi.org/10.1038/ngeo1741http://www.nature.com/ngeo/journal/v6/n4/abs/ngeo1741.html{\#}supplementary-information

Hussain, M., Chen, D., Cheng, A., Wei, H., Stanley, D., 2013. Change detection from remotely sensed images: From pixel-based to object-based approaches. ISPRS Journal of Photogrammetry and Remote Sensing 80, 91–106.

Huth, A., Ditzer, T., Bossel, H., 1998. The rain forest growth model FORMIX3: model description and analysis of forest growth and logging scenarios for the Deramakot Forest Reserve (Malaysia. Deutsche Gesellschaft fur.

Imhoff, M. L., 1995. A theoretical analysis of the effect of forest structure on synthetic aperture radar backscatter and the remote sensing of biomass. IEEE Transactions on Geoscience and Remote Sensing 33 (2), 341–352.

INPA, 2015. Reservas Biológicas do INPA.
URL `http://portal.inpa.gov.br/index.php/reservas-e-estacoes`

INPE, 2011. Dados TerraClass.
URL `http://www.inpe.br/cra/projetos{\_}pesquisas/terraclass.php`

INPE, jan 2013. Projeto PRODES: Monitoramento da Floresta Amazônica Brasileira por Satélite. Instituto Nacional de Pesquisas Espaciais. Tech. rep., INPE, Sao Paulo.

ISRIC, 2013. World Soil Information. SoilGrids: an automated system for global soil mapping.

Jakovac, C. C., Peña-Claros, M., Mesquita, R. C. G., Bongers, F., Kuyper, T. W., 2016. Swiddens under transition: Consequences of agricultural intensification in the Amazon. Agriculture, Ecosystems & Environment 218, 116–125.

Jakovac, C. C., PeñaClaros, M., Kuyper, T. W., Bongers, F., 2015. Loss of secondary-forest resilience by landuse intensification in the Amazon. Journal of Ecology 103 (1), 67–77.

Jensen, J., 2005. Introductory Digital Image Processing: A Remote Sensing Perspective. Prentice Hall, Toronto.

Johansen, K., Coops, N. C., Gergel, S. E., Stange, Y., 2007. Application of high spatial resolution satellite imagery for riparian and forest ecosystem classification. Remote Sensing of Environment 110 (1), 29–44.

Jones, N., 2013. Troubling milestone for CO2. Nature Geoscience 6 (8), 589.

Jordan, C. F., Cuevas, E., Medina, E., 2013. NPP Tropical Forest: San Carlos de Rio Negro, Venezuela, 1975-1984, R1. Data set. Available on-line [http://www. daac. ornl. gov] from Oak Ridge National Laboratory Distributed Active Archive Center, Oak Ridge, Tennessee, USA doi 10.

Kammesheidt, L., Pütz, S., Huth, A., 2011. Sustainable Timber Harvesting in Fragmented Secondary Forests in Paraguay? An Inquiry Through Modelling. In: Silviculture in the Tropics. Springer, pp. 387–396.

Kapos, V., 1989. Effects of isolation on the water status of forest patches in the Brazilian Amazon. Journal of Tropical Ecology 5 (02), 173–185.
URL `href="http://dx.doi.org/10.1017/S0266467400003448`

Kaspari, M., Garcia, M. N., Harms, K. E., Santana, M., Wright, S. J., Yavitt, J. B.,

2008. Multiple nutrients limit litterfall and decomposition in a tropical forest. Ecology Letters 11 (1), 35–43.

Kauffman, J. B., Hughes, R. F., Heider, C., jun 2009. Carbon pool and biomass dynamics associated with deforestation, land use, and agricultural abandonment in the neotropics. Ecological Applications 19 (5), 1211–1222.
URL `http://dx.doi.org/10.1890/08-1696.1`

Keane, R. E., Arno, S. F., Brown, J. K., Tomback, D. F., 1990. Modelling stand dynamics in whitebark pine (Pinus albicaulis) forests. Ecological Modelling 51 (1), 73–95.

Keane, R. E., Austin, M., Field, C., Huth, A., Lexer, M. J., Peters, D., Solomon, A., Wyckoff, P., 2001. Tree mortality in gap models: application to climate change. Climatic Change 51 (3-4), 509–540.

Keane, R. E., Morgan, P., Running, S. W., 1996. Fire-BGC: A mechanistic ecological process model for simulating fire succession on coniferous forest landscapes of the northern Rocky Mountains. Forest Service research paper. Tech. rep., ntermountain Research Station, Ogden.

Keeling, C. D., Piper, S. C., Bacastow, R. B., Wahlen, M., Whorf, T. P., Heimann, M., Meijer, H. A., 2005. Atmospheric CO2 and 13CO2 exchange with the terrestrial biosphere and oceans from 1978 to 2000: observations and carbon cycle implications. In: A history of atmospheric CO2 and its effects on plants, animals, and ecosystems. Springer, pp. 83–113.

Keller, M., Palace, M., Hurtt, G., 2001. Biomass estimation in the Tapajos National Forest, Brazil: examination of sampling and allometric uncertainties. Forest Ecology and Management 154.
URL `http://www.sciencedirect.com/science/article/pii/S0378112701005096`

Keller, M., Varner, R., Dias, J. D., Silva, H., Crill, P., de Oliveira Jr, R. C., Asner, G. P., 2005. Soil-atmosphere exchange of nitrous oxide, nitric oxide, methane, and carbon dioxide in logged and undisturbed forest in the Tapajos National Forest, Brazil. Earth Interactions 9 (23), 1–28.

Kellman, M. C., 1970. Secondary plant succession in tropical montane Mindanao. Tech. rep.

Kellomäki, S., Väisänen, H., 1997. Modelling the dynamics of the forest ecosystem for climate change studies in the boreal conditions. Ecological modelling 97 (1), 121–140.

Kelly, R. H., Parton, W. J., Crocker, G. J., Graced, P. R., Klir, J., Körschens, M.,

Poulton, P. R., Richter, D. D., 1997. Simulating trends in soil organic carbon in long-term experiments using the century model. Geoderma 81 (1), 75–90.

Kent, R. B., 2006. Latin America: regions and people. Guilford Press.

Kercher, J. R., Axelrod, M. C., 1984. A process model of fire ecology and succession in a mixed-conifer forest. Ecology, 1725–1742.

Kimes, D. S., Nelson, R. F., Salas, W. A., Skole, D. L., 1999. Mapping secondary tropical forest and forest age from SPOT HRV data. International Journal of Remote Sensing 20 (18), 3625–3640.
URL `http://www.informaworld.com/openurl?genre=article{\&}doi=10.1080/014311699211246{\&}magic=crossref`

Kimmins, J. P., Mailly, D., Seely, B., 1999. Modelling forest ecosystem net primary production: the hybrid simulation approach used in FORECAST. Ecological modelling 122 (3), 195–224.

Kirby, K. R., Laurance, W. F., Albernaz, A. K., Schroth, G., Fearnside, P. M., Bergen, S., Venticinque, E. M., da Costa, C., may 2006. The future of deforestation in the Brazilian Amazon. Futures 38 (4), 432–453.
URL `http://linkinghub.elsevier.com/retrieve/pii/S0016328705001400`

Kitajima, K., 1994. Relative importance of photosynthetic traits and allocation patterns as correlates of seedling shade tolerance of 13 tropical trees. Oecologia 98 (3-4), 419–428.

Klinge, H., Rodrigues, W. A., 1968. Litter production in an area of Amazonian terra firme forest. Part I. Litter-fall, organic carbon and total nitrogen contents of litter. Amazoniana 1 (4), 287–302.

Köhler, P., 2000. Modelling anthropogenic impacts on the growth of tropical rain forests-using an individual oriented forest growth model for the analyses of logging and fragmentation in three case studies. University of Kassel.

Köhler, P., Huth, A., 1998. The effects of tree species grouping in tropical rainforest modelling: Simulations with the individual-based model FORMIND. Ecological Modelling 109 (3), 301–321.

Köhler, P., Huth, A., 2007. Impacts of recruitment limitation and canopy disturbance on tropical tree species richness. ecological modelling 203 (3), 511–517.

Kong, X., Dao, T. H., Qin, J., Qin, H., Li, C., Zhang, F., 2009. Effects of soil texture and land use interactions on organic carbon in soils in North China cities' urban fringe. Geoderma 154 (1), 86–92.

Körner, C., 1995. Leaf diffusive conductances in the major vegetation types of the globe. In: Ecophysiology of photosynthesis. Springer, pp. 463–490.

Kucherenko, S., Rodriguez-Fernandez, M., Pantelides, C., Shah, N., 2009. Monte Carlo evaluation of derivative-based global sensitivity measures. Reliability Engineering & System Safety 94 (7), 1135–1148.

Kumagai, T., Saitoh, T. M., Sato, Y., Morooka, T., Manfroi, O. J., Kuraji, K., Suzuki, M., feb 2004. Transpiration, canopy conductance and the decoupling coefficient of a lowland mixed dipterocarp forest in Sarawak, Borneo: dry spell effects. Journal of Hydrology 287 (14), 237–251.
URL http://www.sciencedirect.com/science/article/pii/S0022169403004165

Kunert, N., Aparecido, L. M. T., Higuchi, N., dos Santos, J., Trumbore, S., 2015. Higher tree transpiration due to road-associated edge effects in a tropical moist lowland forest. Agricultural and Forest Meteorology 213, 183–192.

Kuplich, T. M., oct 2006. Classifying regenerating forest stages in Amazônia using remotely sensed images and a neural network. Forest Ecology and Management 234 (1-3), 1–9.
URL http://linkinghub.elsevier.com/retrieve/pii/S0378112706003665

Kuplich, T. M., Curran, P. J., Atkinson, P. M., nov 2005. Relating SAR image texture to the biomass of regenerating tropical forests. International Journal of Remote Sensing 26 (21), 4829–4854.
URL http://www.tandfonline.com/doi/abs/10.1080/01431160500239107

Lambin, E. F., Strahlers, A. H., 1994. Change-vector analysis in multitemporal space: a tool to detect and categorize land-cover change processes using high temporal-resolution satellite data. Remote Sensing of Environment 48 (2), 231–244.

Landsberg, J., Waring, R., Coops, N., jan 2003. Performance of the forest productivity model 3-PG applied to a wide range of forest types. Forest Ecology and Management 172 (2-3), 199–214.
URL http://www.sciencedirect.com/science/article/pii/S0378112701008040

Landsberg, J. J., Johnsen, K. H., Albaugh, T. J., Allen, H. L., McKeand, S. E., 2001. Applying 3-PG, a simple process-based model designed to produce practical results, to data from loblolly pine experiments. Forest Science 47 (1), 43–51.

Landsberg, J. J., Sands, P., 2010. Physiological ecology of forest production: principles, processes and models. Vol. 4. Academic Press.

Landsberg, J. J., Waring, R. H., aug 1997. A generalised model of forest productivity

using simplified concepts of radiation-use efficiency, carbon balance and partitioning. Forest Ecology and Management 95 (3), 209–228.
URL http://linkinghub.elsevier.com/retrieve/pii/S0378112797000261

Landsberg, J. J., Waring, R. H., Coops, N. C., 2002. Performance of the forest productivity model 3-PG applied to a wide range of forest types. Forest Ecology and Management 5845, 1–16.

Lasch, P., Badeck, F.-W., Lindner, M., Suckow, F., 2002. Sensitivity of Simulated Forest Growth to Changes in Climate and Atmospheric CO˜ 2. Forstwissenschaftlisches Centralblatt 121, 155–171.

Lasch, P., Badeck, F.-W., Suckow, F., Lindner, M., Mohr, P., mar 2005. Model-based analysis of management alternatives at stand and regional level in Brandenburg (Germany). Forest Ecology and Management 207 (1-2), 59–74.
URL http://www.sciencedirect.com/science/article/pii/S0378112704007273

Lasky, J. R., Uriarte, M., Boukili, V. K., Erickson, D. L., John Kress, W., Chazdon, R. L., sep 2014. The relationship between tree biodiversity and biomass dynamics changes with tropical forest succession. Ecology letters 17 (9), 1158–67.
URL http://www.ncbi.nlm.nih.gov/pubmed/24986005

Laurance, S. G. W., Laurance, W. F., Andrade, A., Fearnside, P. M., Harms, K. E., Vicentini, A., Luizão, R. C. C., feb 2010. Influence of soils and topography on Amazonian tree diversity: a landscape-scale study. Journal of Vegetation Science 21 (1), 96–106.
URL http://doi.wiley.com/10.1111/j.1654-1103.2009.01122.x

Laurance, S. G. W., Stouffer, P. C., Laurance, W. F., 2004. Effects of road clearings on movement patterns of understory rainforest birds in central Amazonia. Conservation Biology 18 (4), 1099–1109.

Laurance, W. F., Balmford, A., 2013. Land use: a global map for road building. Nature 495 (7441), 308–309.

Laurance, W. F., Camargo, J. L. C., Luizão, R. C. C., Laurance, S. G., Pimm, S. L., Bruna, E. M., Stouffer, P. C., Bruce Williamson, G., Benítez-Malvido, J., Vasconcelos, H. L., jan 2011. The fate of Amazonian forest fragments: A 32-year investigation. Biological Conservation 144 (1), 56–67.
URL http://linkinghub.elsevier.com/retrieve/pii/S0006320710004209

Laurance, W. F., Cochrane, M. A., Bergen, S., Fearnside, P. M., Delamônica, P., Barber, C., D'Angelo, S., Fernandes, T., 2001. The future of the Brazilian Amazon. Science(Washington) 291 (5503), 438–439.

Laurance, W. F., Delamonica, P., Laurance, S. G., Vasconcelos, H. L., Lovejoy, T. E., apr 2000. Conservation: Rainforest fragmentation kills big trees. Nature 404 (6780), 836.
URL http://dx.doi.org/10.1038/35009032

Laurance, W. F., Fearnside, P. M., Laurance, S. G., Delamonica, P., Lovejoy, T. E., Rankin-de Merona, J. M., Chambers, J. Q., Gascon, C., jun 1999. Relationship between soils and Amazon forest biomass: a landscape-scale study. Forest Ecology and Management 118 (1-3), 127–138.
URL http://linkinghub.elsevier.com/retrieve/pii/S0378112798004940

Laurance, W. F., Ferreira, L. V., Rankin-de Merona, J. M., Laurance, S. G., 1998. Rain forest fragmentation and the dynamics of Amazonian tree communities. Ecology 79 (6), 2032–2040.

Laurance, W. F., Goosem, M., Laurance, S. G. W., 2009. Impacts of roads and linear clearings on tropical forests. Trends in Ecology & Evolution 24 (12), 659–669.

Laurance, W. F., Laurance, S. G., Ferreira, L. V., Rankin-de Merona, J. M., Gascon, C., Lovejoy, T. E., 1997. Biomass collapse in Amazonian forest fragments. Science 278 (5340), 1117–1118.

Laurance, W. F., Nascimento, H. E. M., Laurance, S. G., Andrade, A. C., Fearnside, P. M., Ribeiro, J. E. L., Capretz, R. L., feb 2006. RAIN FOREST FRAGMENTATION AND THE PROLIFERATION OF SUCCESSIONAL TREES. Ecology 87 (2), 469–482.
URL http://dx.doi.org/10.1890/05-0064

Laurance, W. F., Sayer, J., Cassman, K. G., feb 2014. Agricultural expansion and its impacts on tropical nature. Trends in ecology & evolution 29 (2), 107–16.
URL http://www.sciencedirect.com/science/article/pii/S0169534713002929

Laurance, W. F., Williamson, G. B., dec 2001. Positive Feedbacks among Forest Fragmentation, Drought, and Climate Change in the Amazon. Conservation Biology 15 (6), 1529–1535.
URL http://dx.doi.org/10.1046/j.1523-1739.2001.01093.x

Le Toan, T., Beaudoin, A., Riom, J., Guyon, D., 1992. Relating forest biomass to SAR data. Geoscience and Remote Sensing, IEEE Transactions on 30 (2), 403–411.

Le Toan, T., Quegan, S., Davidson, M. W. J., Balzter, H., Paillou, P., Papathanassiou, K., Plummer, S., Rocca, F., Saatchi, S., Shugart, H., Ulander, L., nov 2011. The BIOMASS mission: Mapping global forest biomass to better understand the terrestrial carbon cycle. Remote Sensing of Environment 115 (11), 2850–2860.

URL http://www.sciencedirect.com/science/article/pii/S0034425711001362

Lederer, M., sep 2011. From CDM to REDD+ What do we know for setting up effective and legitimate carbon governance? Ecological Economics 70 (11), 1900–1907.
URL http://www.sciencedirect.com/science/article/pii/S0921800911000577

Lee, J.-E., Frankenberg, C., van der Tol, C., Berry, J. A., Guanter, L., Boyce, C. K., Fisher, J. B., Morrow, E., Worden, J. R., Asefi, S., 2013. Forest productivity and water stress in Amazonia: observations from GOSAT chlorophyll fluorescence. Proceedings of the Royal Society of London B: Biological Sciences 280 (1761), 20130171.

Lefsky, M. A., Harding, D. J., Keller, M., Cohen, W. B., Carabajal, C. C., Del Bom EspiritoSanto, F., Hunter, M. O., de Oliveira, R., 2005. Estimates of forest canopy height and aboveground biomass using ICESat. Geophysical research letters 32 (22).

Lehmann, S., Huth, A., apr 2015. Fast calibration of a dynamic vegetation model with minimum observation data. Ecological Modelling 301, 98–105.
URL http://www.sciencedirect.com/science/article/pii/S0304380015000320

Lenzen, M., Schaeffer, R., Karstensen, J., Peters, G. P., 2013. Drivers of change in Brazil's carbon dioxide emissions. Climatic change 121 (4), 815–824.

Letcher, S. G., Chazdon, R. L., 2009. Rapid recovery of biomass, species richness, and species composition in a forest chronosequence in northeastern Costa Rica. Biotropica 41 (5), 608–617.

Lewis, S. L., Brando, P. M., Phillips, O. L., van der Heijden, G. M. F., Nepstad, D., feb 2011. The 2010 Amazon Drought. Science 331 (6017), 554.
URL http://www.sciencemag.org/content/331/6017/554.abstract

Lillesand, T., Kiefer, R. W., Chipman, J., 2014. Remote sensing and image interpretation. John Wiley & Sons.

Lines, E. R., Zavala, M. A., Purves, D. W., Coomes, D. A., 2012. Predictable changes in aboveground allometry of trees along gradients of temperature, aridity and competition. Global Ecology and Biogeography 21 (10), 1017–1028.

Lodge, D. J., Cantrell, S. A., González, G., 2014. Effects of canopy opening and debris deposition on fungal connectivity, phosphorus movement between litter cohorts and mass loss. Forest Ecology and Management 332, 11–21.

Lohbeck, M., Poorter, L., Lebrija-Trejos, E., Martínez-Ramos, M., Meave, J. A., Paz, H., Pérez-García, E. A., Romero-Pérez, I. E., Tauro, A., Bongers, F., 2013. Successional

changes in functional composition contrast for dry and wet tropical forest. Ecology 94 (6), 1211–1216.

Lopez-Gonzalez, G., Lewis, S., Burkitt, M., Phillips, O., 2011. ForestPlots.net: a web application and research tool to manage and analyse tropical forest plot data. Journal of Vegetation Science 22, 610–613.

Lu, D., Batistella, M., Moran, E., 2007. Landcover classification in the Brazilian Amazon with the integration of Landsat ETM + and Radarsat data. International Journal of Remote Sensing 28 (24), 5447–5459.
URL http://www.tandfonline.com/doi/abs/10.1080/01431160701227596

Lu, D., Moran, E., Batistella, M., nov 2003. Linear mixture model applied to Amazonian vegetation classification. Remote Sensing of Environment 87 (4), 456–469.
URL http://linkinghub.elsevier.com/retrieve/pii/S0034425703002050

Lucas, R., Held, A., Phinn, S., Saatchi, S., 2004. Tropical Forests. In: Ustin, S. (Ed.), Remote Sensing for Natural Resource Management and Environmental Monitoring. Wiley, Ch. 5, pp. 132 – 186.

Lucas, R., Medcalf, K., Brown, A., Bunting, P., Breyer, J., Clewley, D., Keyworth, S., Blackmore, P., 2011. Updating the Phase 1 habitat map of Wales, UK, using satellite sensor data. ISPRS Journal of Photogrammetry and Remote Sensing 66 (1), 81–102.

Lucas, R. M., Honzak, M., 2002. Forest regeneration on abandoned clearances in central Amazonia. International Journal of Remote Sensing 23 (2002), 37–41.
URL http://www.tandfonline.com/doi/abs/10.1080/01431160110069791

Lucas, R. M., Honzak, M., Curran, P. J., Foody, G. M., Milne, R., Brown, T., Amaral, S., 2000. Mapping the regional extent of tropical forest regeneration stages in the Brazilian Legal Amazon using NOAA AVHRR data. International Journal of Remote Sensing 21 (15), 2855–2881.
URL http://www.tandfonline.com/doi/abs/10.1080/01431160050121285

Lucas, R. M., Mitchell, A. L., Rosenqvist, A., Proisy, C., Melius, A., Ticehurst, C., may 2007. The potential of L-band SAR for quantifying mangrove characteristics and change: case studies from the tropics. Aquatic Conservation: Marine and Freshwater Ecosystems 17 (3), 245–264.
URL http://dx.doi.org/10.1002/aqc.833

Lucas, R. M., Xiao, X., Hagen, S., Frolking, S., 2002. Evaluating TERRA1 MODIS data for discrimination of tropical secondary forest regeneration stages in the Brazilian Legal Amazon. Geophysical Research Letters 29 (8), 2–5.
URL http://onlinelibrary.wiley.com/doi/10.1029/2001GL013375/full

Luckman, A., Baker, J., Kuplich, T. M., da Costa Freitas Yanasse, C., Frery, A. C., apr

1997. A study of the relationship between radar backscatter and regenerating tropical forest biomass for spaceborne SAR instruments. Remote Sensing of Environment 60 (1), 1–13.
URL http://www.sciencedirect.com/science/article/pii/S0034425796001216

Lugo, A., Sanchez, M., Brown, S., 1986. Land use and organic carbon content of some subtropical soils. Plant and Soil 96 (2), 185–196.
URL http://dx.doi.org/10.1007/BF02374763

MacDicken, K., 2012. Forest Resources Assessment 2015.

Mackensen, J., Hölscher, D., Klinge, R., Fölster, H., oct 1996. Nutrient transfer to the atmosphere by burning of debris in eastern Amazonia. Forest Ecology and Management 86 (1-3), 121–128.
URL http://www.scopus.com/inward/record.url?eid=2-s2.0-0030587626{\&}partnerID=tZOtx3y1

Malhi, Y., Aragão, L. E. O. C., Galbraith, D., Huntingford, C., Fisher, R., Zelazowski, P., Sitch, S., McSweeney, C., Meir, P., dec 2009a. Exploring the likelihood and mechanism of a climate-change-induced dieback of the Amazon rainforest. Proceedings of the National Academy of Sciences 106 (49), 20610–20615.
URL http://www.pnas.org/content/106/49/20610.abstract

Malhi, Y., Aragão, L. E. O. C., Metcalfe, D. B., Paiva, R., Quesada, C. A., Almeida, S., Anderson, L., Brando, P., Chambers, J. Q., Da Costa, A. C. L., Hutyra, L. R., Oliveira, P., Patiño, S., Pyle, E. H., Robertson, A. L., Teixeira, L. M., 2009b. Comprehensive assessment of carbon productivity, allocation and storage in three Amazonian forests. Global Change Biology 15 (5), 1255–1274.
URL http://dx.doi.org/10.1111/j.1365-2486.2008.01780.x

Malhi, Y., Baker, T. R., Phillips, O. L., Almeida, S., Alvarez, E., Arroyo, L., Chave, J., Czimczik, C. I., Fiore, A. D., Higuchi, N., 2004. The aboveground coarse wood productivity of 104 Neotropical forest plots. Global Change Biology 10 (5), 563–591.

Malhi, Y., Phillips, O. L., Lloyd, J., Baker, T., Wright, J., Almeida, S., Arroyo, L., Frederiksen, T., Grace, J., Higuchi, N., 2002. An international network to monitor the structure, composition and dynamics of Amazonian forests (RAINFOR). Journal of Vegetation Science 13 (3), 439–450.

Malhi, Y., Roberts, J. T., Betts, R. A., Killeen, T. J., 2008. Climate Change, Deforestation, and the Fate of the Amazon. Science 319 (January), 169–172.
URL http://www.sciencemag.org/content/319/5860/169.short

Malhi, Y., Wood, D., Baker, T. R., Wright, J., Phillips, O. L., Cochrane, T., Meir, P.,

Chave, J., Almeida, S., Arroyo, L., 2006. The regional variation of aboveground live biomass in oldgrowth Amazonian forests. Global Change Biology 12 (7), 1107–1138.

Malhi, Y., Wright, J., 2004. Spatial patterns and recent trends in the climate of tropical rainforest regions. Philosophical Transactions of the Royal Society London 359.
URL http://rstb.royalsocietypublishing.org/content/359/1443/311.short

Marengo, J. A., Nobre, C. A., Tomasella, J., Oyama, M. D., Sampaio de Oliveira, G., de Oliveira, R., Camargo, H., Alves, L. M., Brown, I. F., feb 2008. The Drought of Amazonia in 2005. Journal of Climate 21 (3), 495–516.
URL http://dx.doi.org/10.1175/2007JCLI1600.1

Margono, B. A., Potapov, P. V., Turubanova, S., Stolle, F., Hansen, M. C., aug 2014. Primary forest cover loss in Indonesia over 2000-2012. Nature Clim. Change 4 (8), 730–735.
URL http://dx.doi.org/10.1038/nclimate2277http://10.1038/nclimate2277http://www.nature.com/nclimate/journal/v4/n8/abs/nclimate2277.html{\#}supplementary-information

Martin, P. A., Newton, A. C., Bullock, J. M., 2013. Carbon pools recover more quickly than plant biodiversity in tropical secondary forests. Proceedings of the Royal Society of London B: Biological Sciences 280 (1773), 20132236.

Martin, P. A., Newton, A. C., Bullock, J. M., mar 2014. Carbon pools recover more quickly than plant biodiversity in tropical secondary forests. Proceedings of the Royal Society of London B: Biological Sciences 281 (1782).
URL http://rspb.royalsocietypublishing.org/content/281/1782/20140303.abstract

Martinez, L. J., Zinck, J., jan 2004. Temporal variation of soil compaction and deterioration of soil quality in pasture areas of Colombian Amazonia. Soil and Tillage Research 75 (1), 3–18.
URL http://linkinghub.elsevier.com/retrieve/pii/S0167198703002009

Masek, J. G., Huang, C., Wolfe, R., Cohen, W., Hall, F., Kutler, J., Nelson, P., 2008. North American forest disturbance mapped from a decadal Landsat record. Remote Sensing of Environment 112 (6), 2914–2926.

Mayor, J. R., Wright, S. J., Turner, B. L., jan 2014. Species-specific responses of foliar nutrients to long-term nitrogen and phosphorus additions in a lowland tropical forest. Journal of Ecology 102 (1), 36–44.
URL http://dx.doi.org/10.1111/1365-2745.12190

McDowell, N. G., 2011. Mechanisms linking drought, hydraulics, carbon metabolism, and vegetation mortality. Plant physiology 155 (3), 1051–1059.

MCT (Ministry of Science and Technology), 2010. Second National Communication of Brazil to the United Nations Framework Convention on Climate Change. Tech. rep., Ministry of Science and Technology, Brasilia.

MCT (Ministry of Science and Technology), 2016. Third National Communication of Brazil to the United Nations Framework Convention on Climate Change. Tech. rep., Ministry of Science and Technology, Brasilia.

Medina, E., Klinge, H., 1983. Productivity of tropical forests and tropical woodlands. In: Physiological Plant Ecology IV. Springer, pp. 281–303.

Ménard, A., Dubé, P., Bouchard, A., Canham, C. D., Marceau, D. J., 2002. Evaluating the potential of the SORTIE forest succession model for spatio-temporal analysis of small-scale disturbances. Ecological Modelling 153 (1), 81–96.

Menyailo, O., Lehmann, J., da Silva Cravo, M., Zech, W., 2003. Soil microbial activities in tree-based cropping systems and natural forests of the Central Amazon, Brazil. Biology and Fertility of Soils 38 (1), 1–9.
URL http://dx.doi.org/10.1007/s00374-003-0631-4

Mesquita, R. C. G., Delamônica, P., Laurance, W. F., 1999. Effect of surrounding vegetation on edge-related tree mortality in Amazonian forest fragments. Biological Conservation 91 (2), 129–134.

Mesquita, R. C. G., Ickes, K., Ganade, G., GB, W., 2001. Alternative Successional Pathways in the Amazon Basin. Journal of Ecology 89 (4), 528–537.
URL http://onlinelibrary.wiley.com/doi/10.1046/j.1365-2745.2001.00583.x/full

Mesquita, R. d. C. G., 2000. Management of advanced regeneration in secondary forests of the Brazilian Amazon. Forest Ecology and Management 130 (1), 131–140.

Mesquita, R. d. C. G., dos Santos Massoca, P. E., Jakovac, C. C., Bentos, T. V., Williamson, G. B., 2015. Amazon Rain Forest Succession: Stochasticity or Land-Use Legacy? BioScience 65 (9), 849–861.
URL https://www.researchgate.net/profile/Catarina{_}Jakovac/publication/281470595{_}Amazon{_}Rain{_}Forest{_}Succession{_}Stochasticity{_}or{_}Land-Use{_}Legacy/links/55f1471208aef559dc47020f.pdf

Metcalfe, D., Meir, P., Aragão, L., da Costa, A., Braga, A., Gonçalves, P., de Athaydes Silva Junior, J., de Almeida, S., Dawson, L., Malhi, Y., Williams, M., 2008. The effects of water availability on root growth and morphology in an Amazon rainforest. Plant and Soil 311 (1-2), 189–199.
URL http://dx.doi.org/10.1007/s11104-008-9670-9

Metcalfe, D. B., Meir, P., Aragão, L. E. O. C., Lobo-do Vale, R., Galbraith, D., Fisher, R. A., Chaves, M. M., Maroco, J. P., da Costa, A. C. L., de Almeida, S. S., Braga, A. P., Gonçalves, P. H. L., de Athaydes, J., da Costa, M., Portela, T. T. B., de Oliveira, A. A. R., Malhi, Y., Williams, M., aug 2010. Shifts in plant respiration and carbon use efficiency at a large-scale drought experiment in the eastern Amazon. The New phytologist 187 (3), 608–21.
URL http://www.ncbi.nlm.nih.gov/pubmed/20553394

Metzger, J. P., 2002. Landscape dynamics and equilibrium in areas of slash-and-burn agriculture with short and long fallow period (Bragantina region, NE Brazilian Amazon). Landscape Ecology, 419–431.
URL http://link.springer.com/article/10.1023/A:1021250306481

Minh, D. H. T., Le Toan, T., Rocca, F., Tebaldini, S., D'Alessandro, M. M., Villard, L., 2014. Relating P-band synthetic aperture radar tomography to tropical forest biomass. Geoscience and Remote Sensing, IEEE Transactions on 52 (2), 967–979.

Miranda, 2013. Sustentabilidade Agrícola na Amazonia - 23 anos de monitoramento da agricultura em Machadinho d'Oeste (RO).
URL http://www.machadinho.cnpm.embrapa.br/index.html

Mitchard, E. T. A., Feldpausch, T. R., Brienen, R. J. W., Lopez-Gonzalez, G., Monteagudo, A., Baker, T. R., Lewis, S. L., Lloyd, J., Quesada, C. A., Gloor, M., ter Steege, H., Meir, P., Alvarez, E., Araujo-Murakami, A., Aragão, L. E. O. C., Arroyo, L., Aymard, G., Banki, O., Bonal, D., Brown, S., Brown, F. I., Cerón, C. E., Chama Moscoso, V., Chave, J., Comiskey, J. A., Cornejo, F., Corrales Medina, M., Da Costa, L., Costa, F. R. C., Di Fiore, A., Domingues, T. F., Erwin, T. L., Frederickson, T., Higuchi, N., Honorio Coronado, E. N., Killeen, T. J., Laurance, W. F., Levis, C., Magnusson, W. E., Marimon, B. S., Marimon Junior, B. H., Mendoza Polo, I., Mishra, P., Nascimento, M. T., Neill, D., Núñez Vargas, M. P., Palacios, W. A., Parada, A., Pardo Molina, G., Peña-Claros, M., Pitman, N., Peres, C. A., Poorter, L., Prieto, A., Ramirez-Angulo, H., Restrepo Correa, Z., Roopsind, A., Roucoux, K. H., Rudas, A., Salomão, R. P., Schietti, J., Silveira, M., de Souza, P. F., Steininger, M. K., Stropp, J., Terborgh, J., Thomas, R., Toledo, M., Torres-Lezama, A., van Andel, T. R., van der Heijden, G. M. F., Vieira, I. C. G., Vieira, S., Vilanova-Torre, E., Vos, V. A., Wang, O., Zartman, C. E., Malhi, Y., Phillips, O. L., aug 2014. Markedly divergent estimates of Amazon forest carbon density from ground plots and satellites. Global Ecology and Biogeography 23 (8), 935–946.
URL http://dx.doi.org/10.1111/geb.12168

Mitchard, E. T. A., Saatchi, S. S., Woodhouse, I. H., Nangendo, G., Ribeiro, N. S., Williams, M., Ryan, C. M., Lewis, S. L., Feldpausch, T. R., Meir, P., 2009. Using satellite radar backscatter to predict aboveground woody biomass: A consistent

relationship across four different African landscapes. Geophysical Research Letters 36 (23).

Mladenoff, D. J., dec 2004. LANDIS and forest landscape models. Ecological Modelling 180 (1), 7–19.
URL http://www.sciencedirect.com/science/article/pii/S0304380004003461

Mohren, G. M. J., Bartelink, H. H., Jorritsma, I. T. M., Kramer, K., 1993. A process-based growth model (FORGRO) for analysis of forest dynamics in relation to environmental factors.

Mohren, G. M. J., Garza Caligaris, J. F., Masera, O. R., Kanninen, M., Karjalainen, T., Pussinen, A., Nabuurs, G. J., 1999. CO2FIX for Windows: a dynamic model of the CO2-fixation in forests; version 1.2. Tech. rep., Institute for Forestry and Nature Research, Wageningen.

Molto, Q., Rossi, V., Blanc, L., 2013. Error propagation in biomass estimation in tropical forests. Methods in Ecology and Evolution 4 (2), 175–183.

Monserud, R. A., 2003. Evaluating forest models in a sustainable forest management context. Forest Biometry, Modelling and Information Sciences 1 (1), 35–47.

Monteith, J. L., 1972. Solar radiation and productivity in tropical ecosystems. Journal of applied ecology, 747–766.

Montgomery, R. A., Chazdon, R. L., 2001. Forest structure, canopy architecture, and light transmittance in tropical wet forests. Ecology 82 (10), 2707–2718.

Moore, M. C. H., Krylov, A., Tyukavina, A., Potapov, P. V., Turubanova, S., Zutta, B., Ifo, S., Margono, B., Stolle, F., Rebecca, 2016. Humid tropical forest disturbance alerts using Landsat data. Environmental Research Letters 11 (3), 34008.
URL http://stacks.iop.org/1748-9326/11/i=3/a=034008

Moran, E. F., Brondizio, E. S., Tucker, J. M., da Silva-Forsberg, M. C., McCracken, S., Falesi, I., dec 2000. Effects of soil fertility and land-use on forest succession in Amazônia. Forest Ecology and Management 139 (1-3), 93–108.
URL http://www.sciencedirect.com/science/article/pii/S0378112799003370

Morris, M. D., may 1991. Factorial Sampling Plans for Preliminary Computational Experiments. Technometrics 33 (2), 161–174.
URL http://www.tandfonline.com/doi/abs/10.1080/00401706.1991.10484804

Morton, D. C., DeFries, R. S., Shimabukuro, Y. E., Anderson, L. O., Arai, E., del Bon Espirito-Santo, F., Freitas, R., Morisette, J., 2006. Cropland expansion changes

deforestation dynamics in the southern Brazilian Amazon. Proceedings of the National Academy of Sciences 103 (39), 14637–14641.

Motzer, T., Munz, N., Küppers, M., Schmitt, D., Anhuf, D., 2005. Stomatal conductance, transpiration and sap flow of tropical montane rain forest trees in the southern Ecuadorian Andes. Tree Physiology 25 (10), 1283–1293.

Mustonen, P. S. J., Oelbermann, M., Kass, D. C. L., 2014. Response of the common bean (Phaseolus vulgaris L.) to Tithonia diversifolia (Hamsl.) Gray biomass retention or removal in a slash and mulch agroforestry system. Agroforestry systems 88 (1), 1–10.

Myneni, R. B., Yang, W., Nemani, R. R., Huete, A. R., Dickinson, R. E., Knyazikhin, Y., Didan, K., Fu, R., Juárez, R. I. N., Saatchi, S. S., 2007. Large seasonal swings in leaf area of Amazon rainforests. Proceedings of the National Academy of Sciences 104 (12), 4820–4823.

Nagendra, H., Lucas, R., Honrado, J. P., Jongman, R. H. G., Tarantino, C., Adamo, M., Mairota, P., oct 2013. Remote sensing for conservation monitoring: Assessing protected areas, habitat extent, habitat condition, species diversity, and threats. Ecological Indicators 33, 45–59.
URL http://www.sciencedirect.com/science/article/pii/S1470160X12003317

Nascimento, H. E., Laurance, W. F., sep 2002. Total aboveground biomass in central Amazonian rainforests: a landscape-scale study. Forest Ecology and Management 168 (1-3), 311–321.
URL http://www.sciencedirect.com/science/article/pii/S0378112701007496

Nascimento, H. E. M., Laurance, W. F., 2004. Biomass dynamics in Amazonian forest fragments. Ecological Applications 14 (sp4), 127–138.

Neeff, T., nov 2005. Spatial modeling of primary and secondary forest growth in Amazonia. Forest Ecology and Management 219 (2-3), 149–168.
URL http://linkinghub.elsevier.com/retrieve/pii/S0378112705005025

Neeff, T., dos Santos, J. R., sep 2005. A growth model for secondary forest in Central Amazonia. Forest Ecology and Management 216 (1-3), 270–282.
URL http://www.sciencedirect.com/science/article/pii/S0378112705003737

Neeff, T., Lucas, R. M., dos Santos, J. R., Brondizio, E. S., Freitas, C. C., 2006. Area and Age of Secondary Forests in Brazilian Amazonia 1978-2002: An Empirical

Estimate. Ecosystems 9 (4), 609–623.
URL http://link.springer.com/article/10.1007/s10021-006-0001-9

Negreiros, G., Schlesinger, P., Nepstad, D., Lefebvre, P., Alencar, A., 2009. Pre-LBA RADAMBRASIL Project Data.
URL http://dx.doi.org/10.3334/ORNLDAAC/941

Neill, C., Coe, M. T., Riskin, S. H., Krusche, A. V., Elsenbeer, H., Macedo, M. N., McHorney, R., Lefebvre, P., Davidson, E. A., Scheffler, R., 2013. Watershed responses to Amazon soya bean cropland expansion and intensification. Philosophical Transactions of the Royal Society of London B: Biological Sciences 368 (1619), 20120425.

Neill, C., Fry, B., Melillo, J. M., Steudler, P. A., Moraes, J. F. L., Cerri, C. C., 1996. Forest-and pasture-derived carbon contributions to carbon stocks and microbial respiration of tropical pasture soils. Oecologia 107 (1), 113–119.

Nelson, B. W., Kapos, V., Adams, J. B., Oliveira, W. J., Braun, O. P. G., 1994. Forest Disturbance by Large Blowdowns in the Brazilian Amazon. Ecology 75 (3), 853–858.
URL http://www.jstor.org/stable/1941742

Nelson, B. W., Mesquita, R., Pereira, J. L. G., de Souza, S. G. A., Batista, G. T., Couto, B. L., 1999. Allometric regressions for improved estimate of secondary forest biomass in the central Amazon. Forest Ecology and Management 117, 149–167.

Nepstad, D., Lefebvre, P., Lopes da Silva, U., Tomasella, J., Schlesinger, P., Solorzano, L., Moutinho, P., Ray, D., Guerreira Benito, J., may 2004. Amazon drought and its implications for forest flammability and tree growth: a basin-wide analysis. Global Change Biology 10 (5), 704–717.
URL http://doi.wiley.com/10.1111/j.1529-8817.2003.00772.x

Nepstad, D., Soares-filho, B. S., Merry, F., Lima, A., Moutinho, P., Carter, J., Bowman, M., Cattaneo, A., Rodrigues, H., Schwartzman, S., Mcgrath, D. G., Stickler, C. M., Lubowski, R., Piris-cabezas, P., Rivero, S., Alencar, A., Almeida, O., Stella, O., 2009. The End of Deforestation in the Brazilian Amazon. Science 326.

Nepstad, D., Uhl, C., Serrao, E. A., Anderson, A. B., 1990. Surmounting barriers to forest regeneration in abandoned, highly degraded pastures: a case study from Paragominas, Pará, Brazil. Alternatives to deforestation: steps towards sustainable use of the Amazon rain forest., 215–229.

Nepstad, D. C., McGrath, D. G., Soares-Filho, B., dec 2011. Systemic conservation, REDD, and the future of the Amazon Basin. Conservation biology : the journal of the Society for Conservation Biology 25 (6), 1113–1116.
URL http://www.ncbi.nlm.nih.gov/pubmed/22070264

Nepstad, D. C., Tohver, I. M., Ray, D., Moutinho, P., Cardinot, G., sep 2007. MOR-

TALITY OF LARGE TREES AND LIANAS FOLLOWING EXPERIMENTAL DROUGHT IN AN AMAZON FOREST. Ecology 88 (9), 2259–2269.
URL http://dx.doi.org/10.1890/06-1046.1

Nepstad, D. C., Uhl, C., Pereira, C. A., da Silva, J. M. C., 1996. A comparative study of tree establishment in abandoned pasture and mature forest of eastern Amazonia. Oikos 76 (1), 25–39.
URL http://www.jstor.org/stable/10.2307/3545745

Nepstad, D. C., Verssimo, A., Alencar, A., Nobre, C., Lima, E., Lefebvre, P., Schlesinger, P., Potter, C., Moutinho, P., Mendoza, E., 1999. Large-scale impoverishment of Amazonian forests by logging and fire. Nature 398 (6727), 505–508.

Newbold, T., Hudson, L. N., Hill, S. L. L., Contu, S., Lysenko, I., Senior, R. A., Börger, L., Bennett, D. J., Choimes, A., Collen, B., 2015. Global effects of land use on local terrestrial biodiversity. Nature 520 (7545), 45–50.

Newman, A., 2002. Tropical rainforest: our most valuable and endangered habitat with a blueprint for its survival into the third millennium. Checkmark Books.

Nightingale, J., Phinn, S., Held, A., 2004. Ecosystem process models at multiple scales for mapping tropical forest productivity.

Nightingale, J. M., Hill, M. J., Phinn, S. R., Davies, I. D., Held, A. A., jan 2008a. Use of 3-PG and 3-PGS to simulate forest growth dynamics of Australian tropical rainforests: II. An integrated system for modelling forest growth and scenario assessment within the wet tropics bioregion. Forest Ecology and Management 254 (2), 122–133.
URL http://www.sciencedirect.com/science/article/pii/S0378112707002642

Nightingale, J. M., Hill, M. J., Phinn, S. R., Davies, I. D., Held, A. A., Erskine, P. D., jan 2008b. Use of 3-PG and 3-PGS to simulate forest growth dynamics of Australian tropical rainforests. Forest Ecology and Management 254 (2), 107–121.
URL http://www.sciencedirect.com/science/article/pii/S0378112707002691

Niinemets, Ü., 2010. A review of light interception in plant stands from leaf to canopy in different plant functional types and in species with varying shade tolerance. Ecological Research 25 (4), 693–714.
URL http://dx.doi.org/10.1007/s11284-010-0712-4

Nogueira, E. M., Fearnside, P. M., Nelson, B. W., Barbosa, R. I., Keizer, E. W. H., nov 2008. Estimates of forest biomass in the Brazilian Amazon: New allometric equations and adjustments to biomass from wood-volume inventories. Forest Ecology

and Management 256 (11), 1853–1867.
URL http://linkinghub.elsevier.com/retrieve/pii/S0378112708005689

Nolte, C., Agrawal, A., Silvius, K. M., Soares-Filho, B. S., mar 2013. Governance regime and location influence avoided deforestation success of protected areas in the Brazilian Amazon. Proceedings of the National Academy of Sciences of the United States of America 110 (13), 4956–4961.
URL http://www.pubmedcentral.nih.gov/articlerender.fcgi?artid=3612687{\&}tool=pmcentrez{\&}rendertype=abstract

Norden, N., Angarita, H. A., Bongers, F., Martínez-Ramos, M., Granzow-de la Cerda, I., van Breugel, M., Lebrija-Trejos, E., Meave, J. A., Vandermeer, J., Williamson, G. B., Finegan, B., Mesquita, R., Chazdon, R. L., jun 2015. Successional dynamics in Neotropical forests are as uncertain as they are predictable. Proceedings of the National Academy of Sciences 112 (26), 8013–8018.
URL http://www.pnas.org/content/112/26/8013.abstract

Norden, N., Mesquita, R. C. G., Bentos, T. V., Chazdon, R. L., Williamson, G. B., jan 2011. Contrasting community compensatory trends in alternative successional pathways in central Amazonia. Oikos 120 (1), 143–151.
URL http://doi.wiley.com/10.1111/j.1600-0706.2010.18335.x

Nortcliff, S., 1998. Human Activity and the Tropical Rainforest: Are the Soils the Forgotten Component of the Ecosystem ? In: Maloney, B. (Ed.), Human Activities and the Tropical Rainforest SE - 3. Vol. 44 of The GeoJournal Library. Springer Netherlands, pp. 49–64.
URL http://dx.doi.org/10.1007/978-94-017-1800-4{_}3

Nossent, J., Elsen, P., Bauwens, W., dec 2011. Sobol' sensitivity analysis of a complex environmental model. Environmental Modelling & Software 26 (12), 1515–1525.
URL http://www.sciencedirect.com/science/article/pii/S1364815211001939

Oakley, J. E., O'Hagan, A., 2004. Probabilistic sensitivity analysis of complex models: a Bayesian approach. Journal of the Royal Statistical Society: Series B (Statistical Methodology) 66 (3), 751–769.

Ochieng, R. M., Visseren-Hamakers, I. J., Nketiah, K. S., 2013. Interaction between the FLEGT-VPA and REDD+ in Ghana: Recommendations for interaction management. Forest Policy and Economics 32, 32–39.

Olander, L. P., Scatena, F. N., Silver, W. L., 1998. Impacts of disturbance initiated by road construction in a subtropical cloud forest in the Luquillo Experimental Forest, Puerto Rico. Forest Ecology and Management 109 (1), 33–49.

Oliveira, L. J. C., Costa, M. H., Soares-Filho, B. S., Coe, M. T., jun 2013. Large-scale expansion of agriculture in Amazonia may be a no-win scenario. Environmental Research Letters 8 (2), 24021.
URL http://stacks.iop.org/1748-9326/8/i=2/a=024021?key=crossref.de67cdb5f2b692ad1ff7a051d3f2a414

Oliver, C. D., Larson, B. C., 1990. Forest stand dynamics. McGraw-Hill, Inc.

Olson, D. M., Dinerstein, E., Wikramanayake, E. D., Burgess, N. D., Powell, G. V. N., Underwood, E. C., D'amico, J. A., Itoua, I., Strand, H. E., Morrison, J. C., 2001. Terrestrial Ecoregions of the World: A New Map of Life on Earth A new global map of terrestrial ecoregions provides an innovative tool for conserving biodiversity. BioScience 51 (11), 933–938.

Olson, J. S., Watts, J. A., Allison, L. J., 1983. Carbon in live vegetation of major world ecosystems. Tech. rep., Oak Ridge National Lab, Tennesse.

Ometto, J. P., Bun, R., Jonas, M., Nahorski, Z., Gusti, M. I., 2014. Uncertainties in greenhouse gases inventoriesexpanding our perspective. Climatic Change 124 (3), 451–458.

Ordoñez, J. C., Van Bodegom, P. M., Witte, J. M., Wright, I. J., Reich, P. B., Aerts, R., 2009. A global study of relationships between leaf traits, climate and soil measures of nutrient fertility. Global Ecology and Biogeography 18 (2), 137–149.

Orihuela-Belmonte, D. E., de Jong, B. H. J., Mendoza-Vega, J., Van der Wal, J., Paz-Pellat, F., Soto-Pinto, L., Flamenco-Sandoval, a., may 2013. Carbon stocks and accumulation rates in tropical secondary forests at the scale of community, landscape and forest type. Agriculture, Ecosystems & Environment 171, 72–84.
URL http://linkinghub.elsevier.com/retrieve/pii/S016788091300087X

Overman, J. P. M., Witte, H. J. L., Saldarriaga, J. G., 1994. Evaluation of regression models for above-ground biomass determination in Amazon rainforest. Journal of tropical Ecology 10 (02), 207–218.

Pacala, S. W., Canham, C. D., Silander Jr, J. A., 1993. Forest models defined by field measurements: I. The design of a northeastern forest simulator. Canadian Journal of Forest Research 23 (10), 1980–1988.

Pacheco, P., aug 2009. Agrarian Reform in the Brazilian Amazon: Its Implications for Land Distribution and Deforestation. World Development 37 (8), 1337–1347.
URL http://linkinghub.elsevier.com/retrieve/pii/S0305750X09000497

Palm, C. A., Vosti, S. A., Sanchez, P. A., Ericksen, P. J., 2013. Slash-and-burn agriculture: the search for alternatives. Columbia University Press.

Pan, Y., Birdsey, R. A., Fang, J., Houghton, R., Kauppi, P. E., Kurz, W. A., Phillips,

O. L., Shvidenko, A., Lewis, S. L., Canadell, J. G., Ciais, P., Jackson, R. B., Pacala, S. W., McGuire, A. D., Piao, S., Rautiainen, A., Sitch, S., Hayes, D., aug 2011. A Large and Persistent Carbon Sink in the World's Forests. Science 333 (6045), 988–993. URL `http://www.sciencemag.org/content/333/6045/988.abstract`

Parolin, P., Wittmann, F., Ferreira, L. V., 2013. Fruit and seed dispersal in Amazonian floodplain treesa review. Ecotropica 19, 19–36.

Paul, K. I., Polglase, P. J., O'Connell, A. M., Carlyle, J. C., Smethurst, P. J., Khanna, P. K., 2002. Soil nitrogen availability predictor (SNAP): a simple model for predicting mineralisation of nitrogen in forest soils. Soil Research 40 (6), 1011–1026.

Peña-Claros, M., 2003. Changes in forest structure and species composition during secondary forest succession in the Bolivian Amazon1. Biotropica 35 (4), 450–461.

Peng, C., Liu, J., Dang, Q., Apps, M. J., Jiang, H., jul 2002. TRIPLEX: a generic hybrid model for predicting forest growth and carbon and nitrogen dynamics. Ecological Modelling 153 (12), 109–130.
URL `http://www.sciencedirect.com/science/article/pii/S0304380001005051`

Pereira, M. C., Setzer, A. W., 1993. Spectral characteristics of fire scars in Landsat-5 TM images of Amazonia. Remote Sensing 14 (11), 2061–2078.

Perz, S. G., Skole, D. L., 2003. Social determinants of secondary forests in the Brazilian Amazon. Social Science Research.
URL `http://www.sciencedirect.com/science/article/pii/S0049089X02000121`

Petropoulos, G., Wooster, M. J., Carlson, T. N., Kennedy, M. C., Scholze, M., 2009. A global Bayesian sensitivity analysis of the 1d SimSphere soilvegetationatmospheric transfer (SVAT) model using Gaussian model emulation. Ecological Modelling 220 (19), 2427–2440.

Phillips, O., Baker, T., Brienen, R., 2015. RAINFOR: Field Manual for Plot Establishment and Remeasurement.

Phillips, O., Miller, J. S., Hollowell, V. C., 2002a. Global patterns of plant diversity: Alwyn H. Gentry's forest transect data set. Vol. 89. Missouri Botanical Press Louis, MO.

Phillips, O. L., Aragão, L. E. O. C., Lewis, S. L., Fisher, J. B., Lloyd, J., López-González, G., Malhi, Y., Monteagudo, A., Peacock, J., Quesada, C. A., van der Heijden, G., Almeida, S., Amaral, I., Arroyo, L., Aymard, G., Baker, T. R., Bánki, O., Blanc, L., Bonal, D., Brando, P., Chave, J., de Oliveira, Á. C. A., Cardozo, N. D., Czimczik, C. I., Feldpausch, T. R., Freitas, M. A., Gloor, E., Higuchi, N., Jiménez, E., Lloyd,

G., Meir, P., Mendoza, C., Morel, A., Neill, D. A., Nepstad, D., Patiño, S., Peñuela, M. C., Prieto, A., Ramírez, F., Schwarz, M., Silva, J., Silveira, M., Thomas, A. S., ter Steege, H., Stropp, J., Vásquez, R., Zelazowski, P., Dávila, E. A., Andelman, S., Andrade, A., Chao, K.-J., Erwin, T., Di Fiore, A., C., E. H., Keeling, H., Killeen, T. J., Laurance, W. F., Cruz, A. P., Pitman, N. C. A., Vargas, P. N., Ramírez-Angulo, H., Rudas, A., Salamão, R., Silva, N., Terborgh, J., Torres-Lezama, A., mar 2009. Drought Sensitivity of the Amazon Rainforest. Science 323 (5919), 1344–1347.
URL http://science.sciencemag.org/content/323/5919/1344.abstract

Phillips, O. L., Hall, P., Gentry, A. H., Sawyer, S. A., Vásquez, R., mar 1994. Dynamics and species richness of tropical rain forests. Proceedings of the National Academy of Sciences 91 (7), 2805–2809.
URL http://www.pnas.org/content/91/7/2805.abstract

Phillips, O. L., Malhi, Y., Vinceti, B., Baker, T., Lewis, S. L., Higuchi, N., Laurance, W. F., Vargas, P. N., Martinez, R. V., Laurance, S., Ferreira, L. V., Stern, M., Brown, S., Grace, J., apr 2002b. Changes in growth of tropical forests: evaluating potential biases. Ecological Applications 12 (2), 576–587.
URL http://doi.wiley.com/10.1890/1051-0761(2002)012[0576:CIGOTF]2.0.CO;2

Phillips, O. L., Van der Heijden, G., Lewis, S. L., LópezGonzález, G., Aragão, L. E. O. C., Lloyd, J., Malhi, Y., Monteagudo, A., Almeida, S., Dávila, E. A., 2010. Droughtmortality relationships for tropical forests. New Phytologist 187 (3), 631–646.

Phillips, P. D., van Gardingen, P. R., 2001. The SYMFOR framework for modelling the effects of silviculture on the growth and yield of tropical forests. In: Proceedings of IUFRO 4.11 Conference on Forest Biometry, Modelling and Information Science, University of Greenwich. Citeseer, pp. 25–29.

Piedade, W., Junk, M., 2001. NPP Tropical Forest: Manaus, Brazil, 1963-1990.
URL http://dx.doi.org/10.3334/ORNLDAAC/579

Plourde, B. T., Boukili, V. K., Chazdon, R. L., 2015. Radial changes in wood specific gravity of tropical trees: interand intraspecific variation during secondary succession. Functional Ecology 29 (1), 111–120.

Poorter, H., Niklas, K. J., Reich, P. B., Oleksyn, J., Poot, P., Mommer, L., 2012. Biomass allocation to leaves, stems and roots: metaanalyses of interspecific variation and environmental control. New Phytologist 193 (1), 30–50.

Poorter, L., Bongers, F., Aide, T. M., Almeyda Zambrano, A. M., Balvanera, P., Becknell, J. M., Boukili, V., Brancalion, P. H. S., Broadbent, E. N., Chazdon, R. L., Craven, D., de Almeida-Cortez, J. S., Cabral, G. A. L., de Jong, B. H. J., Denslow, J. S., Dent, D. H., DeWalt, S. J., Dupuy, J. M., Durán, S. M., Espírito-Santo, M. M.,

Fandino, M. C., César, R. G., Hall, J. S., Hernandez-Stefanoni, J. L., Jakovac, C. C., Junqueira, A. B., Kennard, D., Letcher, S. G., Licona, J.-C., Lohbeck, M., Marín-Spiotta, E., Martínez-Ramos, M., Massoca, P., Meave, J. A., Mesquita, R., Mora, F., Muñoz, R., Muscarella, R., Nunes, Y. R. F., Ochoa-Gaona, S., de Oliveira, A. A., Orihuela-Belmonte, E., Peña-Claros, M., Pérez-García, E. A., Piotto, D., Powers, J. S., Rodríguez-Velázquez, J., Romero-Pérez, I. E., Ruíz, J., Saldarriaga, J. G., Sanchez-Azofeifa, A., Schwartz, N. B., Steininger, M. K., Swenson, N. G., Toledo, M., Uriarte, M., van Breugel, M., van der Wal, H., Veloso, M. D. M., Vester, H. F. M., Vicentini, A., Vieira, I. C. G., Bentos, T. V., Williamson, G. B., Rozendaal, D. M. A., feb 2016. Biomass resilience of Neotropical secondary forests. Nature advance on.
URL `http://dx.doi.org/10.1038/nature1651210.1038/nature16512http://www.nature.com/nature/journal/vaop/ncurrent/abs/nature16512.html{\#}supplementary-information`

Potapov, P., Turubanova, S., Hansen, M. C., 2011. Regional-scale boreal forest cover and change mapping using Landsat data composites for European Russia. Remote Sensing of Environment 115 (2), 548–561.

Potapov, P. V., Turubanova, S. A., Hansen, M. C., Adusei, B., Broich, M., Altstatt, A., Mane, L., Justice, C. O., 2012. Quantifying forest cover loss in Democratic Republic of the Congo, 20002010, with Landsat ETM+ data. Remote Sensing of Environment 122, 106–116.

Potithep, S., Yasuoka, Y., may 2011. Application of the 3-PG Model for Gross Primary Productivity Estimation in Deciduous Broadleaf Forests: A Study Area in Japan. Forests 2 (4), 590–609.
URL `http://www.mdpi.com/1999-4907/2/2/590/htm`

Potter, C., Brooks Genovese, V., Klooster, S., Bobo, M., Torregrosa, A., apr 2001. Biomass burning losses of carbon estimated from ecosystem modeling and satellite data analysis for the Brazilian Amazon region. Atmospheric Environment 35 (10), 1773–1781.
URL `http://www.sciencedirect.com/science/article/pii/S1352231000004593`

Powledge, F., 2006. The Millenium Assessment. BioScience 56, 880.
URL `http://www.bioone.org/doi/pdf/10.1641/0006-3568{\%}282006{\%}2956{\%}5B880{\%}3ATMA{\%}5D2.0.CO{\%}3B2http://www.bioone.org/doi/full/10.1641/0006-3568(2006)56{\%}5B880{\%}3ATMA{\%}5D2.0.CO{\%}3B2`

Prates-Clark, C. C., 2004. Remote sensing of tropical regenerating forests in the Brazilian Amazon.

Prates-Clark, C. C., Lucas, R. M., dos Santos, J. R., 2009. Implications of land-use history for forest regeneration in the Brazilian Amazon. Canadian Journal of Remote Sensing 35 (6), 534–553.
URL http://pubs.casi.ca/doi/abs/10.5589/m10-004

Prentice, I. C., Sykes, M. T., Cramer, W., 1993. A simulation model for the transient effects of climate change on forest landscapes. Ecological modelling 65 (1), 51–70.

Primack, R. B., Corlett, R., 2005. Tropical rain forests: an ecological and biogeographical comparison. Blackwell Oxford.

Pütz, S., Groeneveld, J., Alves, L. F., Metzger, J. P., Huth, A., jun 2011. Fragmentation drives tropical forest fragments to early successional states: A modelling study for Brazilian Atlantic forests. Ecological Modelling 222 (12), 1986–1997.
URL http://www.sciencedirect.com/science/article/pii/S030438001100175X

Pütz, S., Groeneveld, J., Henle, K., Knogge, C., Martensen, A. C., Metz, M., Metzger, J. P., Ribeiro, M. C., de Paula, M. D., Huth, A., 2014. Long-term carbon loss in fragmented Neotropical forests. Nature communications 5.

Puyravaud, J.-P., 2003. Standardizing the calculation of the annual rate of deforestation. Forest Ecology and Management 177 (1), 593–596.

Quéré, C. L., Moriarty, R., Andrew, R. M., Peters, G. P., Ciais, P., Friedlingstein, P., Jones, S. D., Sitch, S., Tans, P., Arneth, A., 2015. Global carbon budget 2014. Earth System Science Data 7 (1), 47–85.

Ramankutty, N., Gibbs, H. K., Achard, F., Defries, R., Foley, J. a., Houghton, R. a., jan 2007. Challenges to estimating carbon emissions from tropical deforestation. Global Change Biology 13 (1), 51–66.
URL http://doi.wiley.com/10.1111/j.1365-2486.2006.01272.x

Raupach, M. R., 2011. Pinning down the land carbon sink. Nature Climate Change 1, 148–149.

Ravindranath, N. H., 2007. Mitigation and adaptation synergy in forest sector. Mitigation and Adaptation Strategies for Global Change 12 (5), 843–853.

Reiche, J., Lucas, R., Mitchell, A. L., Verbesselt, J., Hoekman, D. H., Haarpaintner, J., Kellndorfer, J. M., Rosenqvist, A., Lehmann, E. A., Woodcock, C. E., 2016. Combining satellite data for better tropical forest monitoring. Nature Climate Change 6 (2), 120–122.

Réjou-Méchain, M., Muller-Landau, H. C., Detto, M., Thomas, S. C., Toan, T. L., Saatchi, S. S., Barreto-Silvia, J. S., Bourg, N. A., Bunyavejchewin, S., Butt, N., 2014.

Local spatial structure of forest biomass and its consequences for remote sensing of carbon stocks. Biogeosciences Discussions 11, 5711.

Richards, P. W., 1955. The secondary succession in the tropical rain forest. Sci. Prog. London 43, 45–57.

Ritchie, J., 1972. Model [or Predicting Evaporation [roma Row Crop with Incomplete Cover. Water resources research.

Roberts, D. a., 2002. Large area mapping of land-cover change in Rondônia using multitemporal spectral mixture analysis and decision tree classifiers. Journal of Geophysical Research 107 (D20), 8073.
URL `http://doi.wiley.com/10.1029/2001JD000374`

Roberts, J., Cabral, O. M. R., Aguiar, L. F. D., apr 1990. Stomatal and Boundary-Layer Conductances in an Amazonian terra Firme Rain Forest. Journal of Applied Ecology 27 (1), 336–353.
URL `http://www.jstor.org/stable/2403590`

Rodríguez, R., Espinosa, M., Real, P., Inzunza, J., 2002. Analysis of productivity of radiata pine plantations under different silvicultural regimes using the 3-PG process-based model. Australian Forestry 65 (3), 165–172.

Rodríguez-Suárez, J. A., Soto, B., Iglesias, M. L., Diaz-Fierros, F., 2010. Application of the 3PG forest growth model to a Eucalyptus globulus plantation in Northwest Spain. European Journal of Forest Research 129 (4), 573–583.
URL `http://dx.doi.org/10.1007/s10342-010-0355-6`

Rolim, S. G., Jesus, R. M., Nascimento, H. E. M., Do Couto, H. T. Z., Chambers, J. Q., 2005. Biomass change in an Atlantic tropical moist forest: the ENSO effect in permanent sample plots over a 22-year period. Oecologia 142 (2), 238–246.

Rosa, I. M. D., Purves, D., Souza Jr, C., Ewers, R. M., 2013. Predictive modelling of contagious deforestation in the Brazilian Amazon. PloS one 8 (10), e77231.

Rowland, L., Hill, T. C., Stahl, C., Siebicke, L., Burban, B., Zaragoza-Castells, J., Ponton, S., Bonal, D., Meir, P., Williams, M., 2014a. Evidence for strong seasonality in the carbon storage and carbon use efficiency of an Amazonian forest. Global Change Biology 20 (3), 979–991.
URL `http://dx.doi.org/10.1111/gcb.12375`

Rowland, L., Malhi, Y., Silva-Espejo, J. E., Farfán-Amézquita, F., Halladay, K., Doughty, C. E., Meir, P., Phillips, O. L., 2014b. The sensitivity of wood production to seasonal and interannual variations in climate in a lowland Amazonian rainforest. Oecologia 174 (1), 295–306.
URL `http://dx.doi.org/10.1007/s00442-013-2766-9`

Rozendaal, D., Chazdon, R. L., 2015. Demographic drivers of tree biomass change during secondary succession in northeastern Costa Rica. Ecological Applications 25 (2), 506–516.

Rubinstein, R. Y., Kroese, D. P., 2011. Simulation and the Monte Carlo method. Vol. 707. John Wiley & Sons.

Rudel, T. K., Defries, R., Asner, G. P., Laurance, W. F., 2009. Changing drivers of deforestation and new opportunities for conservation. Conservation Biology 23 (6), 1396–1405.

Rüger, N., Gutiérrez, A. G., Kissling, W. D., Armesto, J. J., Huth, A., 2007. Ecological impacts of different harvesting scenarios for temperate evergreen rain forest in southern Chilea simulation experiment. Forest Ecology and Management 252 (1), 52–66.

Rüger, N., Wirth, C., Wright, S. J., Condit, R., 2012. Functional traits explain light and size response of growth rates in tropical tree species. Ecology 93 (12), 2626–2636.

Ruiz, J., Fandiño, M. C., Chazdon, R. L., 2005. Vegetation Structure, Composition, and Species Richness Across a 56year Chronosequence of Dry Tropical Forest on Providencia Island, Colombia1. Biotropica 37 (4), 520–530.

Running, S. W., Coughlan, J. C., 1988. A general model of forest ecosystem processes for regional applications. I. Hydrologic balance, canopy gas exchange and primary production processes. Ecological modelling 42 (2), 125–154.

Running, S. W., Gower, S. T., 1991. FOREST-BGC, a general model of forest ecosystem processes for regional applications. II. Dynamic carbon allocation and nitrogen budgets. Tree physiology 9 (1-2), 147–160.

Ryan, M. G., mar 2011. Tree responses to drought. Tree Physiology 31 (3), 237–239.
URL `http://treephys.oxfordjournals.org/content/31/3/237.short`

Saatchi, S., Asefi-Najafabady, S., Malhi, Y., Aragão, L. E. O. C., Anderson, L. O., Myneni, R. B., Nemani, R., 2013a. Persistent effects of a severe drought on Amazonian forest canopy. Proceedings of the National Academy of Sciences 110 (2), 565–570.

Saatchi, S., Boyce, K., Fisher, J. B., Morrow, E., Worden, J. R., Asefi, S., Badgley, G., 2013b. Forest productivity and water stress in Amazonia: observations from GOSAT chlorophyll fluorescence. Proceedings of the Royal Society of London B: Biological Sciences.

Saatchi, S., Mascaro, J., Xu, L., Keller, M., Yang, Y., Duffy, P., Espírito-Santo, F., Baccini, A., Chambers, J., Schimel, D., may 2015. Seeing the forest beyond the trees. Global Ecology and Biogeography 24 (5), 606–610.
URL `http://dx.doi.org/10.1111/geb.12256`

Saatchi, S., Ulander, L., Williams, M., Quegan, S., LeToan, T., Shugart, H., Chave, J., dec 2012. Forest biomass and the science of inventory from space. Nature Clim. Change 2 (12), 826–827.
URL http://dx.doi.org/10.1038/nclimate1759

Saatchi, S. S., Harris, N. L., Brown, S., Lefsky, M., Mitchard, E. T. a., Salas, W., Zutta, B. R., Buermann, W., Lewis, S. L., Hagen, S., Petrova, S., White, L., Silman, M., Morel, A. C., jun 2011a. Benchmark map of forest carbon stocks in tropical regions across three continents. Proceedings of the National Academy of Sciences of the United States of America 108 (24), 890–904.
URL http://www.pubmedcentral.nih.gov/articlerender.fcgi?artid=3116381{\&}tool=pmcentrez{\&}rendertype=abstract

Saatchi, S. S., Houghton, R. a., Dos Santos Alvalá, R. C., Soares, J. V., Yu, Y., jan 2007. Distribution of aboveground live biomass in the Amazon basin. Global Change Biology 13 (4), 816–837.
URL http://doi.wiley.com/10.1111/j.1365-2486.2007.01323.x

Saatchi, S. S., Marlier, M., Chazdon, R. L., Clark, D. B., Russell, A. E., nov 2011b. Impact of spatial variability of tropical forest structure on radar estimation of aboveground biomass. Remote Sensing of Environment 115 (11), 2836–2849.
URL http://linkinghub.elsevier.com/retrieve/pii/S0034425711001313

Sahney, S., Benton, M. J., Falcon-Lang, H. J., dec 2010. Rainforest collapse triggered Carboniferous tetrapod diversification in Euramerica. Geology 38 (12), 1079–1082.
URL http://geology.gsapubs.org/content/38/12/1079.abstract

Saldarriaga, J. G., Luxmoore, R. J., 1991. Solar energy conversion efficiencies during succession of a tropical rain forest in Amazonia. Journal of Tropical Ecology 7 (02), 233–242.

Saldarriaga, J. G., West, D. C., Tharp, M. L., Uhl, C., 1988. Long-term chronosequence of forest succession in the upper Rio Negro of Colombia and Venezuela. The Journal of Ecology, 938–958.

Saleska, S. R., Wu, J., Guan, K., Araujo, A. C., Huete, A., Nobre, A. D., Restrepo-Coupe, N., 2016. Dry-season greening of Amazon forests. Nature 531 (7594), E4–E5.

Salomão, R. d. P., Lisboa, P. L. B., 1988. Análise ecológica da vegetação de uma floresta pluvial tropical de terra firme, Rondônia.

Saltelli, A., 2002. Making best use of model evaluations to compute sensitivity indices. Computer Physics Communications 145 (2), 280–297.

Saltelli, A., Annoni, P., 2010. How to avoid a perfunctory sensitivity analysis. Environmental Modelling & Software 25 (12), 1508–1517.

Saltelli, A., Tarantola, S., Campolongo, F., Ratto, M., 2004. Sensitivity analysis in practice: a guide to assessing scientific models. John Wiley & Sons.

Saltelli, A., Tarantola, S., Chan, K.-S., 1999. A quantitative model-independent method for global sensitivity analysis of model output. Technometrics 41 (1), 39–56.

Sands, P. J., Battaglia, M., Mummery, D., 2000. Application of process-based models to forest management: experience with PROMOD, a simple plantation productivity model. Tree Physiology 20 (5-6), 383–392.

Sands, P. J., Landsberg, J. J., jun 2002. Parameterisation of 3-PG for plantation grown Eucalyptus globulus. Forest Ecology and Management 163 (1-3), 273–292.
URL http://www.sciencedirect.com/science/article/pii/S0378112701005862

Sano, E. E., Ferreira, L. G., Asner, G. P., Steinke, E. T., 2007. Spatial and temporal probabilities of obtaining cloudfree Landsat images over the Brazilian tropical savanna. International Journal of Remote Sensing 28 (12), 2739–2752.

Sant'Anna, S. J. S., Yanasse, C. d. C. F., Kuplich, T. H., Dutra, L. V., Frery, A. C., dos Santos, P. P., 1995. Secondary forest age mapping in Amazonia using multi-temporal Landsat/TM imagery. In: Geoscience and Remote Sensing Symposium, 1995. IGARSS'95.'Quantitative Remote Sensing for Science and Applications', International. Vol. 1. IEEE, pp. 323–325.

Santiago, L. S., Wright, S. J., Harms, K. E., Yavitt, J. B., Korine, C., Garcia, M. N., Turner, B. L., 2012. Tropical tree seedling growth responses to nitrogen, phosphorus and potassium addition. Journal of Ecology 100 (2), 309–316.

Santos, J. R. d., Narvaes, I. S., Graça, P. M. L. A., Gonçalves, F. G., 2009. Polarimetric responses and scattering mechanisms of tropical forests in the Brazilian Amazon. In: Jedlovec (Ed.), Advances in Geoscience and Remote Sensing. InTech, Ch. 8, pp. 184 – 206.
URL http://www.intechopen.com/books/advances-in-geoscience-and-remote-sensir
polarimetric-responses-and-scattering-mechanisms-of-tropical-forests-in-the-

Sarker, M. L. R., Nichol, J., 2013. Forest biomass estimation from the fusion of C-band SAR and optical data using wavelet transform. In: SPIE Remote Sensing. International Society for Optics and Photonics, pp. 88870S–88870S.

Scariot, A., jan 1999. Forest fragmentation effects on palm diversity in central Amazonia. Journal of Ecology 87 (1), 66–76.
URL http://dx.doi.org/10.1046/j.1365-2745.1999.00332.x

Scatena, F. N., Walker, R. T., Homma, A. K. O., 1996. Cropping and fallowing sequences of small farms in the " terra firme " landscape of the Brazilian Amazon : a case study

from Santarem, Para. Ecological Economics 18, 29–40.
URL http://www.sciencedirect.com/science/article/pii/0921800995000550

Scheller, R. M., Mladenoff, D. J., 2004. A forest growth and biomass module for a landscape simulation model, LANDIS: design, validation, and application. Ecological Modelling 180 (1), 211–229.

Schippers, P., Sterck, F., Vlam, M., Zuidema, P. A., jul 2015. Tree growth variation in the tropical forest: understanding effects of temperature, rainfall and CO2. Global Change Biology 21 (7), 2749–2761.
URL http://dx.doi.org/10.1111/gcb.12877

Schroeder, P. E., Winjum, J. K., 1995. Assessing Brazil's carbon budget: II. Biotic fluxes and net carbon balance. Forest Ecology and Management 75 (1), 87–99.

Schuldt, B., Leuschner, C., Horna, V., Moser, G., Köhler, M., Van Straaten, O., Barus, H., 2011. Change in hydraulic properties and leaf traits in a tall rainforest tree species subjected to long-term throughfall exclusion in the perhumid tropics.

Scott, D. A., Proctor, J., Thompson, J., 1992. Ecological studies on a lowland evergreen rain forest on Maracá Island, Roraima, Brazil. II. Litter and nutrient cycling. Journal of Ecology, 705–717.

Selaya, N. G., Anten, N. P. R., Oomen, R. J., Matthies, M., Werger, M. J. A., jan 2007. Above-ground Biomass Investments and Light Interception of Tropical Forest Trees and Lianas Early in Succession. Annals of Botany 99 (1), 141–151.
URL http://aob.oxfordjournals.org/content/99/1/141.abstract

Serráo, E. A., 1995. Possibilities for sustainable agricultural development in the Brazilian Amazon: an EMBRAPA proposal.

Serrao, E. A. S., Falesi, I. C., da Veiga, J. B., Teixeira Neto, J. F., 1979. Productivity of cultivated pastures on low fertility soils in the Amazon of Brazil. Pasture production in acid soils of the tropics. Cali, Colombie, CIAT, 195–225.

Shimada, M., Itoh, T., Motooka, T., Watanabe, M., Shiraishi, T., Thapa, R., Lucas, R., 2014. New global forest/non-forest maps from ALOS PALSAR data (20072010). Remote Sensing of Environment 155, 13–31.

Shimada, M., Watanabe, M., Motooka, T., Shiraishi, T., Isoguchi, O., Mukaida, A., Okumura, H., Otaki, T., Itoh, T., 2011. Generation of 10m resolution PALSAR and JERS-1 SAR MOSAIC and forest/non-forest maps for forest carbon trackning. In: Synthetic Aperture Radar (APSAR), 2011 3rd International Asia-Pacific Conference on. IEEE, pp. 1–4.

Shugart, H. H., West, D. C., 1981. Long-Term Dynamics of Forest Ecosystems: Computer simulation models, which allow for numerous seedlings and the long lives of

large trees, predict how forests will respond to different management techniques. American Scientist 69 (6), 647–652.

Shuttleworth, W. J., 1988. Evaporation from Amazonian rainforest. Proceedings of the Royal Society of London B: Biological Sciences 233 (1272), 321–346.

Silva, J. M. C., Uhl, C., Murray, G., 1996. Plant succession, landscape management, and the ecology of frugivorous birds in abandoned Amazonian pastures. Conservation biology 10 (2), 491–503.

Silva, J. M. N., Carreiras, J. M. B., Rosa, I., Pereira, J. M. C., 2011. Greenhouse gas emissions from shifting cultivation in the tropics, including uncertainty and sensitivity analysis. Journal of Geophysical Research: Atmospheres (19842012) 116 (D20).

Silva, J. N. M., 1989. The behaviour of the tropical rain forest of the Brazilian Amazon after logging.

Silva, J. N. M., Lopes, J., Montagner, L. H., 1985. regeneracao natural de Vochysia maxima Ducke em floresta secundaria no Planalto do Tapajos, Belterra-PARA. Boletim de pesquisa Florestal.

Silver, W. L., Ostertag, R., Lugo, A. E., 2000a. The potential for carbon sequestration through reforestation of abandoned tropical agricultural and pasture lands. Restoration ecology 8 (4), 394–407.

Silver, W. L., Ostertag, R., Lugo, A. E., dec 2000b. The Potential for Carbon Sequestration Through Reforestation of Abandoned Tropical Agricultural and Pasture Lands. Restoration Ecology 8 (4), 394–407.
URL http://doi.wiley.com/10.1046/j.1526-100x.2000.80054.x

Simon, M. F., Garagorry, F. L., 2005. The expansion of agriculture in the Brazilian Amazon. Environmental Conservation 32 (03), 203–212.

Sirén, A. H., 2007. Population growth and land use intensification in a subsistence-based indigenous community in the Amazon. Human Ecology 35 (6), 669–680.

Sirois, M.-C., Margolis, H. A., Camiré, C., 1998. Influence of remnant trees on nutrients and fallow biomass in slash and burn agroecosystems in Guinea. Agroforestry Systems 40 (3), 227–246.
URL http://dx.doi.org/10.1023/A{\%}3A1006093329468

Slik, J. W. F., Arroyo-Rodríguez, V., Aiba, S.-I., Alvarez-Loayza, P., Alves, L. F., Ashton, P., Balvanera, P., Bastian, M. L., Bellingham, P. J., van den Berg, E., 2015. An estimate of the number of tropical tree species. Proceedings of the National Academy of Sciences 112 (24), 7472–7477.

Slot, M., Rey-Sánchez, C., Gerber, S., Lichstein, J. W., Winter, K., Kitajima, K., sep

2014. Thermal acclimation of leaf respiration of tropical trees and lianas: response to experimental canopy warming, and consequences for tropical forest carbon balance. Global Change Biology 20 (9), 2915–2926.
URL http://dx.doi.org/10.1111/gcb.12563

Smith, K., Gholz, H. L., de Assis Oliveira, F., 1998. Litterfall and nitrogen-use efficiency of plantations and primary forest in the eastern Brazilian Amazon. Forest Ecology and Management 109 (1), 209–220.

Sobol, I. M., 2001. Global sensitivity indices for nonlinear mathematical models and their Monte Carlo estimates. Mathematics and computers in simulation 55 (1), 271–280.

Sobol, I. M., Kucherenko, S., 2010. Derivative based global sensitivity measures. Procedia - Social and Behavioral Sciences 2 (6), 7745–7746.
URL http://www.sciencedirect.com/science/article/pii/S1877042810013492

Solberg, S., Riegler, G., Nonin, P., 2015. Estimating forest biomass from TerraSAR-X stripmap radargrammetry. Geoscience and Remote Sensing, IEEE Transactions on 53 (1), 154–161.

Sommer, R., Vlek, P. L. G., Fölster, H., 2000. Slash-and-mulch to reduce nutrient losses in shifting cultivation in the Eastern Amazon. Seminário sobre manejo da Vegetação Secundária para a Sustentabilidade da Agricultura Familiar. ANAIS, Belém, EMBRAPA Amazônia Oriental/CNPq. Pg, 80–82.

Song, X., Bryan, B. A., Paul, K. I., Zhao, G., 2012. Variance-based sensitivity analysis of a forest growth model. Ecological Modelling.
URL http://www.sciencedirect.com/science/article/pii/S0304380012004024

Spiegelhalter, D. J., Best, N. G., Carlin, B. P., Van Der Linde, A., 2002. Bayesian measures of model complexity and fit. Journal of the Royal Statistical Society: Series B (Statistical Methodology) 64 (4), 583–639.

Stackhouse, P. W., 2015. NASA Surface meteorology and Solar Energy: Daily Averaged Data.
URL https://eosweb.larc.nasa.gov/cgi-bin/sse/daily.cgi?email=skip@larc.nasa.gov

Stark, S. C., Enquist, B. J., Saleska, S. R., Leitold, V., Schietti, J., Longo, M., Alves, L. F., Camargo, P. B., Oliveira, R. C., 2015. Linking canopy leaf area and light environments with tree size distributions to explain Amazon forest demography. Ecology letters 18 (7), 636–645.

Steiner, C., Teixeira, W., Lehmann, J., Nehls, T., de Macêdo, J., Blum, W., Zech,

W., 2007. Long term effects of manure, charcoal and mineral fertilization on crop production and fertility on a highly weathered Central Amazonian upland soil. Plant and Soil 291 (1-2), 275–290.
URL http://dx.doi.org/10.1007/s11104-007-9193-9

Steininger, M. K., 2000. Satellite estimation of tropical secondary forest above-ground biomass : Data from Brazil and Bolivia. International Journal of Remote Sensing 21, 1139–1157.
URL http://www.tandfonline.com/doi/abs/10.1080/014311600210119

Stibig, H.-J., Achard, F., Carboni, S., Raši, R., Miettinen, J., 2014. Change in tropical forest cover of Southeast Asia from 1990 to 2010. Biogeosciences 11 (2), 247–258.

Stone, T. A., Schlesinger, P., Houghton, R. A., Woodwell, G. M., 1994. Map of the vegetation of South America based on satellite imagery. Photogrammetric Engineering and Remote Sensing 60 (5).

Sugiyama, A., Peterson, C. J., jan 2013. Edge Effects Act Differentially on Multiple Early Regeneration Stages of a Shade-tolerant Tree Tapirira mexicana. Biotropica 45 (1), 37–44.
URL http://dx.doi.org/10.1111/j.1744-7429.2012.00897.x

Surendran Nair, S., Kang, S., Zhang, X., Miguez, F. E., Izaurralde, R. C., Post, W. M., Dietze, M. C., Lynd, L. R., Wullschleger, S. D., 2012. Bioenergy crop models: descriptions, data requirements, and future challenges. GCB Bioenergy 4 (6), 620–633.

Szott, L. T., Palm, C. A., Buresh, R. J., 1999. Ecosystem fertility and fallow function in the humid and subhumid tropics. Agroforestry Systems 47 (1-3), 163–196.
URL http://dx.doi.org/10.1023/A{\%}3A1006215430432

Tabarelli, M., Peres, C. A., Melo, F. P., oct 2012. The few winners and many losers' paradigm revisited: Emerging prospects for tropical forest biodiversity. Biological Conservation 155, 136–140.
URL http://www.sciencedirect.com/science/article/pii/S0006320712002893

Team, R. C., 2015. R: A Language and Environment for Statistical Computing.
URL https://www.r-project.org

Tenenbein, A., 1972. A double sampling scheme for estimating from misclassified multinomial data with applications to sampling inspection. Technometrics 14 (1), 187–202.

Tian, H., Melillo, J. M., Kicklighter, D. W., McGuire, A. D., Helfrich, J. V. K., Moore, B., VoÈroÈsmarty, C. J., 1998. Effect of interannual climate variability on carbon storage in Amazonian ecosystems. Nature 396 (6712), 664–667.

Toledo, J. J., Magnusson, W. E., Castilho, C. V., 2013. Competition, exogenous disturbances and senescence shape tree size distribution in tropical forest: evidence from tree mode of death in Central Amazonia. Journal of Vegetation Science 24 (4), 651–663.

Toledo, M., Poorter, L., Peña-Claros, M., Alarcón, A., Balcázar, J., Leaño, C., Licona, J. C., Llanque, O., Vroomans, V., Zuidema, P., Bongers, F., jan 2011a. Climate is a stronger driver of tree and forest growth rates than soil and disturbance. Journal of Ecology 99 (1), 254–264.
URL http://doi.wiley.com/10.1111/j.1365-2745.2010.01741.x

Toledo, M., Poorter, L., Peña-Claros, M., Alarcón, A., Balcázar, J., Leaño, C., Licona, J. C., Llanque, O., Vroomans, V., Zuidema, P., Bongers, F., 2011b. Climate is a stronger driver of tree and forest growth rates than soil and disturbance. Journal of Ecology 99 (1), 254–264.
URL http://dx.doi.org/10.1111/j.1365-2745.2010.01741.x

Tomé, J., Tomé, M., Fontes, L., Soares, P., Pacheco, C., Araújo, C., 2004. Testing 3PG with irrigated and fertilized plots established in Eucalyptus globulus plantations in Portugal. In: Modeling Forest Production" Proc. Conf. Vienna. pp. 19–21.

Trancoso, R., Tomasella, J., Silva, R., Monteiro, M. T. F., Rodriguez, D. A., Cuartas, L. A., 2007. Hydrological impacts of deforestation in small catchments in Brazilian Amazonian. In: 21st Conference on Hydrology, Session J. Vol. 1.

Trumbore, S., Barbosa De Camargo, P., 2009. Soil Carbon Dynamics. In: Amazonia and Global Change. American Geophysical Union, pp. 451–462.
URL http://dx.doi.org/10.1029/2009GM000882

Turner, I. M., 2001. The Ecology of Trees in the Tropical Rain Forest. publisherName-Cambridge University Press.
URL http://dx.doi.org/10.1017/CBO9780511542206

Turner, M. G., Baker, W. L., Peterson, C. J., Peet, R. K., 1998. Factors influencing succession: lessons from large, infrequent natural disturbances. Ecosystems 1 (6), 511–523.

Uhl, C., 1987. Factors Controlling Succession Following Slash-and-Burn Agriculture in Amazonia. Journal of Ecology 75 (2), 377–407.
URL http://www.jstor.org/stable/10.2307/2260425

Uhl, C., Buschbacher, R., Serrao, E. A. S., 1988. Abandoned Pastures in Eastern Amazonia. I. Patterns of Plant Succession. The Journal of Ecology 76 (3), 663–681.
URL http://www.jstor.org/stable/10.2307/2260566

Uhl, C., Clark, H., Clark, K., Maquirino, P., 1982. Successional Patterns Associated

with Slash-and-Burn Agriculture in the Upper Rio Negro Region of the Amazon Basin. Biotropica 14 (4), 249–254.
URL http://agris.fao.org/agris-search/search/display.do?f=2012/OV/OV201201360001360.xml;US19840013199

Uhl, C., Clark, K., 1983. Seed Ecology of Selected Amazon Basin Successional Species. Botanical Gazette 144 (3), 419–425.
URL http://www.jstor.org/stable/10.2307/2474440

Uhl, C., Clark, K., Clark, H., Murphy, P., 1981. Early Plant Succession after Cutting and Burning in the Upper Rio Negro Region of the Amazon Basin. Journal of Ecology 69 (2), 631–649.
URL http://www.jstor.org/stable/10.2307/2259689

Uhl, C., Jordan, C. F., 1984. Succession and nutrient dynamics following forest cutting and burning in Amazonia. Ecology, 1476–1490.

Valladares, F., Niinemets, Ü., 2008. Shade tolerance, a key plant feature of complex nature and consequences. Annual Review of Ecology, Evolution, and Systematics, 237–257.

van Breugel, M., Ransijn, J., Craven, D., Bongers, F., Hall, J. S., oct 2011. Estimating carbon stock in secondary forests: Decisions and uncertainties associated with allometric biomass models. Forest Ecology and Management 262 (8), 1648–1657.
URL http://www.sciencedirect.com/science/article/pii/S0378112711004579

Van Daalen, J. C., Shugart, H. H., 1989. OUTENIQUAA computer model to simulate succession in the mixed evergreen forests of the Southern Cape, South Africa. Landscape Ecology 2 (4), 255–267.

van der Pijl, L., 1982. Ecological Developments in Leguminous Fruits. In: Principles of Dispersal in Higher Plants. Springer, pp. 150–159.

van der Sleen, P., Groenendijk, P., Vlam, M., Anten, N. P. R., Boom, A., Bongers, F., Pons, T. L., Terburg, G., Zuidema, P. A., jan 2015. No growth stimulation of tropical trees by 150 years of CO2 fertilization but water-use efficiency increased. Nature Geosci 8 (1), 24–28.
URL http://dx.doi.org/10.1038/ngeo231310.1038/ngeo2313http://www.nature.com/ngeo/journal/v8/n1/abs/ngeo2313.html{\#}supplementary-information

van Gardingen, P. R., Valle, D., Thompson, I., 2006. Evaluation of yield regulation options for primary forest in Tapajos National Forest, Brazil. Forest Ecology and Management 231, 184–195.

URL http://www.sciencedirect.com/science/article/pii/S0378112706003562

van Oijen, M., Reyer, C., Bohn, F., Cameron, D., Deckmyn, G., Flechsig, M., Härkönen, S., Hartig, F., Huth, A., Kiviste, A., Lasch, P., Mäkelä, A., Mette, T., Minunno, F., Rammer, W., feb 2013. Bayesian calibration, comparison and averaging of six forest models, using data from Scots pine stands across Europe. Forest Ecology and Management 289, 255–268.
URL http://www.sciencedirect.com/science/article/pii/S0378112712005944

van Schaik, C. P., Terborgh, J. W., Wright, S. J., 1993. The phenology of tropical forests: adaptive significance and consequences for primary consumers. Annual Review of Ecology and Systematics, 353–377.

Vanclay, J. K., 1994. Modelling forest growth and yield : applications to mixed tropical forests. School of Environmental Science and Engineering Papers.
URL http://epubs.scu.edu.au/cgi/viewcontent.cgi?article=1538{\&}context=esm{_}pubs

Vanclay, J. K., Sands, P. J., 2009. Calibrating the self-thinning frontier. Forest Ecology and Management 259 (1), 81–85.

Varela, R. A. D., Rego, P. R., Iglesias, S. C., Sobrino, C. M., 2008. Automatic habitat classification methods based on satellite images: A practical assessment in the NW Iberia coastal mountains. Environmental monitoring and assessment 144 (1-3), 229–250.

Varner, R. K., Keller, M., Cosme de Oliveira, R., Crill, P. M., Palace, M. W., Hunter, M. O., Silva, H. P., Dias, J., Neto, E., 2010. Temporal and spatial variability of greenhouse gas fluxes from soil in an undisturbed forest in the Brazilian Amazon. In: American Geophysical Union.

Verbeeck, H., Peylin, P., Bacour, C., Bonal, D., Steppe, K., Ciais, P., 2011. Seasonal patterns of CO2 fluxes in Amazon forests: fusion of eddy covariance data and the ORCHIDEE model. Journal of Geophysical Research: Biogeosciences 116 (G2).

Verbeeck, H., Samson, R., Verdonck, F., Lemeur, R., jun 2006. Parameter sensitivity and uncertainty of the forest carbon flux model FORUG: a Monte Carlo analysis. Tree Physiology 26 (6), 807–817.
URL http://treephys.oxfordjournals.org/content/26/6/807.abstract

Vieira, I., Uhl, C., Nepstad, D., 1994. The role of the shrub Cordia multispicata Cham. as a succession facilitator' in an abandoned pasture, Paragominas, Amazônia.

Vegetatio 115 (2), 91–99.
URL http://dx.doi.org/10.1007/BF00044863

Vieira, I. C. G., de Almeida, A. S., Davidson, E. A., Stone, T. A., de Carvalho, C. J. R., Guerrero, J. B., nov 2003. Classifying successional forests using Landsat spectral properties and ecological characteristics in eastern Amazônia. Remote Sensing of Environment 87 (4), 470–481.
URL http://linkinghub.elsevier.com/retrieve/pii/S0034425703002062

Vieira, S., de Camargo, P., Selhorst, D., da Silva, R., Hutyra, L., Chambers, J., Brown, I., Higuchi, N., dos Santos, J., Wofsy, S., Trumbore, S., Martinelli, L., 2004. Forest structure and carbon dynamics in Amazonian tropical rain forests. Oecologia 140 (3), 468–479.
URL http://dx.doi.org/10.1007/s00442-004-1598-z

Villela, D. M., Nascimento, M. T., Aragão, L. E. O. C., Da Gama, D. M., 2006. Effect of selective logging on forest structure and nutrient cycling in a seasonally dry Brazilian Atlantic forest. Journal of Biogeography 33 (3), 506–516.

Vlam, M., Baker, P. J., Bunyavejchewin, S., Zuidema, P. A., 2014. Temperature and rainfall strongly drive temporal growth variation in Asian tropical forest trees. Oecologia 174 (4), 1449–1461.

Vogelmann, J. E., Gallant, A. L., Shi, H., Zhu, Z., 2016. Perspectives on monitoring gradual change across the continuity of Landsat sensors using time-series data. Remote Sensing of Environment.

Vourlitis, G. L., Hayashi, M., de S Nogueira, J., Caseiro, F. T., Campelo, J. H., 2002. Seasonal variations in the evapotranspiration of a transitional tropical forest of Mato Grosso, Brazil. Water resources research 38 (6).

Vourlitis, G. L., Priante Filho, N., Hayashi, M. M. S., Nogueira, J. D. S., Caseiro, F. T., Holanda Campelo, J., 2001. Seasonal variations in the net ecosystem CO2 exchange of a mature Amazonian transitional tropical forest (cerradão). Functional Ecology 15 (3), 388–395.
URL http://dx.doi.org/10.1046/j.1365-2435.2001.00535.x

Vulinec, K., 2013. Acoustic analyses of bat activity in fragmented central Amazonian forest. In: New Frontiers in Tropical Biology: The Next 50 Years (A Joint Meeting of ATBC and OTS). Atbc, p. Online.

Walker, W. S., Stickler, C. M., 2010. Large-Area Classification and Mapping of Forest and Land Cover in the Brazilian Amazon: A Comparative Analysis of ALOS/PALSAR and Landsat Data Sources. IEEE Journal of Selected Topics in Applied Earth

Observation Remote Sensing 3 (4), 594–604.
URL http://ieeexplore.ieee.org/xpls/abs{_}all.jsp?arnumber=5623307

Walsh, T. A., Burk, T. E., 1993. Calibration of satellite classifications of land area. Remote Sensing of Environment 46 (3), 281–290.

Walters, F., 1999. Sequential simplex optimization - An update. Analytical Letters 32 (2), 193–212.

Wandelli, E. V., Fearnside, P. M., jul 2015. Secondary vegetation in central Amazonia: Land-use history effects on aboveground biomass. Forest Ecology and Management 347 (0), 140–148.
URL http://www.sciencedirect.com/science/article/pii/S0378112715001498

Wang, F., Mladenoff, D. J., Forrester, J. A., Keough, C., Parton, W. J., 2013a. Global sensitivity analysis of a modified CENTURY model for simulating impacts of harvesting fine woody biomass for bioenergy. Ecological Modelling 259, 16–23.

Wang, W., Ciais, P., Nemani, R. R., Canadell, J. G., Piao, S., Sitch, S., White, M. A., Hashimoto, H., Milesi, C., Myneni, R. B., aug 2013b. Variations in atmospheric CO2 growth rates coupled with tropical temperature. Proceedings of the National Academy of Sciences 110 (32), 13061–13066.
URL http://www.pnas.org/content/110/32/13061.abstract

Wang, Y., Davis, F. W., Melack, J. M., Kasischke, E. S., Christensen Jr, N. L., 1995. The effects of changes in forest biomass on radar backscatter from tree canopies. Remote Sensing 16 (3), 503–513.

Waring, R. H., 2000. A process model analysis of environmental limitations on the growth of Sitka spruce plantations in Great Britain. Forestry 73 (1), 65–79.

Watt, A. D., Stork, N. E., Eggleton, P., Srivastava, D., Bolton, B., Larsen, T. B., Brendell, M. J. D., Bignell, D. E., 1997. Impact of forest loss and regeneration on insect abundance and diversity. Forests and insects, 273–286.

Way, D. A., Oren, R., 2010. Differential responses to changes in growth temperature between trees from different functional groups and biomes: a review and synthesis of data. Tree physiology 30 (6), 669–688.

Wensel, L. C., Meerschaert, W. J., Biging, G. S., 1987. Tree height and diameter growth models for northern California conifers. Agriculture and Natural Resources Publ., University of Calif.

Wertz-Kanounnikoff, S., Verchot, L. V., Kanninen, M., Murdiyarso, D., 2008. How can we monitor, report and verify carbon emissions from forests? In: Angelsen,

A. (Ed.), Moving Ahead with REDD: Issues, Options and Implications. Center for International Forestry Research (CIFOR), Bogor, Indonesia, pp. 88 – 98.

West, T. A. P., Vidal, E., Putz, F. E., feb 2014. Forest biomass recovery after conventional and reduced-impact logging in Amazonian Brazil. Forest Ecology and Management 314, 59–63.
URL http://www.sciencedirect.com/science/article/pii/S0378112713007779

White, D. A., Beadle, C. L., Sands, P. J., Worledge, D., Honeysett, J. L., 1999. Quantifying the effect of cumulative water stress on stomatal conductance of Eucalyptus globulus and Eucalyptus nitens: a phenomenological approach. Functional Plant Biology 26 (1), 17–27.

White, J. D., Coops, N. C., Scott, N. A., jul 2000. Estimates of New Zealand forest and scrub biomass from the 3-PG model. Ecological Modelling 131 (2-3), 175–190.
URL http://www.sciencedirect.com/science/article/pii/S0304380000002519

White, J. D., Scott, N. a., Hirsch, A. I., Running, S. W., feb 2006. 3-PG Productivity Modeling of Regenerating Amazon Forests: Climate Sensitivity and Comparison with MODIS-Derived NPP. Earth Interactions 10 (8), 1–26.
URL http://journals.ametsoc.org/doi/abs/10.1175/EI137.1

Whitmore, 1990. Tropical Rain Forest. Claredon Press, Oxford.

Wijdeven, S. M. J., Kuzee, M. E., dec 2000. Seed Availability as a Limiting Factor in Forest Recovery Processes in Costa Rica. Restoration Ecology 8 (4), 414–424.
URL http://dx.doi.org/10.1046/j.1526-100x.2000.80056.x

Williams, J. W., Jackson, S. T., Kutzbach, J. E., apr 2007. Projected distributions of novel and disappearing climates by 2100 AD. Proceedings of the National Academy of Sciences 104 (14), 5738–5742.
URL http://www.pnas.org/content/104/14/5738.abstract

Williamson, G. B., Bentos, T. V., Longworth, J. B., Mesquita, R. C. G., apr 2014. Convergence and divergence in alternative successional pathways in Central Amazonia. Plant Ecology & Diversity 7 (1-2), 341–348.
URL http://dx.doi.org/10.1080/17550874.2012.735714

Williamson, G. B., Laurance, W. F., Oliveira, A. A., Delamônica, P., Gascon, C., Lovejoy, T. E., Pohl, L., 2000. Amazonian Tree Mortality during the 1997 El Niño Drought. Conservation Biology 14 (5), 1538–1542.
URL http://dx.doi.org/10.1046/j.1523-1739.2000.99298.x

Wirth, R., Weber, B., Ryel, R. J., sep 2001. Spatial and temporal variability of canopy

structure in a tropical moist forest. Acta Oecologica 22 (56), 235–244.
URL http://www.sciencedirect.com/science/article/pii/S1146609X01011237

Wolf, S., Eugster, W., Majorek, S., Buchmann, N., 2011. Afforestation of tropical pasture only marginally affects ecosystem-scale evapotranspiration. Ecosystems 14 (8), 1264–1275.

Woodhouse, I. H., Mitchard, E. T. a., Brolly, M., Maniatis, D., Ryan, C. M., jul 2012. Radar backscatter is not a 'direct measure' of forest biomass. Nature Climate Change 2 (8), 556–557.
URL http://www.nature.com/doifinder/10.1038/nclimate1601

Woodward, S., 2008. Tropical Broadleaf Evergreen Forest: The Rainforest.
URL http://www.radford.edu/{~}swoodwar/CLASSES/GEOG235/biomes/rainforest/rainfrst.html

Wright, S. J., Yavitt, J. B., Wurzburger, N., Turner, B. L., Tanner, E. V. J., Sayer, E. J., Santiago, L. S., Kaspari, M., Hedin, L. O., Harms, K. E., Garcia, M. N., Corre, M. D., mar 2011. Potassium, phosphorus, or nitrogen limit root allocation, tree growth, or litter production in a lowland tropical forest. Ecology 92 (8), 1616–1625.
URL http://dx.doi.org/10.1890/10-1558.1

Wu, Q.-L., Cournède, P.-H., Mathieu, A., 2012. An efficient computational method for global sensitivity analysis and its application to tree growth modelling. Reliability Engineering & System Safety 107, 35–43.

Xian, G., Homer, C., Fry, J., 2009. Updating the 2001 National Land Cover Database land cover classification to 2006 by using Landsat imagery change detection methods. Remote Sensing of Environment 113 (6), 1133–1147.

Xiao, X., Zhang, Q., Saleska, S., Hutyra, L., De Camargo, P., Wofsy, S., Frolking, S., Boles, S., Keller, M., Moore, B., 2005. Satellite-based modeling of gross primary production in a seasonally moist tropical evergreen forest. Remote Sensing of Environment 94 (1), 105–122.

Yaussy, D. A., feb 2000. Comparison of an empirical forest growth and yield simulator and a forest gap simulator using actual 30-year growth from two even-aged forests in Kentucky. Forest Ecology and Management 126 (3), 385–398.
URL http://www.sciencedirect.com/science/article/pii/S0378112799001115

Zanne, A. E., Lopez-Gonzalez, G., Coomes, D. A., Ilic, J., Jansen, S., Lewis, S. L., Miller, R. B., Swenson, N. G., Wiemann, M. C., Chave, J., 2009. Global wood density database. Dryad. Identifier: http://hdl. handle. net/10255/dryad 235.

Zar, J. H., 1999. Biostatistical analysis. Pearson Education India.

Zarco-Tejada, P. J., Ustin, S. L., 2001. Modeling canopy water content for carbon estimates from MODIS data at Land EOS validation sites. In: Geoscience and Remote Sensing Symposium, 2001. IGARSS'01. IEEE 2001 International. Vol. 1. IEEE, pp. 342–344.

Zarin, D. J., Davidson, E. A., Brondizio, E., Vieira, I. C. G., Moran, E. F., Delamonica, P., Ducey, M. J., Hurtt, G. C., Salimon, C., Denich, M., 2005. Legacy of fire slows carbon accumulation in Amazonian forest regrowth. Frontiers in Ecology and the Environment 3 (7), 365–369.
URL http://www.esajournals.org/doi/abs/10.1890/1540-9295(2005)003{\%}5B0365:LOFSCA{\%}5D2.0.CO{\%}3B2

Zarin, D. J., Ducey, M. J., Tucker, J. M., Salas, W. A., 2001. Potential biomass accumulation in Amazonian regrowth forests. Ecosystems 4 (7), 658–668.

Zeng, N., Yoon, J.-H., Marengo, J. A., Subramaniam, A., Nobre, C. A., Mariotti, A., Neelin, J. D., 2008. Causes and impacts of the 2005 Amazon drought. Environmental Research Letters 3 (1), 14002.

ZermeñoHernández, I., MéndezToribio, M., Siebe, C., BenítezMalvido, J., MartínezRamos, M., 2015. Ecological disturbance regimes caused by agricultural land uses and their effects on tropical forest regeneration. Applied Vegetation Science 18 (3), 443–455.

Zhao, M., Running, S. W., aug 2010. Drought-Induced Reduction in Global Terrestrial Net Primary Production from 2000 Through 2009. Science 329 (5994), 940–943.
URL http://science.sciencemag.org/content/329/5994/940.abstract

Zhao, M., Xiang, W., Peng, C., Tian, D., 2009. Simulating age-related changes in carbon storage and allocation in a Chinese fir plantation growing in southern China using the 3-PG model. Forest Ecology and Management 257 (6), 1520–1531.

Zhu, Z., Piao, S., Myneni, R. B., Huang, M., Zeng, Z., Canadell, J. G., Ciais, P., Sitch, S., Friedlingstein, P., Arneth, A., Cao, C., Cheng, L., Kato, E., Koven, C., Li, Y., Lian, X., Liu, Y., Liu, R., Mao, J., Pan, Y., Peng, S., Penuelas, J., Poulter, B., Pugh, T. A. M., Stocker, B. D., Viovy, N., Wang, X., Wang, Y., Xiao, Z., Yang, H., Zaehle, S., Zeng, N., apr 2016. Greening of the Earth and its drivers. Nature Clim. Change advance on.
URL http://dx.doi.org/10.1038/nclimate3004http://10.1038/nclimate3004http://www.nature.com/nclimate/journal/vaop/ncurrent/abs/nclimate3004.html{\#}supplementary-information

Appendix A

Appendix

A.1 Deforestation and regrowth rates

Table A.1: Deforestation and regrowth rates between consecutive dates in the Manaus time-series (MF - mature forest; SF - secondary forest).

Transitions (year)	MF annual rate of deforestation		SF annual rate of deforestation		Annual rate of deforestation		Annual rate of regrowth	
	(% yr^{-1})	(% yr^{-1})	(% yr^{-1})	(% yr^{-1})	(% yr^{-1})	(% yr^{-1})	(% yr^{-1})	(% yr^{-1})
[1973-1977]	0.14	691	0.00	0	0.14	691	0.00	0
[1977-1978]	0.51	2,517	0.00	0	0.51	2,517	7.91	230
[1978-1979]	0.67	3,267	0.00	0	0.67	3,267	0.00	0
[1979-1983]	0.35	1,700	0.00	0	0.35	1,700	0.00	0
[1983-1985]	2.87	13,451	0.95	2	2.87	13,453	55.41	8,974
[1985-1988]	0.87	3,911	8.40	1,349	1.13	5,260	28.70	6,142
[1988-1989]	2.30	10,063	27.69	7,873	3.84	17,936	61.09	12,584
[1989-1991]	0.45	1,956	5.58	1,968	0.84	3,924	29.06	6,455
[1991-1992]	0.70	2,976	17.30	7,345	2.19	10,321	44.38	8,674
[1992-1994]	0.28	1,187	6.38	2,850	0.86	4,037	17.45	3,627
[1994-1995]	0.23	986	9.76	4,568	1.18	5,554	55.48	10,579
[1995-1996]	0.07	277	3.06	1,662	0.41	1,940	109.50	13,037
[1996-1999]	0.31	1,291	4.99	3,083	0.91	4,374	19.60	1,431
[1999-2001]	0.30	1,239	4.41	2,601	0.81	3,839	20.76	3,085
[2001-2002]	1.51	6,228	13.20	7,733	2.96	13,961	46.29	8,338
[2002-2003]	2.74	11,092	7.37	4,482	3.35	15,574	133.89	24,738
[2003-2006]	0.51	2,036	5.09	3,938	1.26	5,974	26.79	3,490
[2006-2007]	0.29	1,128	4.94	3,955	1.08	5,083	20.07	4,230
[2007-2008]	0.13	509	3.07	2,488	0.63	2,996	25.63	5,356
[2008-2009]	0.38	1,482	10.45	8,453	2.11	9,935	10.64	2,233
[2009-2010]	0.09	360	3.16	2,453	0.60	2,813	23.95	6,134
[2010-2011]	0.09	364	5.33	4,287	0.99	4,651	12.67	3,035
Minimum	0.07	277	0.00	0	0.14	691	0.00	0
Minimum	0.07	277	0.00	0	0.14	691	0.00	0
Maximum	2.87	13,451	27.69	8,453	3.84	17,936	133.89	24,738
Mean	0.72	3,123	6.42	3,231	1.35	6,355	34.06	6,017
Standard deviation	0.85	3,726	6.51	2,699	1.05	4,905	33.71	5,756

Table A.2: Deforestation and regrowth rates between consecutive dates in the Santarém time-series (MF - mature forest; SF - secondary forest).

Transitions (year)	MF annual rate of deforestation		SF annual rate of deforestation		Annual rate of deforestation		Annual rate of regrowth	
	(% yr^{-1})	(% yr^{-1})	(% yr^{-1})	(% yr^{-1})	(% yr^{-1})	(% yr^{-1})	(% yr^{-1})	(% yr^{-1})
[1984-1985]	1.51	1,467	28.89	2,883	4.05	4,350	83.91	1,708
[1985-1986]	2.17	2,075	30.14	2,683	4.55	4,759	79.01	3,190
[1986-1987]	1.79	1,674	3.63	386	1.98	2,060	182.93	6,332
[1987-1988]	3.25	2,964	82.27	9,401	11.97	12,366	40.92	897
[1988-1989]	0.47	420	6.65	531	0.97	952	136.41	10,350
[1989-1990]	0.89	796	17.19	2,856	3.46	3,651	126.01	3,330
[1990-1991]	0.94	826	20.27	3,404	4.03	4,230	116.16	3,362
[1991-1993]	4.55	3,817	7.39	1,272	5.03	5,089	60.71	2,200
[1993-1995]	0.89	710	10.83	1,983	2.75	2,694	79.46	4,808
[1995-1996]	1.41	1,100	23.63	5,475	6.48	6,575	32.88	2,070
[1996-1997]	1.52	1,175	6.15	1,349	2.55	2,524	84.85	7,016
[1997-1998]	15.60	11,046	23.42	5,906	17.65	16,952	261.50	7,063
[1998-1999]	2.50	1,617	48.71	11,352	14.70	12,969	113.26	11,726
[1999-2000]	2.04	1,286	11.00	3,104	4.80	4,390	102.31	12,257
[2000-2001]	0.38	235	6.04	2,285	2.51	2,520	63.61	4,920
[2001-2003]	0.86	531	9.82	3,710	4.26	4,241	11.06	832
[2003-2005]	2.17	1,301	10.64	3,434	5.13	4,735	20.01	2,760
[2005-2006]	0.79	459	3.18	1,079	1.67	1,538	18.75	3,238
[2006-2007]	0.85	493	1.32	482	1.03	975	45.88	6,385
[2007-2008]	0.87	499	12.59	5,036	5.68	5,535	10.52	1,183
[2008-2009]	0.45	254	0.50	194	0.47	448	27.37	3,861
[2009-2010]	0.71	404	3.25	1,354	1.79	1,758	30.34	3,359
Minimum	0.38	235	0.50	194	0.47	448	10.52	832
Maximum	15.60	11,046	82.27	11,352	17.65	16,952	261.50	12,257
Mean	2.12	1,598	16.71	3,189	4.89	4,787	78.54	4,675
Standard deviation	3.18	2,292	18.74	2,849	4.42	4,188	61.51	3,332

Table A.3: Deforestation and regrowth rates between consecutive dates in the Machadinho d'Oeste time-series (MF - mature forest; SF - secondary forest).

Transitions (year)	MF annual rate of deforestation		SF annual rate of deforestation		Annual rate of deforestation		Annual rate of regrowth	
	(% yr^{-1})	(% yr^{-1})	(% yr^{-1})	(% yr^{-1})	(% yr^{-1})	(% yr^{-1})	(% yr^{-1})	(% yr^{-1})
[1984-1986]	4.12	6,893	0.00	0	4.12	6,893	9.49	103
[1986-1987]	1.49	2,369	8.63	17	1.50	2,386	67.68	7,320
[1987-1989]	1.83	2,844	20.16	1,246	2.53	4,090	29.61	2,448
[1989-1990]	2.83	4,251	10.33	973	3.27	5,224	84.18	8,881
[1990-1991]	3.65	5,311	88.05	10,434	9.97	15,744	16.77	1,501
[1991-1994]	3.00	4,092	8.06	636	3.27	4,729	21.47	4,409
[1994-1995]	7.33	9,223	33.42	5,741	10.46	14,964	25.38	5,886
[1995-1996]	5.20	6,139	9.48	1,841	5.80	7,979	62.72	17,389
[1996-1997]	5.73	6,407	30.75	9,505	11.14	15,912	22.28	5,245
[1997-1998]	3.30	3,528	10.58	3,177	4.90	6,706	29.70	9,302
[1998-1999]	6.34	6,463	24.17	8,110	10.75	14,573	31.25	9,466
[1999-2001]	3.71	3,529	16.04	5,369	6.91	8,898	11.84	4,282
[2001-2003]	5.41	4,699	2.48	895	4.55	5,594	15.95	7,458
[2003-2005]	5.82	4,517	17.43	7,370	9.90	11,887	12.40	5,345
[2005-2006]	9.95	6,933	21.32	8,836	14.19	15,768	25.69	14,039
[2006-2007]	2.13	1,394	20.97	9,693	9.91	11,087	10.87	6,050
[2007-2008]	2.32	1,491	43.26	16,711	17.66	18,202	3.68	2,309
[2008-2009]	1.75	1,101	4.98	1,612	2.85	2,713	11.04	8,335
[2009-2010]	1.21	748	7.18	2,766	3.50	3,514	14.58	10,011
[2010-2011]	1.48	904	12.55	5,560	6.13	6,464	9.80	6,293
Minimum	1.21	748	0.00	17	1.50	2,386	3.68	103
Maximum	9.95	9,223	88.05	16,711	17.66	18,202	84.18	17,389
Mean	3.93	4,142	19.49	5,289	7.17	9,286	25.82	6,804
Standard deviation	2.31	2,394	19.50	4,467	4.36	5,248	21.46	4,141

A.2 Separating stand properties by land use history

Figure A.1 a demonstrates illustrates the lack of separability in the avDBH, BA, stem density or AGB between the forests with a FC of 1 and $\geq$2 over 37 years of regrowth. Seperability was not improved when the forests were seperated by PALU ($\leq$2 and $\geq$3 years) (Figure A.2).

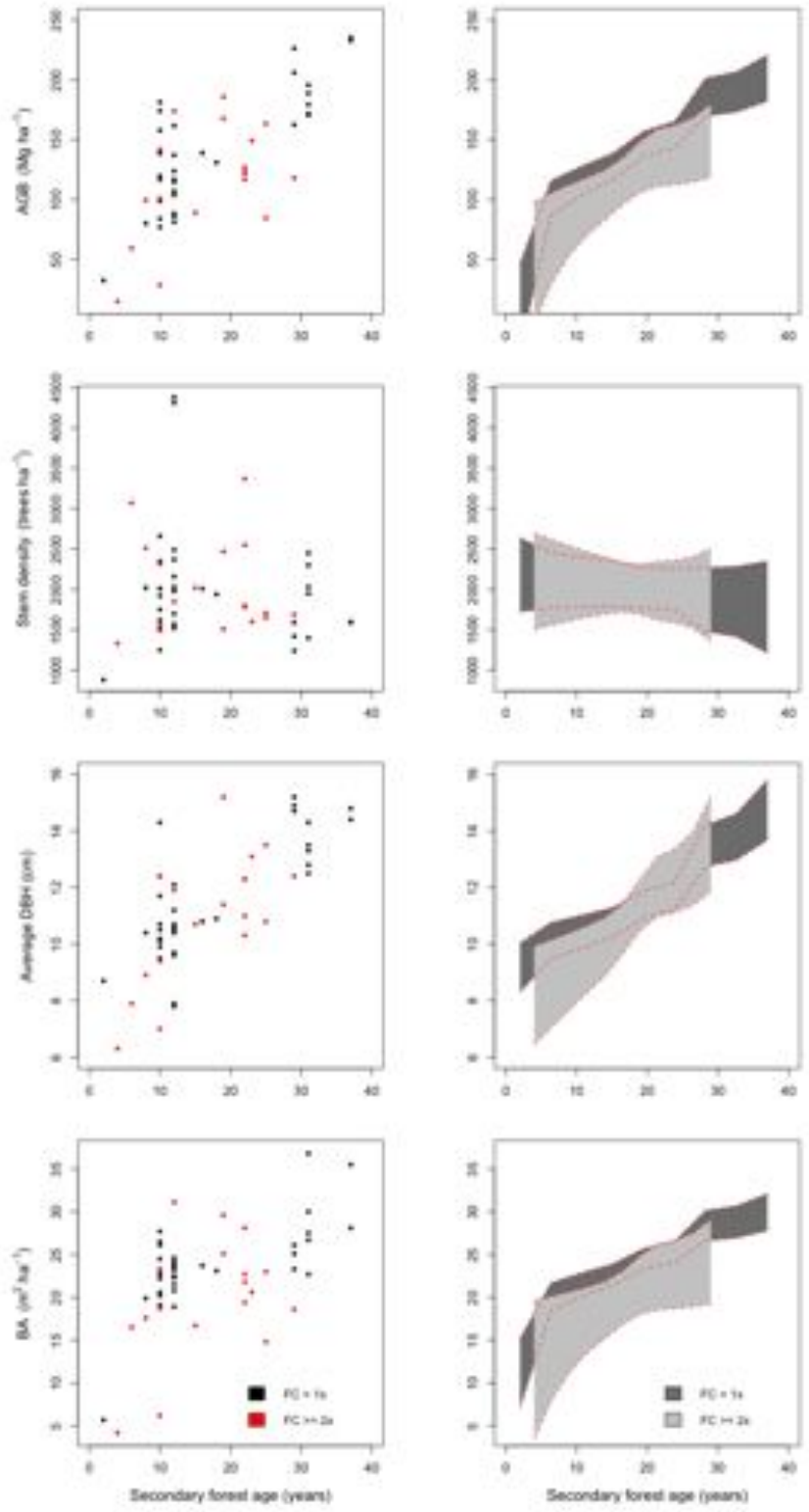

Figure A.1: Comparison of field plots seperated by frequency of clearance (FC). The graphs on the left show each plot. The graphs on the right show the 95% confidence intervals.

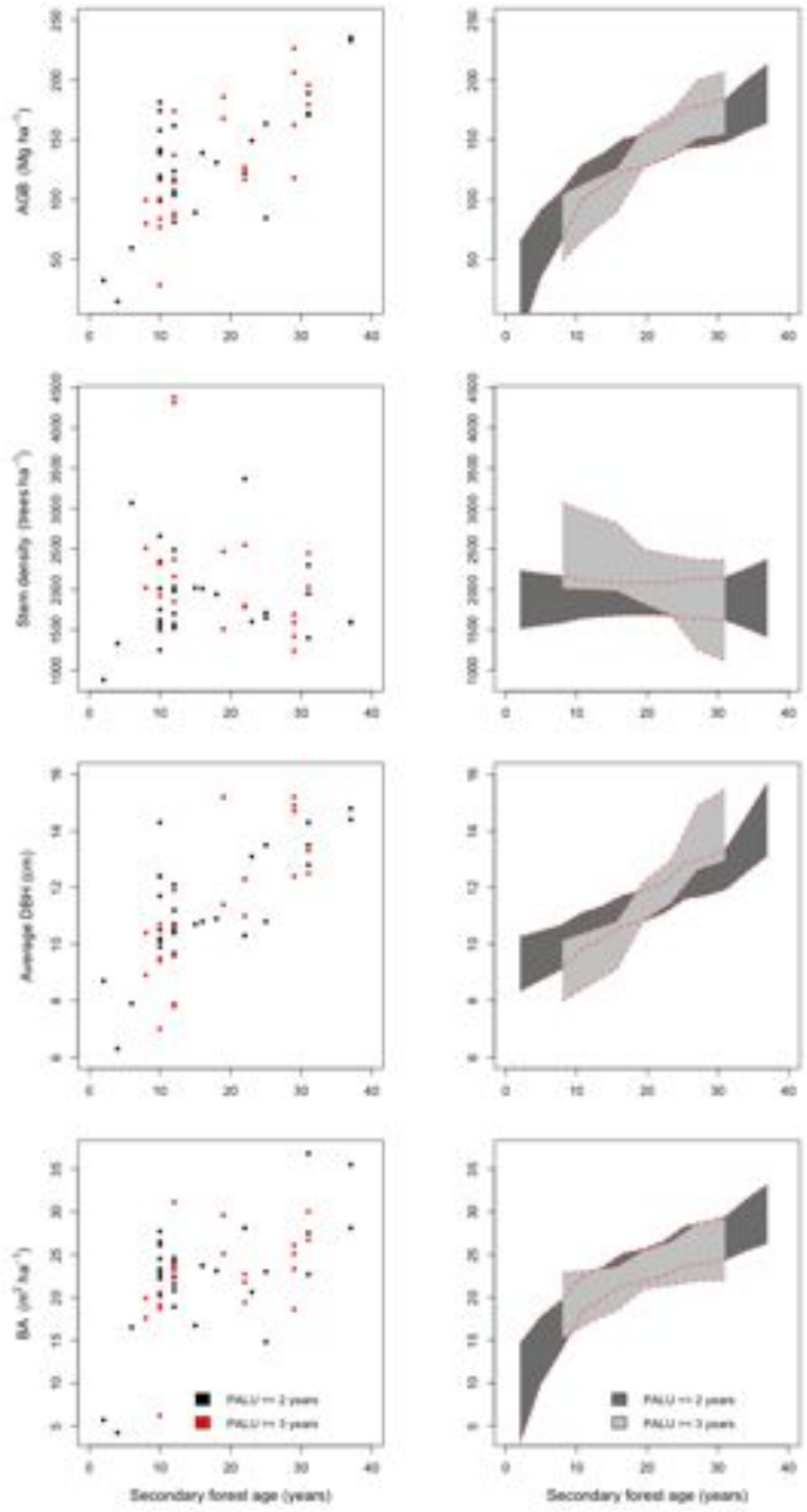

Figure A.2: Comparison of field plots seperated by period of active land use (PALU). The graphs on the left show each plot. The graphs on the right show the 95% confidence intervals.

A.3 Forest growth models

Table A.4: Forest growth models which have been implemented globally to study biomass and/or structural changes.

Model name	Carbon sequestration	Climate change	Distance dependent	Distance independent	Empirical	Gap model	Succession model	Mixed-species	Process based	Single species	Stand level	Tree-based	Source
3-PG (Physiological Processes Predicting Growth)								•	•	•			Landsberg and Waring (1997)
FORMIND						•		•				•	Köhler and Huth (1998)
JABOWA						•							Botkin et al. (1972)
OUTENIQUA						•		•	•			•	Van Daalen and Shugart (1989)
SYMFOR			•		•		•						Phillips and van Gardingen (2001)
TROLL			•					•	•				Chave (1999)
4C FORESEE (Forest Ecosystems in a Changing Environment)						•							Lasch et al. (2005)
BOJRES				•	•		•					•	Carpentier and de la recherche Forestière (1996)
CABALA (CArbon BALAnce)									•				Battaglia et al. (2004)
CACTOS (CAlifornia Conifer Timber Output Simulator)				•	•							•	Wensel et al. (1987)
CAFOGRAM					•		•	•					Alder (1996)
CO2FIX	•				•						•		Mohren et al. (1999)
DFSIM (Douglas-fir Simulator)											•		Curtis et al. (1981)
FINNFOR		•	•				•						Kellomäki and Väisänen (1997)
FIRE-BGC (FIRE BioGeoChemical process model)						•			•				Keane et al. (1996)
FIRESUM						•							Keane et al. (1990)
FORECAST		•							•		•		Kimmins et al. (1999)
Forest-BGC (Forest-BioGeoChemical process model)									•				Running and Gower (1991)
FORET (Forests of Eastern Tennessee)						•							Shugart and West (1981)
ForGro Forest Growth Model									•		•		Mohren et al. (1993)
FORSKA		•				•							Prentice et al. (1993)
MOSAIC			•				•	•	•				Frelich et al. (1993)
SILVA						•			•			•	Kercher and Axelrod (1984)
SORTIE				•						•	•		Pacala et al. (1993)
TASS (Tree and Stand Simulator) and TADAM			•								•	•	García (2005)

A.4 Description of 3-PG$_2$ model

3-PG$_2$ is a process based model (PBM) that involves a series of casual loops which link a series of sub models, to provide a number of monthly outputs (Table A.5).

Table A.5: Monthly outputs provided by 3-PG$_2$

Output Name	Description	Unit
StemNo	Stand stocking	trees ha^{-1}
avDBH	Mean diameter at breast height	cm
BasArea	Basal area	m^2 ha^{-1}
StandVol	Stand volume	m^3 ha^{-1}
MAI	Mean annual increment	cm yr^{-1}
LAI	Leaf area index	m^2 m^{-2}
WF	Foliage biomass	Mg ha^{-1}
WS	Stem biomass	Mg ha^{-1}
WR	Root biomass	Mg ha^{-1}
fracBB	Branch and bark fraction	-

At the core of 3-PG$_2$ is a carbon balance model. Radiation is intercepted by the canopy and converted into sugars in photosynthesis. This is the gross primary productivity (GPP). A proportion of the carbon is lost to respiration and is expelled as CO_2. The remainder of these products, the net primary productivity (NPP), are then allocated to foliage, stem and roots. Further carbon is lost through litterfall and root turnover. This is represented by the green shapes in Figure A.3.

The next step of the model to consider is assimilation and allocation (pink boxes Figure A.3). These are based on simple, well established principles and robust observations (Landsberg et al., 2003). Intercepted solar radiation (Q_{int}) varies as a function of LAI via Beers law (Equation A.1). Production in trees is primarily driven by the absorption of and utilisation of incident radiation. Photosynthetically active radiation (PAR) is estimated from short wave radiation (MJm^{-2}d^{-1}) assuming that 50% is photosynthetically active. This assumption is used in Beer's law to determine how much light is transmitted through the canopy. Thus radiation intercepted (Q_{int}) by the canopy is

$$Q_{int} = (1 - e^{-kL})Q_0 \tag{A.1}$$

where k is the radiation extinction coefficient with a constant value of 0.7 (Saldarriaga

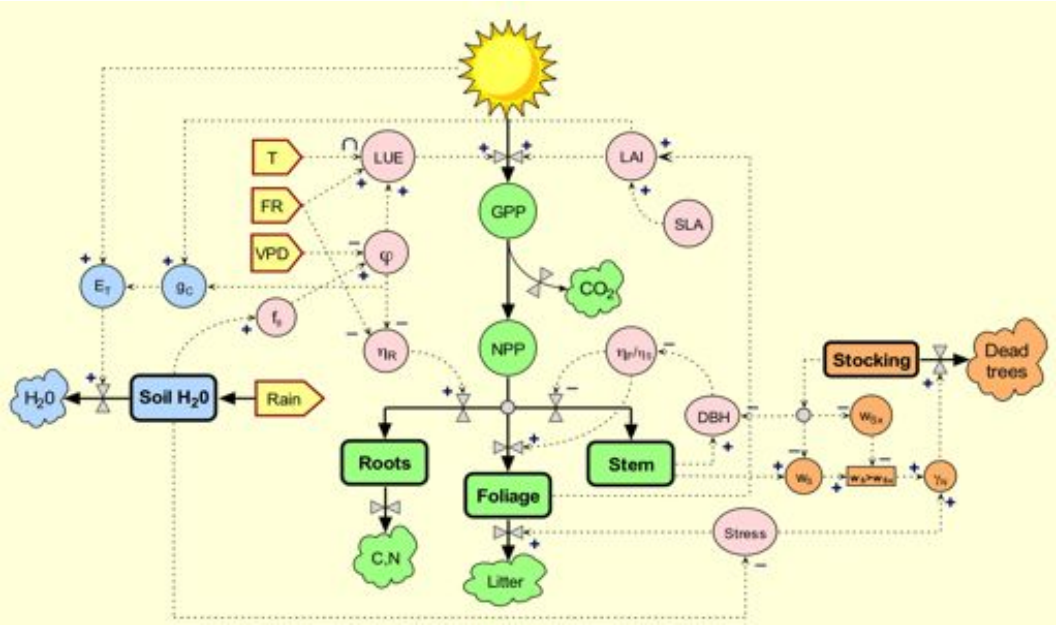

Figure A.3: Structure of 3-PG with it's carbon balance model, in green, that is influenced by causal loops involving the surrounding sub-models Landsberg and Sands (2010).

and Luxmoore, 1991) in Amazonia, L is the leaf area index (LAI) and Q_0 represents total PAR. Beer's law assumes that foliage is uniformly distributed across the stand. LAI is determined from the foliage biomass present at the end of each month and input parameter values of specific leaf area (SLA, m^2kg^{-1}). Figure A.4 demonstrates the diminishing returns, in terms of intercepted solar radiation, with increasing LAI. Secondary forest near Manaus rapidly attains a high LAI (>4) within 9 years (Lucas and Honzak, 2002) and therefore would intercept >80 % of Q_0.

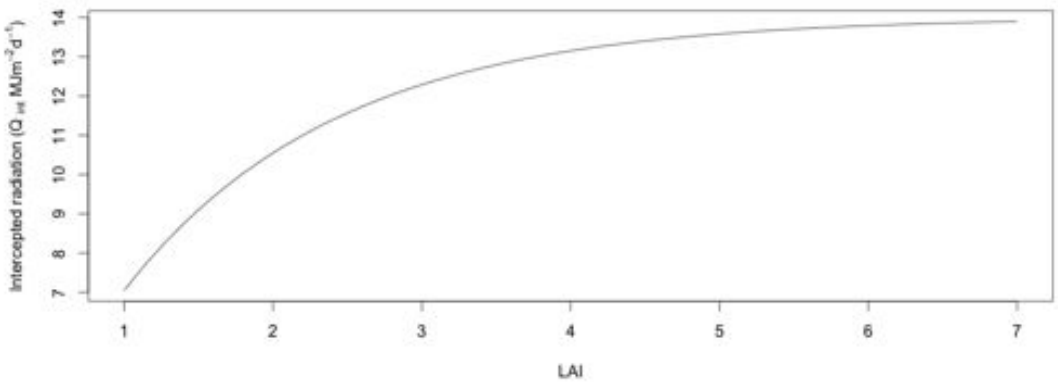

Figure A.4: Asymptotic relationship between increasing LAI and intercepted radiation assuming total incident radiation is 14 $MJm^{-2}d^{-1}$

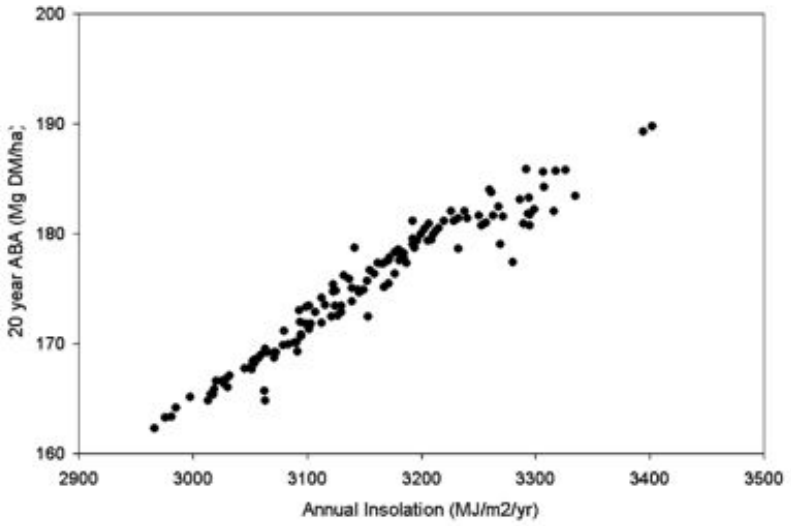

Figure A.5: The linear relationship between shortwave radiation and above ground biomass accumulation after 20 years is the LUE (White et al., 2006)

The assimilation of this intercepted radiation is described by the light use efficiency (LUE) relationship (Anderson et al., 2000). Observations show that above ground biomass and gross production are linearly related to intercepted radiation (Figure A.5). The slope of these relationships is a measure of the LUE. This simple relationship is the basis for many simple growth models. Annual stand-level LUE is stable and species specific.

LUE is known as the canopy quantum efficiency in 3-PG$_2$ and is denoted by α_C. GPP is proportional to the intercepted radiation (Equation A.2)

$$P_g = \alpha_C(1 - e^{-kL})Q_0 \tag{A.2}$$

Where P_g is GPP and α_C is determined by a series of physiological growth modifiers that reduce Q_{int} (Figure A.6). These growth modifiers are derived from environmental constraints which represent partial to complete stomatal closure. This prevents gas exchange and subsequently transpiration. These modifiers range from 0, total limitation, and 1, no limitation of growth (Equation A.3).

$$\alpha_C = f_T f_F f N min\{f_D, f_\theta\} f_{age} \alpha_{Cx} \tag{A.3}$$

where f_T is the factor representing temperature; f_F is the frost modifier; f_N is site

nutrition which is governed by the fertility rating; f_D is the vapour pressure deficit (VPD) modifier; f_θ is the soil water modifier; f_{age} represents the effect of age and α_{Cx} is the maximum canopy quantum efficiency.

A.4.1 Physiological Growth modifiers

The effect of the VPD is represented by the VPD modifier (Equation A.4). VPD is the difference (deficit) between the amount of moisture in the air and how much moisture the air can hold when it is saturated (**?**). It is a key factor when considering transpiration, the gaseous transfer of water vapour, as it is an important measure of the drying power of the air.

$$f_D(D) = e^{-k_D D} \tag{A.4}$$

where D (kPa) is the average day-time vapour pressure deficit and the species-specific parameter k_D (kPa) determines the strength of the effect of VPD. This modifier is determinant of canopy conductance and k_D can be assigned based on observed effects of VPD on stomatal conductance. *fVPD* declines exponentially with D (Figure A.6a)

In 3-PG$_2$ the soil water modifier (f_θ) (Equation A.5) represents the relative plant available soil water (θ_r) in the root zone, rather than in the entire soil profile as in previous versions of 3-PG. This growth modifier simulates the effect of the soil water balance in calculating α_C, which is calculated by differencing the monthly transpiration, as calculated by the Penman Montieth equation, and monthly precipitation. The SW balance can be negative if transpiration is greater than precipitation. Available soil water varies between no plant available water ($\theta_r = 0$) to unlimited soil water ($\theta_r = 1$).

$$f_\theta(\theta_r) = \frac{1 - (1 - \theta_r)^{n_\theta}}{1 + [(1 - 2c_\theta{}^{n_\theta})/c_\theta]^{n_\theta}} \tag{A.5}$$

where c_θ and n_θ determine the shape of the modifier and depend on the soil texture (Figure A.6b). If θ_r is $<\theta$ it is set to the same value as θ. the excess water is assumed to have drained out of the system.

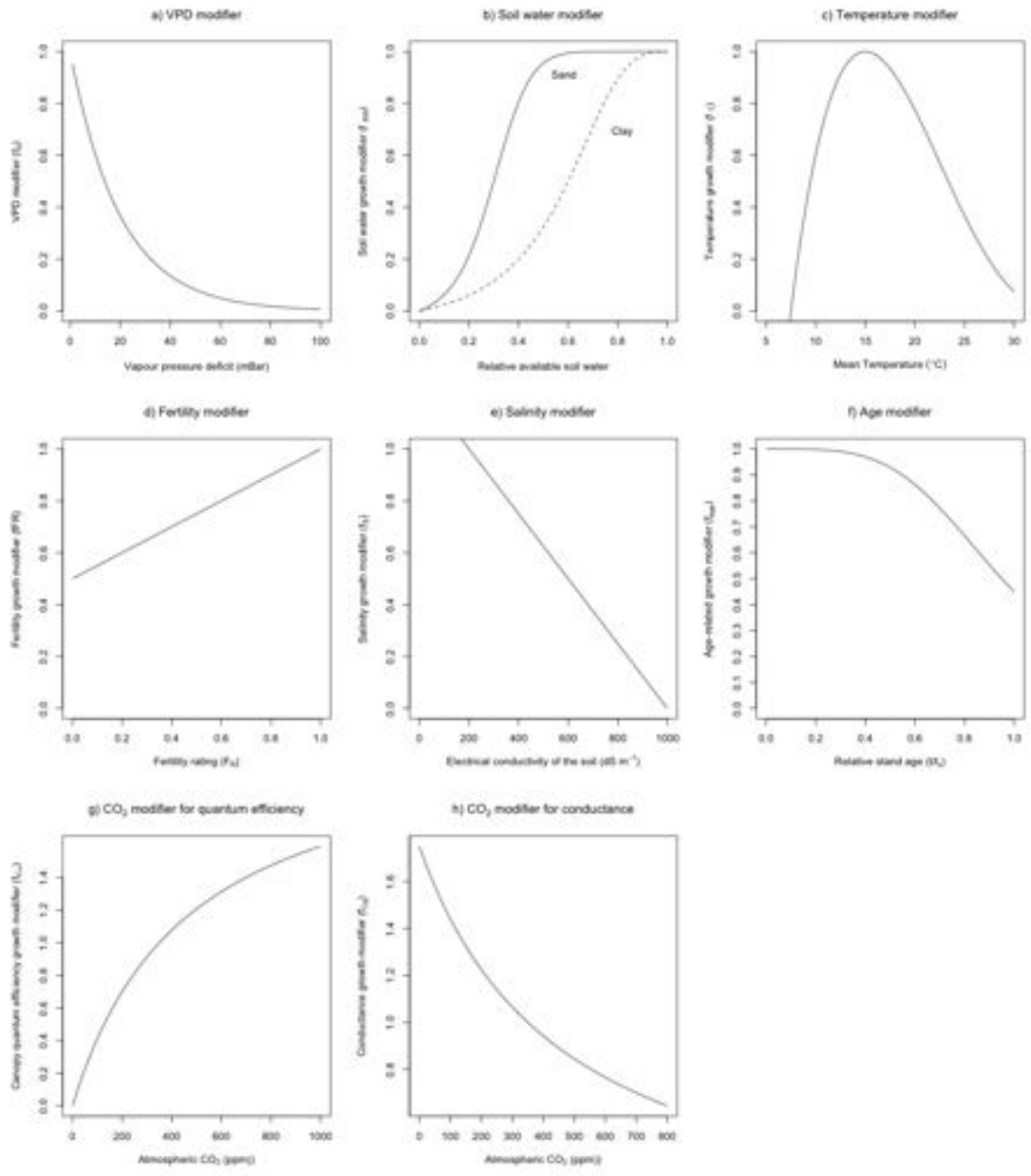

Figure A.6: a) The VPD dependent modifier showing increased stomatal closure with an increase in the VPD. b) The soil water-dependent modifier for sand and clay soils. c) Temperature-dependent modifier, showing increasing productivity with increasing temperatures up to an optimum before declining as the temperature continues to rise. d) The site fertility-dependent modifier e) The salinity-dependent modifier, illustrating the salinity below which growth is not affected and that which ceases growth f) The age-dependent modifier only decreases when the stand age nears the maximum specified age. g) The modifier applied to canopy quantum efficiency takes into account atmospheric CO_2. h) The modifier applied to canopy conductance into account atmospheric CO_2 concentration. Not shown is the growth modifier that takes into account the number of frost days which has a simple linear relationship.

The temperature modifier (Equation A.6) simulates the observed increase in production with increasing temperature up to an optimum before declining as temperature continues to rise (Figure A.6c).

$$f_T(T_{max}) = \left(\frac{T_{max} - T_{min}}{T_{opt} - T_{min}}\right)\left(\frac{T_{max} - T_{max}}{T_{max} - T_{opt}}\right)^{(T_{max}-T_{opt})/(T_{opt}-T_{min})} \tag{A.6}$$

where T_{min}, T_{opt} and T_{max} are the minimum, optimum and maximum, temperatures for growth respectively. In 3-PG$_2$ the temperature modifier is based on maximum temperature as it is daytime temperature that affects the productivity and water use (White et al., 1999).

The effect of frost is determined by a single parameter in the frost growth modifier (Equation A.7).

$$f_F(d_F) = 1 - k_F(d_F/30) \tag{A.7}$$

where d_F is the number of days of frost per month and parameter k_F is the number of days growth lost for each day of frost. The relationship follows a linear relationship where k_F is assumed as 1.

The soil nutrition modifier (Equation A.8) is determined as a linear function of the fertility rating F_R (Figure A.6d)

$$fFR(F_R) = 1 - (1 - fN0)(1 - F_R)^{fNn} \tag{A.8}$$

where F_R is the site fertility rating, *fNn* determines the shape of the response and *fN0* is the value of *fFR* when $F_R = 0$. It is recognised that this is a crude procedure to account for the differences in soil fertility ans hence 3-PG is often coupled with models of nitrogen availability such as CENTURY (Kelly et al., 1997) or SNAP (Paul et al., 2002).

The salinity modifier (f_S) (Equation A.9) accounts for the effect of soil salinity on canopy light use efficiency and canopy conductance as a function of soil electrical conductivity.

$$f_S(C_S) = 1 - \left(\frac{(C_S - C_{S0})}{(C_{S1} - C_{S0})} \right)^{n_{C_S}} \tag{A.9}$$

where C_s (dS m^{-1}) is the electrical conductivity of the soil, the thresholds C_{S0} and C_{S1} are the conductivities at which salinity begins to affect and stops growth, respectively, while n_{C_S} is a power that determines the shape of the response (Figure A.6e). The effects of salinity have yet to be parameterised for 3-PG (Landsberg and Sands, 2010) and a salt balance model has not been implemented (Almeida et al., 2007a). Therefore changes in soil water content do not change soil solution salinity, i.e. salinity is a static site factor and is not modelled dynamically.

The age effect modifier (Equation A.10) is close to 1 for young stands and only decreases when the stand age approaches the maximum age parameter value t_x (Figure A.6f).

$$f_{age}(t) = \frac{1}{1 + (t/r_{age}t_x)^{n_{age}}} \tag{A.10}$$

where t (years) is stand age and t_x is the maximum age expected for a stand of these species. Whilst r_{age} is the relative age (t/t_X) at which $f_{age} = 0.5$ and n_{age} determines the strength of the response.

The atmospheric CO_2 modifier is separated into the effects of CO_2 (C_a) concentration (ppm) on α_c (Equation A.11a, Figure A.6g) and the effect on conductance g_c (Equation A.11b, Figure A.6h). However these have yet to be tested. Proper implementation will follow physiological studies of the effects of CO_2 enrichment, and the results of applications of models to study such effects (Almeida et al., 2007a).

$$f\alpha_C(C_a) = \frac{f_{C\alpha x}C_a}{350(f_{C\alpha x} - 1) + C_a} \tag{A.11a}$$

$$f_{Cg}(C_a) = \frac{f_{Cg0}}{1 + (f_{Cg0} - 1)C_a/350} \tag{A.11b}$$

respectively, where

$$f_{C\alpha x} = \frac{f_{C\alpha 700}}{2 - f_{C\alpha 700}} \tag{A.12a}$$

$$f_{Cg0} = \frac{f_{Cg700}}{2f_{Cg700} - 1} \tag{A.12b}$$

express $f_{C\alpha x}$ and f_{Cg0} in terms of the parameters $f_{C\alpha 700}$ and f_{Cg700}. The modifiers have the value 1 when C_a = 350ppm, and the values $f_{C\alpha 700}$ and f_{Cg700} are also 1 when C_a = 700ppm. The effects of these formulas are consistent with observations of the response of single-leaf gas-exchange data to changes in CO_2 concentration (Malhi et al., 2009b).

In 3-PG_2, the combination of the soil water, salt and age modifiers is called *'PhysMod'* (Equation A.13). Unlike the original version which included the VPD modifier as this does not affect NPP (Almeida et al., 2007a).

$$\varphi = f_\theta f_{age} f_S \tag{A.13}$$

A.4.2 Biomass partitioning

3-PG_2 assumes that a constant fraction (Y, 0.47) of GPP is lost as construction and maintenance of respiration is carried out, this process is known as the carbon use efficiency (CUE). The remainder, NPP, (P_n) is defined by the equation A.14.

$$P_n = YP_g = \varepsilon Y(1 - e^{-kL})Q_0 \tag{A.14}$$

NPP is partitioned into the biomass pools (Mg ha^{-1}) representing foliage (W_F), above ground woody tissue (W_S) and roots (W_R) (Equation A.15). Partitioning rates (η_F, η_R, η_S) depend on site and growth conditions and the average DBH of the stand. This approach allows root allocation and LAI to vary with growing conditions, but forces the model to allocate carbon in realistic manner that replicates actual structures.

Litter-fall (γ_F) and root-turnover (γ_R) are also taken into account whereby:

$$\begin{aligned} \Delta W_F &= \eta_F P_n - \gamma_F W_F \\ \Delta W_R &= \eta_R P_n - \gamma_R W_R \\ \Delta W_S &= \eta_S P_n \end{aligned} \tag{A.15}$$

A.4.3 Allocation in 3-PG$_2$

Root allocation is determined by fertility and available soil water (ASW). Poor fertility conditions favour below-ground growth (Figure A.7). High F_R results in low allocation to roots and higher volume leaf growth (Ordoñez et al., 2009). This increases the LUE and the overall biomass production. The effects of VPD on allocation of NPP to roots originally assumed by 3-PG is excluded in 3-PG$_2$. This results in slightly higher allocation to above ground pools, requiring a lower canopy quantum efficiency α_C to achieve the same volume growth. These changes were made so that more realistic values for α_C can be used in line with fundamental plant physiology (Almeida et al., 2007a).

Root allocation is affected by growth conditions through φ and soil fertility through m (Equation A.16). As roots grow the volume of soil they access changes. The new volume of the root zone accessed due to root growth is calculated as the roots grow. Its upper limit is reached when the soil profile is full. The model then takes into account the soil water that is moved from the root-free zone to the root zone, or conversely if the root zone volume decreases.

$$\eta_R = \frac{\eta_{Rx}\eta_{Rn}}{\eta_{Rn} + (\eta_{Rx} - \eta_{Rn})m\varphi} \tag{A.16}$$

Where m = m_0 + (1-m_0)F_R. m_0 is a potential species specific parameter but is usually assigned a value of $m_0 = 0$. η_{Rx} represents root allocation under poor fertility conditions and η_{Rn} denotes root allocation under optimal conditions when neither site F_R or ASW is limiting.

Above ground allocation is based on the foliage:stem partitioning ratio (Equation A.17). This ratio is determined by tree size. Large trees allocate more NPP to stem wood.

$$p_{FS} = \eta_F/\eta_s = a_p B^{n_p} \tag{A.17}$$

Where η_F denotes the allocation of NPP to foliage (Equation A.18a) and η_S the allocation of NPP to the woody stem (Equation A.18a). B is DBH determined from an allometric relationship between stem mass and B, whilst a_p and n_p are coefficients

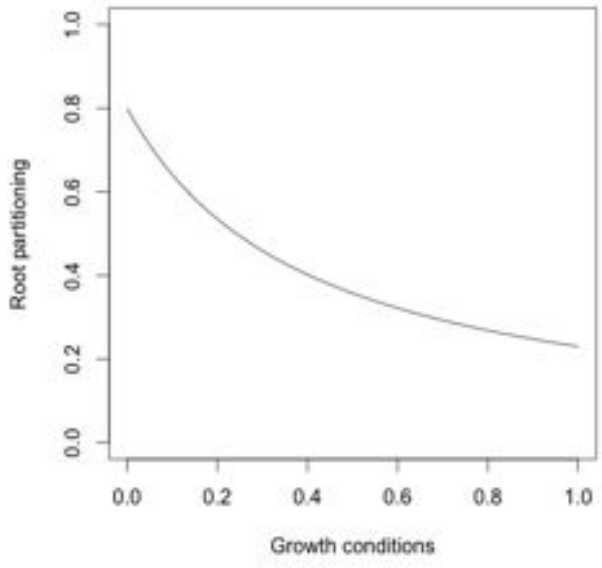

Figure A.7: Fertile soils with adequate available soil water result in lower partitioning of NPP to roots.

determined from p_{FS} at $B = 2$ and 20 cm.

$$\eta_S = \frac{1 - \eta_R}{1 + p_{FS}} \tag{A.18a}$$

$$\eta_F = p_{FS}\eta_S \tag{A.18b}$$

η_R is a function of the site fertility, and soil water status. Increasing DBH decreases foliage allocation and increases stem allocation. This response is illustrated in Figure A.8.

A.4.4 Litter-fall and root-turnover

Litter-fall is an age dependant function of foliage biomass (Equation A.19)

$$\gamma_F(t) = \frac{\gamma_{Fx}\gamma_{F0}}{\gamma_{F0} + (\gamma_{Fx} - \gamma_{F0})e^{kt}}, k = \frac{1}{t_{\gamma F}} \ln(1 + \frac{\gamma_{Fx}}{\gamma_{F0}}) \tag{A.19}$$

where γ_{F0} is the litter-fall rate at age 0. γ_{Fx} is maximum litter-fall rate, which may be stress-related. $t_{\gamma F}$ is age when $\gamma_F = \frac{1}{2}(\gamma_{F0} + \gamma_{Fx})$. Root-turnover is a constant fraction of root biomass (γ_R=0.015 month-1)

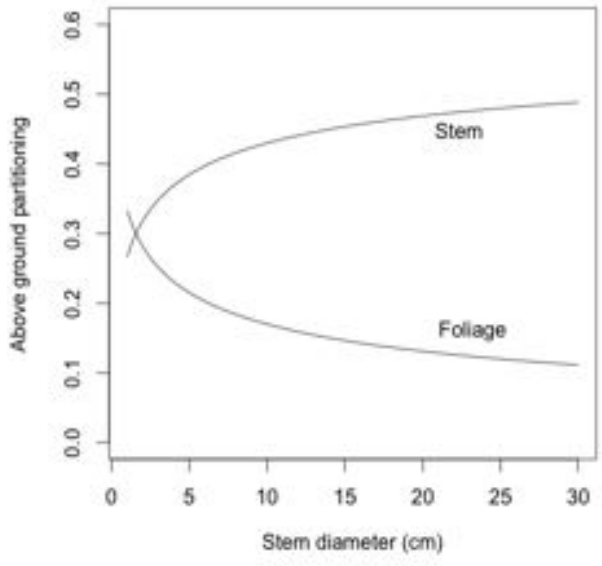

Figure A.8: The stem:foliage partitioning ratio

A.4.5 Summary of carbon-balance model

The basic carbon balance equations include light interception, assimilation, biomass allocation and mortality (litter-fall and root turnover). Canopy quantum efficiency and root allocation are determined by the site conditions. Whilst rates of allocation are age-dependant and stress related.

A.4.6 Stem mortality

3-PG$_2$ includes density independent mortality through probability of death (γ_N). This is related to age and stress (Equation A.20)

$$\Delta N = -\gamma_N N \tag{A.20}$$

γ_N increases in times of stress, e.g. in response to low long-term average *f0* (drought) it can also be representative of continuous background mortality.

Stem mortality also occurs through self-thinning in 3-PG$_2$. This is influenced by stocking via single-tree stem mass. Self thinning gives maximum single-tree stem mass (kg/tree) at current stocking (Equation A.21)

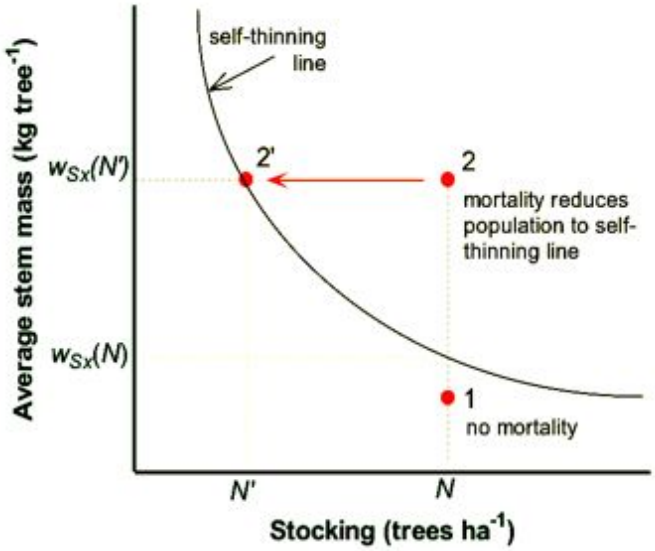

Figure A.9: At point 1 there is no mortality whilst at point 2 the population is reduced to 2' (Landsberg and Sands, 2010)

$$w_{Sx}(N) = w_{Sx0}(1000/N)^{3/2} \tag{A.21}$$

Where W_{Sx0} is maximum stem mass at 1000 trees ha^{-1}. When $W_S > w_{Sx}$(N), stocking is reduced. This is illustrated in Figure A.9.

The process of self-thinning is calculated by Figure A.10. As self thinning decreases the number of stems the basal areas increases causing self-thinning to accelerate. This is based on the model developed by Vanclay and Sands (2009). In which it is continuous during stand development.

Stem volume is calculated either from allometric relationships with respect to DBH or from density using (Equation A.22):

$$V = (1 - p_{BB})W_S/\rho \tag{A.22}$$

Where p_{BB} is fraction of stem biomass in branch and bark and ρ is stem density. p_{BB} and ρ can vary widely across a site and calculation of stem volume from W_S can be error prone.

‘

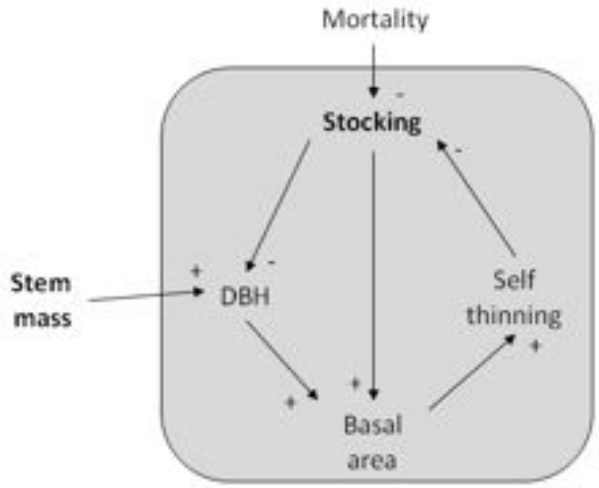

Figure A.10: Density-independent, or environmentally induced mortality, is modelled in 3-PG$_2$ as an age dependent process and is shown as an input here. Stem number is the primary output of this sub-model. The inward pointing arrows identify environmental inputs or inputs from other sub-models, while outward arrows identify outputs from this sub-model. Bold text denotes state variables. Arrows show casual influences whilst positive and negative symbols show the type of influence. The sub-model is based on the work of Vanclay and Sands (2009) and is driven by basal area.

A.4.7 Water Balance

In 3-PG$_2$ the determination of soil water stress is set by the water content of a zone of soil surrounding the roots. This zone changes in volume as the plant grows and the root system occupies a greater volume of the soil profile. The water involved in transpiration is drawn from the root zone, an area that dries out more easily than the bulk soil (Almeida and Sands, 2015). The recharge of the root zone is modelled by movement of water at a rate proportional to the difference in volumetric soil water content in the two zones considering the saturated hydraulic conductivity.

The soil water balance separately calculates forest and understorey rainfall interception, transpiration, and soil evaporation. The understorey component is not utilised in this study due to a lack of data pertaining to it. Implementation would however provide a more realistic model of rainfall interception. A leaf water retention model is used in calculating rainfall interception that assumes rainfall occurs as a single event. This first wets leaves to a maximum thickness of retained water, and any subsequent rain becomes throughfall. Retained water is evaporated at the wet-surface rate which is calculated using the Penman-Monteith equation driven by the soil aerodynamic conductance (g_{As},

ms^{-1}), Q_{int} on the soil and VPD above the soil, both accounting for the presence of a canopy prior to canopy closure. Following a rainfall event, all retained water is evaporated. Thus all water lost through interception is that which is evaporated and retained on the leaves. Total monthly interception loss is then obtained by summing over individual events.

3-PG_2 is capable of utilising a daily time step in calculating the water balance however this adds extra complexity to a model who's design is supposed to be simple. The alternative is to provide the number of rainy days per month. The rainfall interception and soil evaporation are then modelled on a rainfall event basis. The month is divided into (d_R) equal periods with an amount (R/d_R) of rain falling as a single event at the beginning of each period. R is total monthly rainfall and d_R is the number of rainy days. The water balance is performed separately over each period.

Transpiration in the forest canopy is modelled using the Penman-Monteith equation. It is driven by canopy aerodynamic conductance (g_{Ac}), Q_{int} and VPD above the canopy. g_{Ac} is modelled using a model described by White et al. (1999). It is canopy conductance is affected by VPD, soil water and stand age through φ, and increases with canopy LAI (Equation A.23).

Water lose through soil evaporation is confined to a shallow upper soil layer. This layer acts as a barrier to further evaporation as the soil dries. Evaporation is high when the soil surface is wet after rain, and declines as it dries out (Ritchie, 1972). The amounts of water evaporated during this process are determined by E_{S1} and E_{S2} (Table A.6. All soil evaporation is modelled in this way in 3-PG_2.

If the volume of rain falling exceeds θ the soil becomes saturated (θ_{sat}) and the excess becomes surface run-off. Remaining water then becoming available for evaporation and transpiration. If θ exceeds the field capacity (θ_{fc}) the excess soil water is available for drainage. Soil drainage proceeds at a rate (k_{Drain}) proportional to the excess and is a soil texture dependent property.

$$g_C = g_{Cx}\varphi min\{L/L_{gCx}, 1\} \tag{A.23}$$

where g_{Cx} represents the maximum canopy conductance and L_{gCx} is the value of LAI

when maximum conductance is reached.

Table A.6: Soil Parameters used in $3PG_2$

Description	**Symbol**	**Soil Parameters**							**Composition (%)**		
		θ_{sat}	θ_{fc}	θ_{wp}	c_θ	n_θ	kSCond	kDrain	Silt	Sand	Clay
Clay	C	0.49	0.42	0.30	0.40	3.00	0.11	0.22	20.00	30.00	50.00
Clay loam	CL	0.47	0.35	0.21	0.50	5.00	0.21	0.24	33.00	33.00	34.00
Loam	L	0.46	0.27	0.13	0.55	6.00	0.60	0.30	40.00	42.00	18.00
Loamy sand	LS	0.46	0.12	0.06	0.65	8.00	13.51	0.59	12.00	82.00	6.00
Sand	S	0.47	0.10	0.05	0.70	9.00	15.21	0.66	3.00	92.00	5.00
Sandy clay	SC	0.44	0.38	0.26	0.45	4.00	0.19	0.37	6.00	52.00	42.00
Sand clay loam	SCL	0.43	0.28	0.18	0.53	5.50	0.55	0.43	12.00	60.00	28.00
Sandy loam	SL	0.45	0.18	0.08	0.60	7.00	2.99	0.47	25.00	65.00	10.00
Silt	T	0.49	0.32	0.06	0.63	7.50	0.00	0.05	87.00	7.00	6.00
Silty clay	TC	0.53	0.42	0.28	0.43	3.50	0.09	0.05	46.00	7.00	47.00
Silty clay loam	TCL	0.51	0.38	0.21	0.48	4.50	0.15	0.07	56.00	10.00	34.00
Silty loam	TL	0.49	0.32	0.14	0.58	6.50	0.62	0.14	60.00	20.00	20.00